NASA CONTRACTOR REPORT 166271

Study of Aerodynamic Technology for Single-Cruise-Engine V/STOL Fighter/Attack Aircraft

Final Report

H. H. Driggers
S. A. Powers
R. T. Roush
Vought Corporation

CONTRACT NAS2–11003
February 1982

NASA

NASA CONTRACTOR REPORT 166271

Study of Aerodynamic Technology for Single-Cruise-Engine V/STOL Fighter/Attack Aircraft

Final Report

H. H. Driggers
S. A. Powers
R. T. Roush
Vought Corporation
Dallas, Texas

Prepared for
Ames Research Center
Under Contract NAS2-11003

National Aeronautics and
Space Administration

Ames Research Center
Moffett Field, California 94035

FOREWORD

This study of aerodynamic technology for single-cruise-engine V/STOL fighter/attack aircraft was Phase I of a research program jointly sponsored by the National Aeronautics and Space Administration and the United States Navy. Technical Monitors for Ames Research Center were Mr. D. A. Durston and Mr. W. P. Nelms, Aircraft Aerodynamics Branch. Navy representatives included Mr. M. W. Brown, Naval Air Systems Command and Mr. J. H. Nichols, David W. Taylor Naval Ship Research and Development Center.

Mr. H. H. Driggers was the Principal Investigator. Mr. S. A. Powers was responsible for the aerodynamic analysis; Mr. R. T. Roush performed the propulsion analysis. The following individuals made significant contributions to the Phase I study effort:

W. B. Brooks	Aerodynamics
T. D. Beatty	Aerodynamics
T. C. Dull	Mass Properties
K. W. Higham	Mass Properties
G. W. Hillman	Design
S. E. Orner	Aerodynamics
W. B. Sears	Aerodynamics
H. E. Sherrieb	Aerodynamics
M. K. Worthey	Aerodynamics

U.S. Customary Units are used throughout this report. A Metric (SI) conversion table is provided in Appendix I.

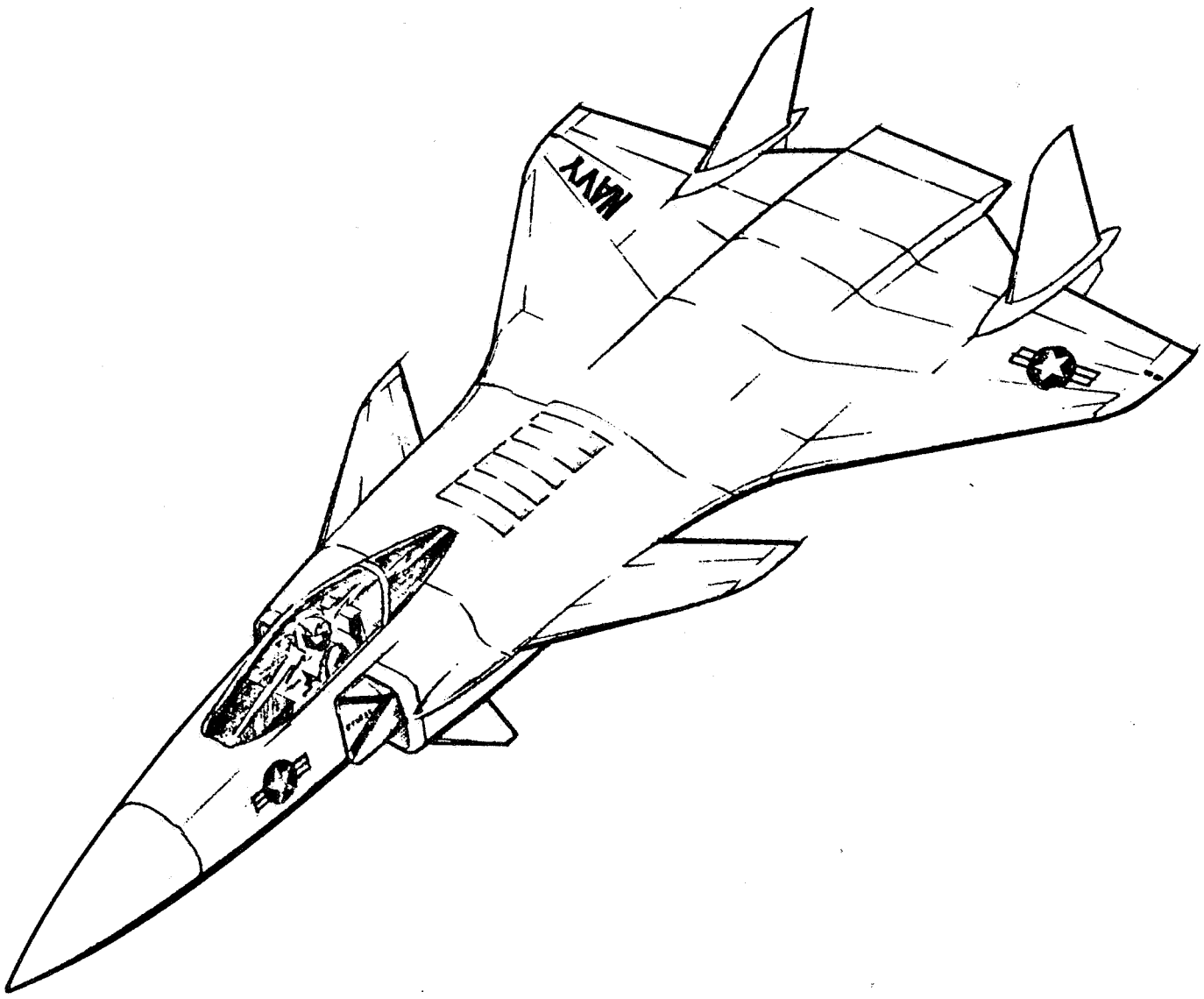
NAVY

SUMMARY

The Vought Series Flow Tandem Fan (SFTF) variable cycle propulsion concept was integrated into a high performance, single engine V/STOL fighter/attack aircraft. The resulting configuration was the focus of a conceptual design and aerodynamic analysis study emphasizing the identification of aerodynamics uncertainties. The TF120 study configuration is a canard delta arrangement with extensive wing-body blending and three pairs of all-moving vertical control surfaces to maintain control in the post-stall flight regime. Side inlets feed the SFTF propulsion unit, which exhausts through a two-dimensional deflecting nozzle. In the V/STOL mode the forward fan efflux exits through a ventral nozzle; an auxiliary inlet feeds the aft fan and core, which utilize the aft deflecting nozzle. Exhaust temperature of both streams is 950°F for vertical takeoff, enhancing shipboard compatibility. In high speed flight the SFTF converts to an afterburning turbofan cycle which yields exceptionally high fighter performance.

Estimates of TF120 aerodynamics characteristics were made for Mach numbers from 0.2 to 2.4 range. An advanced computer code used in the analysis predicted complex interactions between the configuration and deflected control surfaces. An investigation was made of unconventional control modes, in which simultaneous deflections were commanded to augment a desired single-axis response while suppressing all unwanted responses.

Identification of aerodynamic uncertainties was a principal study objective. All the computer-based estimates were considered inadequate due to inherent limitations imposed by linear theory as well as anomalies encountered during the course of the study. Aerodynamic characteristics at high angles of attack (including post-stall), large control deflections and the close-coupled, highly integrated and blended configuration were judged beyond the capabilities available methods. Vought believes a wind tunnel test program is mandatory to supply the data base needed to validate the TF120 configuration and assess current aerodynamic analysis methods. A concurrent benefit from the proposed test program is that since the TF120 is only minimally compromised to achieve V/STOL capability, the aerodynamic configuration is representative of advanced CTOL fighters.

SYMBOLS

a	–	Acceleration in ft/sec^2
A/B	–	Afterburner
a.c.	–	Aerodynamic Center in fraction of Mean Geometric Chord
A_j	–	Total jet exit area in ft^2
AOA	–	Angle of attack
C_l	–	Rolling moment coefficient
C_D	–	Drag coefficient
C_{fg}	–	Gross thrust coefficient
c.g.	–	Center of gravity
C_L	–	Lift coefficient
C_m	–	Pitching moment
C_n	–	Yawing moment coefficient
C_Y	–	Side force coefficient
ΔD	–	Drag increment in pounds
D_e	–	Equivalent nozzle diameter in ft
ΔL	–	Propulsion induced suckdown in lbs
e	–	Oswald span efficiency factor
ECS	–	Environmental control system
FPR	–	Fan pressure ratio
g	–	Acceleration of gravity in ft/sec^2
h	–	Altitude in feet
I_x, I_y, I_z	–	Moments of inertia about the x, y or z axis, respectively.
IGV	–	Inlet guide vanes
k, k_1	–	Constants of proportionality
M	–	Mach number
MGC	–	Mean Geometric Chord in feet
p	–	Ratio of elevon to vertical fin deflection
P	–	Jet static pressure
$P_{t,n}$	–	Jet total pressure in lb/ft^2
PR	–	Pressure ratio
q	–	Dynamic pressure in lb/ft^2

SYMBOLS (Continued)

q	–	Ratio of elevon to aft ventral fin deflection
r	–	Ratio of elevon to forward ventral deflection
RCS	–	Reaction control system
S	–	Wing reference area in ft^2
SFC	–	Specific fuel consumption, lb/hr/lb
SLS	–	Sea level static conditions
STO	–	Short takeoff
T	–	Total jet thrust
TOGW	–	Takeoff gross weight in lbs
T4	–	Turbine outlet temperature
T/W	–	Thrust to weight ratio
V	–	Velocity, kts
w	–	Airflow in lb/sec
X	–	Downstream distance in ft
α	–	Angle of attack in degrees
β	–	Sideslip angle
δ	–	Control surface deflection in degrees
δ	–	Pressure ratio, P/P_{SL}
γ	–	Flight path angle in degrees
θ	–	Temperature ratio, T/T_{SL}

CONTENTS

CONTENTS (Continued)

CONTENTS (Continued)

FIGURES

FIGURES (Continued)

TABLES

1.0 INTRODUCTION

This section shows how Vought experience in conceptual design of high performance V/STOL aircraft led to the present Series Flow Tandem Fan Configuration Concept.

1.0 INTRODUCTION

The TF120 V/STOL fighter concept which is the subject of this report is the latest in a series of Vought high performance V/STOL designs. The design philosophy discussed in Section 2.0 derives from experience gained in earlier conceptual design analyses. Two concepts of particular relevance will be briefly discussed.

In 1977-78 Vought performed a study of aerodynamic technology of a vertical attitude takeoff and landing (VATOL) fighter for Ames Research Center under Contract NAS2-9772. This work is reported in Reference 1. The SF-121 study configuration, illustrated in Figure 1-1, was a canard-delta arrangement powered by two conventional afterburning turbofan engines with vectoring exhaust nozzles for VATOL mode operation. The SF-121 was essentially uncompromised to achieve V/STOL capability and exhibited excellent performance, but the unorthodox takeoff and landing mode required special platform installations not presently on Naval aviation ships. This unusual characteristic led Vought to seek alternative horizontal attitude V/STOL propulsion concepts.

A major operational problem inherent to jet lift propulsion concepts such as lift-plus-lift/cruise or remote augmentation lift systems (RALS) is very hot gas impingement on the ship or runway. If exhaust gas temperature is limited to, say, 1000°F the impact on operating facilities and personnel would be minimal.

Vought has devised a promising solution to the problem of combining high performance and moderate footprint in one configuration: the Series Flow Tandem Fan. The SFTF was first applied in 1979 to the design shown in Figure 1-2. The V-536 was a relatively large fighter, in which two SFTF engines were cross-shafted together to prevent thrust asymmetry and to permit a vertical landing with one engine disabled. The V-536 was evaluated against VATOL, L+L/C and RALS concepts (Reference 2) and found competitive in weight and superior in performance.

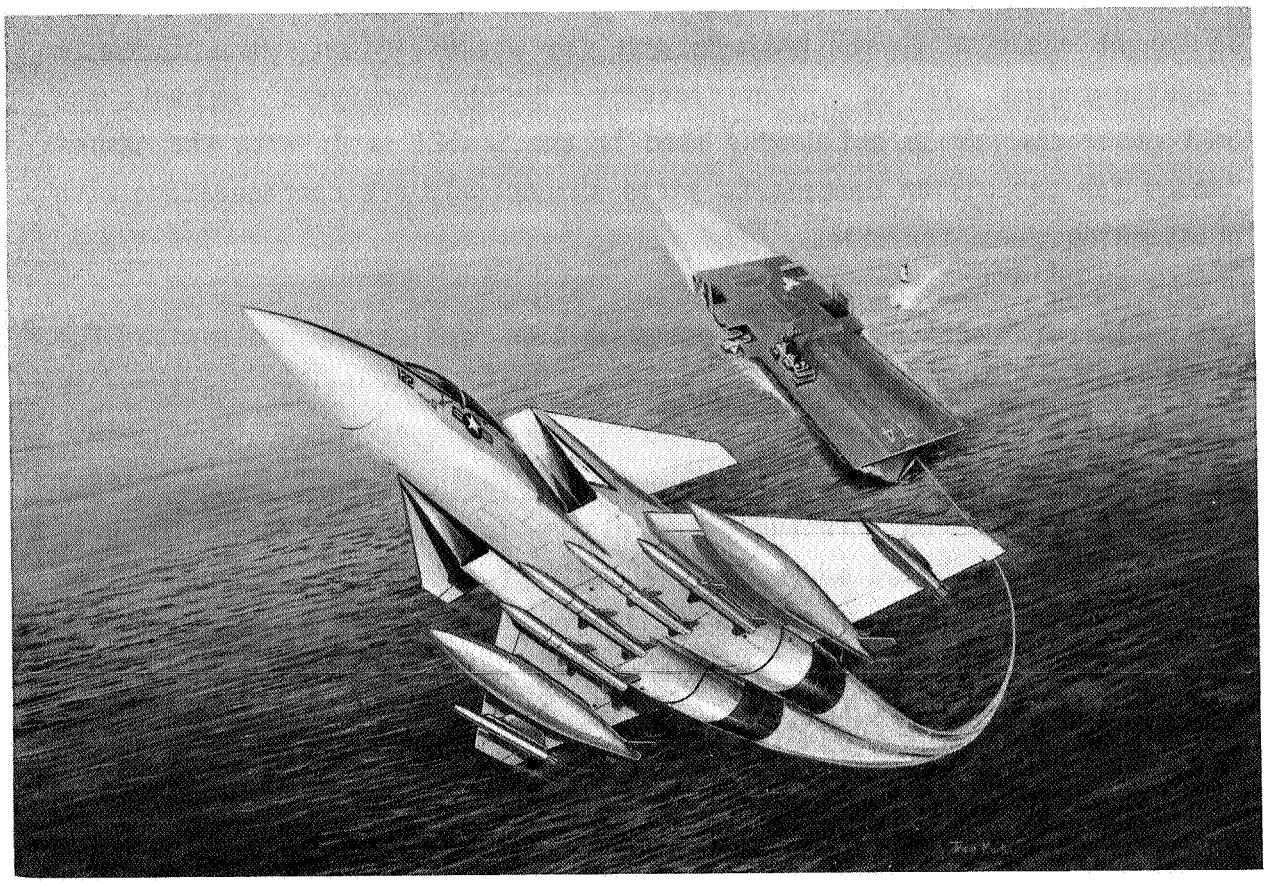

Figure 1-1 - SF-121 VATOL Fighter Concept

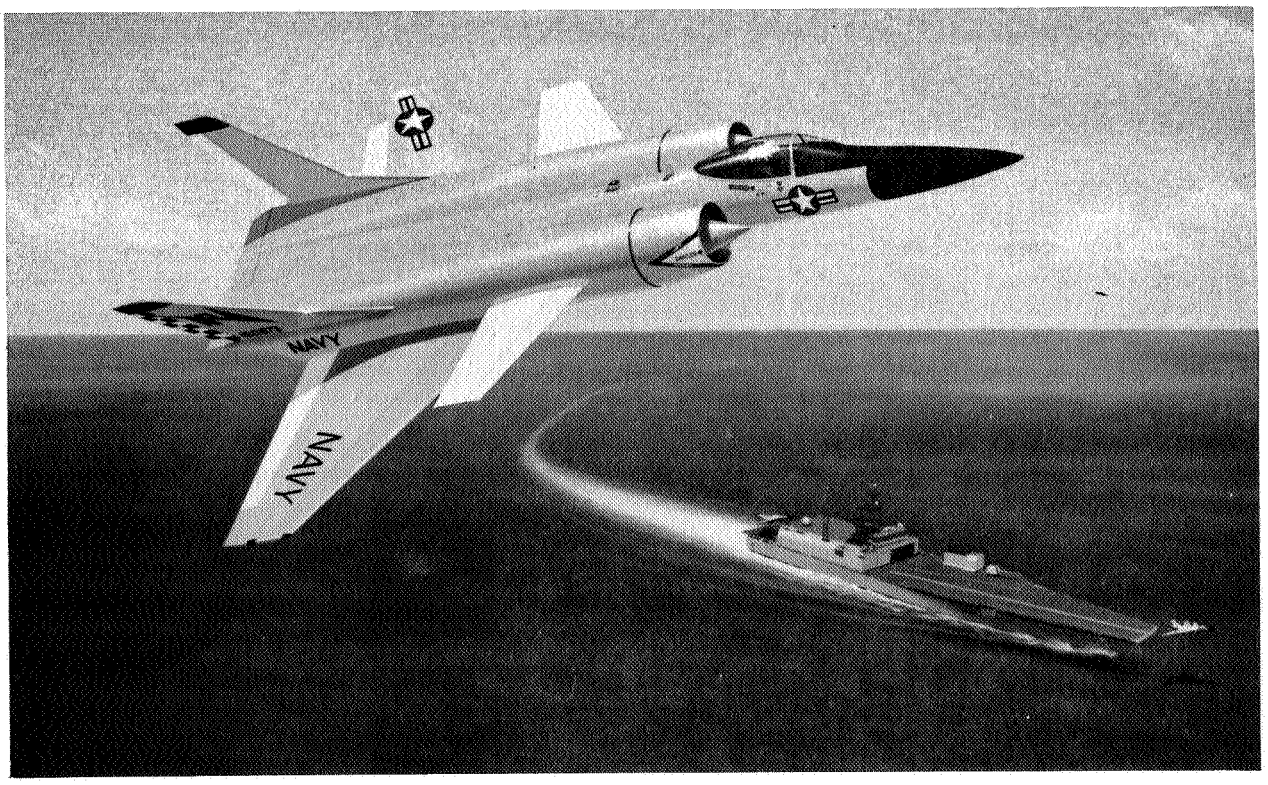

Figure 1-2 - V-536 Tandem Fan Fighter Concept

The Vought response to the NASA request for proposal (Reference 3) for a single-cruise-engine V/STOL fighter/attack design analysis melded the minimum-fighter-compromise philosophy used in the SF-121 study with the series flow tandem fan propulsion concept to yield an entirely new configuration with some outstanding characteristics.

The following sections will discuss design philosophy, describe the resulting fighter concept and its powerplant, derive detailed aerodynamic characteristics and present performance characteristics. Aerodynamic uncertainties arising from unique configuration features will be identified and a wind tunnel program structured to resolve principal uncertainties will be proposed. SFTF installed performance and aircraft performance sensitivites are collected in Appendices at the end of the report.

2.0 AIRCRAFT DESIGN

This section contains a discussion of the design philosophy behind the TF120 V/STOL concept, the NASA performance guidelines and sizing criteria.

This section includes:

2.1 DESIGN PHILOSOPHY

> The design philosophy was to achieve V/STOL capability with minimal compromise to an efficient fighter configuration.

The V/STOL fighter/attack concept described and analyzed in this report reflects the philosophy that the means used to achieve V/STOL capability should have minimal impact on fighter capability. This objective is best achieved by a propulsion concept which can be integrated into an aerodynamic configuration which is desirable for a CTOL fighter/attack role. Given the current situation of limited research funds and the uncertainty of V/STOL as an operational requirement, it is important to develop a data base of potentially broad application. The configuration to be described achieves this objective.

General requirements for future fighters will include the ability to maneuver at high angle of attack and to remain controllable at and beyond the stall. The post-stall regime is characterized by the development of strong vortices and separated flow. The Vought TF120 design employs a clipped delta wing planform with a canard and wing-body blending to exploit the lift potential of vortex flow and to achieve a smooth variation in aerodynamic characteristics with increasing angle of attack. This approach yields a wing with the light weight vital to V/STOL aircraft and the volume to accommodate large integral fuel cells. Directional stability at high angles of attack is enhanced by locating vertical fins outboard on the wings and on the underside of the vehicle.

Fly-by-wire control technology will facilitate use of redundant, distributed aerodynamic controls. The TF120 control system elements are arranged to prevent a total loss of control power due to separated flow, mechanical failure or battle damage. The decision was made to limit static instability in order to minimize control surface size required to recover from a post-stall excursion.

Characteristics sought for the propulsion system were ease of design integration, moderate footprint during VTOL, compatibility with Mach 2+ performance, good STO performance at overload weights and minimal weight penalty to acquire V/STOL capability. Previous Vought work (Contract NAS2-9772) on a twin engine Vertical Attitude Takeoff and Landing (VATOL) concept revealed its excellent performance, a simple propulsion system and one-engine-out vertical landing capability. It was obvious that a single engine VATOL design would encounter even fewer uncertainties. We elected to concentrate on a horizontal attitude concept which will ease operational problems on shipboard or land bases, yet still achieve fighter performance goals at low takeoff weight.

The study configuration was designed to meet or exceed NASA performance guidelines.

The TF120 was specifically designed to meet or exceed all performance and operational capability guidelines specified in the contract statement of work, Section 3.1.1, which states that:

"The conceptual analysis shall be for an aircraft based on the following guidelines:

- o high performance, single-cruise-engine, VSTOL fighter/attack aircraft
- o supersonic dash capability with sustained Mach number capability of at least 1.6
- o operational from land and from ships smaller than CVs without catapults and arresting gear (good STO capability)
- o sustained load factor of 6.2 at Mach 0.6, 10,000 foot altitude at 88 percent VTOL gross weight
- o specific excess power at 1G (Ps1G) of 900 fps at Mach 0.9, 10,000 foot altitude at 88 percent VTOL gross weight
- o VTOL gross weight of approximately 15,000 to 30,000 pounds
- o STO sea-based gross weight = VTOL gross weight plus approximately 8,000 to 10,000 pounds."

In addition to the NASA guidelines we sought these performance capabilities:

- Mach 2.0 dash capability at altitude
- Mach 1.2 dash capability at Sea Level
- Mach 1+ dash capability at altitude at Intermediate thrust
- Acceleration from Mach 0.8 to 1.6 at 36,089 feet altitude in less than 60 seconds
- Maximum thrust ceiling above 60,000 feet
- Intermediate thrust ceiling above 50,000 feet
- STO deck run of 400 feet or less with zero wind, Tropical Day, at VTO weight plus approximately 10,000 pounds

2.3 SIZING CRITERIA

> The study configuration was sized to realistic mission and combat constraints.

High performance V/STOL fighters are typically sized by the combination of three requirements:

(1) radius of action on a specified mission profile (fuel load)

(2) a VTOL or V/STOL thrust-to-weight ratio constraint (engine size)

(3) a maneuver constraint (wing area)

For the Tandem Fan fighter we elected to size to a 200 nautical mile radius Mach 1.6 Supersonic Intercept (SI or DLI) mission, a VTO thrust-to-weight ratio sufficient to meet MIL-STD-83300 Level 1 hover control power requirements (as in the SF-121 VATOL analysis, Reference 1), and all NASA guidelines. We also generated performance on six alternate missions with design mission internal fuel, with external fuel and on numerous maneuver and STO conditions, as reported in Section 6 and Appendix IV.

3.0 CONCEPT DESCRIPTION

This section describes the physical characteristics of the TF120 V/STOL fighter design, from the outside in.

This section contains:

3.1 AERODYNAMIC CONFIGURATION

> The study configuration is designed for efficient supersonic cruise and for high combat maneuverability to extreme angle of attack.

The TF120 is a high performance, single engine V/STOL fighter designed around the Vought series flow tandem fan (SFTF) propulsion concept. The tandem fan is a unique dual mode, variable cycle engine which is described in Section 5.1. Integration of the SFTF into an efficient fighter configuration was accomplished with minimal compromise to the aerodynamic configuration, as illustrated by the TF120 general arrangement, Figure 3-1.

The TF120 is a canard delta configuration featuring extensive wing body blending in both planform and cross section. Canard control surfaces are located on the wing strakes. Small booms extend aft from the wing to carry outboard vertical fins and ventrals. Two small control fins mounted on the lower corners of the inlets pivot from vertical to horizontal depending on flight regime. Table 3-1 summarizes geometric properties of all aerodynamic surfaces for the Point Design.

The TF120 is a control configured vehicle with control surfaces whose deflections be optimally coordinated throughout the operating envelope. In addition to providing direct lift and direct sideforce, this system can cope with battle damage or random failures with fewer channels of redundancy than usually postulated for fly-by-wire because of the multiplicity of controls.

The forward ventral fins below the inlets are all-moving control surfaces with two axes of travel. In addition to pivoting to generate normal forces, these surfaces can be adjusted to any dihedral angle between -15 and -75 degrees. In the down position they help generate direct side forces and aid in directional control. At supersonic speeds they fold outward to reduce the rearward shift in the aerodynamic center and augment longitudinal and lateral

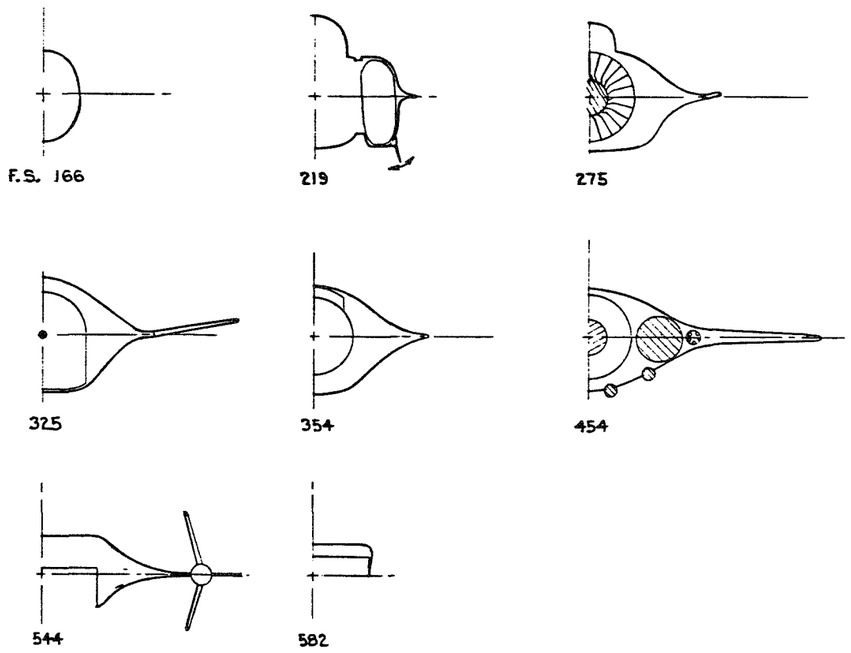

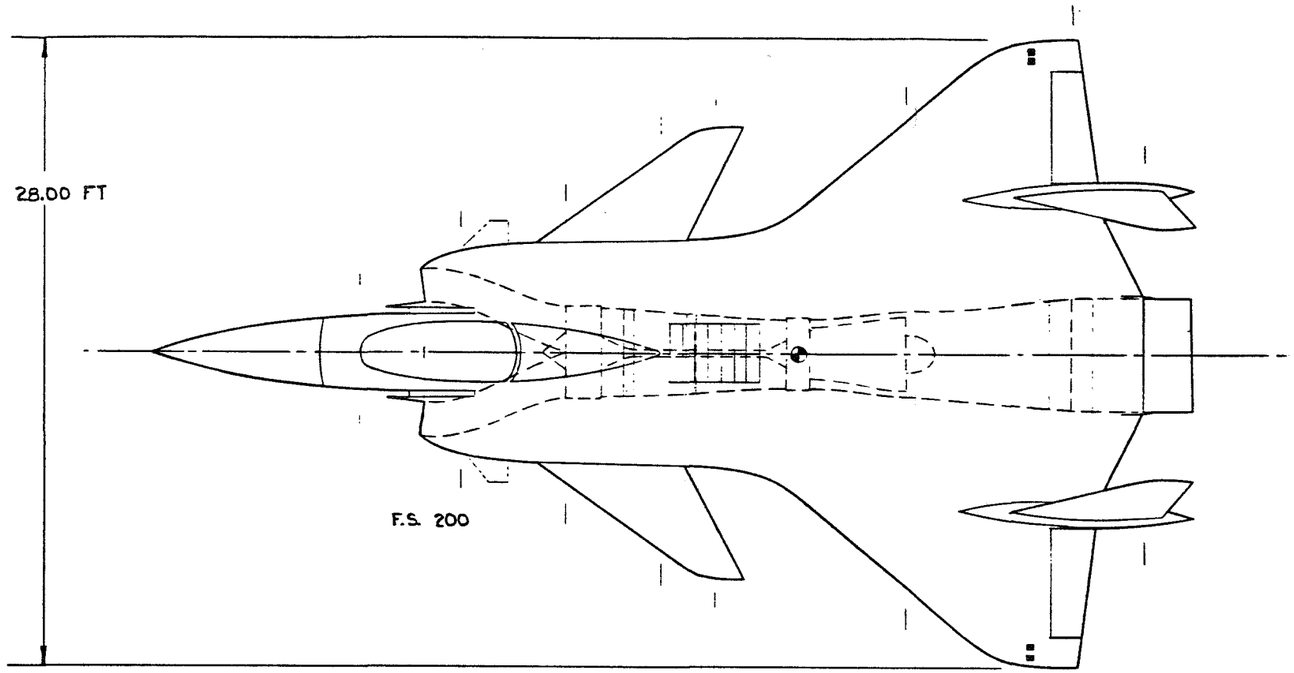

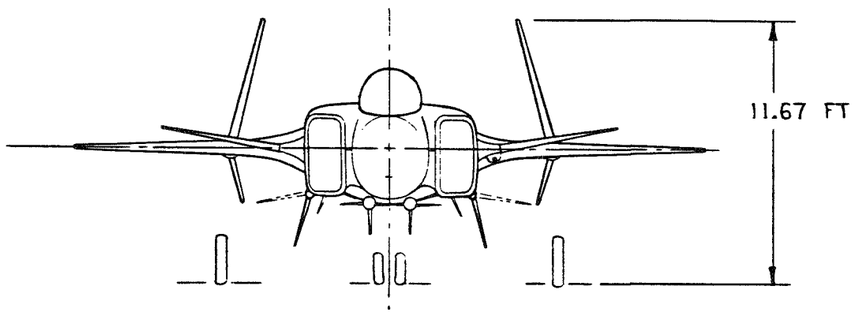

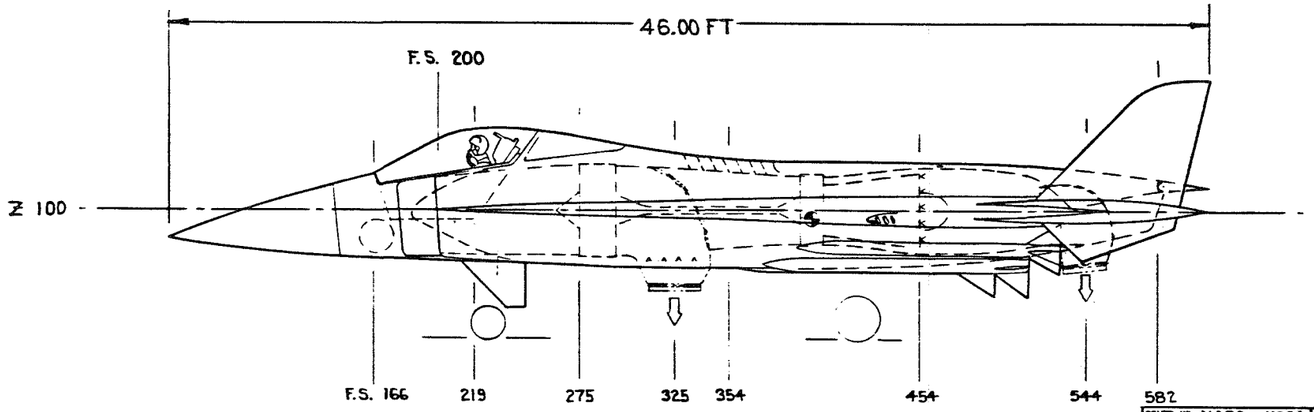

CONTR NO. NAS2 - 11003		VOUGHT CORPORATION
PREP HILLMAN	5/1/81	GENERAL ARRA
CHKD		TF120 VSTOL TANDEM
DESIGN GROUP NAME ADV. AIRCRAFT		SIZE FSCM NO. 80378 DWG NO. VTF - SCALE 1/40

FOLD-OUT #

Figure 3-1 - TF120 General Arrangemer

FOLD-OUT #2

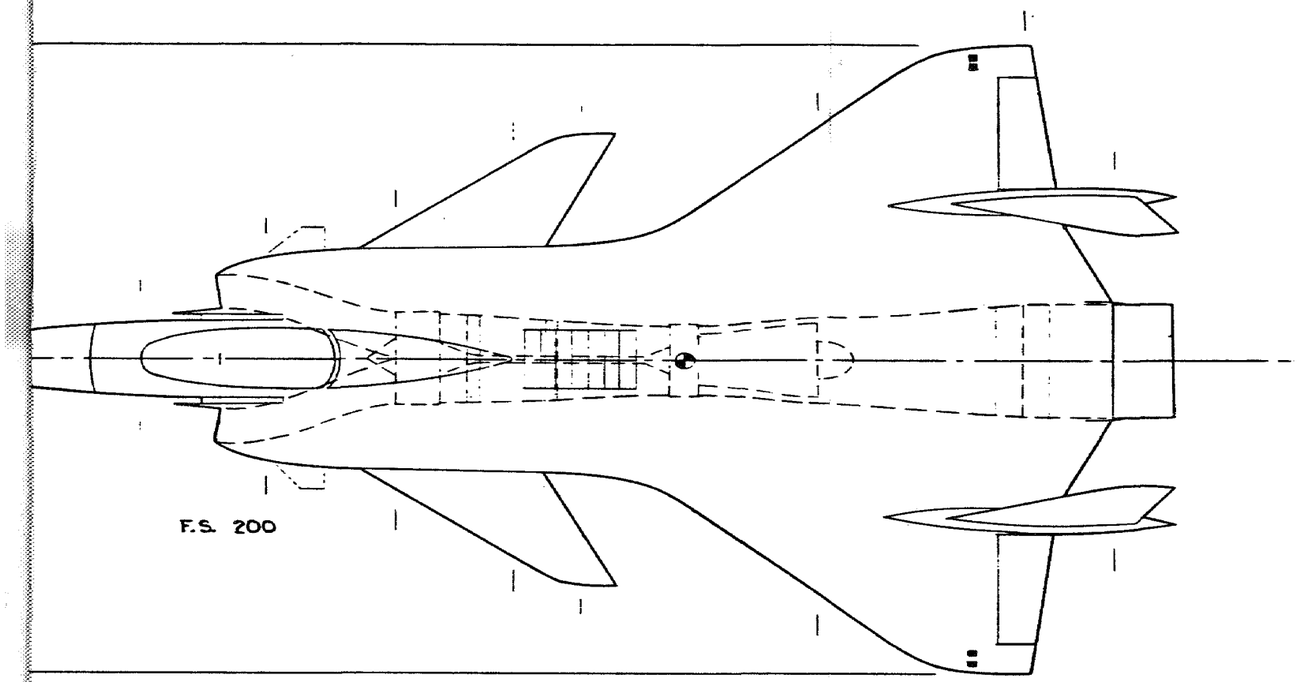

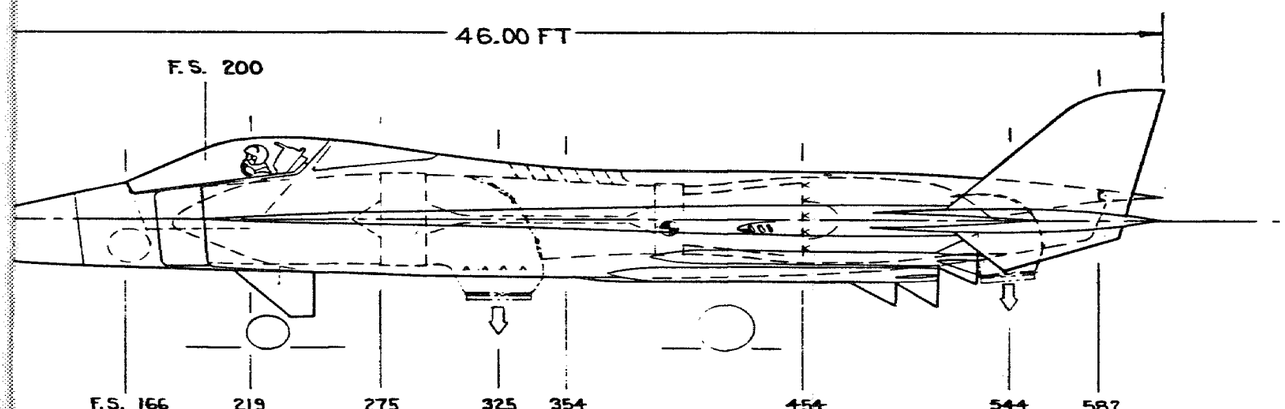

CONTR NO. NAS2 - 11003		
PREP	HILLMAN	5/1/81
CHKD		
DESIGN GROUP NAME: ADV. AIRCRAFT		

VOUGHT CORPORATION

GENERAL ARRANGEMENT
TF120 VSTOL TANDEM FAN FIGHTER

SIZE	FSCM NO.	DWG NO.	REV
	80378	VTF-00-02	
SCALE 1/40		SHEET 1 OF 1	

Figure 3-1 - TF120 General Arrangement

FOLD-OUT #2

TABLE 3-1 - TF120 WING AND TAIL GEOMETRY

	WING (TOTAL)	CANARD (EACH)	VERTICAL FIN (EACH)	AFT VENTRAL (EACH)	FWD VENTRAL (EACH)
AREA ft^2	350.0	20.8	26.2	8.5	3.6
ASPECT RATIO	2.24	1.20	1.30	0.58	1.12
TAPER RATIO	0.15	0.28	0.35	0.0	0.30
SPAN ft	28.00	5.00	5.84	2.21	2.00
ROOT CHORD ft	21.74	6.51	6.65	6.67	2.75
TIP CHORD ft	3.26	1.82	2.33	0.0	0.83
MEAN GEOMETRIC CHORD ft	14.78	4.60	4.84	5.10	1.97
LEADING EDGE SWEEP - DEG	50.0	55.0	45.0	45.0	45.0
THICKNESS RATIO, ROOT/TIP	0.06/0.05	0.04	0.04	0.03	0.04
AIRFOIL, ROOT/TIP	65A006/65A005	65A004	65A004	65A003	65A004
DIHEDRAL - DEG	0	10	-	-	-15
FIN CANT - DEG	-	-	15	-15	15
DEFINITION	Idealized - No Strake or T.E. Extension	Root Chord At Strake	From Wing Ref. Plane	From Wing Ref. Plane	Exposed Area

control. At a -45 degree setting the fins can be used as two-axis controls for gust alleviation and precision target tracking. The vertical fins and aft ventral fins are mechanically independent all-moving controls. Therefore a total of six control surfaces are available to generate side forces. The four ventrals provide control effectiveness into the post-stall regime to enhance combat agility.

Force controls available for longitudinal and lateral control are wing trailing edge flaps (elevons), canards and the forward ventral fins. A trailing edge flap at the extreme aft fuselage provides longitudinal trim and high speed thrust vectoring capability.

With the control surface group under integrated software control, it is possible to compensate for wide-ranging flight conditions, control nonlinearites and component failures to achieve a very high level of system performance. However a high quality aerodynamic data base will be required to realize this potential.

The Vought series flow tandem fan propulsion system provides V/STOL capability with minimal compromise to a high performance fighter configuration.

The propulsion system for the TF120 is the series flow tandem fan (SFTF) variable cycle engine. The system is based on a mixed flow, augmented turbofan driving a remote front fan through an extension shaft. The novelty of this arrangement is that the front fan contributes to aircraft propulsion at all times, but in two totally distinct operating modes. In high speed flight, the propulsion cycle is a conventional afterburning turbofan with all airflow passing through both fans in series. For V/STOL operations, the front fan flow is separated from the aft fan/core engine flow, greatly increasing effective bypass ratio. The way Vought accomplishes this transformation is illustrated in Figure 3-2. A unique pivoting vane assembly isolates and redirects the front fan efflux through a low temperature burner and ventral nozzle. Simultaneously, an aft auxiliary inlet opens to supply the aft fan and core engine. The mixed flow is exhaused through an aft vectoring nozzle. Maximum VTO exhaust temperature is less than that of the Harrier. A series flow transition section is undergoing testing at the NASA Lewis Research Center.

Both fans employ variable inlet guide vanes (VIGV) for height and pitch control in the V/STOL mode and for fan matching in both operating modes. The TF120 introduces vanes in both exhaust streams to provide yaw control in hover. Roll control is achieved using bleed reaction jet system.

Fixed geometry vertical ramp, external compression side inlets supply air to the forward fan through a short, bifurcated duct. Blow-in doors are used to augment low speed inlet performance.

The tandem fan propulsion system inherently provides very high fighter performance, because virtually all of the propulsion system contributes thrust throughout the "up and away" flight envelope. This provides an opportunity to combine dramatic advances in combat agility with an operationally attractive V/STOL capability in an aircraft of moderate size and weight.

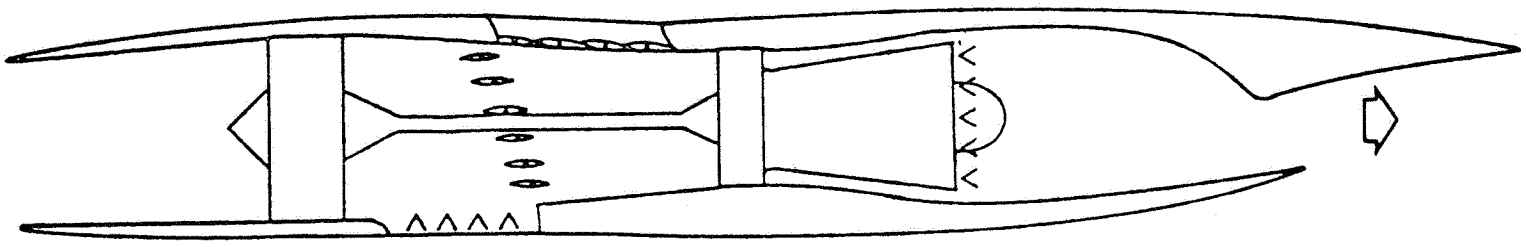

Series Flow Mode – High Speed

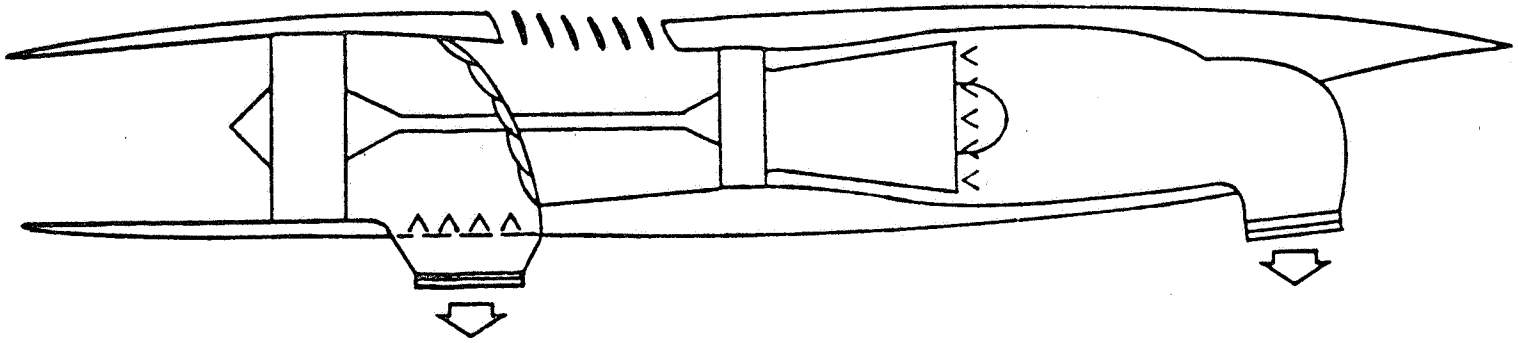

Parallel Flow Mode – V/STOL

Figure 3-2 - Tandem Fan Operating Principle

Fuel cells and fixed equipment are located on either side of the propulsion system to facilitate engine access from below and to achieve a low profile.

Figure 3-3 shows the location of TF120 fixed equipment and fuel system. The distribution of these elements was determined by several major design constraints. The two views in Figure 3-2 emphasize the dominant attributes of the configuration: minimal profile height and the broad blended planform. Since the tandem fan propulsion system would require access at several points, fuel and fixed equipment flank the powerplant, allowing engine access through doors on the aircraft centerline. Engine-driven accessories and the internal gun are accommodated in the wing-body blending on opposite sides of the core engine. Other fixed equipment, including avionics, environmental control system, and armament are located as far aft as practical in order to make center of mass and resultant thrust vector in the VTOL mode coincide.

The fuel system includes subdivided integral tanks in wings and strakes, with protected cells in the fuselage. Referring to Figure 3-2, tanks 1 and 4 are the principal longitudinal c.g. management reservoirs. Saddle tank 5, located above the core engine bypass duct, and forward of the afterburner, is not needed to meet design radius of action, but can be used to extend range.

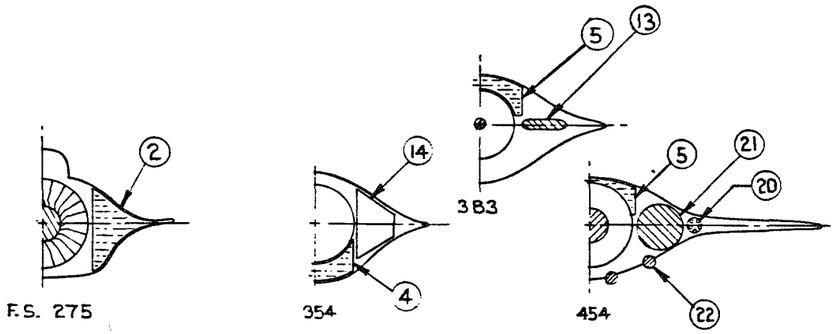

NO.	ITEM	
1	FWD FUS. FUEL	959 LB
2	LEFT STRAKE FUEL	1394
3	RIGHT STRAKE FUEL	1394
4	SUMP FUEL	350
5	SADDLE TANK FUEL	627
6	RIGHT FUS. FUEL	440
7	LEFT FUS. FUEL	915
8	RIGHT WING FUEL	2190
9	LEFT WING FUEL	1152
	TOTAL FUEL	9421 LB
10	RADAR, 27-INCH DISH	
11	FLIR DISPLAY	
12	DUAL NOSE TIRES, 18 x 4.4	
13	MAIN TIRE, 24 x 5.5, TYP. L&R	
14	AVIONICS BAY, TYP. L&R, 170 LB PER SIDE	
15	BLEED-AIR DUCT, 2.25 SQ. IN. INNER CROSS SECT., TYP. L&R	
16	ROLL CONTROL VALVE, TYP. L&R	
17	DOWNWARD EJECTOR, TYP. L&R	
18	UPWARD EJECTOR, TYP. L&R	
19	ACCESSORIES & DRIVE	
20	20-mm GATLING GUN	
21	400 ROUND AMMO DRUM	
22	ADV. MED. RANGE AIR-TO-AIR MISSILE (AMRAAM), 4 PLACES	
23	E.C.M. BAY, TYP. L&R	
24	PILOT EYE	

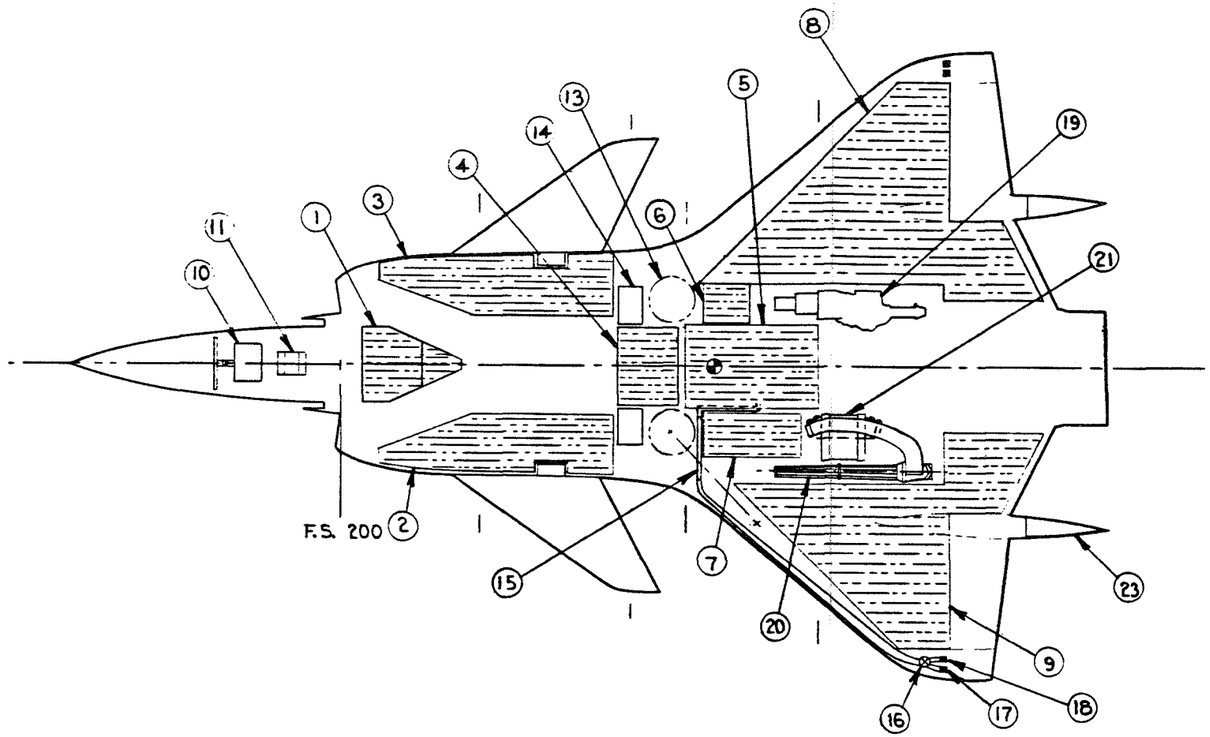

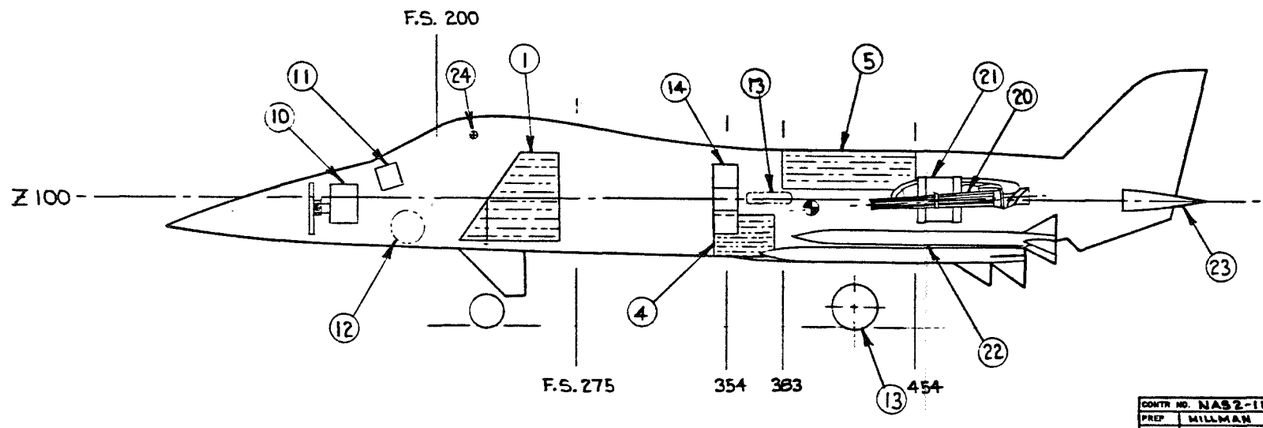

CONTR NO. NAS2-11003		
PREP	MILLMAN	9/3/81
CHKD		
DESIGN GROUP NAME	ADV. AIRCRAFT	

VOUGHT CORPORATION

INBOARD PROFILE
TF120 VSTOL TANKER

SIZE	FSCM NO.	DWG NO.
	80378	VT

SCALE 1/40

FOLD-OUT #1

Figure 3-2 - TF120 Internal Arrange

FOLD-OUT #2

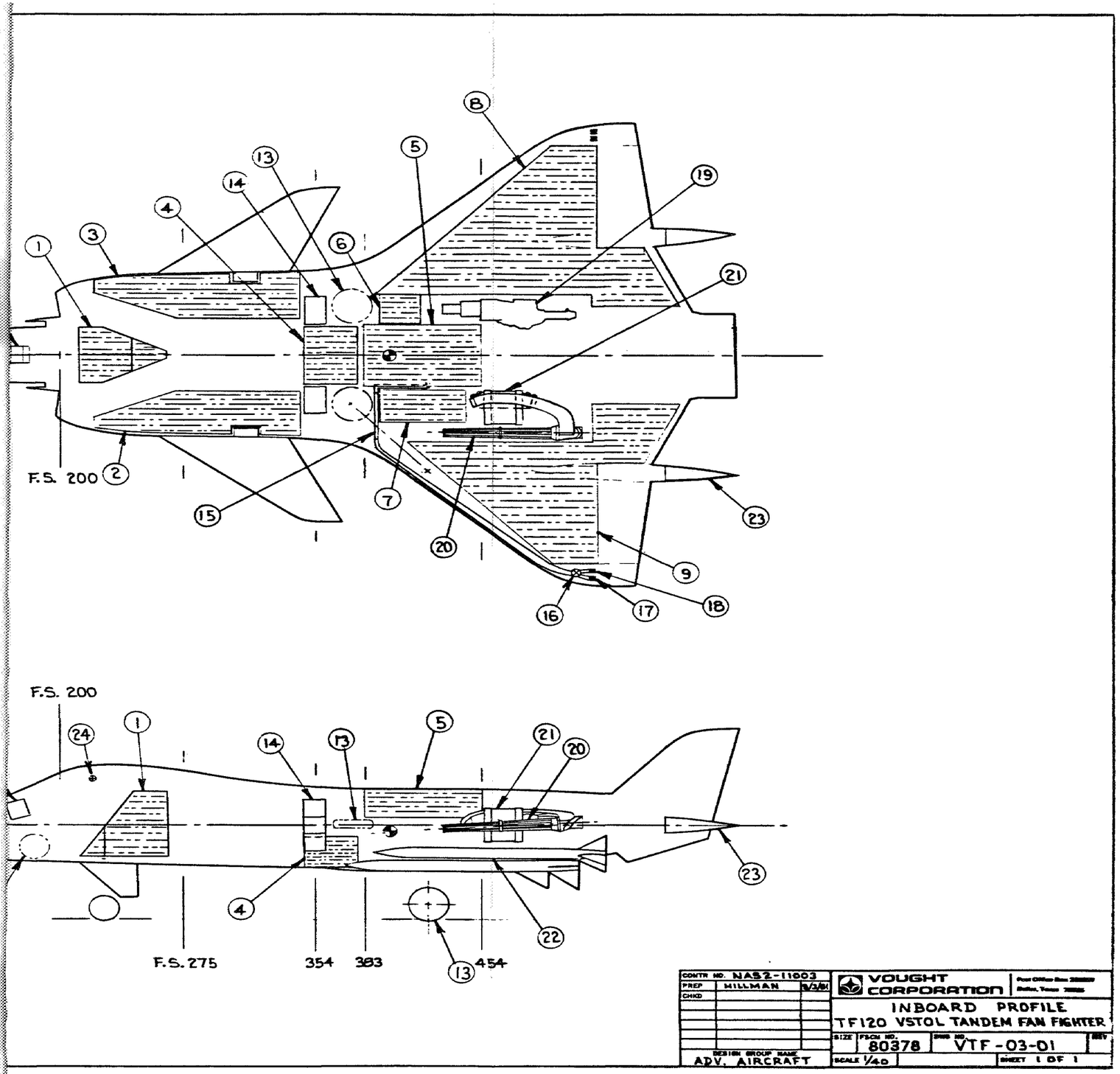

Figure 3-2 - TF120 Internal Arrangement

FOLD-OUT #2

The TF120 design incorporates advanced materials and subsystems technology. A weight breakdown and inertias are presented.

The component weights for the TF120 were derived by semianalytical analyses, statistical equations or Vendor quoted values. The effects of technological improvements anticipated by 1990 are discussed in the following paragraphs.

Composite material usage on the TF120 is projected to save approximately 20 percent of the structural weight. Composite material application is separated into three major levels depending on the state-of-art and the status of supporting R&D efforts.

Level I Components are fabricated composite materials where production capability and payoff has been proven. No new R&D programs are necessary. Level I components could be incorporated into a prototype today.

Level II Components are fabricated composite materials where proof of concept has not been thoroughly demonstrated; however, necessary R&D efforts are either currently being funded or funding is planned. Level II components will be available for design in the 1985 time period. Some Level II components could be available for a near-term prototype.

Level III Components are fabricated of advanced composite materials for which little or no design experience exists and for which R&D funding is just now being appropriated. Most Level III components will be available for design in the early 1990's.

Figure 3-3 shows the weight payoff for the three application levels and identifies the components considered for each level. The 20 percent structural weight saving assessed for the TF120 is between Levels II and III, reflecting composite fuselage bulkheads but conventional landing gear materials.

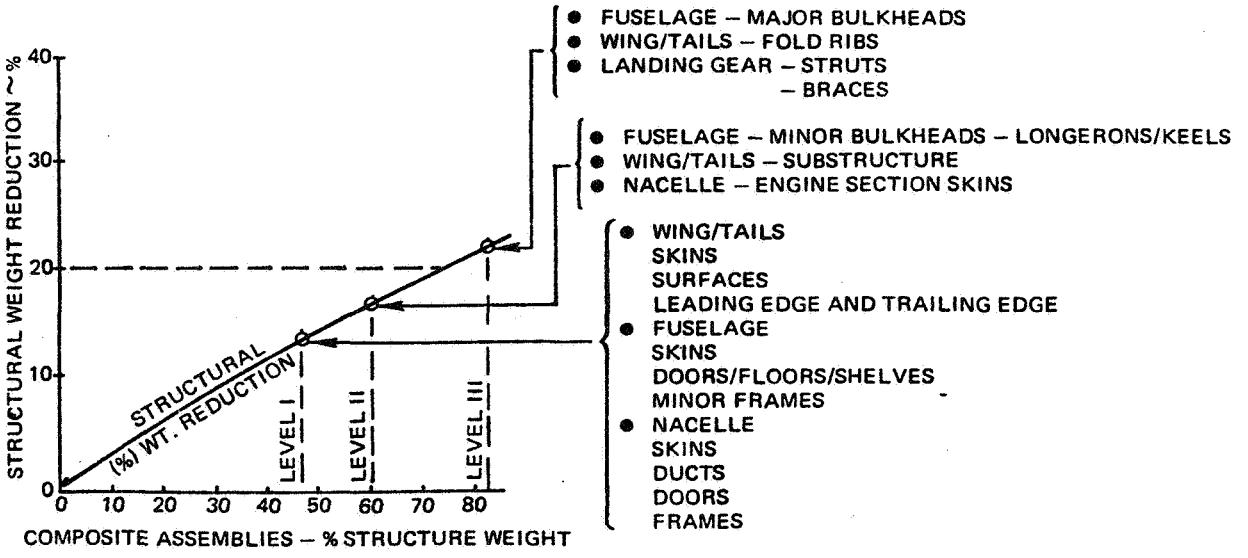

Figure 3-4 - Weight Payoff for Composite Materials

The TF120 avionics suite is the same as defined for the SF-122 V/STOL strike fighter. The details of the suite and the technology projection method used to derive it are provided in Reference 4.

Propulsion system weights are discussed in Section 5.3.1.

All the considerations just discussed were represented in the aircraft design weight module as calculated quantities or input factors. Table 3-2 is the TF120 point design weight statement, including payload for the Supersonic Intercept design mission.

Inertias were calculated using the internal component distribution illustrated in Figure 3-2. Table 3-3 summarizes complete configuration weight, center of mass location and inertias for the TF120 point design.

SHORT GROUP WEIGHT STATEMENT **NAVAIR FORM 13060/3** (Rev. 9-78) DATE

	MODEL	TF120				
1.	TOTAL STRUCTURE	5,384				
2.	WING		1,381			
3.	ROTOR					
4.	TAIL		562			
5.	BODY		2,305			
6.	ALIGHTING GEAR		970			
7.	ENGINE SECTION		57			
8.	AIR INDUCTION		109			
9.						
10.						
11.	TOTAL PROPULSION	5,629				
12.	ENGINE INSTALLATION		4,747			
13.	ACCESS GR. BOXES/DRIVE		100			
14.	EXHAUST SYSTEM					
15.	WATER INJECTION					
16.	ENGINE CONTROLS		19			
17.	STARTING SYSTEM		30			
18.	PROPELLER INSTALLATION					
19.	LUBRICATION SYSTEM		30			
20.	FUEL SYSTEM		703			
21.	DRIVE SYSTEM					
22.						
23.						
24.	TOTAL EQUIPMENT	3,240				
25.	FLIGHT CONTROLS		565			
26.	AUXILIARY POWER PLANT					
27.	INSTRUMENTS		137			
28.	HYDRAULIC & PNEUMATICS		326			
29.	ELECTRICAL		409			
30.	AVIONICS		976			
31.	ARMAMENT		332			
32.	FURNISHINGS & EQUIPMENT		215			
33.	AIR CONDITIONING		280			
34.	ANTI-ICING					
35.	LOAD AND HANDLING					
36.						
37.						
38.	TOTAL WEIGHT EMPTY	14,253				
39.	CREW		200			
40.						
41.	OIL		60			
42.	FUEL-UNUSABLE		85			
43.	FUEL-INTERNAL		8,480			
44.						
45.	Internal Gun, Less Drum		250			
46.	400 Rds Ammunition		224			
47.	Missile Suspension		200			
48.	4 Conceptual AMRAAM		1,188			
49.						
50.						
51.						
52.						
53.						
54.						
55.	USEFUL LOAD	10,687				
56.	GROSS WEIGHT	24,940				

REPLACES NAVAIR FORM 13060/3 (4-72) WHICH IS OBSOLETE.

TABLE 3-3 - TF120 MASS PROPERTIES

LOADING			DESIGN MISSION VTO WEIGHT	NO STORES, NO FUEL
GROSS WEIGHT	-	LB	24,940	14,253
CENTER OF MASS	-	PERCENT MGC	7.8	9.6
ROLL INERTIA I_{xx}	-	SLUG-FT^2	12,789	5,882
PITCH INERTIA I_{yy}	-	SLUG-FT^2	64,469	42,902
YAW INERTIA I_{zz}	-	SLUG-FT^2	74,622	46,738
PRODUCT OF INERTIA I_{xz}	-	SLUG-FT^2	-5.4	270

4.0 AERODYNAMIC CHARACTERISTICS

This section describes the procedures used to estimate TF120 aerodynamic characteristics, the results and assessment of flying qualities.

This section contains:

4.1 DRAG

4.1.1 Minimum Drag

> TF120 minimum drag characteristics were estimated using correlation methods and far-field wave drag estimates.

The zero lift drag buildup of the TF120 was determined by using the best available theoretical, empirical, and experimental methods and data. Friction drag was estimated by determining the effective skin friction coefficients for each surface over a range of Mach numbers. Multiplying the skin friction coefficient by its appropriate wetted area results in the skin friction D/q, which in turn is converted into a drag coefficient. These calcualtions were carried out in the Vought Aircraft Synthesis Analysis Program (ASAP) (Reference 5).

The ASAP program was also used to determine the form and interference factors. These ASAP methods are based on those of the USAF Datcom (Reference 6).

No aerodynamic allowance was provided for base drag corrections since these effects are accounted for in the propulsion data. Protuberance, cooling, and ventilation drags were assumed to be the same as for the SF-121. Roughness, waviness, and leakage drag were scaled from SF-121 values by the ratio of wetted areas. Boundary layer diverter drag was estimated by scaling the SF-121 values by the ratio of the engine capture areas and the local boundary layer thickness. Table I in Appendix II summarizes the miscellaneous drag values over the Mach number range.

In the transonic and supersonic speed ranges, the wave drag was estimated by using the area rule program imbedded in the (Aerodynamic Preliminary Analysis System (APAS), Reference 7). For these wave drag calculations the mathematical model of the TF120 included the strakes as part of the body. The skin friction, form and interference, wave, and miscellaneous drags were summed to determine the total maximum drag values. This minimum drag value is plotted versus Mach number in Figure 4-1, and tabulated in Table II of Appendix II. Also in Appendix II is the TF120 normal (M=1) area distribution.

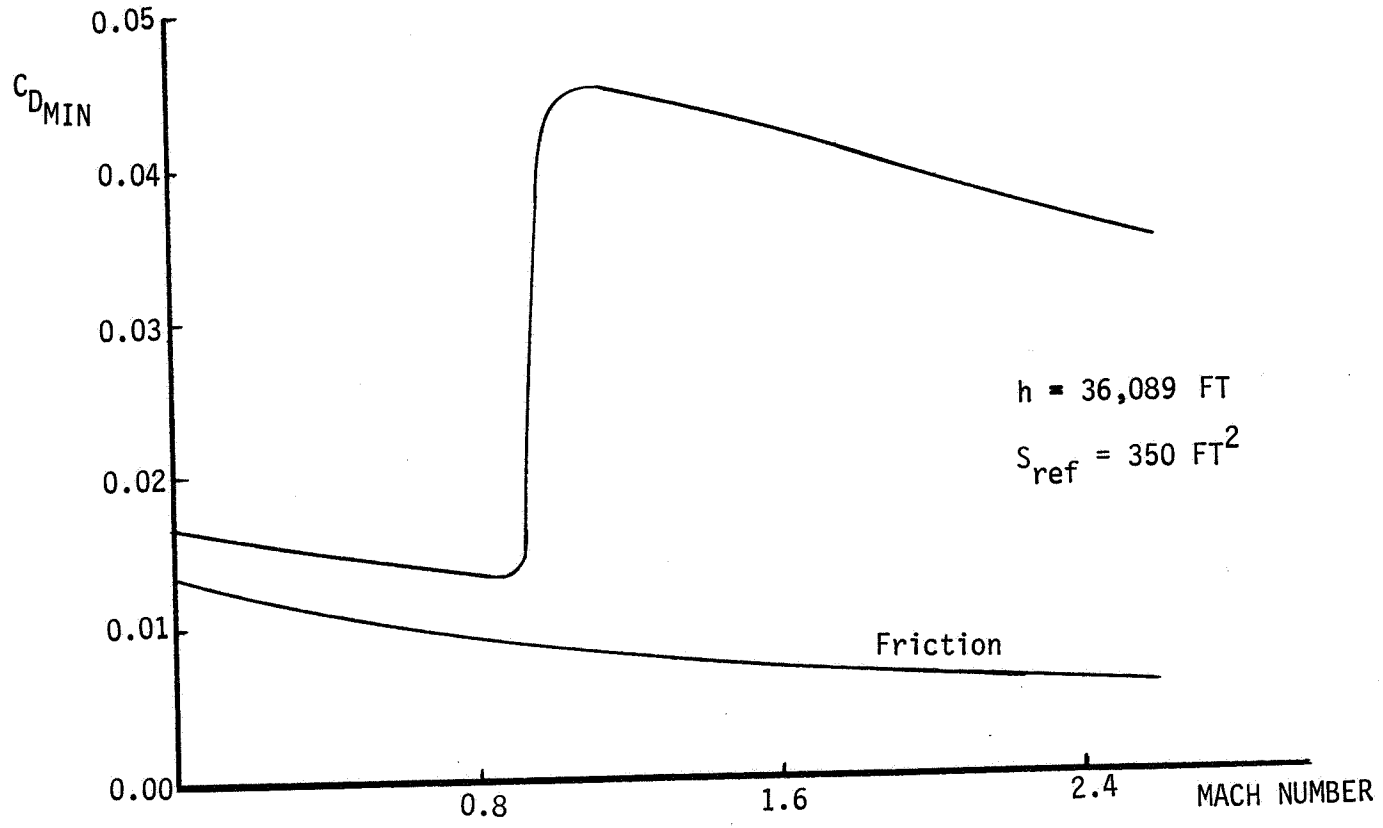

Figure 4-1 - TF120 V/STOL Fighter Minimum Drag as a Function of Mach Number

4.1.2 Drag Due to Lift

> Empirical methods and wind tunnel tests of a similar configuration was the basis for TF120 drag due to lift estimates.

Drag due to lift is difficult to predict accurately without a foundation of empirical data for the specific configuration. Figure 4-2 shows the variation of e, the Oswald span efficiency factor, as a function of Mach number as predicted by several methods:

- The Linden-O'Brimski/VAC/DATCOM method, which is a correlation of existing data on actual aircraft.
- APAS solutions, which are based on Trefftz plane results from a Vortex Lattice analysis for subsonic speeds and linear theory for supersonic speeds.
- The SF-121 VATOL fighter estimates (Reference 1), which are based on adjusted of experimental and correlated data.
- A General Dynamics correlation method (Reference 8), which determines e as a function of the percent leading edge suction,which is a correlated function of sweep, Mach number, Reynolds number, and leading edge radius.

Based on the above data, and past studies, the variation of e with Mach number for the TF120 was chosen to follow the Linden-O'Brimski solution up to approximately M = 1.2, and to follow the SF-121 experimentally based predictions up through M = 2.4. The resultant variation of e with lift coefficient is shown in Figure 4-3.

Using the $C_{D_{min}}$ data from Figure 4-1 and the e data from Figure 4-3, drag polars for several Mach numbers were calculated and presented in Figure 4-4. The corresponding lift-to-drag ratios, are presented in Figure 4-5.

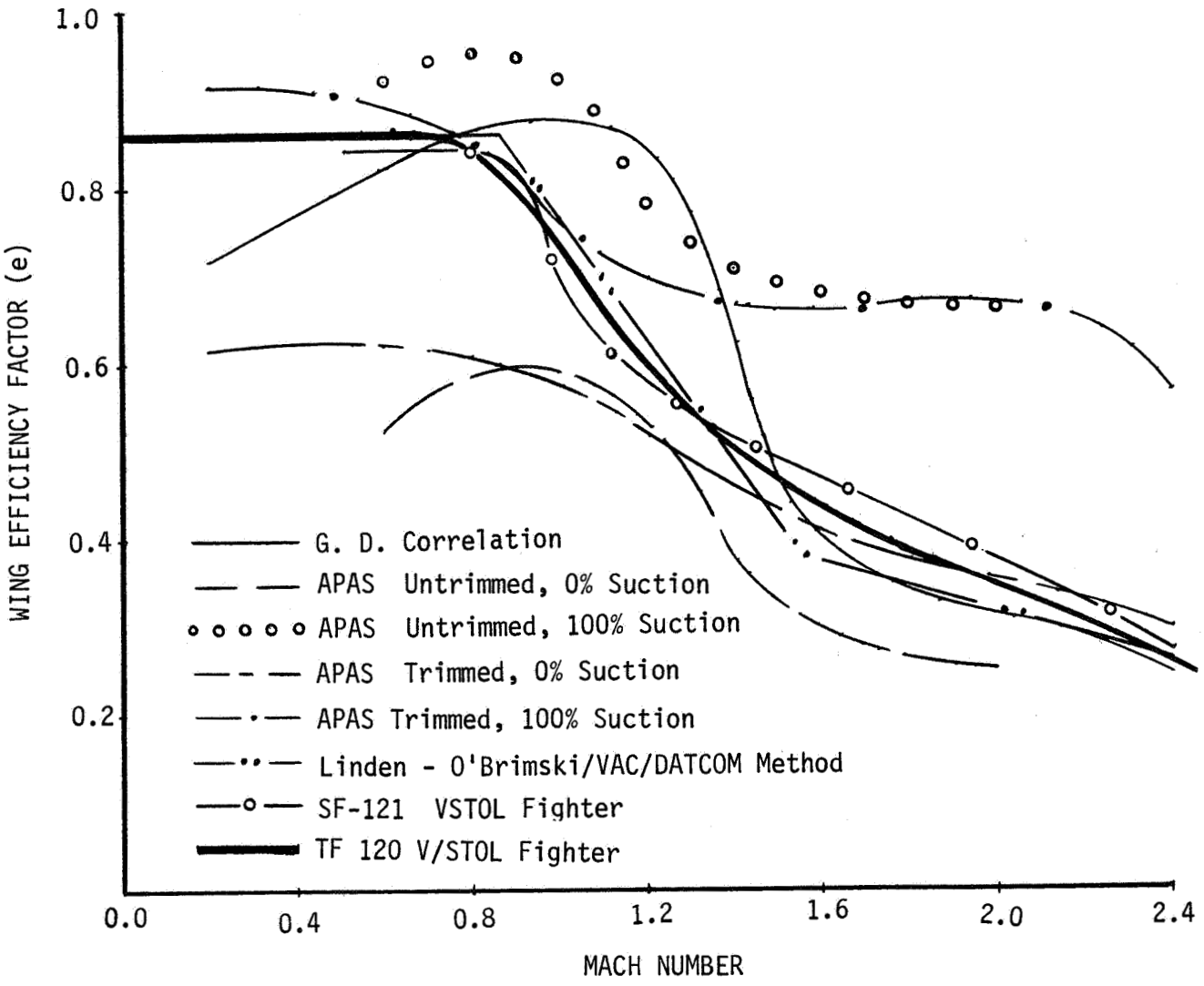

Figure 4-2 - TF120 Wing Efficiency as a Function of Mach Number

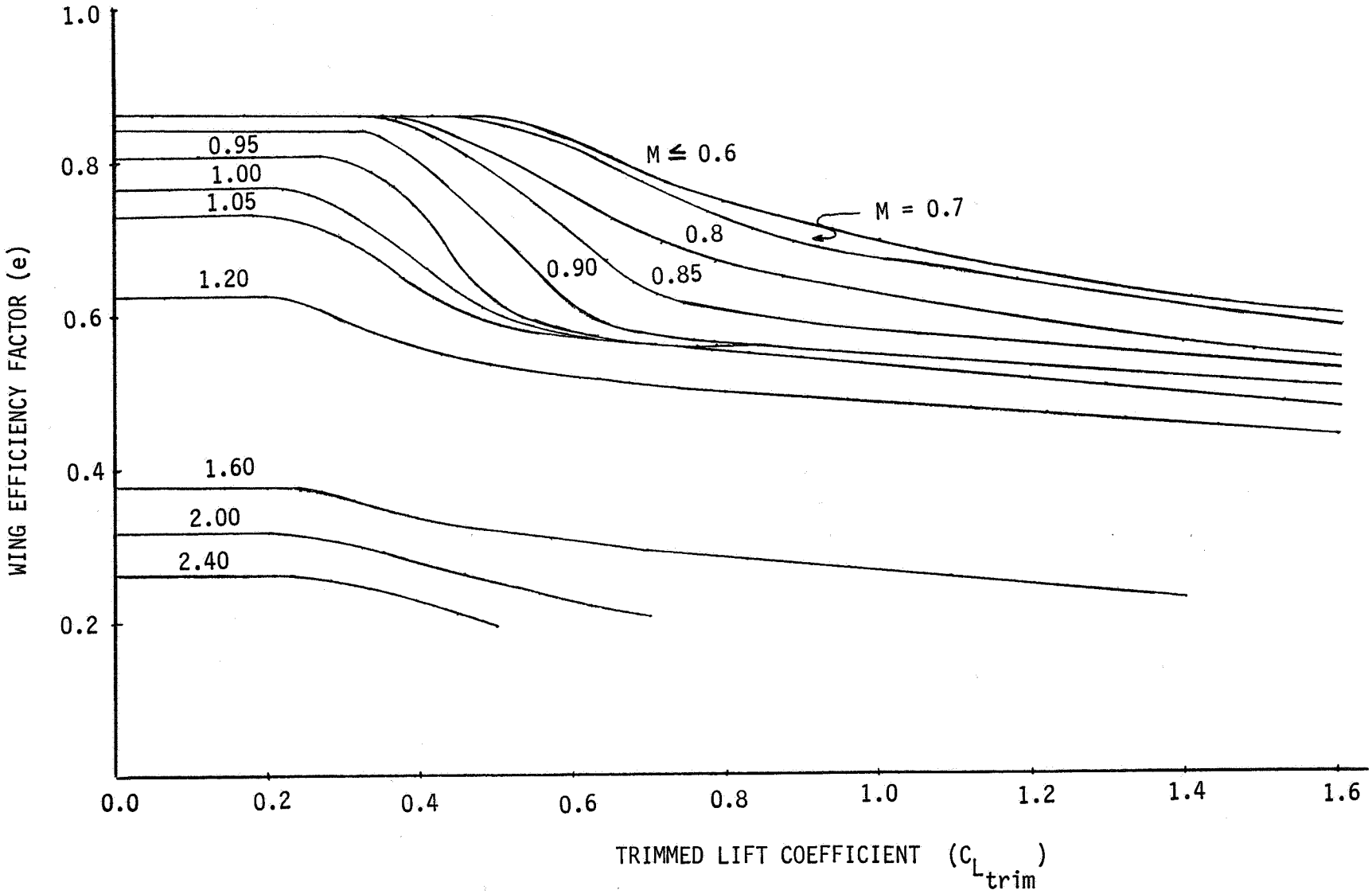

Figure 4-3 - TF120 Wing Efficiency as a Function of Lift Coefficient for Various Mach Numbers

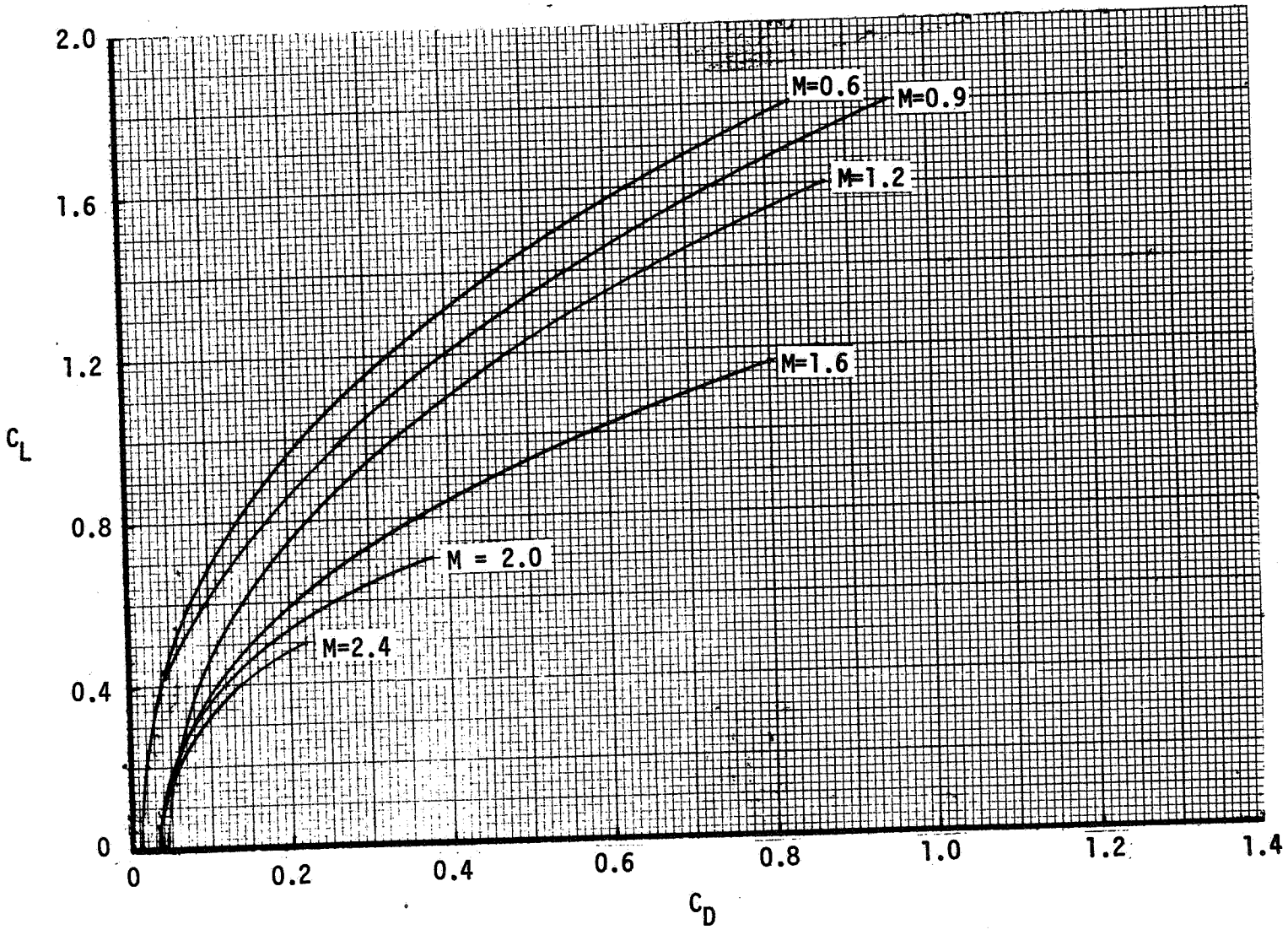

Figure 4-4 – TF120 Trimmed Drag Polars for Selected Mach Numbers

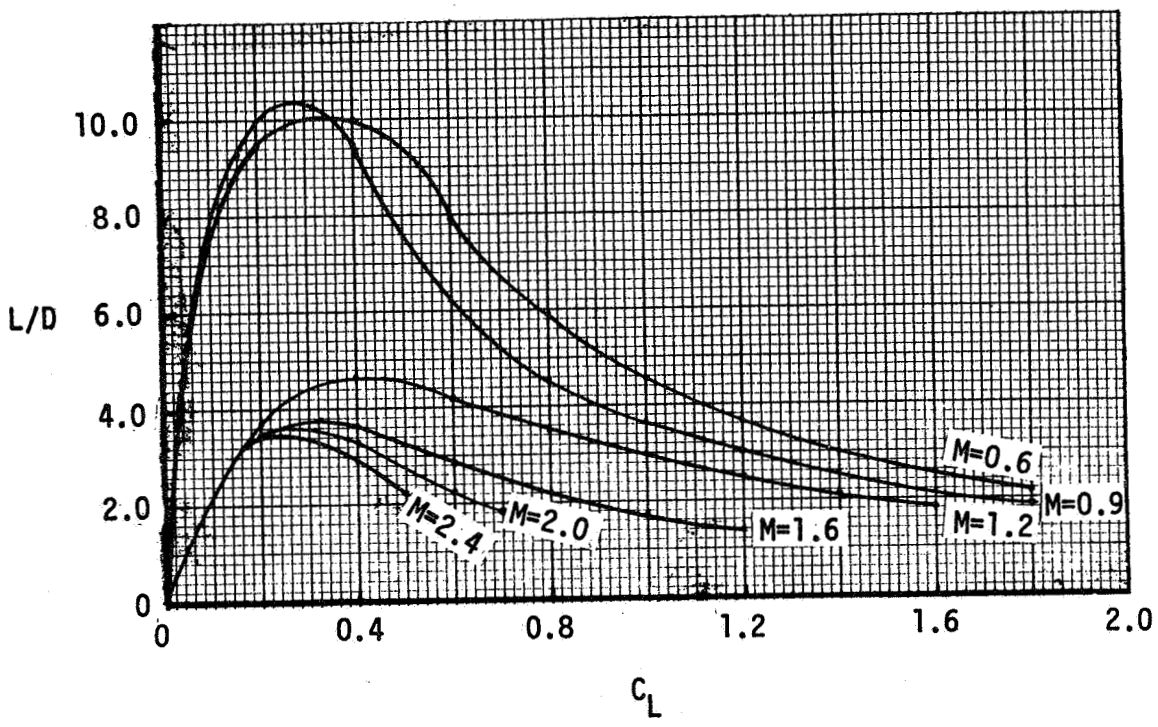

Figure 4-5 - Variation of TF120 Trimmed L/D Ratio With Lift Coefficient for Various Mach Numbers

4.1.3 Installed Store Drag

> Store drag estimates made for a similar fighter configuration were applied to the TF120.

Store drag for the TF120 was adapted from estimates in Reference 4. Four conceptual Advanced Medium Range Air-to-Air Missiles (AMRAAM) missiles are carried on the Supersonic Intercept design mission and on the Fighter Escort mission. The missiles are conformally installed on the TF120 lower fuselage. Two are semisubmerged and would normally be carried. The other two are tangent mounted to facilitate carrying alternative conformal stores. Figure 4-6 shows incremental drag for both installations, as well as for two Short Range Air-to-Air missiles (SRAAM) similar to the AGILE missile. SRAAMs are mounted on outboard wing pylons to avoid interference with the wingtip roll jets.

The LGB1100 conceptual laser guided bomb drag in Figure 4-7 was constructed by adjusting installed drag for tangent mounted MK83LD bombs for the higher drag of the LGB control unit and aft fins. The MK83LD drag was determined from Vought wind tunnel tests.

Unpublished Vought wind tunnel data was available for the 370 gallon external fuel tank shape. Figure 4-8 was used without adjustment.

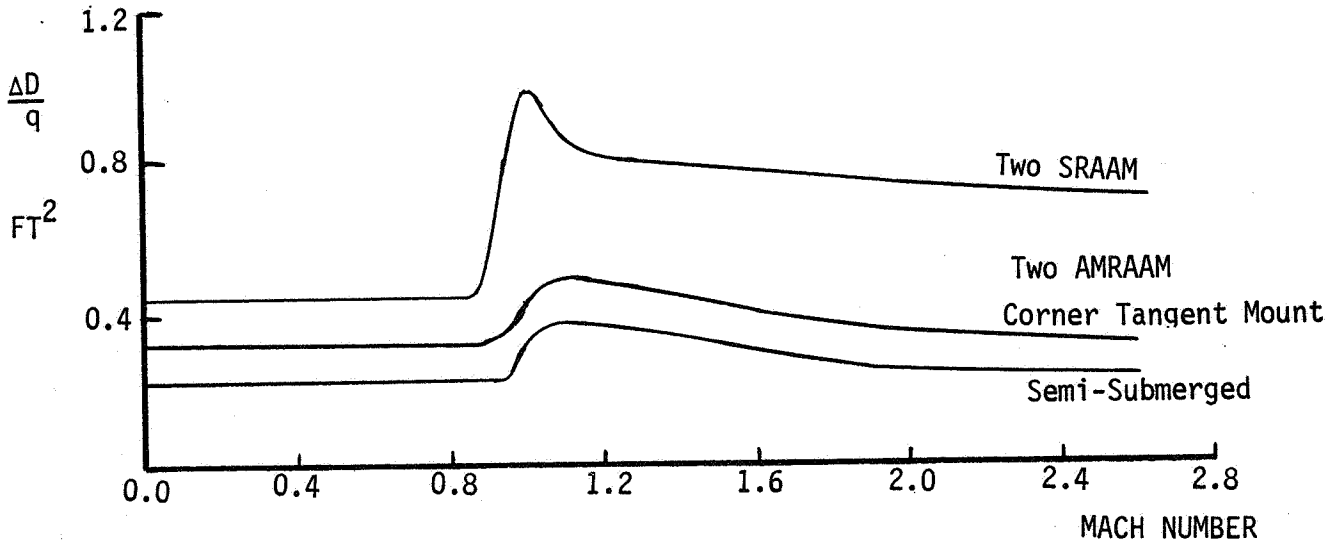

Figure 4-6 - Installed Drag of Air-to-Air Missiles

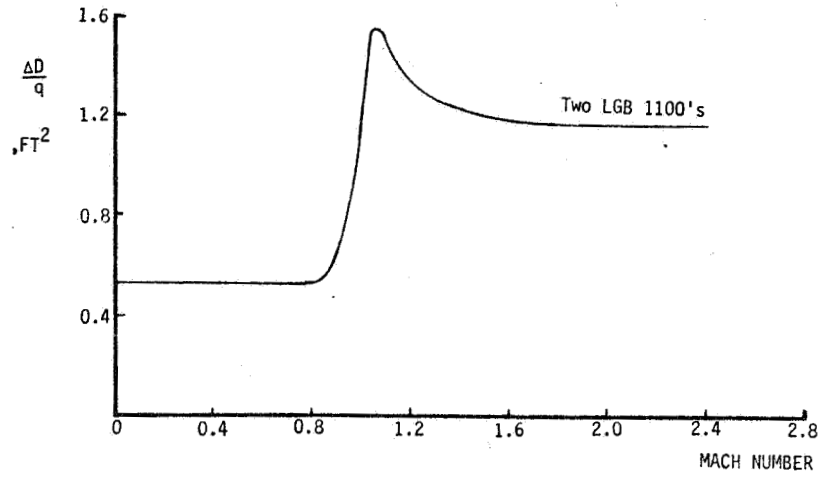

Figure 4-7 - Installed Drag of LGB1100 Conceptual Laser-Guided Bombs

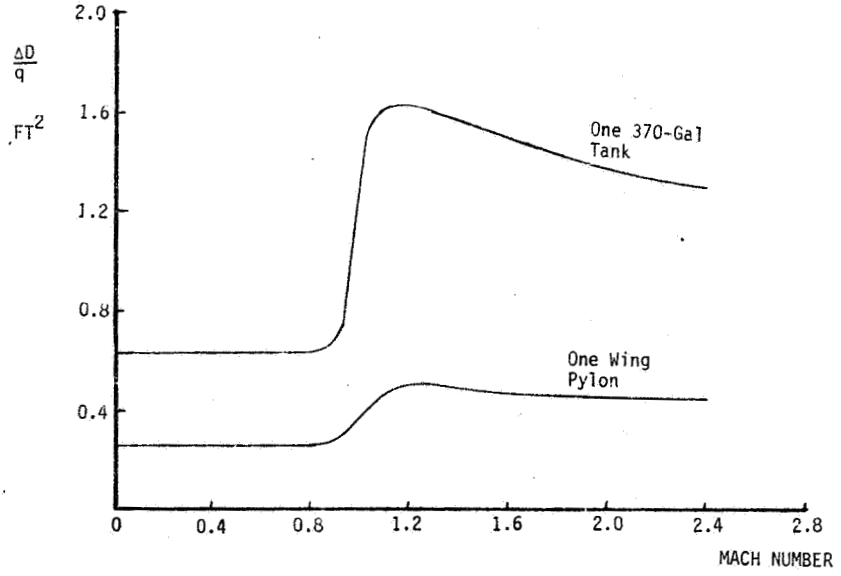

Figure 4-8 - Installed Drag of 370 Gallon External Tank and Wing Pylon

4.2 LIFT

4.2.1 Untrimmed Lift

> The untrimmed lifting characteristics of the TF120 were estimated using theoretical and experimental data.

The variation of lift coefficient with angle of attack in the linear aerodynamics region was based on data provided by APAS. Values of $C_{L_{\alpha=0}}$ and $dC_L/d\alpha$ were determined over the Mach number range from 0.2 to 2.4. The wings of the TF120 are uncambered, and therefore the changes in $C_{L_{\alpha=0}}$ represent the influence of the fuselage on the configuration aerodynamics.

Figure 4-9 presents $C_{L_{\alpha=0}}$ and $C_{m_{\alpha=0}}$ vs Mach number for the TF120 configuration. Note that the $C_{L_{\alpha=0}}$ plot uses a rather large vertical scale. This large scale overemphasizes the changes in $C_{L_{\alpha=0}}$ with Mach number. In actuality, these values are very small, and the change with Mach number is of little consequence.

The lift curve slope variation with Mach number follows the expected trends. At subsonic speeds C_{L_α} increases with increasing Mach number; at supersonic speeds, C_{L_α} decreases with increasing Mach number.

The values of C_{m_o} vary little with Mach number outside of the transonic region. At subsonic speeds C_{m_o} has a moderately negative value, which is decreased (in the absolute sense) by about half at supersonic speeds. The body provides the major portion of the C_{m_o}. At subsonic speeds, the moments induced by the fuselage are very small, but at supersonic speeds these induced effects result in a large positive increment in C_{m_o}.

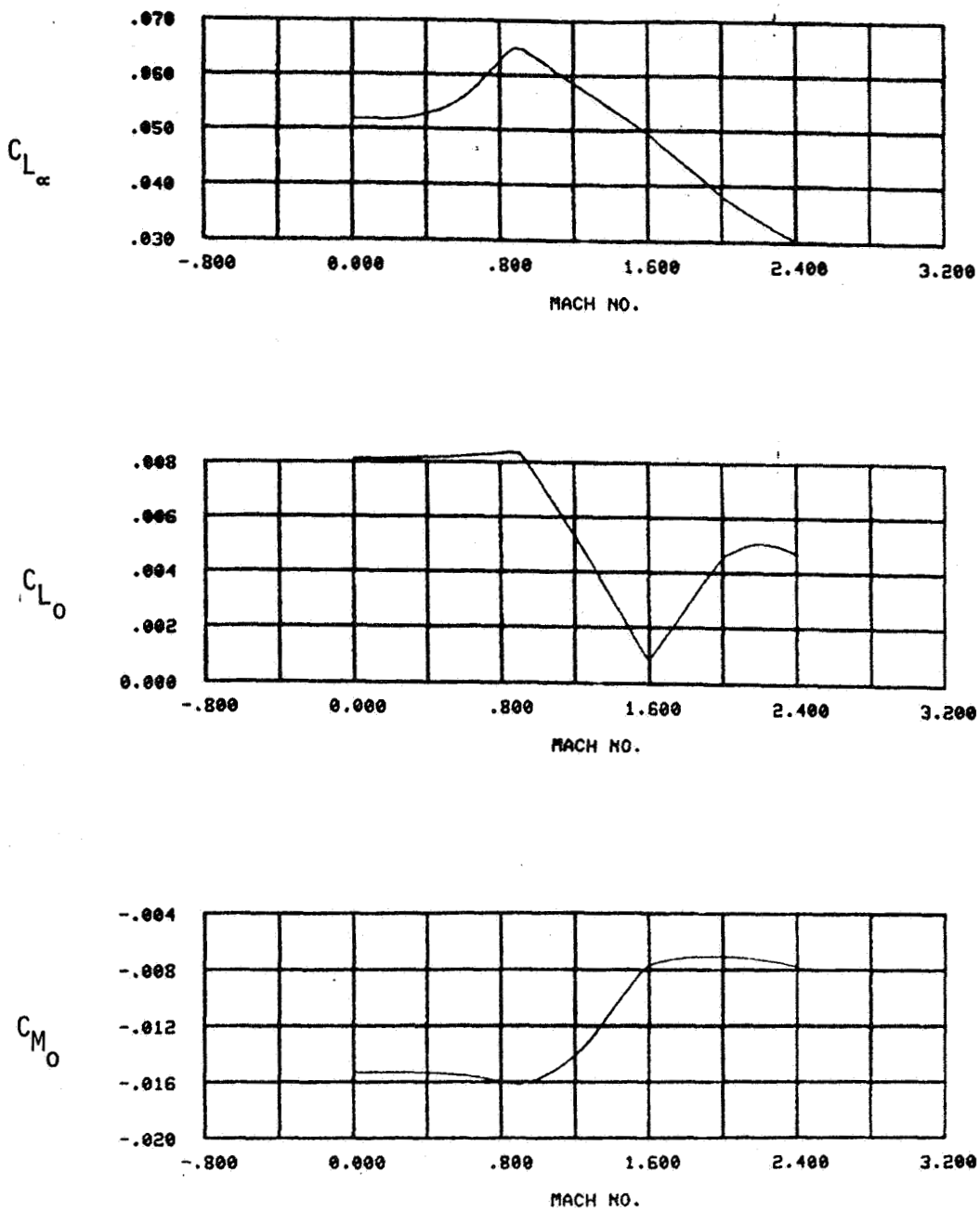

Figure 4-9 - TF120 Lift Curve Slope, Zero Angle of Attack Lift and Moment Coefficients as a Function of Mach Number

For the nonlinear aerodynamics estimates, the results of the previous study were utilized as guides. The linear aerodynamics results were faired smoothly into the $C_{L_{max}}$ and/or α_{max} values. The resulting data are presented in Figure 4-10.

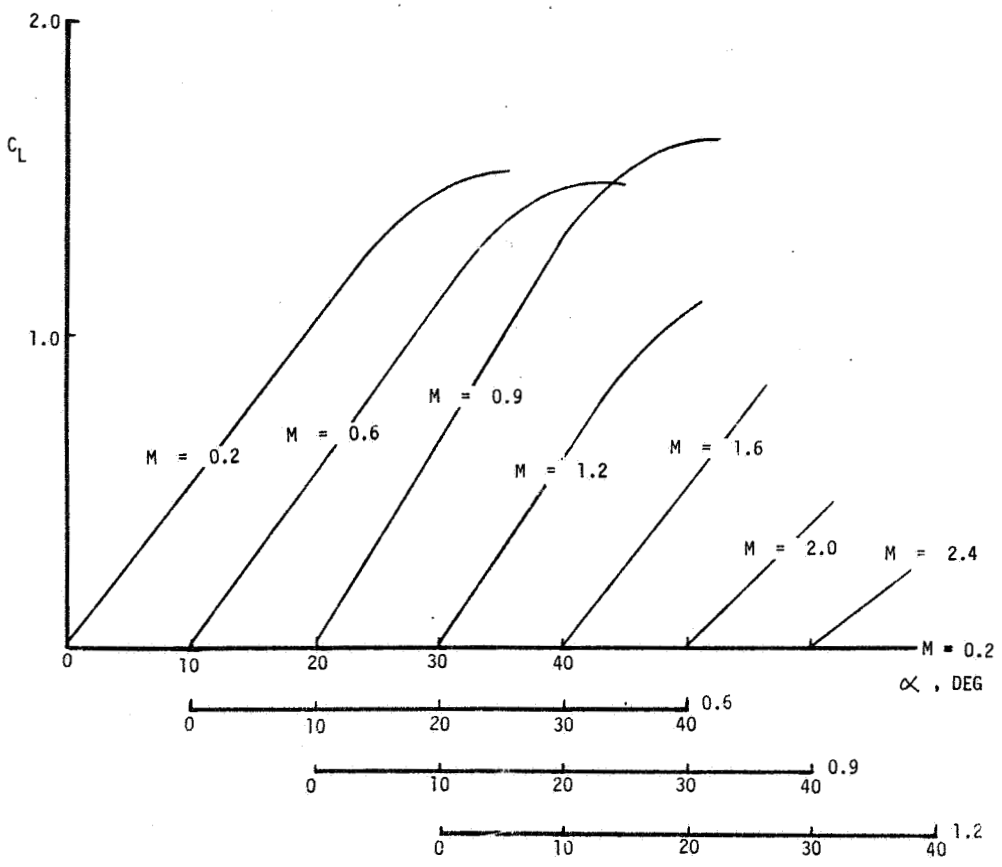

Figure 4-10 - Untrimmed Lift Coefficient as a Function of Angle of Attack for Several Mach Numbers

4.2.2 Aerodynamic Center

> A combination of slender body theory and lifting surface theory was used to estimate aerodynamic center location.

The APAS code was used to determine the lift and pitching moments of the TF120 aircraft in the linear aerodynamics range. The TF120 configuration was more difficult to model than most due to the integrated strakes upon which the main wing panels and the canards are mounted. The initial math model of the TF120 included the integrated strakes as part of the fuselage. When run on APAS we found that the predicted aerodynamic center was considerably further aft than the location predicted by the NASA-Langley Vortex Lattice program (Reference 9), which has proven a useful preliminary design tool. The APAS program implements a Vortex Lattice method for subsonic wing-like surfaces, and a slender body method for fuselage shapes. When the strakes were accurately modeled as a portion of the fuselage, the slender body contribution was unrealistically large.

A revised math model was prepared in which the strakes were defined as elongated wing roots. The fuselage contribution was then much smaller. The resulting aerodynamic center locations were found to be in reasonable agreement with the results of Vortex Lattice calculations. Figure 4-11 shows the aerodynamic center location as a function of Mach number as predicted by APAS, Vortex Lattice, and Digital DATCOM (Reference 10). The a.c. determined by the APAS program is somewhat further aft than that given by the Vortex Lattice method. This is a result of the use of slender body theory in APAS as opposed to the flat lifting plate approach used in the Vortex Lattice approach. The Digital Datcom results are somewhat further aft than the APAS data, and do not appear to have a realistic trend with Mach number. Due to the operational difficulties experienced when using Digital Datcom, these data are somewhat suspect. On balance, it appears that the revised APAS data represents the most accurate variation of aerodynamic center with Mach number and was used throughout the remainder of the study.

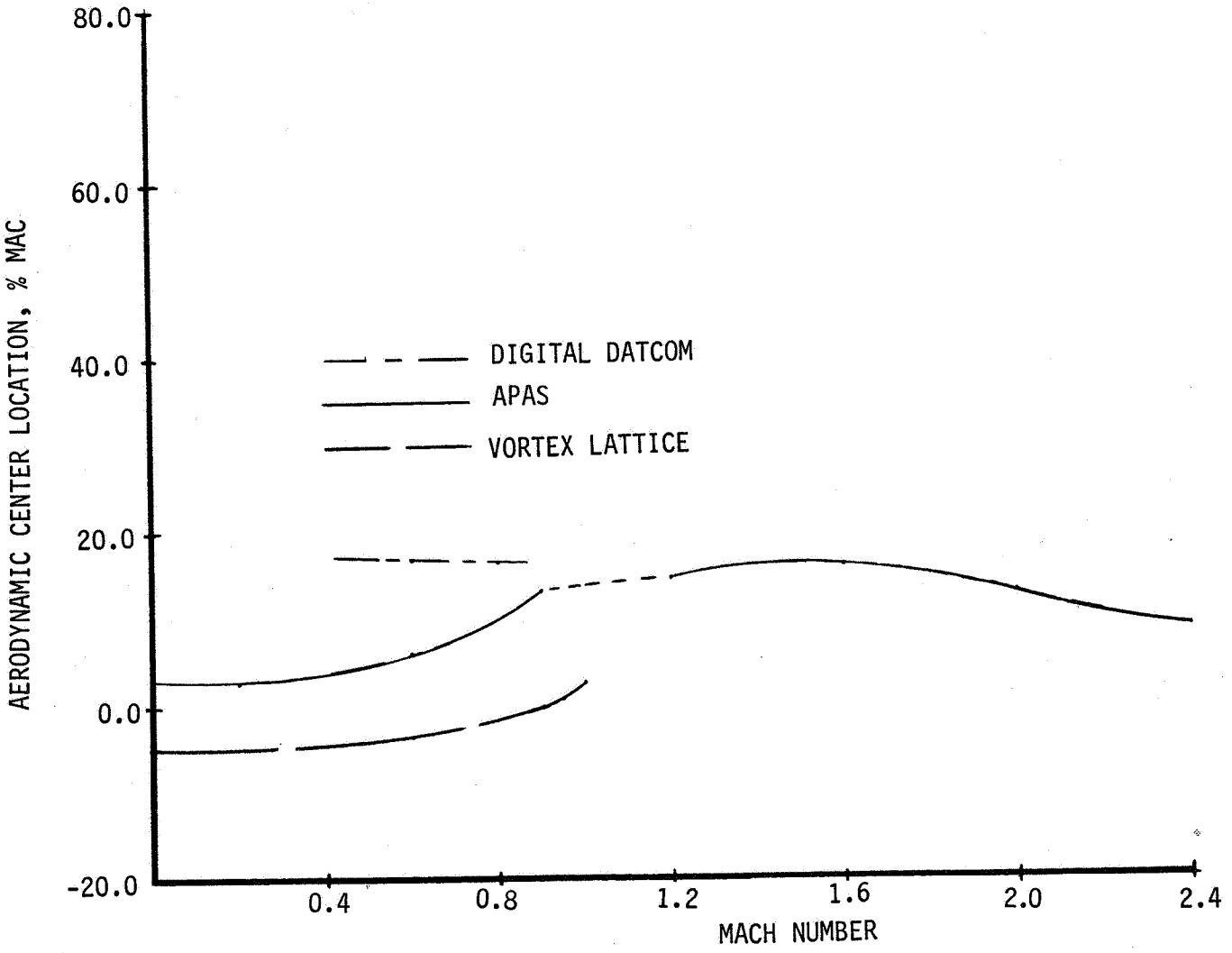

Figure 4-11 - Variation of the Aerodynamic Center With Mach Number

4.2.3 Trimmed Lift

Lift and pitching moment estimates, control effectiveness predictions and center of mass location was combined to get trimmed lift.

Using the APAS aerodynamic data and the a.c. and c.g. locations, the elevon and canard deflections required to trim the aircraft were determined.

Figure 4-12 shows C_L as a function of C_m for three elevon deflections: 0 and $\pm$ 10 degrees. The basic plot is made for the most aft c.g. location. The influence of moving the center of gravity to the forward limit is also shown. From this figure it is apparent that sufficient control power exists for this flight condition since reasonably large C_L values can be reached for $C_m = 0$ with moderate control deflections.

Figure 4-13 shows the same type plot for deflections of the canards. Comparisons of the two plots reveals that, as is to be expected, the trimming ability of the canards is about twice that of the elevons.

Figure 4-14 shows the control deflections required for trim the aircraft using canards alone and elevons alone. Note that since the basic airframe has been designed to have a negative static margin the trends in the three charts discussed above are opposite to those expected for stable aircraft.

Using these results, the impact of trim in the lift curves was determined. Figure 4-15 shows the variation in $C_{L_{\alpha=0}}$ and $dC_L/d\alpha$ with Mach number for the untrimmed case, and the two trimmed cases; one for trimming with the canard, the other for trimming with the elevons. The changes in C_{L_α} are due to the C_L values generated by the fuselage. Note that the changes in lift curve slope are opposite to those for a normal vehicle because of the negative static margin. Here, the lift curve slope is increased at subsonic speeds when trimming by elevon, and decreased when trimming by canard. The change due to trim changes sign at transonic and supersonic speeds.

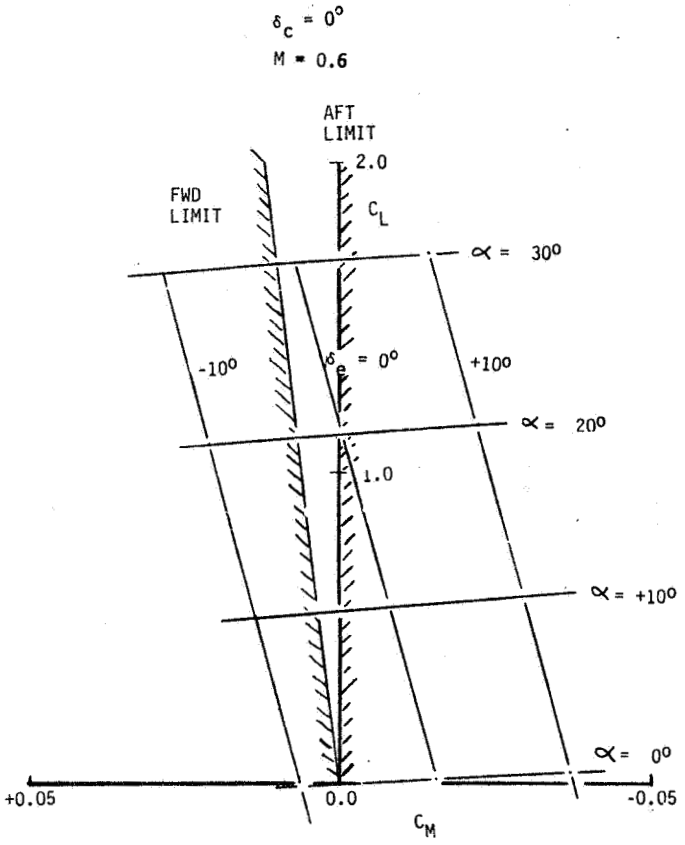

Figure 4-12 - Elevon Ability to Generate Pitching Moments About the Aircraft C.G.

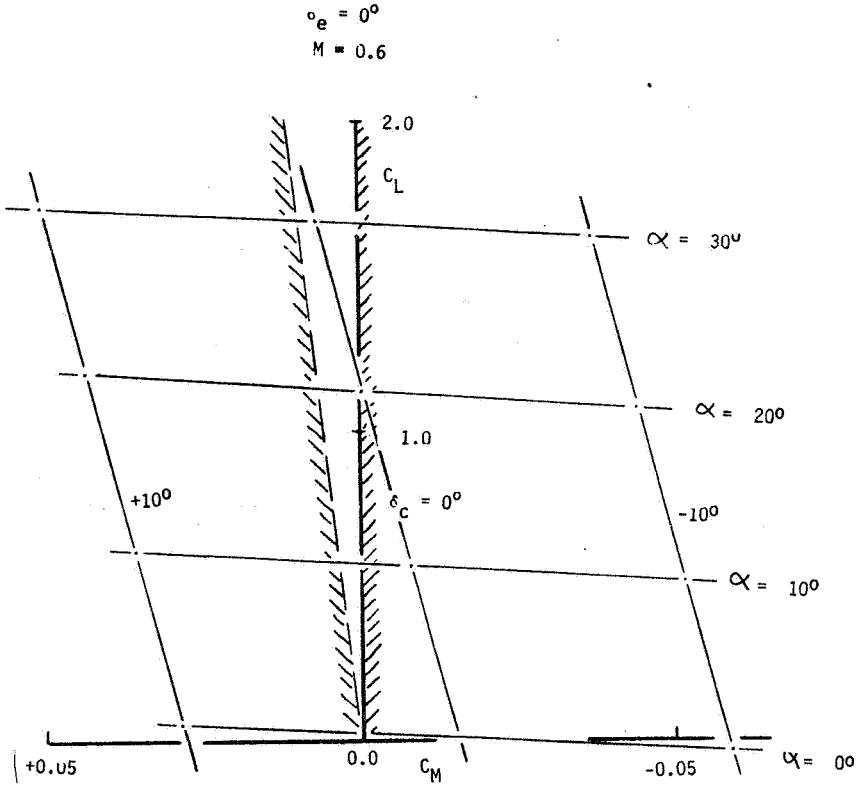

Figure 4-13 - Canard Ability to Generate Pitching Moments About the Aircraft C.G.

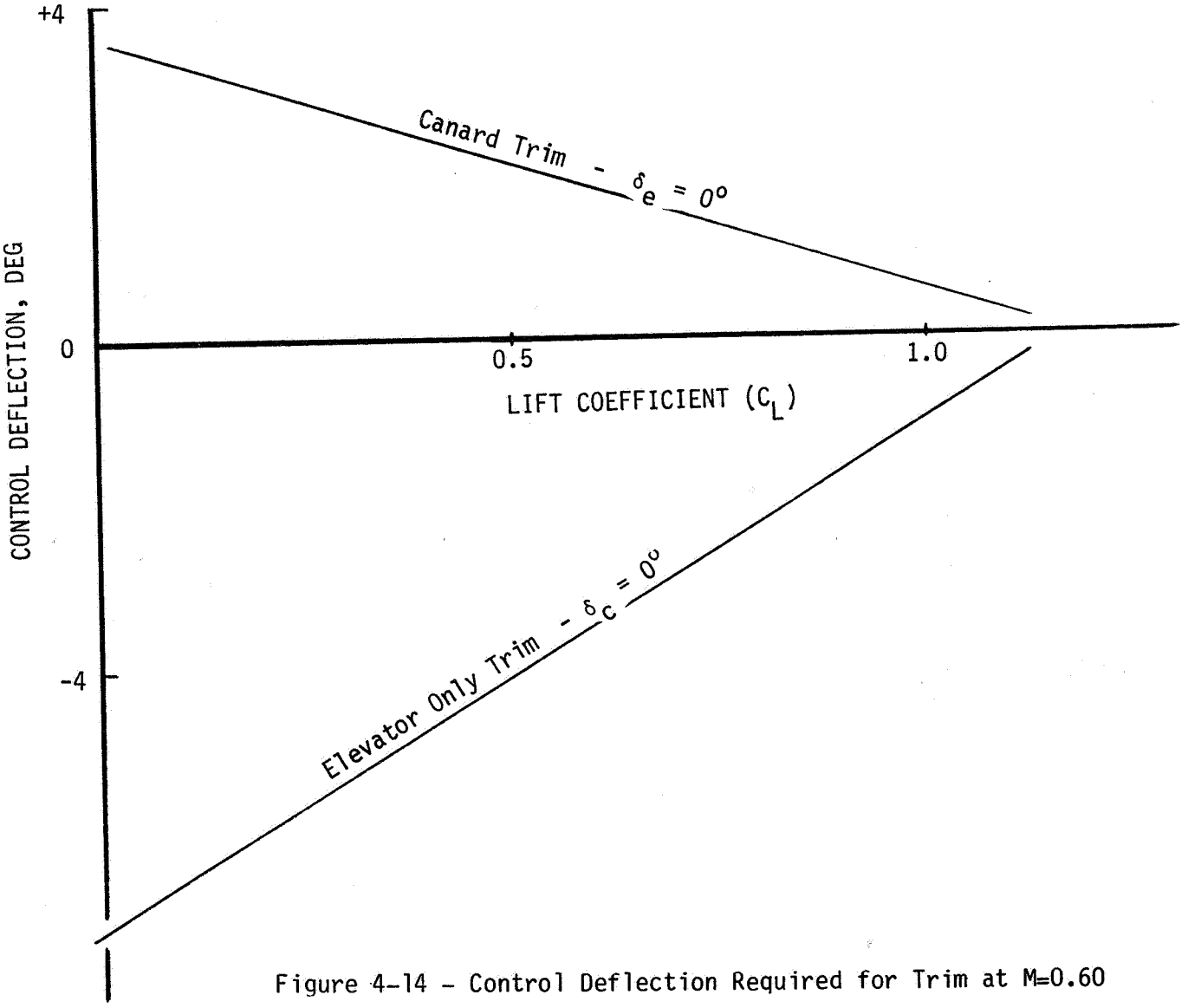

Figure 4-14 - Control Deflection Required for Trim at M=0.60

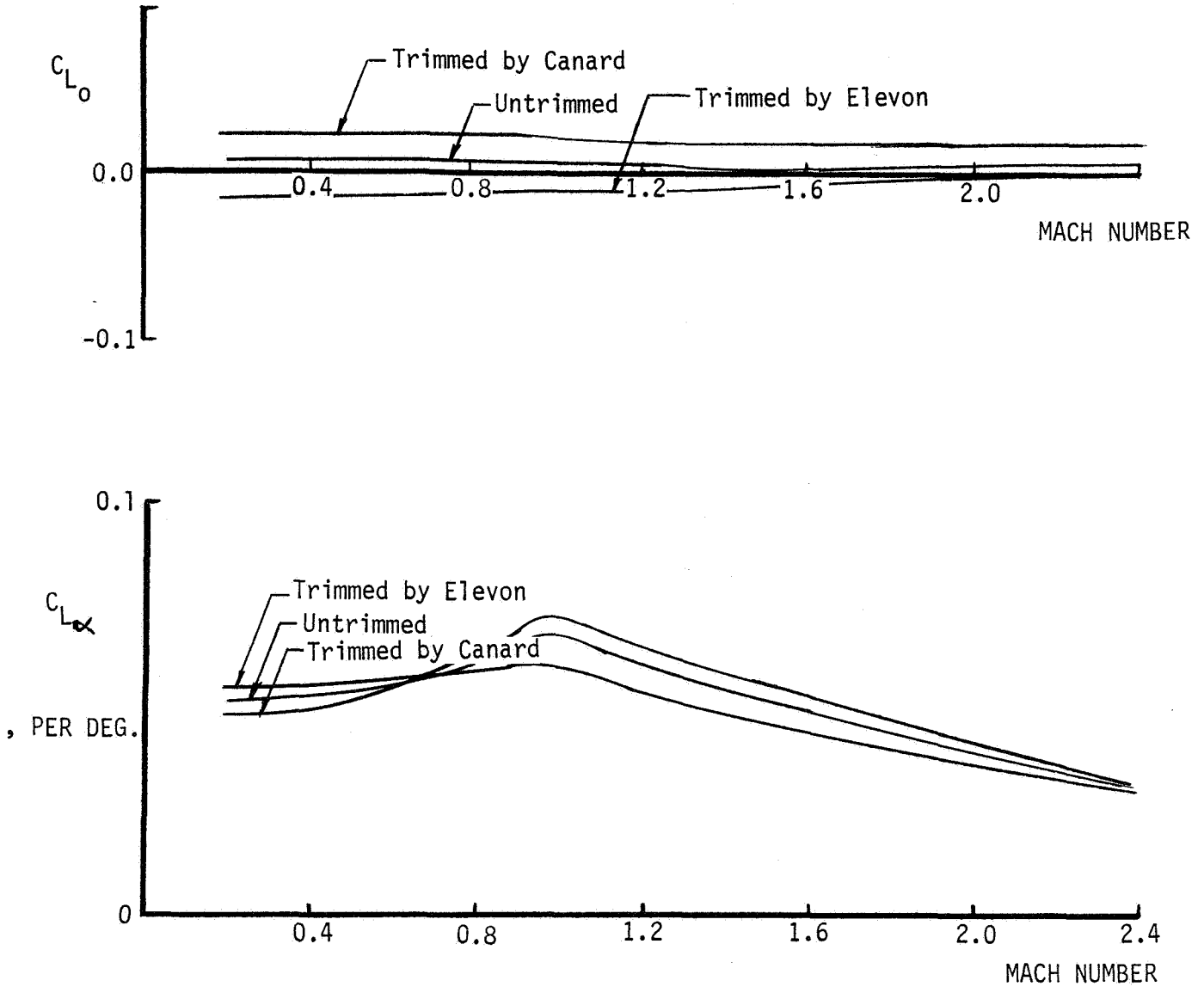

Figure 4-15 - Trim Effects on Lift at Zero Angle of Attack and on Lift Curve Slope

Figure 4-16 presents the variation of $C_{L_{max}}$ and $C_{L_{bo}}$ (C_L for buffet onset) with Mach numbers. These experimentally based data were adapted from the previous SF-121 configuration (Reference 1), which has a very similar canard-wing planform.

Figure 4-17 presents the variation of trimmed lift coefficient with angle of attack for several Mach numbers in the 0.2 to 2.4 range.

The availability of both canards forward and elevons aft for longitudinal control provides a direct lift control capability. The lift and moment equations due to elevon and canard deflections may be solved to determine the control deflections required to generate incremental values of C_L, with the incremental pitching moment set to zero. Figure 4-18 summarizes these results for the case of M = 0.6. If the elevon deflection is limited to 20 degrees, the resulting C_L increment is 0.106. This corresponds to an incremental load factor of 0.62 at h = 10,000 feet.

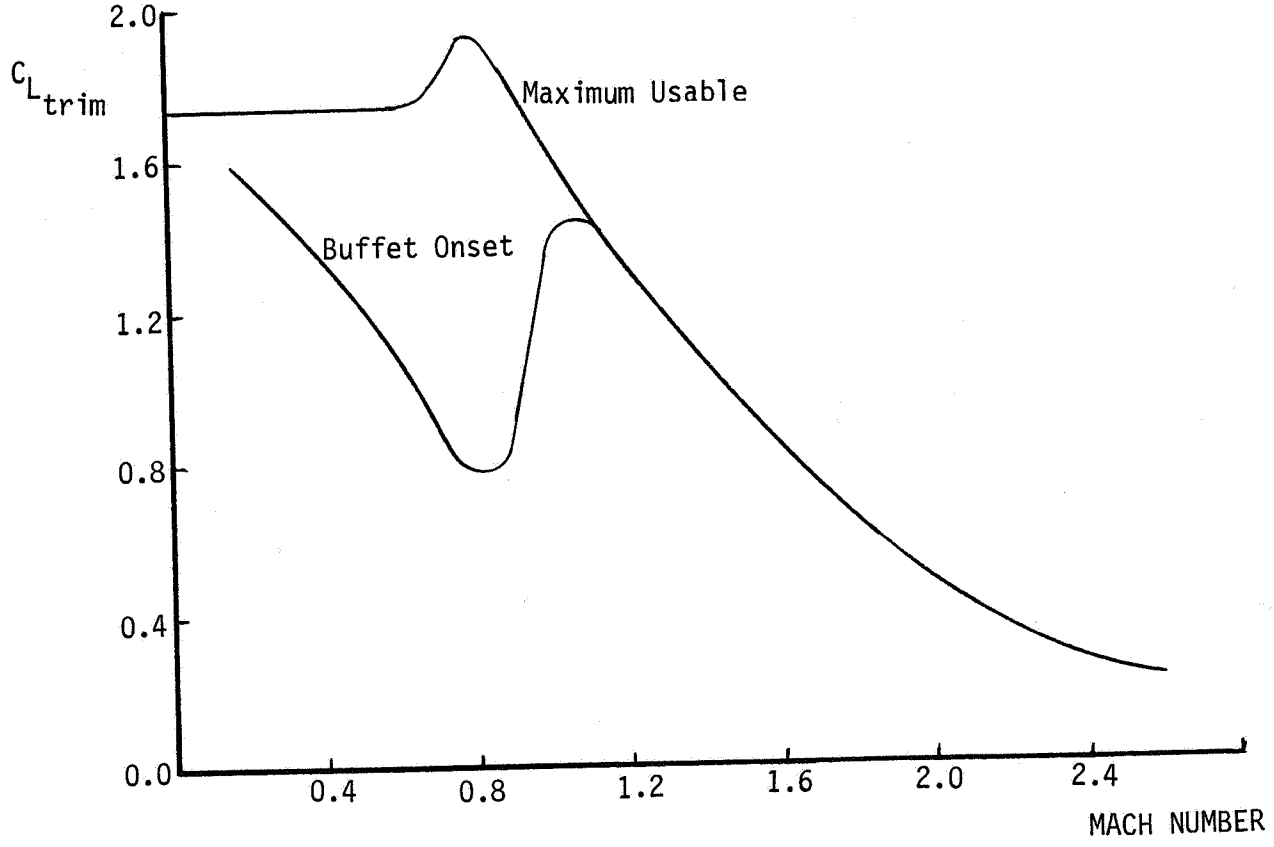

Figure 4-16 - Maximum Usable and Buffet Onset Lift Coefficients as a Function of Mach Number

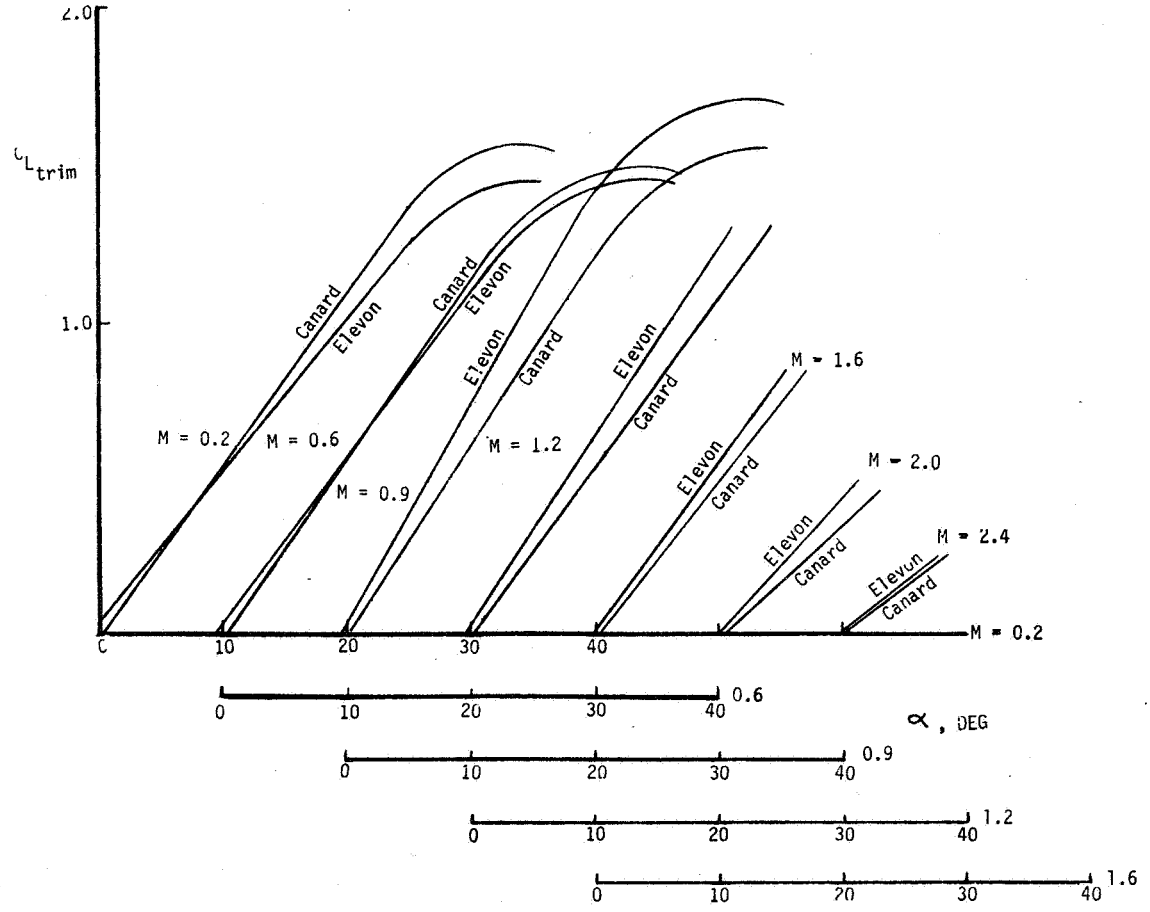

Figure 4-17 - Trimmed Lift Coefficient as a Function of Angle of Attack for Several Mach Numbers

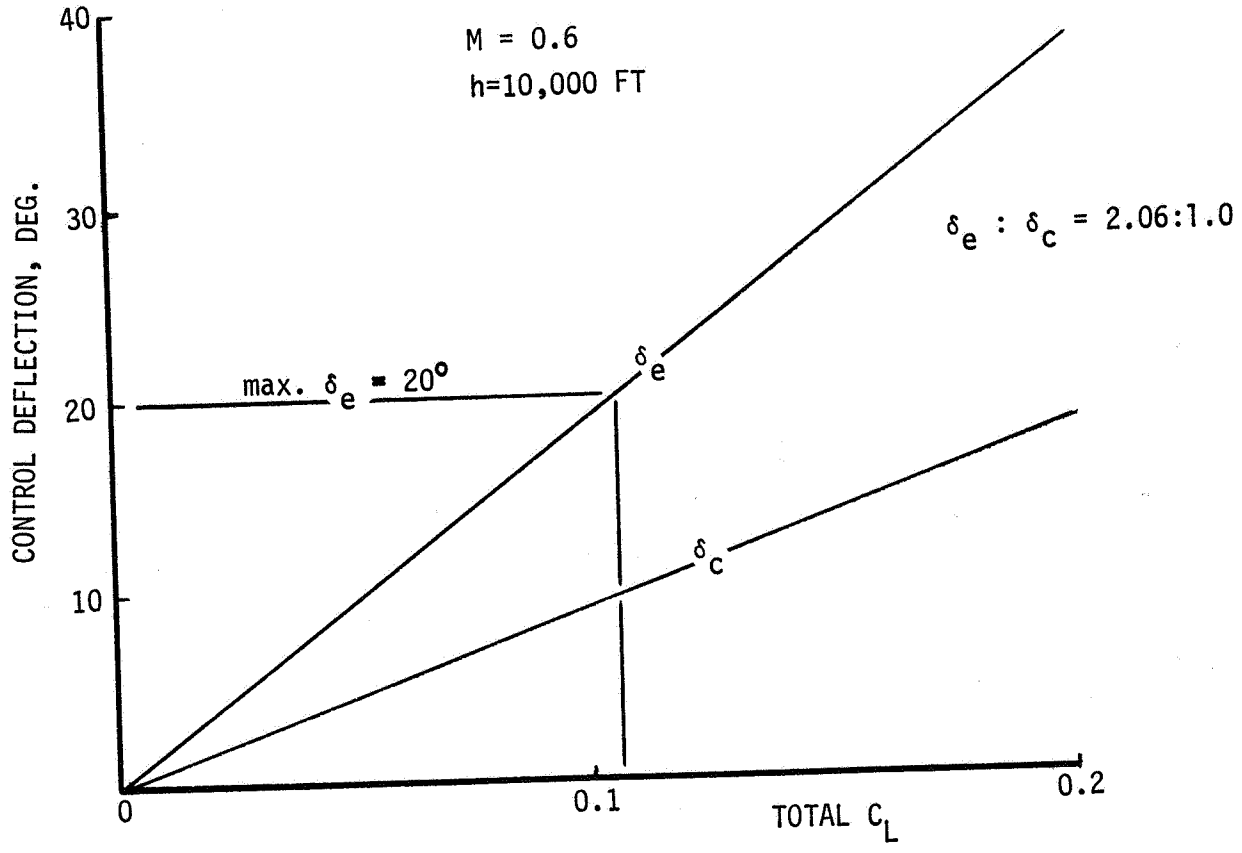

Figure 4-18 - Control Deflections Required for Direct Lift Generation

The lateral/directional aerodynamic characteristics and control effectiveness of the TF120 were estimated using analytical methods.

The predicted values of the rolling and yawing moments and the side force coefficients of the TF120 were generated using the APAS program. Within APAS these calculations were carried out using the Woodward unified subsonic/supersonic panel method. For subsonic speed the calculations are made using a Vortex-lattice method, while for transonic and supersonic speeds a linear theory method is used. Separate computer runs were made in which the elevons, the vertical fins, the aft ventral fins, and the forward ventral fins were asymmetrically deflected, one set at a time. When compared with the zero deflection case, these runs yielded the incremental moments and force coefficient due to unit deflections of each surface.

Figure 4-19 shows the variation of rolling moment capability, C_{l_δ}, with Mach number for each of the five deflectable surfaces. Note that the vertical and aft ventral fins both have C_{l_δ} values larger than the value for the elevons. Each vertical fin has an area of 26 ft^2 compared to 8 ft^2 for each elevon, and is an all moving surface, which increases the amount of force and moment generated per unit deflection. In the case of the vertical fin, 86 percent of the rolling moment at M = 0.6 is generated by the loads induced by the vertical fin on the wing. For the aft ventrals almost all of the rolling moment (99.5 percent) is due to the induced forces on the wing. The rolling moment generated by side force on the forward ventrals is almost exactly cancelled out by the rolling moment induced on the canard by the forward ventrals. A larger rolling moment, counter to the rolling moment caused by the forward ventrals, is induced on the wing, and is essentially the remaining quantity shown in Figure 4-19. This unusual result was checked with wind tunnel test data on an AFTI F-15 model in Reference 11 and the same general results were found: deflection of the forward ventrals results in a roll in the direction counter to the ventral fin force.

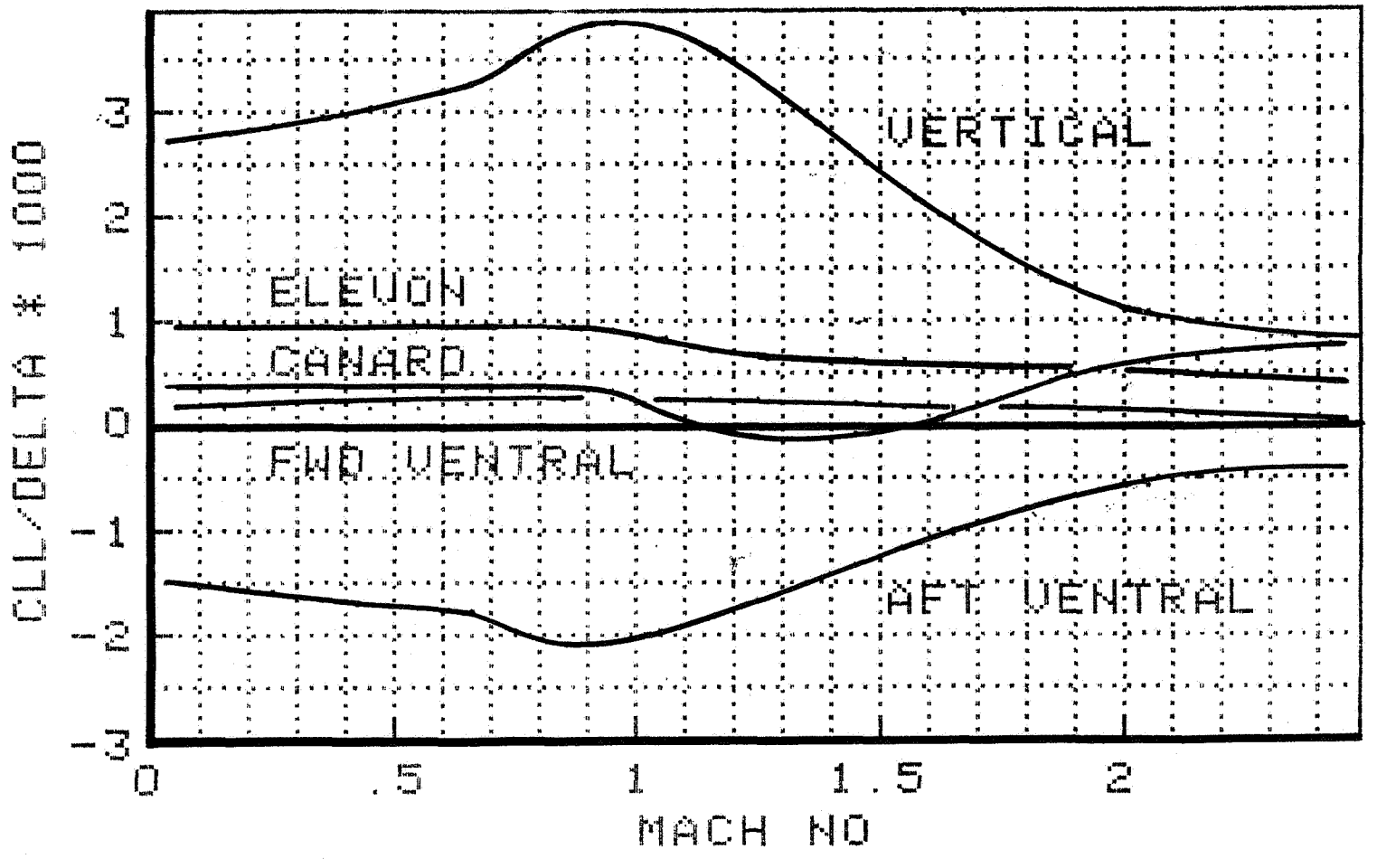

Figure 4-19 - Rolling Moment Due to Control Surface Deflection as a Function of Mach Number

The rolling moment at M = 0.6 generated by the canard itself is some 340 percent of the resultant rolling moment. An opposing rolling moment of 240 percent of the resultant moment is induced on the wing by the downwash from the canard. In the M = 1.1 to 1.3 region the interaction of the canard and wing results in an opposing rolling moment. This supports the empirical observation that canards are not efficient generators of rolling moment.

The side forces caused by asymmetrical surface deflections, C_{y_δ}, are shown in Figure 4-20. The forces generated by the vertical fins and the forward and aft ventral fins are in the direction expected. The side force due to elevon deflection is caused by induced forces on the vertical fins. The side force generated by the canard is due to the asymmetric deflection of a wing-like surface with dihedral.

The yawing moments induced by asymmetric control surface deflections are shown in Figure 4-21. The yawing moments generated by the vertical fins, the aft ventral fins, the forward ventral fins and the canard are all in the direction to be expected. The yawing moment due to elevon deflection is caused by the forces induced by the elevons on the vertical fins.

These control effectiveness data are tabulated in Appendix II.

Due to the linear nature of the equations used in these analyses, asymmetric control surface deflections did not cause any changes in lift or pitching moment. In reality, significant cross couplings of this type occur. As a result, some of our conclusions may need modification when wind tunnel results become available.

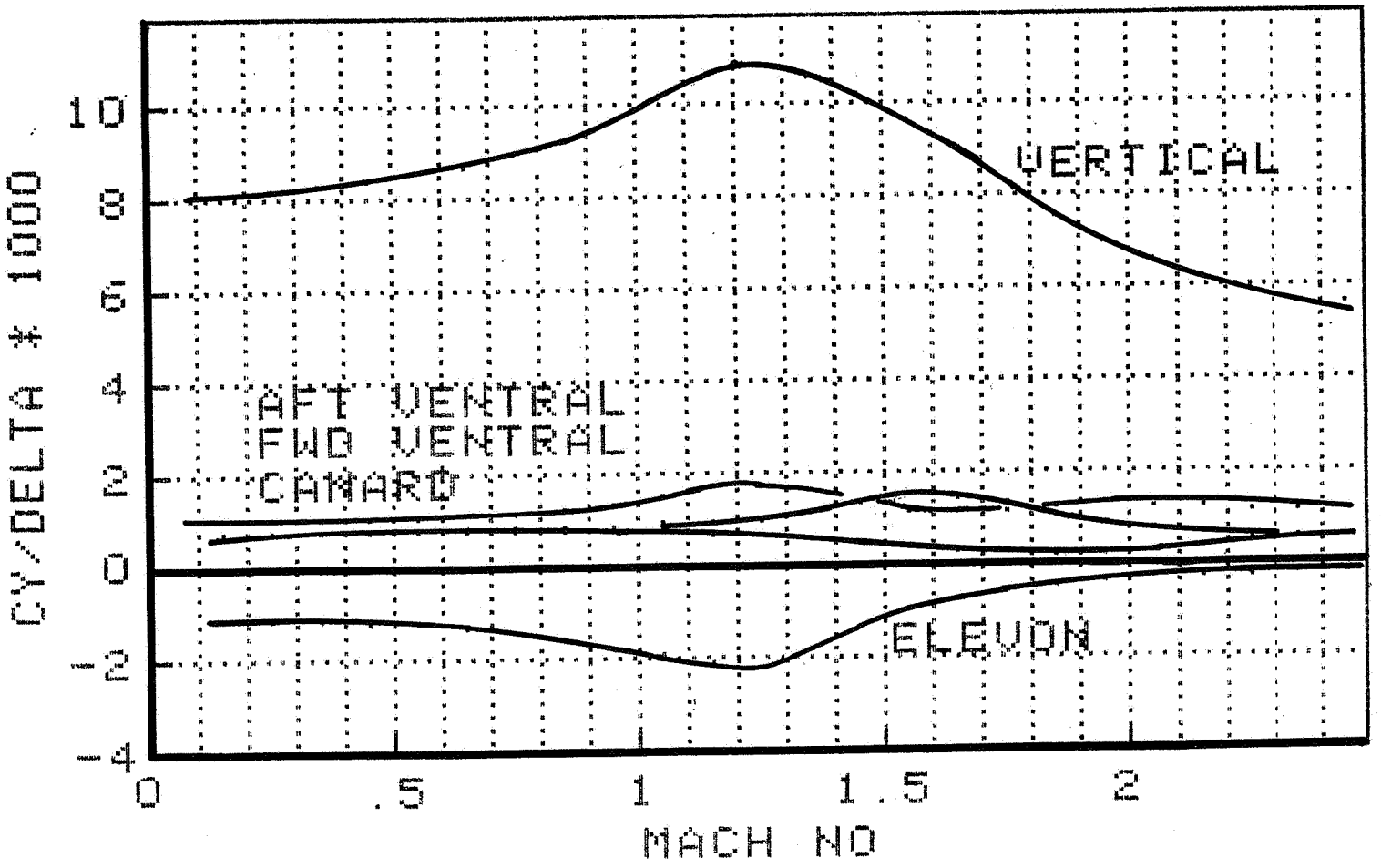

Figure 4-20 - Side Force Due to Control Surface Deflections as a Function of Mach Number

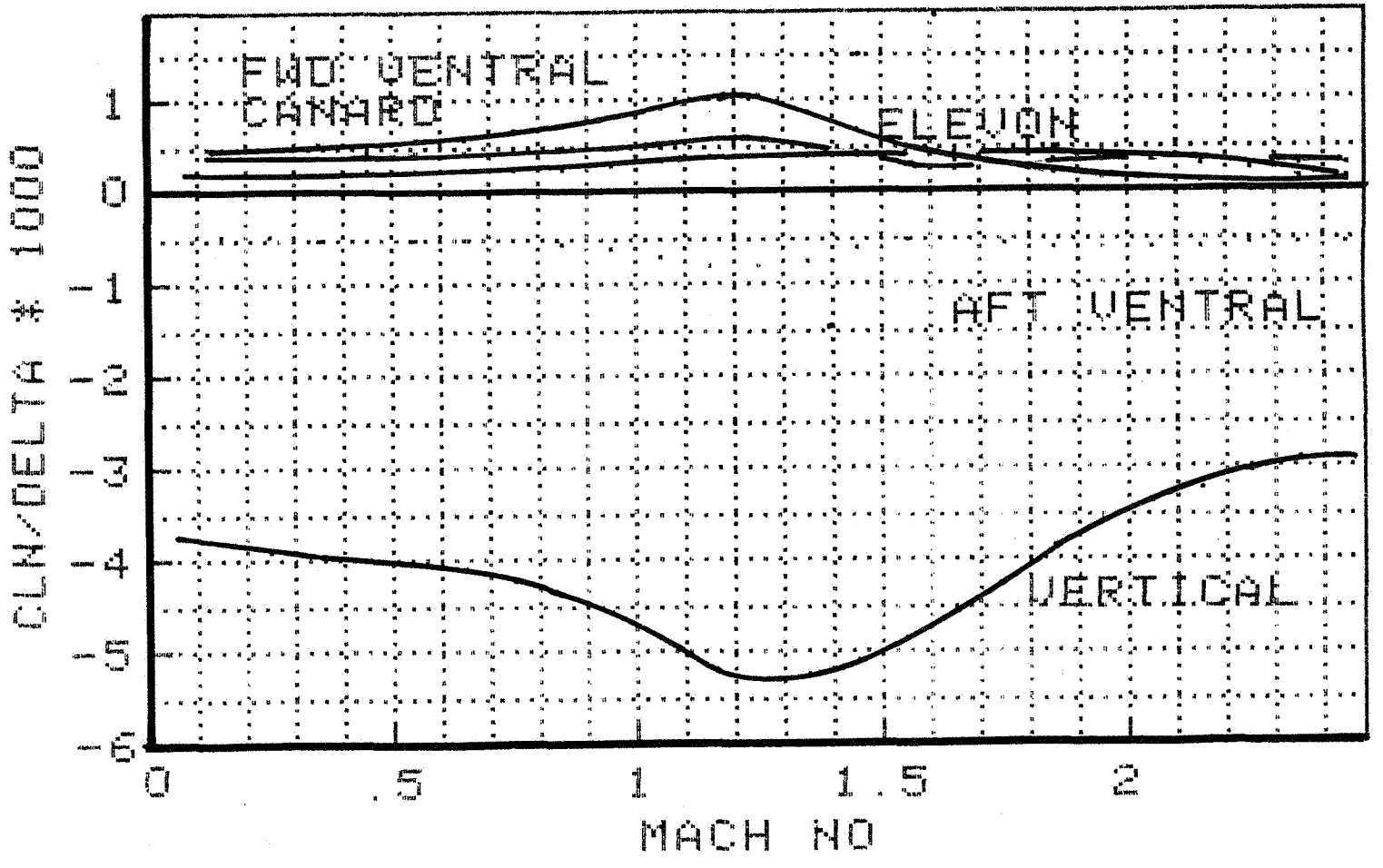

Figure 4-21 - Yawing Moment Due to Control Surface Deflections as a Function of Mach Number

The control deflections necessary to generate rolling, yawing and sideward motions have been determined.

On the TF120 the elevons, verticals and forward and aft ventral fins can be deflected independently of each other. The actual deflections will be governed by the control laws built into the digital fly-by-wire control system. As a prelude to the development of the actual control laws, the ability to generate pure rolling moments and pure side forces using a "conventional" control system was evaluated. This conventional control system used elevons for roll control, and the vertical and aft ventral fins as coordinating surfaces.

The three equations to be evaluated are:

$$C_{l_{\delta_e}} \delta_e + C_{l_{\delta_v}} \delta_v + C_{l_{\delta_{av}}} \delta_{av} = C_l \quad (1)$$

$$C_{n_{\delta_e}} \delta_e + C_{n_{\delta_v}} \delta_v + C_{n_{\delta_{av}}} \delta_{av} = C_n \quad (2)$$

$$C_{Y_{\delta_e}} \delta_e + C_{Y_{\delta_v}} \delta_v + C_{Y_{\delta_{av}}} \delta_{av} = C_Y \quad (3)$$

where the control effectiveness coefficients are those provided in Figures 4-19 through 4-21.

If a pure rolling moment is desired, the equations for yawing moment (C_n) and side force (C_y) are set equal to zero and the system is solved for values of elevon (δ_e), forward ventral (δ_v) and lower aft ventral (δ_{av}) deflections corresponding to the desired value of C_l. If pure side force or pure yawing moment is desired the other two equations are constrained to zero and the solution is repeated. While this analysis neglects coupling with the longitudinal degrees of freedom (which should be small) it illustrates how the data can be used to synthesize a program for the DFBW control system.

Using values appropriate to M = 0.6 the resulting control deflection for various levels of $C_{l\ total}$ are given in Figure 4-22. The powerful rolling moment capability of the vertical fins is accompanied by a large yawing moment generated by the same surfaces. Thus, the maximum rolling moment that can be generated is limited by the maximum usable elevon deflection. If the maximum usable elevon deflection is 20 degrees, the resulting $C_{l_{TOTAL}}$ is approximately 0.037.

If the equations for the rolling moment and yawing moment are set to zero in Equation (3), the control deflections required for generation of a pure side force, C_y, can be evaluated. The results for M = 0.6 are shown in Figure 4-23. Again the powerful effects of the vertical tails are limited by the effectiveness of the elevons. If the maximum usable elevon deflection is 20 degrees the resulting C_y is only 0.00167. At an altitude of 10,000 feet, this results in a side force a/g of only 0.01; a level that is far to low to be useful (Note that this side force is generated using only the conventional controls; the forward ventral has not been used).

A pure yawing moment can be generated by the same technique.

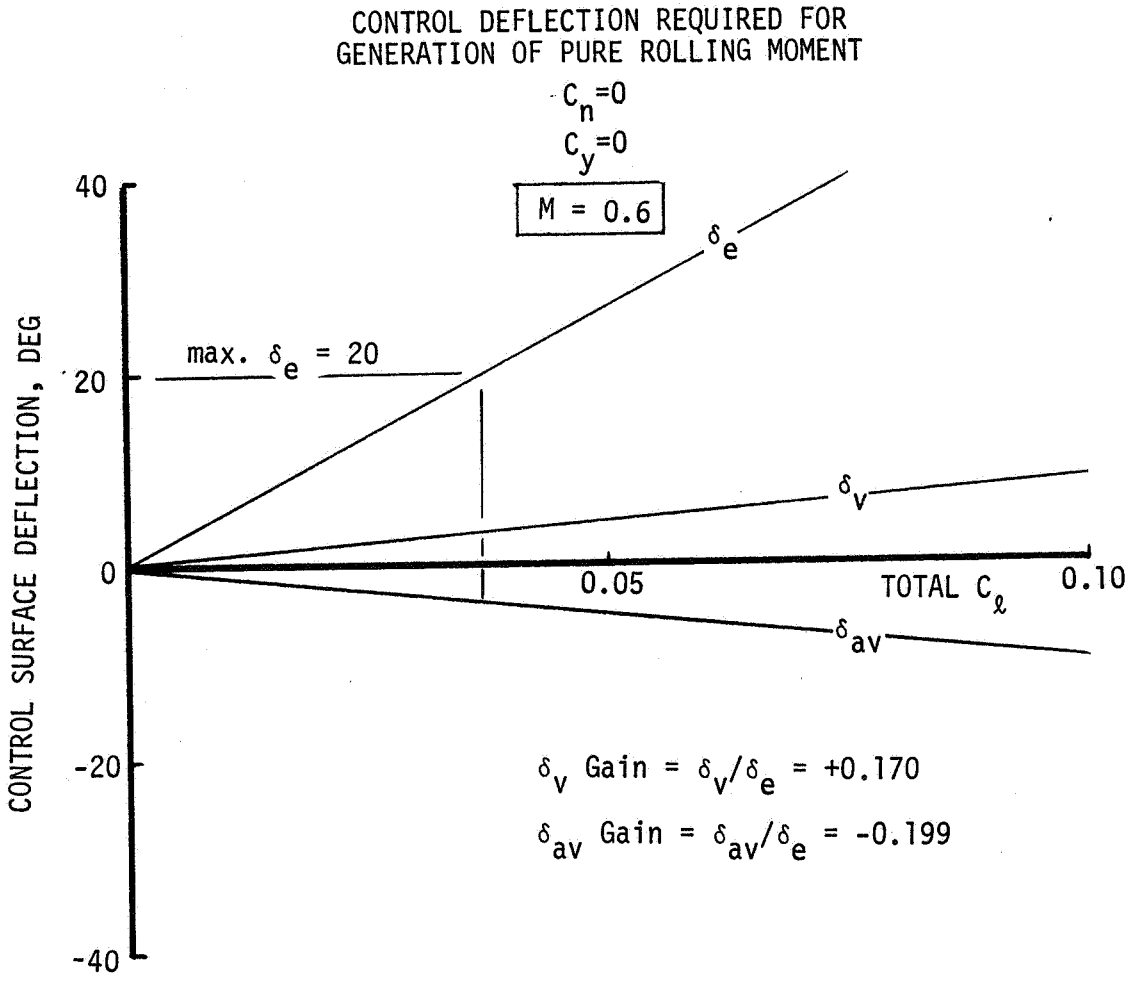

Figure 4-22 - Control Surface Deflections Required to Generate Pure Rolling Moment

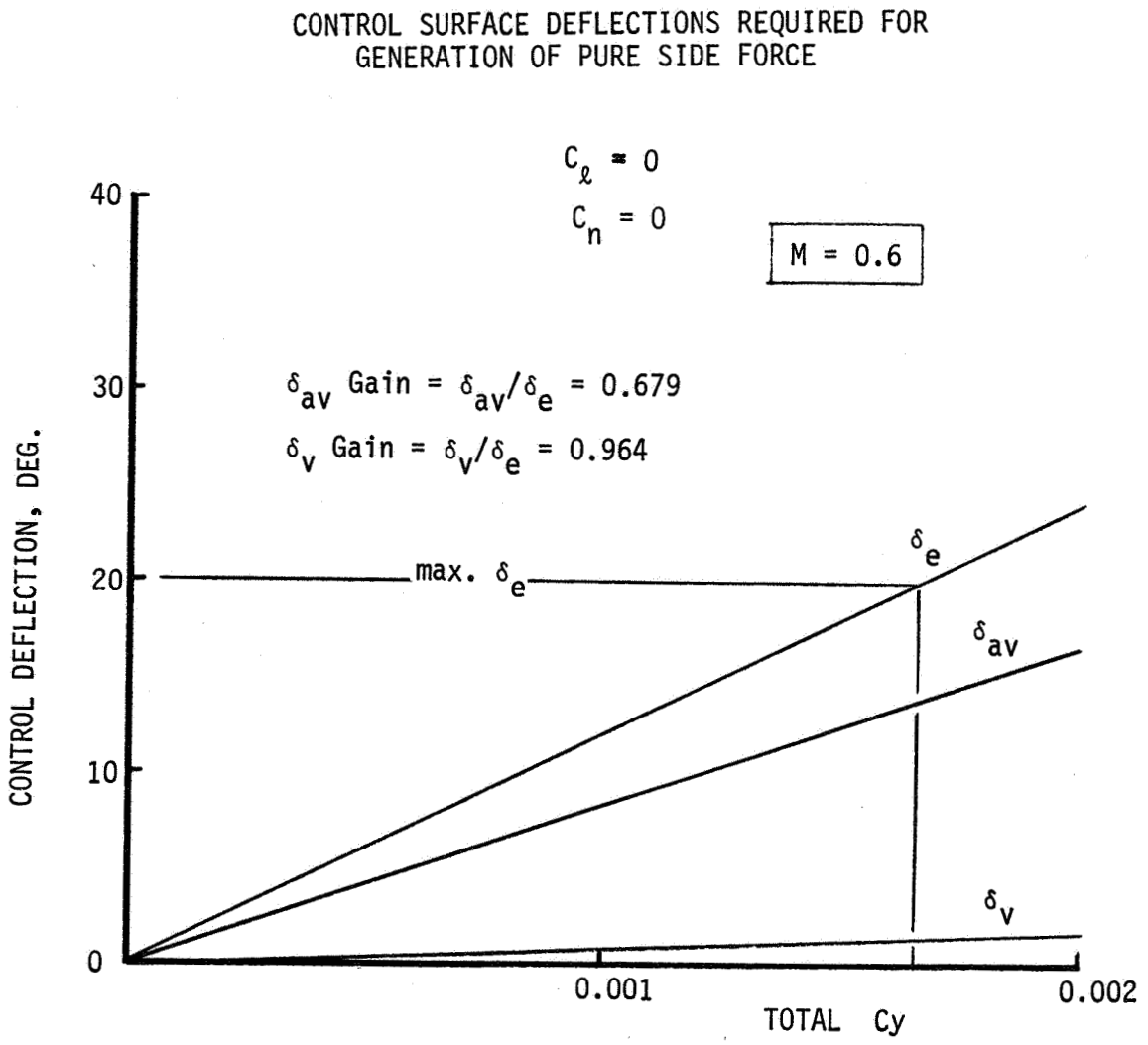

Figure 4-23 – Control Surface Deflections Required to Generate Pure Side Force

Unconventional use of aerodynamic controls augments rolling performance.

Direct side force capability has proven useful in air-to-ground weapon delivery and in air-to-air combat. During air-to-ground delivery of weapons, the application of direct side force can materially assist in acquiring and tracking the target. The TF120 was designed with twin forward ventrals for use in generating direct side forces. However, during the aerodynamic analysis we discovered alternative ways to generate forces and moments to enhance maneuverability.

The determination of the force and moment generation capabilities of all control surfaces was discussed in Section 4.4. From that analysis it appears that the elevon-type roll control system is limited because of the yawing moments and side forces generated by the three control surfaces, all of which are aft of the center of gravity. Due to aerodynamic interactions, the rolling moments generated by the vertical and aft ventral fins are predicted to be larger than that generated by the elevons. Thus, it appeared logical to investigate replacing the elevons by the forward ventrals. This exchange put into the control system surfaces capable of generating the large side forces needed to compensate for the side forces and yawing moment produced by the vertical tails and aft ventral fins.

As in Section 4.4, we can write the equations for total rolling moment, total yawing moment and total side force coefficients as functions of the individual control surface deflections. If we specify a finite value for the rolling moment and zero for the yawing moment and side force, these three equations can be solved for the three required control deflections. In Section 4.4 these equations were written using elevons, verticals, and aft ventral fins. We now rewrite these equations using the vertical, aft ventral and forward ventral fins, leaving the elevon contributions out entirely. The solution to this set of equations is then straight forward.

Figure 4-24 shows the control deflections required to generate various levels of rolling moment while trimming the yawing moments and side forces to zero. If the maximum usable deflection of the aft ventral fin is 20 degrees as for the elevons, the TF120 configuration can develop a rolling moment coefficient of 0.043. This rolling moment is 16 percent larger than the value of 0.037 generated by the configuration by using the elevons. The aft ventral fins operate in "clean air", have a much lower aspect ratio than the elevons and are all-moving surfaces. Hence, a reasonable maximum deflection for the aft ventral fins is 25 degrees. As shown in Figure 4-24, this increased deflection results in a rolling moment of 0.054, which is a 45 percent increase over the baseline elevon-based configuration.

The vertical, aft ventral and the forward ventral fins are all efficient side force generators. They also generate substantial yawing and rolling moments. We investigated the magnitude of side force that could be achieved by again solving the three force and moment equations for the control surface deflections required to generate various levels of side force with zero rolling or yawing moments. Figure 4-25 shows the results in terms of lateral accelerations, a/g, at M = 0.6 and h = 10,000 ft. If the maximum usable forward ventral deflection is 20 degrees, the TF120 configuration can generate a lateral acceleration of 0.23 a/g. If the maximum usable deflection of the forward ventral is 25 degrees, for the same reasons cited above for the aft ventral, the resulting lateral acceleration is 0.29 a/g. Thus the TF120 can develop appreciable side forces.

Having four surfaces which generate rolling and yawing moments, and side forces permits us to look at alternatives to the conventional elevon-vertical-aft ventral control concept. The large rolling moment capability of the vertical tail is accompanied by large yawing moment and large side forces. To determine if the rolling effectiveness of the configuration could be improved, a roll control system consisting of the elevons, and the forward and aft ventrals was investigated. In this system the large yawing moment and large side force contributions of the vertical fins did not have to be trimmed out, It was found that the maximum roll capability of this configuration was limited to about half that of the elevon-vertical-aft ventral configuration.

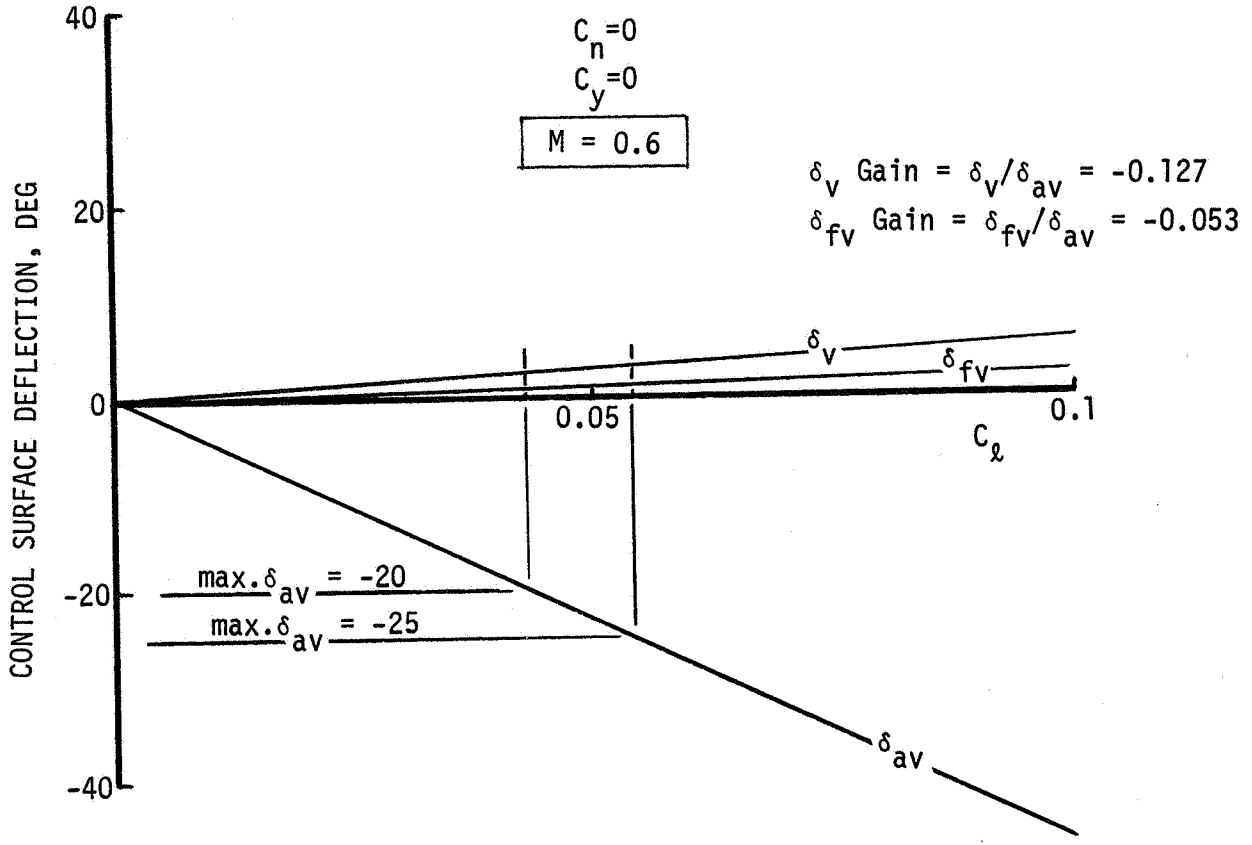

Figure 4-24 - Rolling Moment Generated by Control System Using Forward Ventrals Instead of Elevons

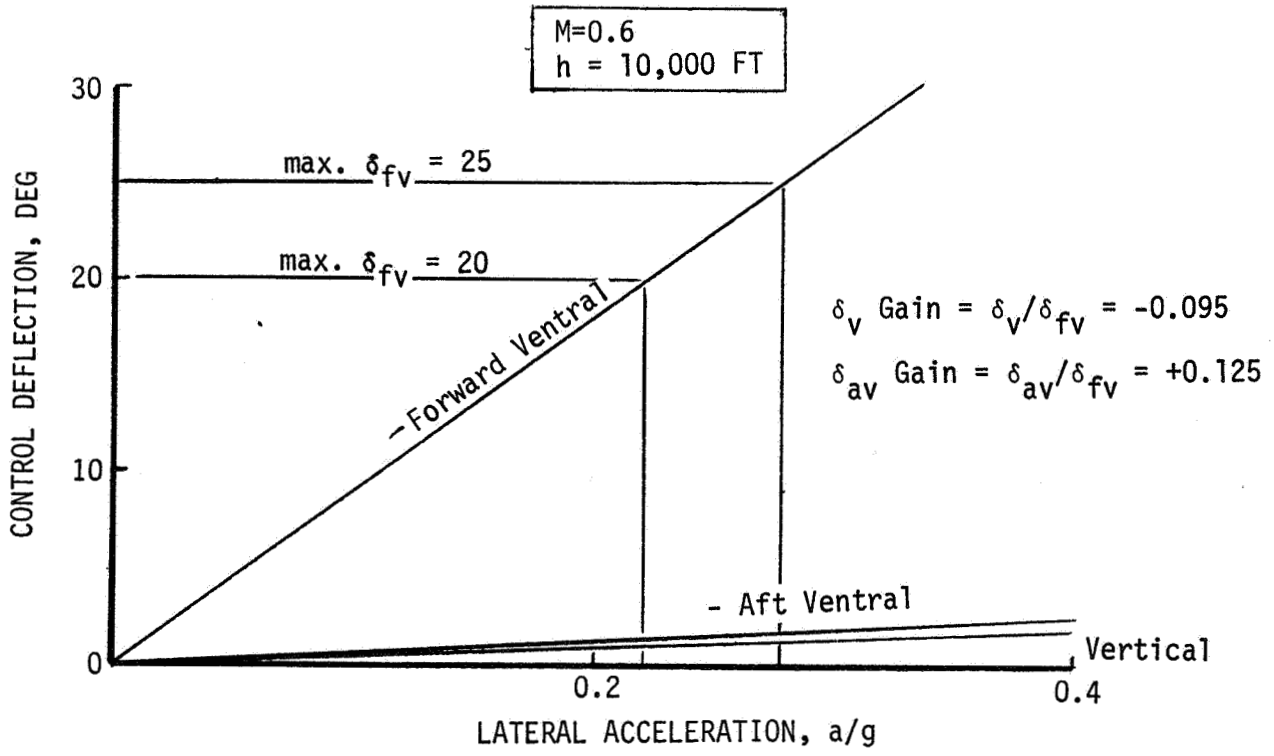

Figure 4-25 - Control Surface Deflections Required to Generate Various Lateral Accelerations

Another roll control system consisting of all four roll-inducing controls was investigated. In this case the three equations for roll, yaw and side force must be supplemented by a fourth equation. For the fourth equation we assumed a linear relationship between elevon and the other control deflections, such that

$$\delta_e + p\delta_v + q\,\delta_{av}\, r\,\delta_{fv} = 0 \qquad (4)$$

Here p, q, and r are arbitrary mixing ratios of elevon-to-control surface deflections (these are equivalent to the gains in a control system). The values for p, q, and r may range from $-\infty$ to $+\infty$. The object is then to solve the three force and moment equations plus this auxiliary equations for the rolling moment corresponding to control deflection less than or equal to the maximum allowable deflection. This "limited" maximum rolling moment is a function of the values of p, q, and r. The values of p, q, and r required to maximize the limited maximum rolling moment were then determined.

For the case considered here, M = 0.6 at 10,000 feet, the maximum rolling moment occured when p and q were equal to zero and r was about 18. Figure 4-26 shows the variation of the limited maximum rolling moment with mixing ratio, r, at M = 0.6. For r = 0, no elevons deflection occurs with forward ventrals deflection. For r = ∞, no forward ventral deflection occurs with elevon deflection. As the value of r is increased from 0 (thus phasing in the elevons) the total rolling moment increases at a rate set by the maximum usable deflection for the aft ventrals (25 degrees in the present instance). At r ~ 18, the limit of maximum usable elevon deflection (20 degrees) is also reached. For larger values of the ratio, the total rolling moment decreases, due to the limited elevon deflection available. The maximum rolling moment generated by this four control system is some 123 percent greater than the original conventional elevon system rolling moment.

The control deflection for each of the four surfaces corresponding the limited maximum rolling moments of Figure 4-26 (with C_n and C_y = 0) are shown shown in Figure 4-27, also as a function of the mixing ratio, r. These deflections together generate a rolling moment while holding the yawing moment and side force to zero. Any other combinations of controls will unbalance the

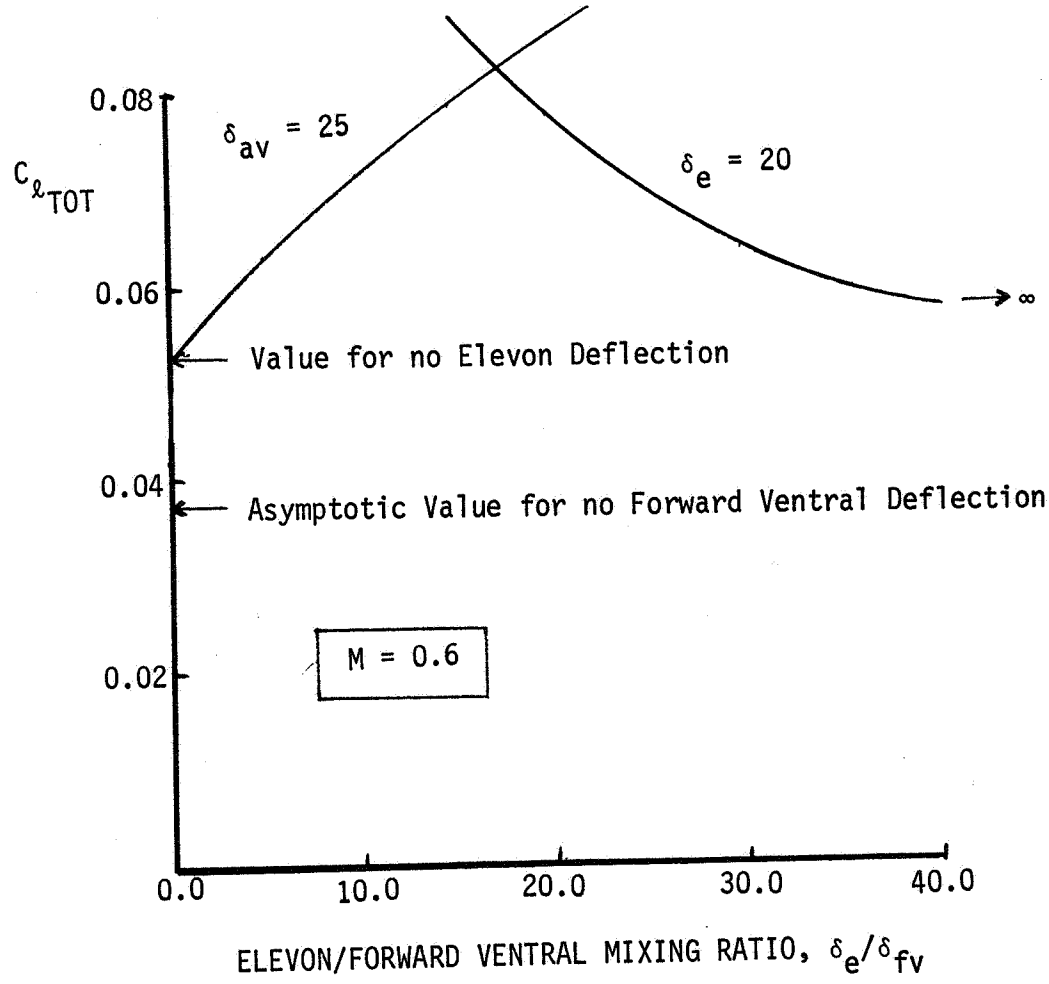

Figure 4-26 - Total Subsonic Rolling Moment as a Function of Elevon/Forward Ventral Mixing Ratio

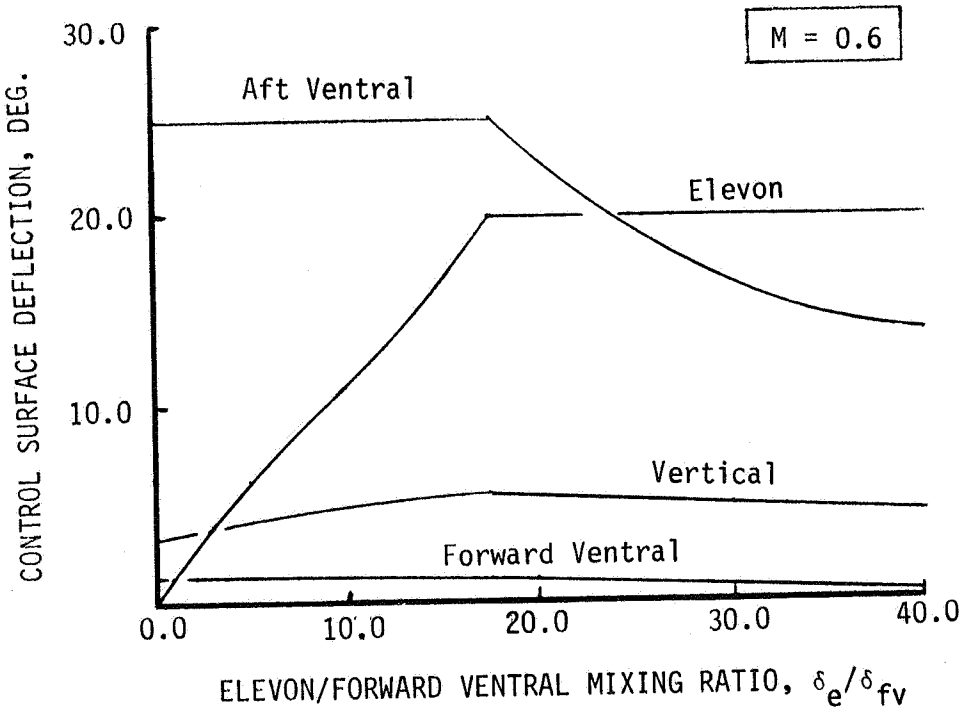

Figure 4-27 - Control Surface Deflections as a Function of Elevon/Forward Ventral Mixing Ratio

forces and moments. Note that at low values of r the aft ventral is the limiting surface. As r increases the amount of elevon input increase until the limit of 20 degrees is reached at about r = 18. Above this value of r, the elevon deflection is held constant, while the aft ventral deflection decreases.

The difference between the three-control and four-control systems for roll can be understood by considering the following data:

Evaluation of the Rolling, Sideforce and Yawing Equations

1. Four-Control

Contributions

	$\delta_e = 20^\circ$	$\delta_v = 6.06^\circ$	$\delta_{av} = -25.00^\circ$	$\delta_{fv} = 1.11^\circ$	
(C_l)	0.237	+0.233	+0.527	+0.003 =	1.00
(C_y)	-0.300	+0.633	-0.345	+0.012 =	0
(C_n)	0.143	-0.297	+0.148	+0.006 =	0

2. Three-Control

Contributions

	$\delta_e = 20^\circ$	$\delta_v = 3.39^\circ$	$\delta_{av} = -3.94^\circ$	$\delta_{fv} = 0^\circ$	
(C_l)	0.237	+0.131	+0.083	+ 0 =	0.451
(C_y)	-0.300	+0.355	-0.055	+ 0 =	0
(C_n)	0.143	-0.166	+0.023	+ 0 =	0

Here, all data are normalized by the rolling moment generated by the four-control system. Note that the addition of the forward ventral to the control systems allows aft ventral deflections to -25 degrees, at which point the aft ventral contributes more than 50 percent of the total rolling moment. The forward ventral contributes a very small amount of rolling moment, and what appears to be small amounts of side force and yawing moment. These latter contributions however allow the vertical and aft ventral fins to increase their deflection and hence add significantly to the total rolling moment.

The rolling performance of these control systems are compared to the requirements of MIL-F-8785B in Figure 4-28. There it is seen that with a step input of roll control, the conventional and the vertical-aft ventral-forward ventral control systems will not meet the MIL Spec requirements. The four control system handily exceeds the specified value. When the systems' performances are degraded (by using ramp input, etc), the four-control system is still expected to meet the MIL Spec requirements.

Figure 4-29 shows the rolling moment generated by the four-control system at M = 1.6. The shape of the curves are similar to those of the M = 0.6 data presented in Figure 4-26. The general magnitudes of the rolling coefficients at M = 1.6 are generally smaller than those for M = 0.6, and the improvements due to using the four control system are not as large.

All of the analyses discussed above have been carried out using the linear aerodynamics data generated by APAS. Significant angle of attack effects will be found in the actual aircraft, but methods for predicting these effects are not available at the present time.

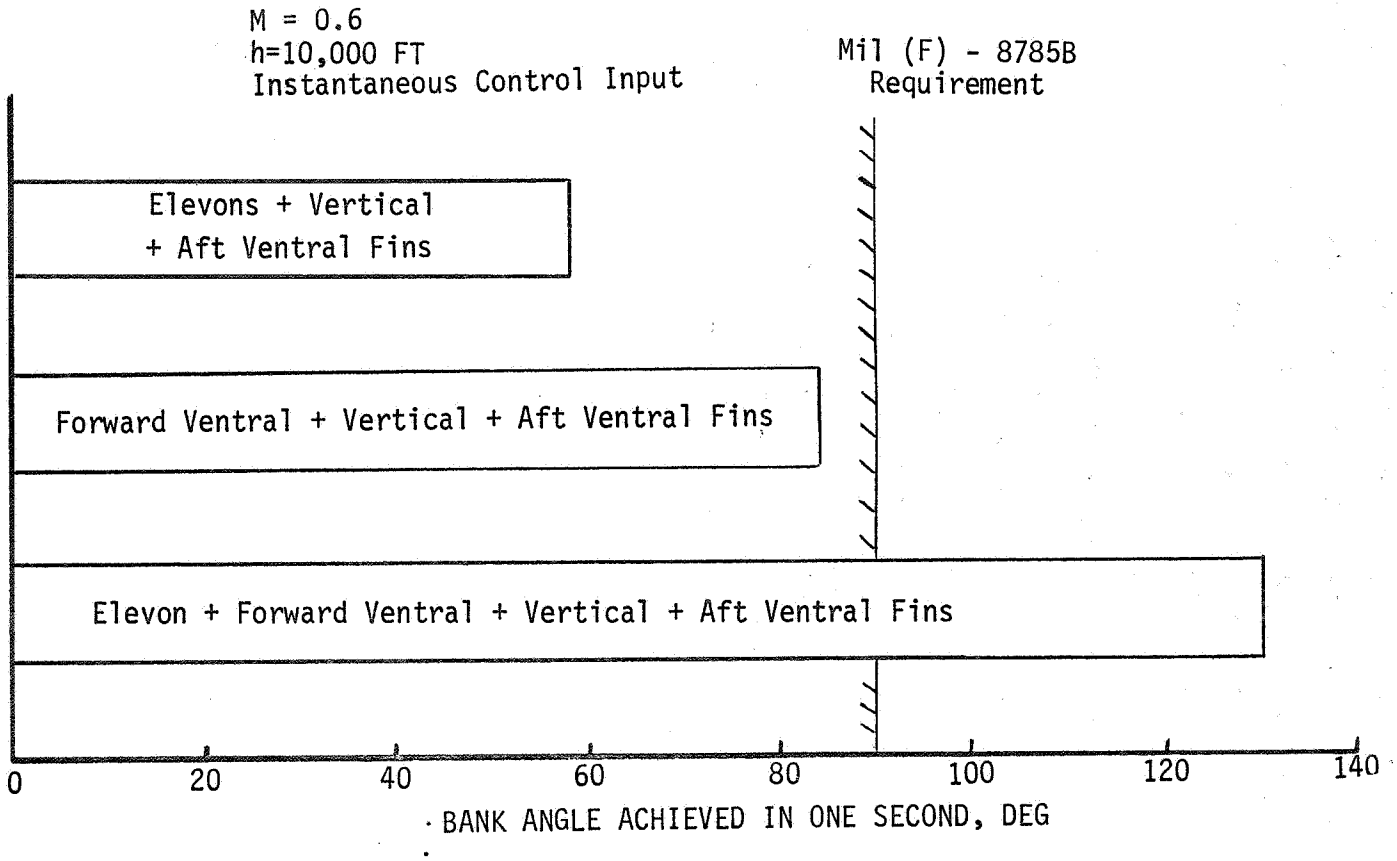

Figure 4-28 - Comparison of Rolling Capabilities of Three Roll Control Systems

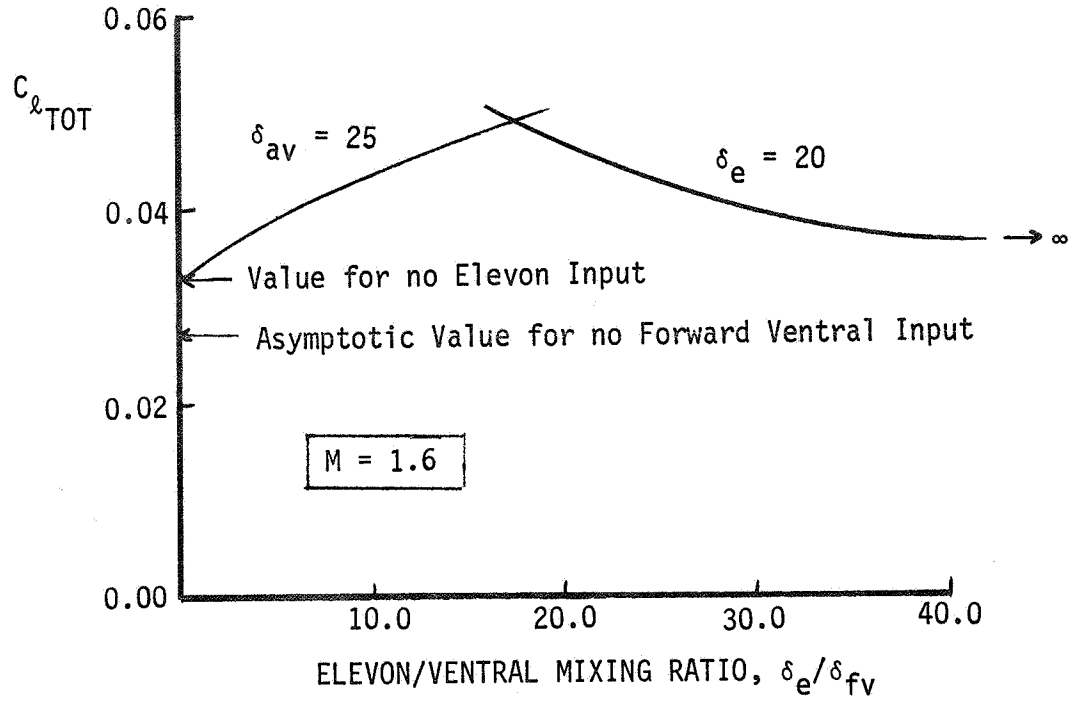

Figure 4-29 - Total Supersonic Rolling Moment as a Function of Elevon/Forward Ventral Mixing Ratio

4.6 PROPULSION INDUCED EFFECTS

Jet induced vertical lift loss for the TF120 in and out of ground effect was estimated using correlation methods.

Jet induced suckdown in hover out of ground effect was estimated for the TF120 configuration from a correlation of the jet exhaust properties and the corresponding induced loads. The method, summarized in Reference 12, was developed by Gentry and Margason in Reference 13. It was reasoned that increased suckdown was due to a higher rate of entrainment of ambient air into the jet exhaust, and higher entrainment rates were related to a faster decay of the jet. A jet decay correlation parameter was developed by assuming the rate of entrainment and the distance from the nozzle exit to the region of maximum entrainment was proportional to the maximum change of jet dynamic pressure decay and inversely proportional to the distance downstream where the maximum decay occurs. Figure 4-30 illustrates a typical jet dynamic pressure decay with distance downstream showing the max rate of decay and the downstream point where that slope occurs.

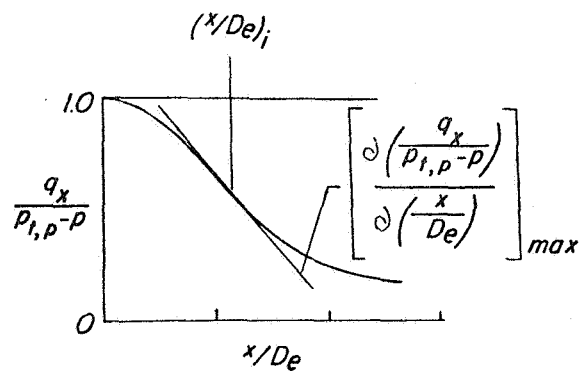

Figure 4-30 - Determination of Jet Dynamic Pressure Decay Parameter

It was found that suckdown could be correlated to the aircraft planform area and this jet decay parameter by

$$\Delta L/T = k \sqrt{S/A_j} \sqrt{-\left[\frac{\partial(q_x/q_n)}{\partial(x/D_e)}\right]_{max} \Big/ \left(\frac{x}{D_e}\right)_i}$$

where k is the constant of proportionality. Downstream distance is x, D_e is the equivalent nozzle diameter based on the total jet exit area A_j, S is aircraft planform area, q is dynamic pressure, and T is total jet thrust. The jet decay parameter is independent of airframe characteristics and affected only by nozzle shape. Nozzle shapes that increase the rate of decay close to the nozzle promote rapid entrainment and high suckdown loads.

Further investigations in Reference 14 supported this correlation. A nozzle pressure ratio effect was found and the correlation equation was revised to

$$\Delta L/T = k_1 \sqrt{S/A_j} \, (P_{t,n}/P)^{-.64} \sqrt{-\left[\frac{\partial(q_x/q_n)}{\partial(x/D_e)}\right]_{max} \Big/ \left(\frac{x}{D_e}\right)_i}$$

The constant of proportionality, k_1 is now dependent only on the aircraft configuration, such as wing height, flaps, landing gear, nozzle doors, etc. Figure 4-31 shows the correlation obtained for a mid-wing configuration, a mid wing with landing gear down, and a low wing. The slope of these curves give k.

Jet induced lift loss was estimated with the mid wing with gear down correlation. The lift loss attributed to each nozzle was estimated independent of the others because of the large difference in thrust between the nozzles. Total lift loss was then calculated as the sum of the lift losses attributed to each nozzle ratioed to the thrust from each nozzle.

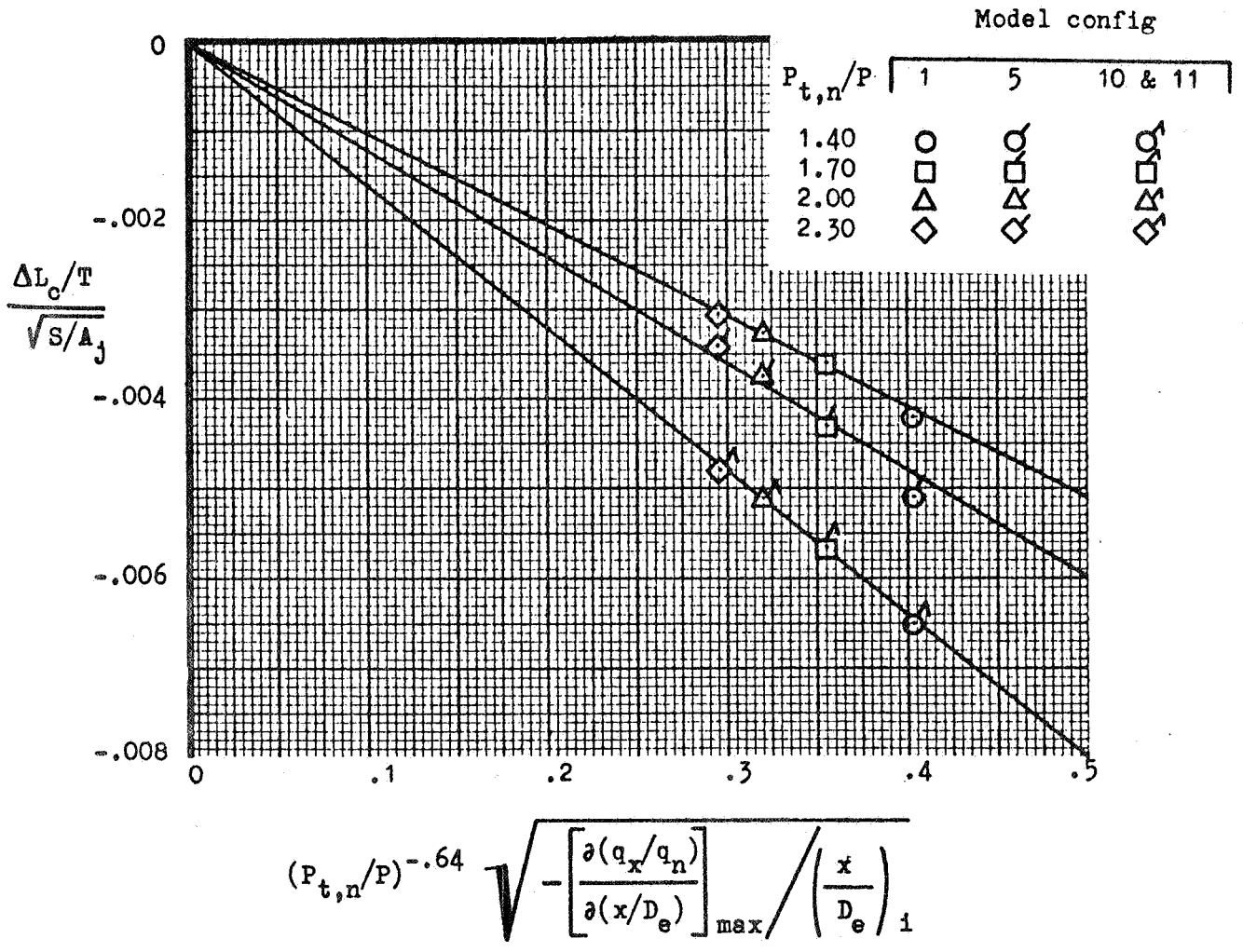

Figure 4-31 – Correlation of Lift Loss With Nozzle Pressure Ratio and Jet Decay Parameters

In ground effect the TF120 was estimated to have a suckdown profile comparable to a similar configuration with published test data. Several sources were reviewed to find data on a similar jet arrangement. With this arrangement a fountain is expected near the aircraft c.g. Suckdown as a function of height above the ground was normalized to the out of ground effect suckdown from Reference 15. This ratio was then applied to the TF120 to obtain the suckdown profile in Figure 4-32.

Reingestion was qualitatively assessed. In hover the TF120 planform shields the top inlet from any direct upflow from the ground reflected jet exhaust. The cruise inlets are well forward of the jet exhausts reducing any direct ingestion effects. The low exhaust temperatures (950°F front and rear) minimize the consequences of any reingestion which does occur. With any forward motion or aft deflection reingestion is negligible in these inlets.

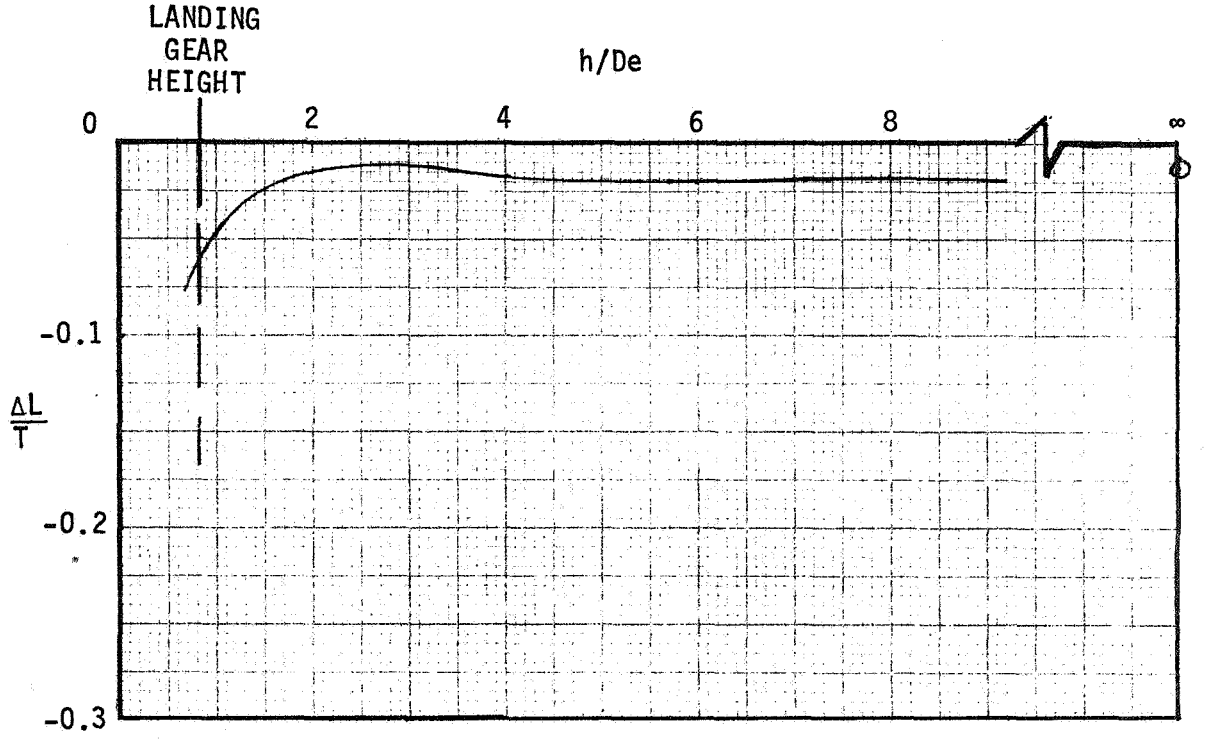

Figure 4-32 - TF120 Lift Loss in Ground Effect

5.0 PROPULSION SYSTEM

This section describes how the Series Flow Tandem Fan cycle works and how installed performance was estimated for high speed flight and for V/STOL operation.

This section contains:

5.1 INTRODUCTION TO THE TANDEM FAN

> The series flow Tandem Fan is an innovative, high performance propulsion cycle for supersonic V/STOL aircraft.

The Tandem Fan is a variable cycle propulsion system for V/STOL application. The system operates at low fan pressure ratio and high airflow for vertical takeoff and landing and at high fan pressure and low airflow for horizontal cruise. The high bypass ratio vertical mode allows takeoffs and landings moderate jet velocities, temperatures, and fuel consumption. The low bypass ratio cruise mode is an efficient cycle for supersonic aircraft. The Tandem Fan further utilizes virtually all engine components in both cruise and vertical mode, thus minimizing total propulsion system weight.

The propulsion system consists of a remote front fan connected by shaft to a rear mixed flow turbofan unit. Each fan has its own inlet and deflecting nozzle for vertical mode. This mode is referred to as the parallel flow mode due to separate flow streams. During transition to the series flow cruise mode, the front fan nozzle and rear fan inlet close in conjunction with the pivoting vane transition mechanism, which functions as a variable porosity wall to minimize flow distortion. In the series flow cruise mode, all air enters the forward inlet and passes sequentially through both fans and supercharges the engine core. The system is shown schematically in Figure 5-1.

Performance of the Tandem Fan was calculated using the Vought TECSON routine (Turbine Engine Cycle Simulation) and NNEP (Navy-NASA Engine Program). The performance is based on composite engine technology trends and fan characteristics provided during Navy Type A V/STOL studies. These trends have been periodically reviewed with engine companies and customer areas. The technology levels used in this study are considered conservative for the post-1990 period.

The following sections describe Tandem Fan cycle selection, propulsion system components, and propulsion system performance. The point design engine cycle for the TF120 aircraft is designated SSTF011.

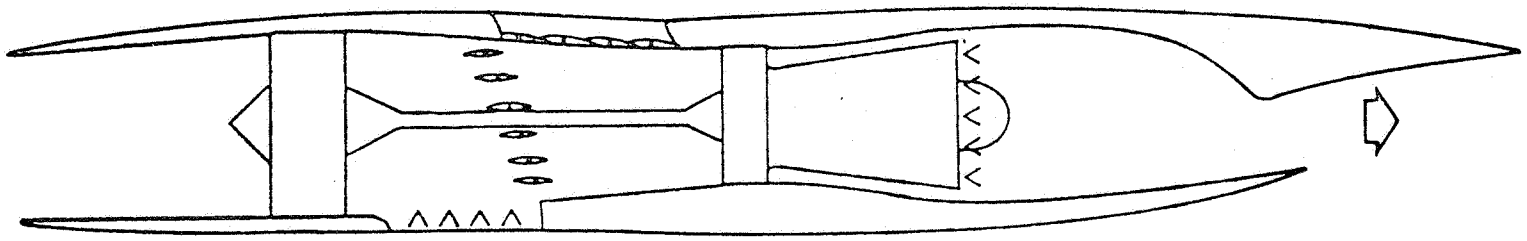

Series Flow Mode – High Speed

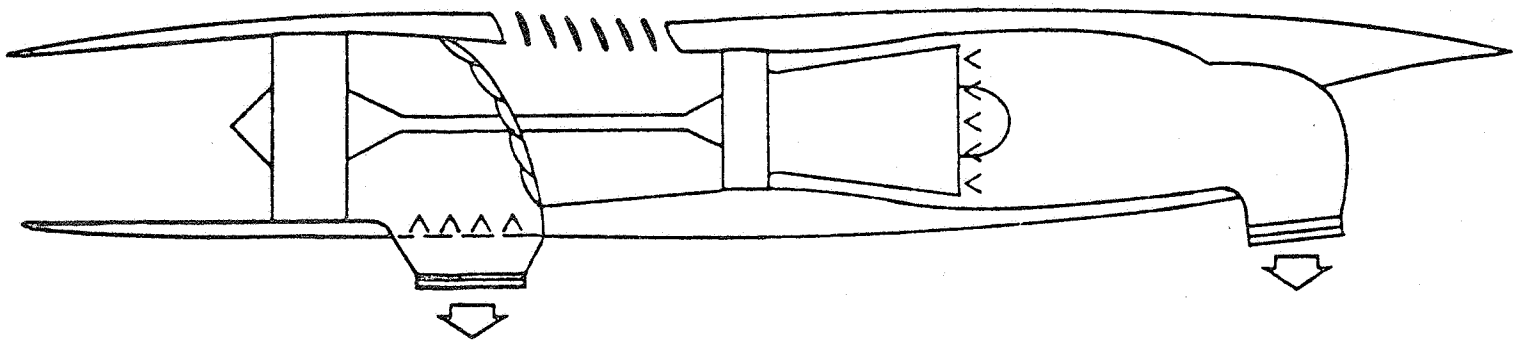

Parallel Flow Mode – V/STOL

Figure 5-1 - Tandem Fan Propulsion Schmetic

5.2 CYCLE SELECTION

SFTF cycle parameter selection was based on recent propulsion trade studies and a preliminary analysis of the Phase I configuration.

Vought has performed extensive tandem fan cycle analysis from 1976 to the present and supported powered model testing at the NASA Lewis Research Center. The TF120 conceptual analysis benefited from recent cycle trade studies. Following initial analysis of the TF100 proposal configuration a new flow tandem fan cycle, the SSTF011, was defined and incorporated into the definitive TF120 design.

The cycle design point is based on a max vertical thrust at Sea Level static on a Tropical Day in the parallel flow mode. The engine is sized for 25,000 lb of installed, non-augmented thrust with a 60/40 thrust split between the two vertical force generating nozzles. In this condition, the fans are at max flow and max pressure ratio with the core at Intermediate power. The front and rear operating fan pressure ratios are 2.2 and 1.75, respectively. The engine core operates at 2,800°F with a compressor pressure ratio of 10:1.

Cycle properties during vertical mode and series flow cruise are summarized in Table 5-1. Factors influencing propulsion system definition are listed in Figure 5-2.

Table 5-1 - SSTF011 Cycle Characteristics

	Parallel Flow (VTOL)	Series Flow (High Speed)
Fan pressure ratio	2.2/1.75	3.44
Bypass ratio	3.43	1.00
Compressor PR	10.0	7.33
Overall PR	17.5	25.2
Combustor temperature °F	2,800	2,695
Exhaust temperature °F	950/950	3,400
Thrust, augmented, lb	29,286	43,845
SFC, augmented	0.977	2.024
Thrust, unaugmented lb	25,000	26,486
SFC	0.541	0.665
Corrected airflow lb/sec	433/254	433
Actual airflow lb/sec	400/234	412
Core actual airflow, lb/sec	143	206

Tandem Fan Design Variables

Vehicle Sizing
o fan thrust requirements for pitch control o bleed thrust requirements for roll control o fore/aft thrust split for neutral balance o degree of augmentation for takeoff o engine scale factor or thrust/weight at takeoff o cruise mode thrust requirements

Propulsion Design
o front fan pressure ratio o relative size of front and rear fans o rear fan pressure ratio (fallout for given thrust split) o core cycle: pressure ratio and temperature o engine flat rating schedule o component technology levels o component map locations o engine control philosophy o bleed station location o inlet and nozzle design

Figure 5-2 - Design Variables for Propulsion System

5.3 PROPULSION SYSTEM DESCRIPTION

5.3.1 Engine Components and Weight

> The Tandem Fan engine component characteristics are based on technology projections for mixed flow turbofans.

The engine configuration basically is a mixed flow, augmented turbofan driving a remote front fan through an extended shaft. The front and rear fans are two stage fixed pitch fans with variable inlet guide vanes (VIGV). The front fan is designed for a pressure ratio of 2.2. The rear fan is designed for a pressure ratio of 1.75 in the vertical mode.

The engine core is an advanced cycle based on current and projected engine technology. The design pressure ratio is 10.0. In the series flow mode, the compressor operates at a pressure ratio of 7.33. The overall pressure ratios in parallel and series flow are 17.5 and 25.2, respectively.

The rear augmentor is a conventional afterburner designed for a maximum temperature of 3400°F and total fuel/air ratio of 0.06. In the STO takeoff mode, the rear augmentor operates at a temperature of 2800°F. The nominal front augmentor operating temperature is 950°F. The burner operates at a max fuel/air ratio of 0.011 and throttles along with the front fan IGV for pitch control.

The SFTF engine physical characteristics and weight were estimated by Vought methodology which relates each component to similar existing hardware. A technology projection factor is then applied to each item. For the SFTF011 cycle used in the TF120 point design, the engine installation weight is 4,747 lb. Total propulsion system weight is 5,629 lb.

5.3.2 Air Induction System

> The Tandem Fan air induction system consists of the forward high speed inlet, the aft vertical mode inlet, and the transition blocker doors.

The forward air induction comprises a fixed geometry external compression inlet with bleed and bypass. The external compression surfaces are 7 degree two-dimensional ramps without sidewalls. Boundary layer diverters and diffuser bleed are used to control the boundary layer on the external ramps and inner walls of the subsonic diffuser. Overboard bypass is used for airflow matching and drag reduction in supersonic flight. Auxiliary takeoff doors are used to increase pressure recovery at low speeds. The takeoff door flow area is sized for 0.30 of the inlet throat area and reduces the throat Mach number from 0.75 to 0.48.

Figure 5-3 shows front inlet low speed pressure recovery as a function of flight Mach number and front fan specific flow. The nominal recovery levels are 0.95 for static takeoff and 0.98 to 0.99 for subsonic cruise. Figure 5-4 shows high speed inlet recovery at max power airflow. This curve includes shock losses, diffuser losses, and cowl lip losses. Inlet spillage drag characteristics are shown in Figure 5-5. The inlet bypasses excess flow above Mach 1.4 and spills subcritically below Mach 1.4. Engine-inlet airflow matching characteristics are shown in Figure 5-6.

The aft fan inlet consists of auxiliary takeoff doors in the upper nacelle section between the front and rear fans. The takeoff doors are sized for a flow area of 980 in^2 and a Mach number of 0.50. The aft fan inlet is used only during the parallel flow mode for vertical/short takeoff, hover, and landing and closes progressively during transition to series flow. The estimated recovery characteristics of this inlet are shown in Figure 5-7. For vertical takeoff, the nominal recovery level is 0.95.

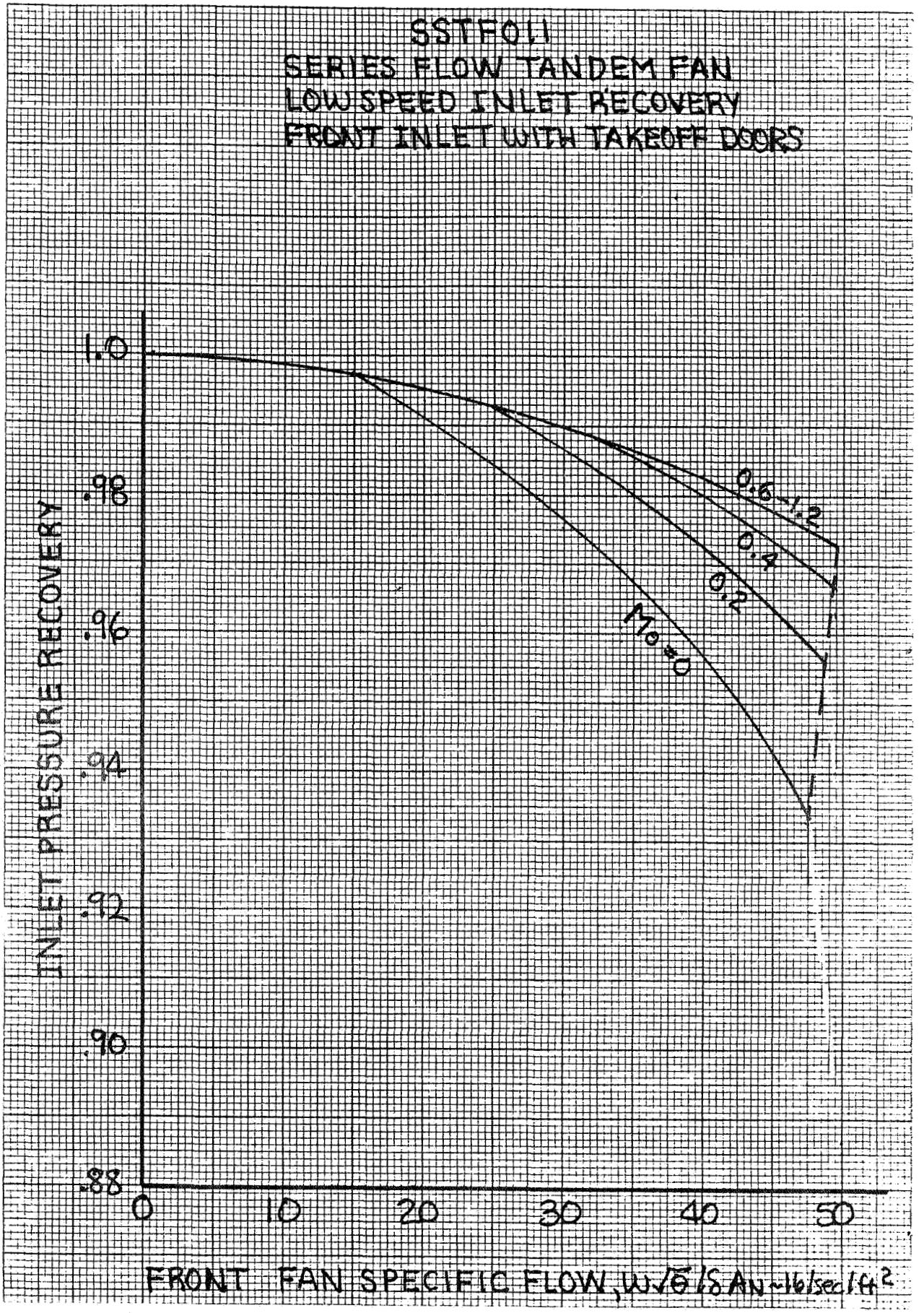

Figure 5-3 - Front Inlet Low Speed Recovery

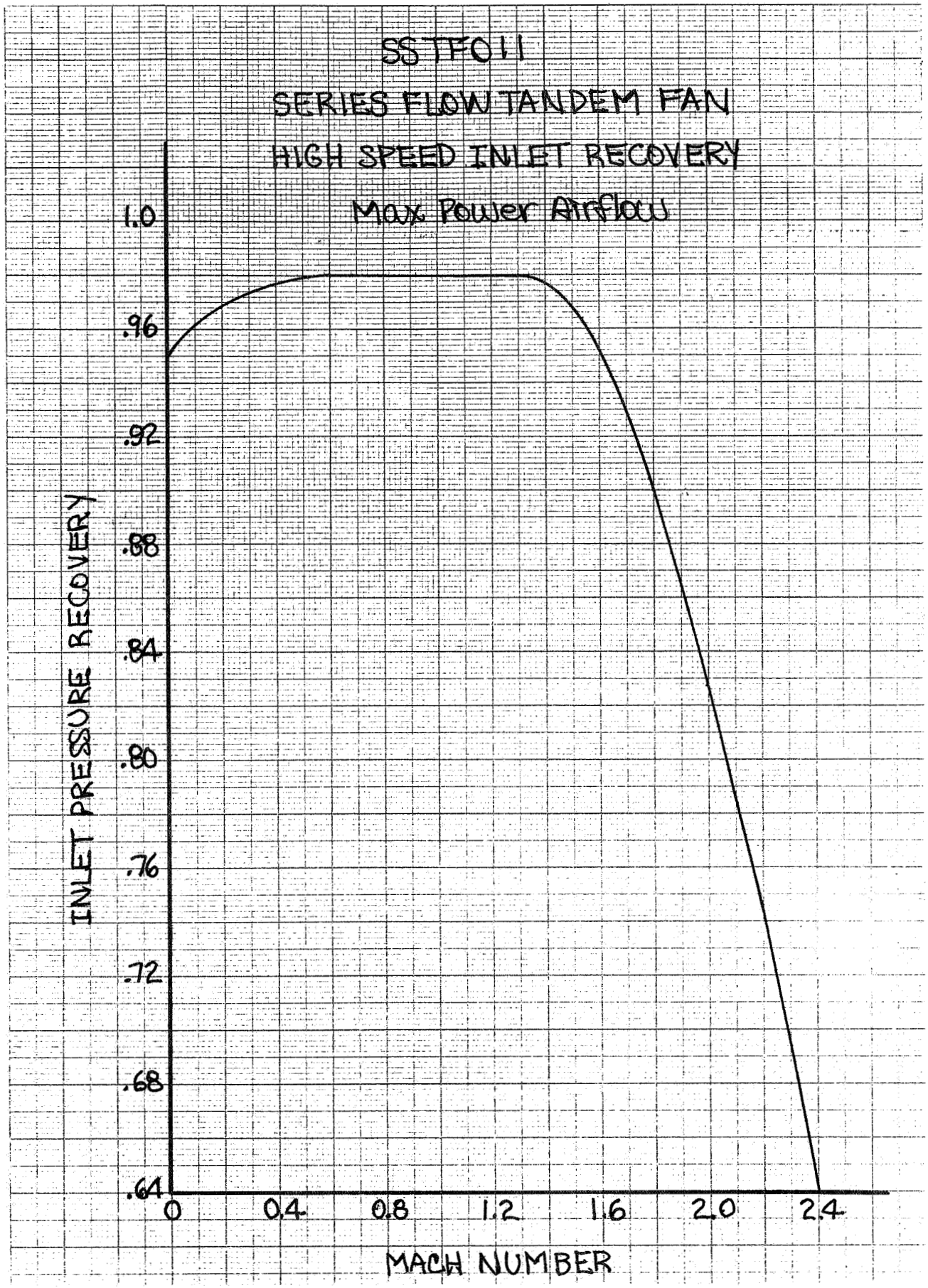

Figure 5-4 - Front Inlet High Speed Recovery

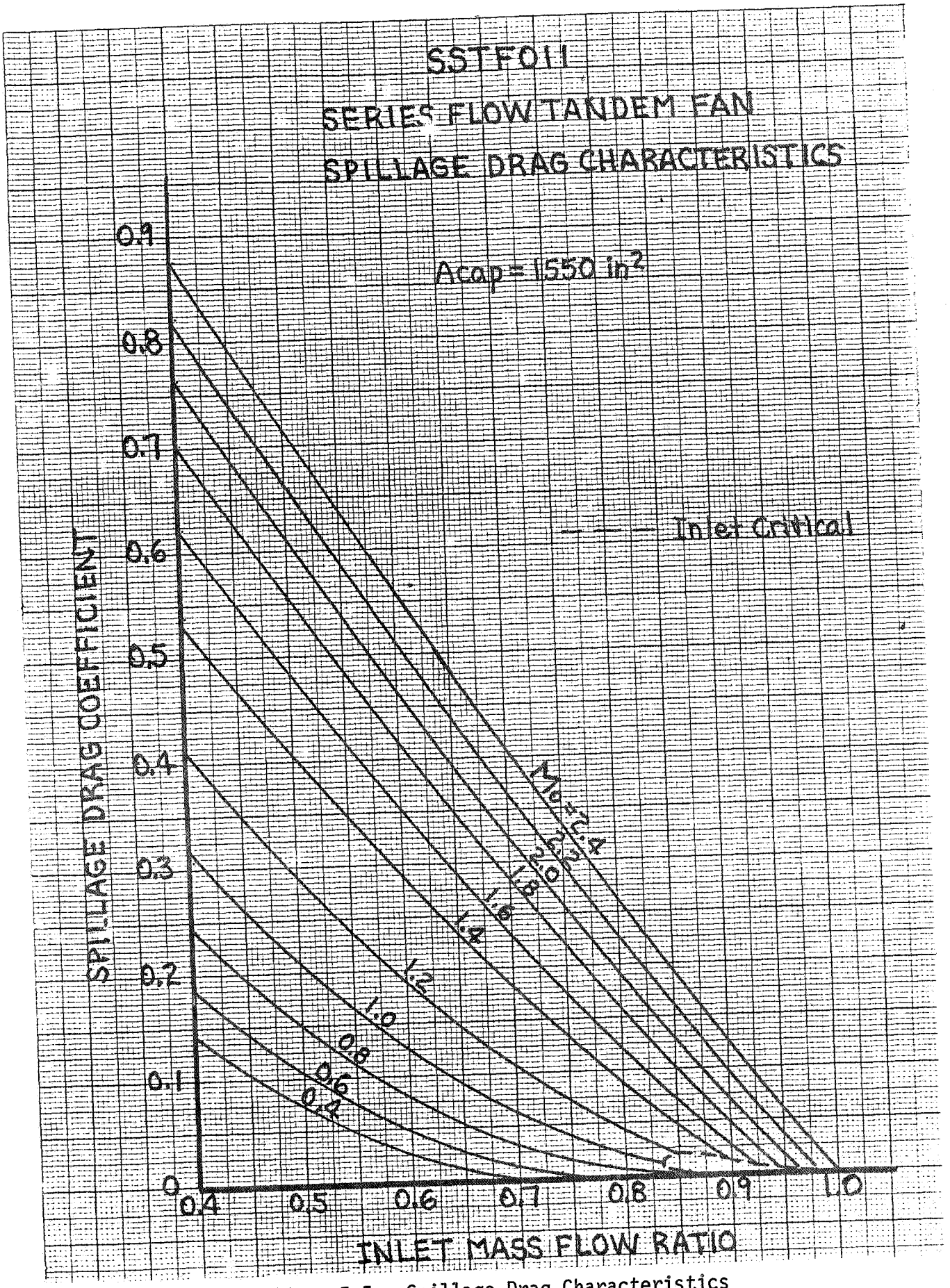

Figure 5-5 - Spillage Drag Characteristics

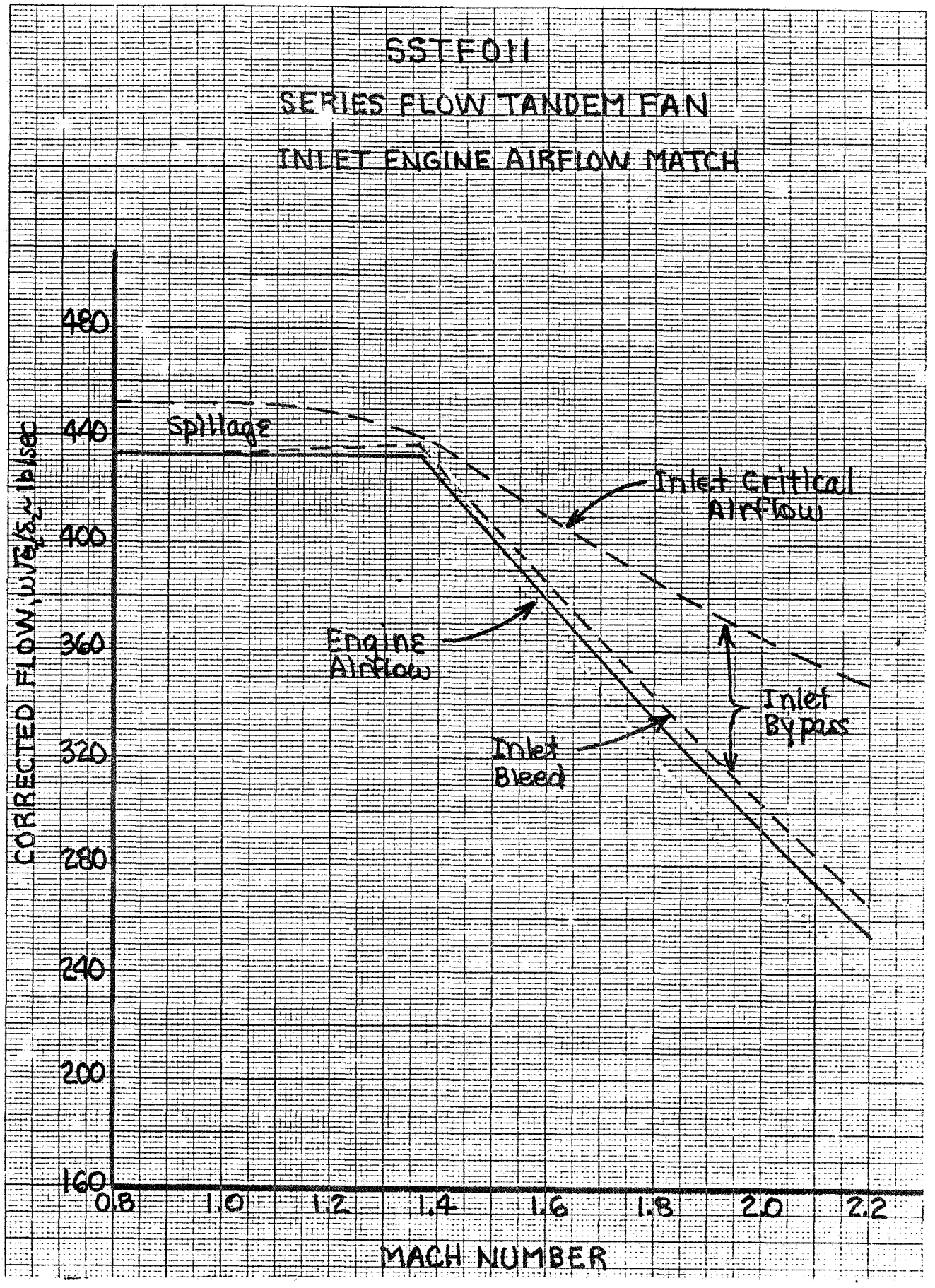

Figure 5-6 – Engine-Inlet Airflow Matching

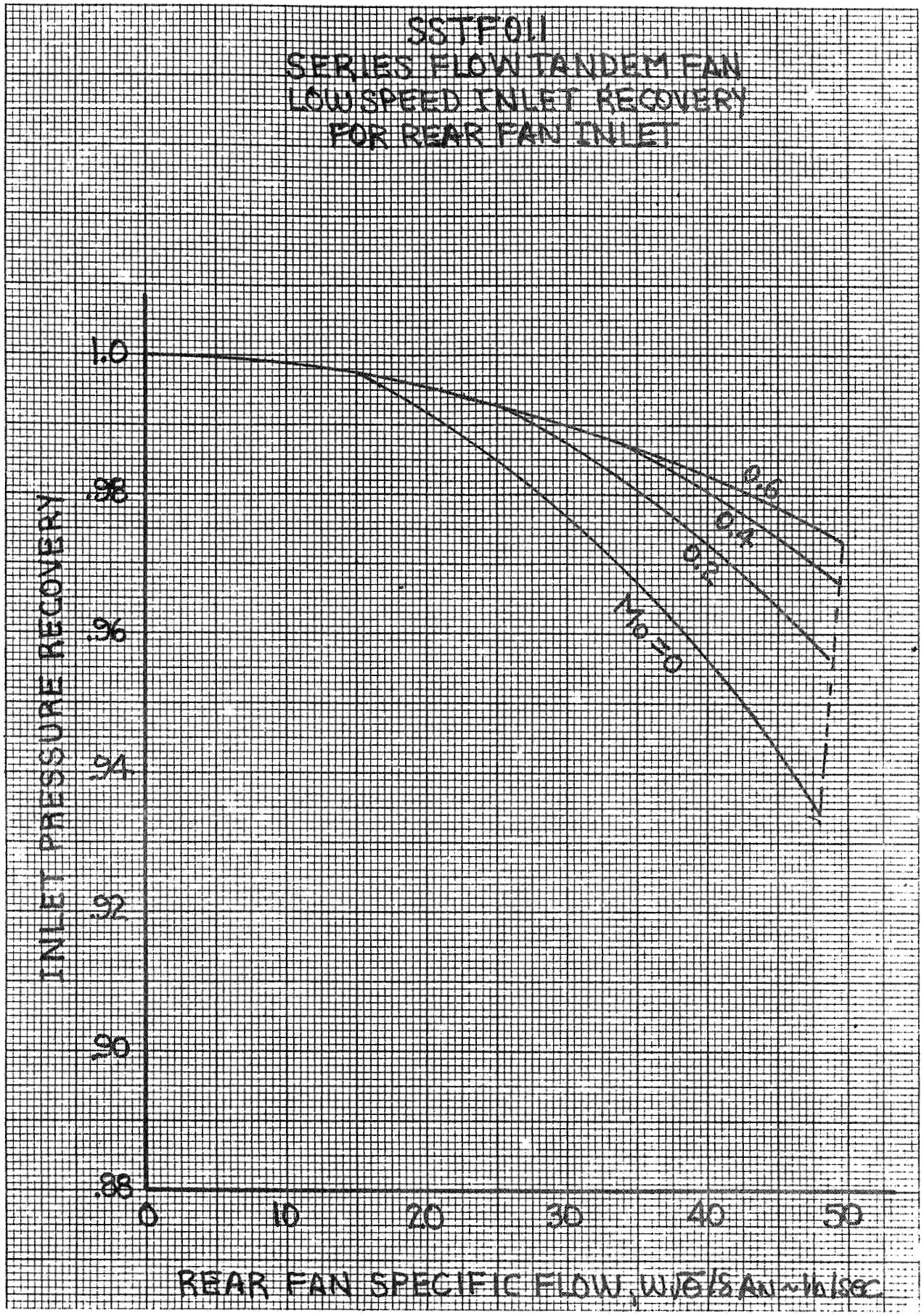

Figure 5-7 - Aft Inlet Pressure Recovery

5.3.3 Exhaust System

> The Tandem Fan incorporates deflecting forward and aft nozzles for vertical and cruise mode operation.

The front fan nozzle is used only used during vertical mode operation and transition. Variable flaps are used for nozzle exit area control and for deflecting thrust for attitude control and transition. The thrust vector is variable longitudinally up to ± 30 degrees. The front nozzle throat area varies between 680 and 1,020 in^2 depending upon the front burner exit temperature. For vertical mode operation, the throat area is typically 1,020 in^2 for maximum augmented takeoff and 680 in^2 for non-augmented landing. The thrust coefficient of this nozzle is estimated to be 0.95 for vertical operation.

The rear nozzle is a two dimensional, deflecting hooded nozzle for vertical mode or cruise operation. The nozzle in the cruise position consists of an adjustable upper ramp and a rotating lower flap to vary throat area. The effective area of the exit streamtube depends upon internal and external flow conditions. Performance of this nozzle was calculated as an optimum expanding C-D nozzle limited by a maximum streamtube area of 1,624 in^2. During afterburning cruise, the nozzle throat area varies from 693 to 1,552 in^2, changing the nozzle aspect ratio from 5.2 to 2.3. Without afterburning, the nozzle throat area is 693 in^2 with an aspect ratio of 5.2.

During vertical or STO operation, a deflecting hood rotates downward from the upper ramp to form a new external boundary. The lower variable flap then rotates downward through a range of positions to vary throat area from 777 to 1440 in^2 but can be set at a predetermined value similar to the front nozzle. Throat area variation is required only during STO takeoff. The thrust coefficient during vertical operation is estimated to be 0.95.

5.3.4 Attitude Control System

> The Tandem Fan uses a combination of variable inlet guide vanes, engine bleed, and deflector vanes for aircraft attitude control.

The Tandem Fan uses variable fan inlet guide vanes (VIGV) for pitch control. The guide vanes change the incoming flow velocity and direction ahead of the fan rotor, producing changes in fan airflow and pressure ratio. By closing the IGVs and reducing flow by 40 percent, thrust modulation of 50 to 70 percent can be achieved depending upon fan pressure ratio. The SSTF011 Tandem Fan can vary front fan thrust ±5,000 lb and rear fan thrust ±3,500 lb while maintaining constant 100 percent fan speed. During augmented takeoff, the fan IGVs and burner fuel flows are varied simultaneously while holding nozzle area constant. This simultaneous variation maintains a constant fan operating line and avoids the necessity for a rapid response variable area nozzle.

Aircraft roll control is accomplished by means of engine bleed. Air is taken from compressor discharge and ducted to roll nozzles in the aircraft wingtips. A demand bleed system is used. At the nominal takeoff condition with max roll commands, the engine supplies 2 percent of the core airflow, which produces 250 lb of bleed thrust. The bleed ducts are approximately 2 inch diameter lines and experience a 15 percent pressure drop at max flow conditions.

Yaw control and lateral translation is achieved by asymmetric and symmetric deflection of deflector vanes in the aft nozzle and the exit flaps of the front nozzle. The vane system is capable of providing up to 8 degrees of thrust deflection for yaw control, resulting in a 1 percent loss in the vertical thrust component.

5.4 INSTALLED PERFORMANCE

5.4.1 Installation Losses

> Tandem Fan installation losses include inlet and nozzle losses plus engine bleed and power extraction.

Vertical and cruise mode performance calculations included the following installation effects:

- o inlet pressure recovery
- o inlet system drag
- o ECS bleed extraction
- o RCS bleed extraction
- o horsepower extraction
- o nozzle thrust coefficient
- o nozzle reference drag

Characteristics of the fore and aft inlets are described in Section . Front inlet critical mass flow, pressure recovery, and drag characteristics are shown in Figures 5-3 through 5-6. The front inlet system drag includes critical and subcritical spillage drag, bleed drag, and bypass drag. Boundary layer diverter drag is included in the airplane drag. Pressure recovery of the aft inlet is shown in Figure 5-7. Nominal pressure recovery of both inlets at takeoff is 0.95.

Compressor bleed and power extraction include environmental control, hydraulic, and electrical system loads plus attitude control in the vertical mode. The ECS bleed extraction on a Standard Day is shown in Figure 5-8. Vertical takeoff, hover, and landing bleed on a Tropical Day is 1.0 lb/sec. The power extraction is 70 hp with for afterburning and 50 hp unaugmented.

Nozzle thrust coefficient effects are included in engine performance. During vertical mode operation, both nozzles have a constant 0.95 thrust coefficient. In the cruise mode, the aft nozzle is modeled as an optimum expansion C-D nozzle with a constrained exit streamtube area. The effects of exit streamtube area variations is included in aircraft drag.

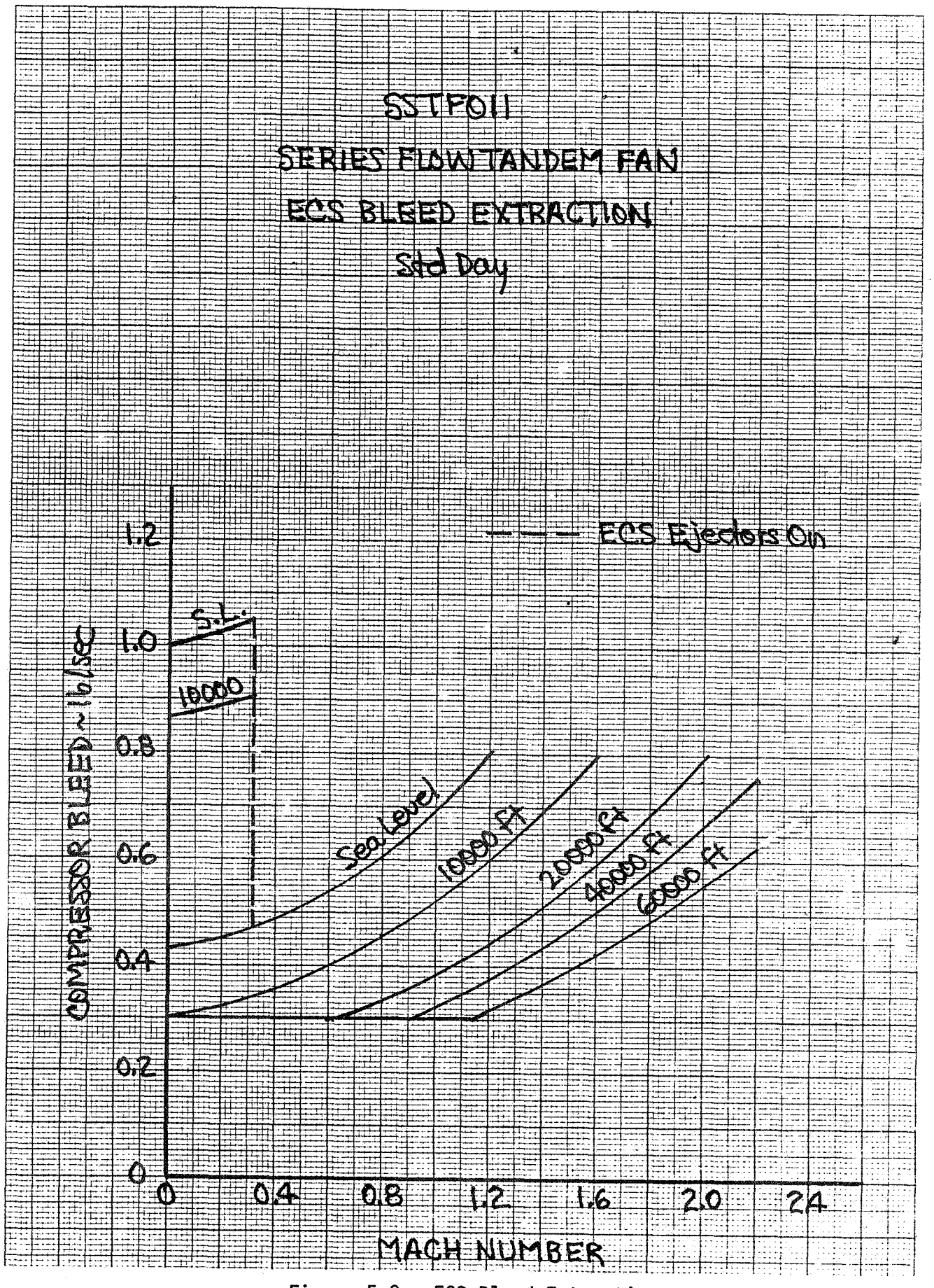

Figure 5-8 - ECS Bleed Extraction

Installation losses at typical operating points are summarized in Table 5-2.

Table 5-2 - Representative Installation Losses

Altitude	SL	10,000	40,000	40,000	60,000
Mach	0	0.9	0.85	1.6	2.0
Type Day	Trop	Std	Std	Std	Std
Rating	Max Dry Vertical	Max A/B Combat	Non A/B Cruise	Max A/B Combat	Part A/B Cruise
Net Thrust, lb	25,000	43,560	2,630	25,685	7,625
Fuel Flow, lb/hr	13,520	96,590	2,210	56,820	17,975
Front Inlet Recovery	0.95	0.982	0.995	0.953	0.827
Aft Inlet Recovery	0.95	-	-	-	-
Front Inlet Drag, lb	0	75	80	625	570
Engine Bleed, lb/sec	1.0	0.49	0.30	0.50	0.55
Power Extraction, hp	50	70	50	70	70
Front Nozzle Cfg	0.95	-	-	-	-
Rear Nozzle Cfg	0.95	0.98	0.98	0.94	0.93

5.4.2 Cruise Mode Performance

> The SSTF011 Tandem Fan in the cruise mode is an efficient cycle for supersonic tactical aircraft.

In the cruise mode the Tandem Fan operates as a conventional mixed flow turbofan. Air enters the front fan inlet and passes through both fan units, thus supercharging the engine core. The net resulting fan pressure ratio is 3.43 with a bypass ratio near 1.0. The engine exhaust then exits through the aft 2-D deflecting nozzle.

Cruise mode performance was calculated using the Vought TECSON turbine engine cycle simulation routine. Non-afterburning power settings were generated by commanding lines of corrected fan speed while applying combustor temperature limits. A combustor temperature limit of 2,800°F was used for Intermediate power and a limit of 2,600°F for maximum continuous. Afterburning power settings were generated from Min to Max A/B, limited by a fuel/air ratio of 0.06 and an exit temperature of 3,400°F.

Cruise mode performance at representative mission points is summarized in Table 5-3. The performance is based on the installation losses discussed in Section 5.4.1.

During cruise mode operation, the fan IGV angles are scheduled to maintain constant fan operating lines while matching flow between the front and rear fans. The operating lines maintain peak fan efficiency and the desired stall margin at all operating points. The aft nozzle throat area is held constant during non-afterburning and varies during afterburning to maintain the fan operating lines. The IGV schedules required for optimum flow matching depend upon the design fan pressure ratios and the ratio of annulus areas between fans.

Table 5-3 - Cruise Performance Summary

Altitude ~ ft	Mach	Power Setting	Thrust ~ lb	Fuel Flow ~ lb/hr	SFC ~ lb/hr/lb
SL	0	Interm	26,485	17,600	0.665
SL	0.85	Interm	23,277	23,066	0.991
10,000	0.90	Interm	19,817	19,305	0.974
30,000	0.90	Interm	9,687	8,633	0.891
40,000	0.85	Interm	5,786	4,895	0.846
40,000	0.85	Cruise	2,600	2,314	0.890
SL	0.27	Loiter	2,000	2,250	1.125
SL	0	Max A/B	43,842	88,749	2.024
10,000	0.90	Max A/B	43,518	96,237	2.211
30,000	0.90	Max A/B	22,095	47,844	2.165
40,000	1.60	Max A/B	25,720	56,870	2.211
50,000	1.60	Part A/B	8,056	10,965	1.361
60,000	2.00	Part A/B	7,626	17,975	2.357
50,000	2.40	Max A/B	14,734	43,618	2.960

5.4.3 VTOL Performance

> The Tandem Fan propulsion system provides vertical lift for a supersonic aircraft with moderate jet velocities, exit temperatures, and fuel consumption.

The cycle characteristics of the Tandem Fan allow the propulsion system to operate at high airflow and bypass ratio during vertical mode operation. This translates into reduced jet velocities and exit temperatures, which in turn reduce footprint profiles and reingestion losses. The cycle operates at a specific fuel consumption of approximately 1.0 for takeoff and 0.5 for landing, much reducing the fuel allowances usually associated with supersonic V/STOL. Limited augmentation at the front nozzle reduces propulsion system size without exceeding the rear nozzle temperature.

V/STOL parallel flow mode performance and cycle characteristics is summarized in Table 5-4 for typical operating points. "Max Lift, Dry" is the cycle design point for component flows and pressure ratios. "Max Lift A/B" is the corresponding point with maximum augmentation front and rear. This rating is used for STO. "Max Takeoff, A/B" is the maximum takeoff thrust for an aircraft with a 67/33 thrust split. The Max Takeoff rating provides an aircraft thrust/weight of 1.17 for maximum heave and pitch commands. The 'Nominal Takeoff, A/B" case is the normal takeoff thrust level without pitch commands. The "Max Vertical, Dry" case is the maximum nonaugmented thrust level at 67/33 thrust split. "Nominal Landing, Dry" is for a typical landing weight with normal return stores and fuel reserves.

Table 5-4 - VTOL Performance Summary

Rating	Aircraft T/W	Total Thrust ~ lb	Total Fuel Flow ~ lb/hr	Thrust Split	Front Fan FPR	Rear Fan FPR	Front Nozzle Temp ~ °F	Rear Nozzle Temp ~ °F
Max Lift, Dry(1)	-	25,000	13,520	60/40	2.20(1)	1.75	250	975
Max Lift, A/B(2)	-	34,000	60,285	60/40	2.20(1)	1.75	950	2,800(3)
Max Takeoff/A/B	1.17(3)	29,285(5)	27,550	67/33	2.11	1.73	950	910
Nominal Takeoff, A/B	1.10(4)	27,535	26,405	67/33	2.06	1.70	910	860
Max Vertical, Dry	1.232	22,400	12,105	67/33	2.20	1.51	250	985
Nominal Landing, Dry	1.10	20,000(6)	10,435	67/33	2.03	1.46	235	900

Notes:
(1) Cycle design point, not used for aircraft sizing
(2) Same as (2) with max A/B, used only for STO takeoff
(3) Includes margin for reingestion, suckdown, engine deterioration, max vertical acceleration and pitch up commands
(4) Same as (3) but without pitch thrust commands
(5) Used for aircraft sizing, TOGW = 24,930 lb.
(6) Actual landing weight and thrust depend on fuel and stores returned

5.4.4 STO Performance

> The Tandem Fan propulsion system provides high thrust for short takeoff.

Short takeoff performance (STO) for parallel flow mode is shown in Figure 5-16 and 5-17. The performance is with and without afterburning at Sea Level, Tropical Day. The figures include ram drag and gross thrust for each stream versus flight Mach number and nozzle deflection angle in addition to net thrust and fuel flow.

During short takeoff the front nozzle is deflected aft 10 to 30 degrees to increase forward thrust, while the aft nozzle is deflected 20 to 45 degrees to cancel the front fan pitching moment.

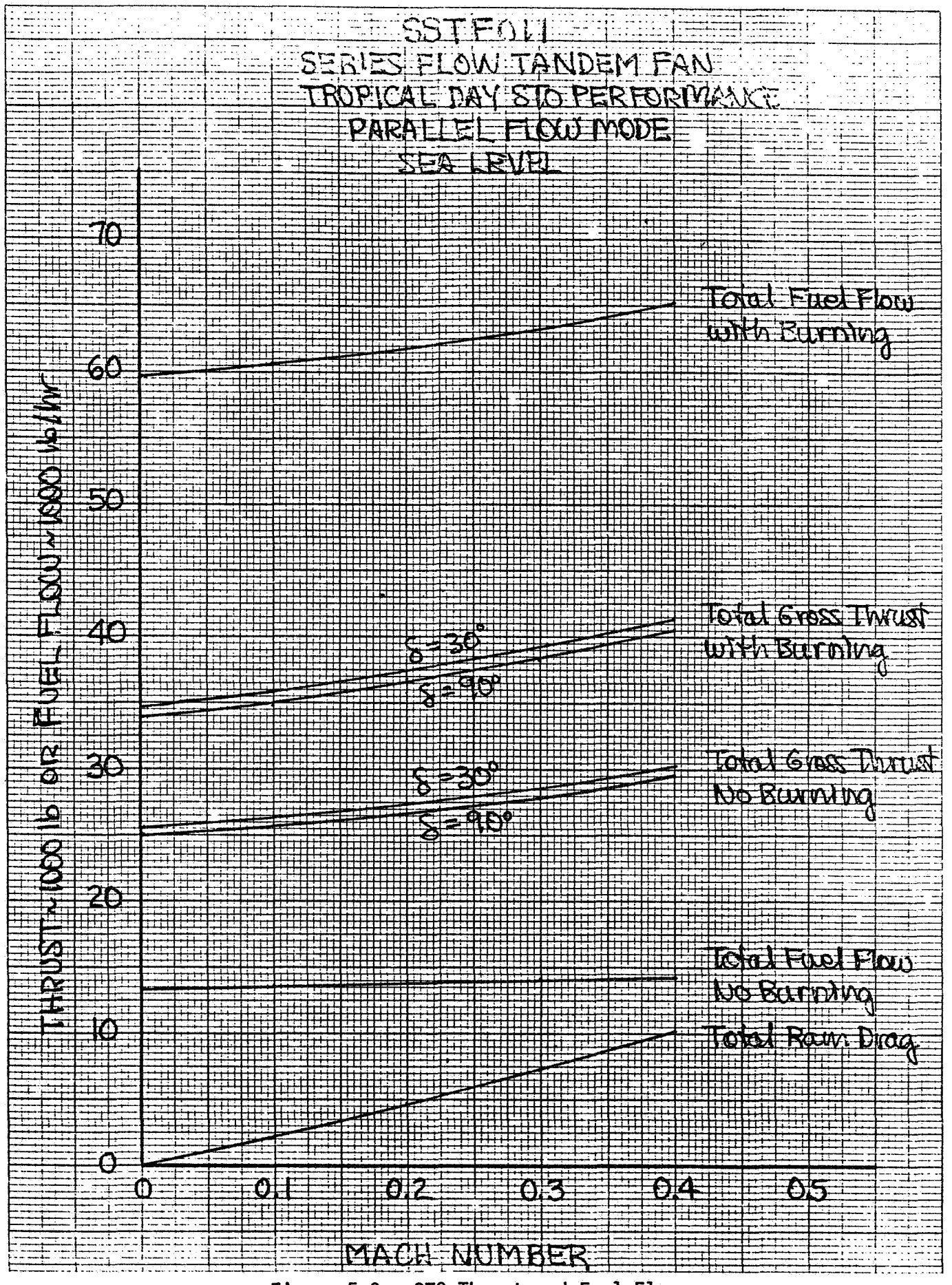

Figure 5-9 - STO Thrust and Fuel Flow

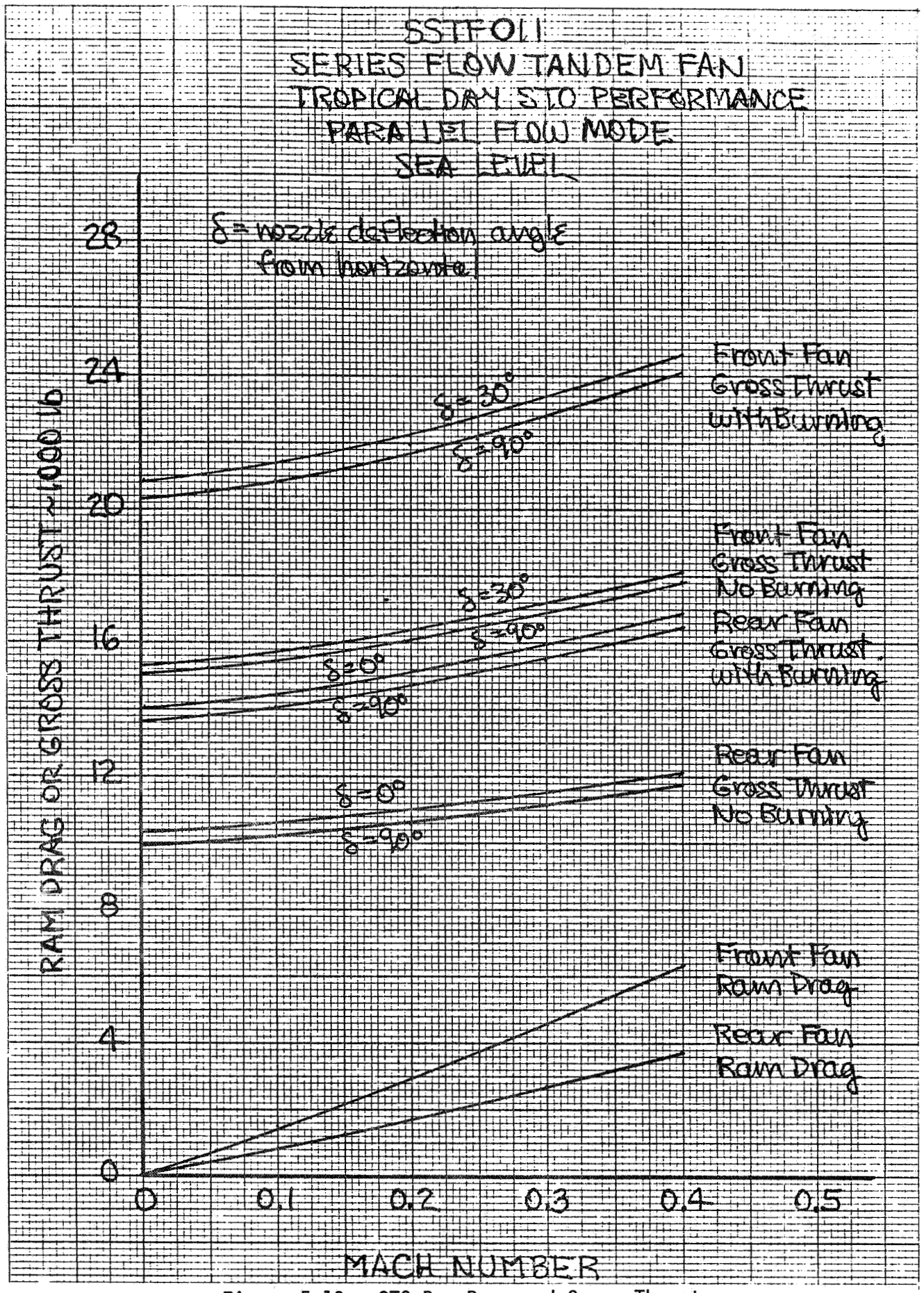

Figure 5-10 - STO Ram Drag and Gross Thrust

6.0 TF120 PERFORMANCE

This section presents mission, combat and takeoff performance of the TF120 point design sized to the study guidelines, design sensitivities, and an analysis of VSTOL transition.

This section contains:

6.1 POINT DESIGN

6.1.1 Sizing

> The TF120 was sized for a supersonic intercept mission and to VTOL thrust-to-weight and maneuver constraints.

Design synthesis was accomplished using the Vought Aircraft Synthesis Analysis Program (ASAP) implemented on a Control Data Corporation CYBER 175 computer with interactive graphics capability. ASAP is also used by Naval Air Systems Command and is being implemented at the Naval Air Development Center. The ASAP modular architecture is diagrammed in Figure 6-1. ASAP integrates the estimation methods from the various technical disciplines required to define an aircraft (for this study, aerodynamics, propulsion, weights and performance) and generates a design space for a matrix of configuration variables. Wing area and engine scale factor were selected as independent variables since the wing planform had previously been optimized for the same mission and maneuverability requirements as described in Reference 1.

The TF120 baseline configuration (wing reference area = 350 ft^2 and unity engine scale factor) was the center of a nine point design space. Figure 6-2 shows the takeoff weight variation with Engine Scale Factor (ESF) and Wing Area. All aircraft represented in Figure 6-2 have been fuel balanced to yield the same radius of action (200 NMi) for the Supersonic Intercept (or DLI) design mission defined in Section 6.1.2. The two critical sizing constraints are overlaid to show the portion of the design space in which the aircraft meet or exceed all performance requirements. All aircraft in the design space exceed the other performance guidelines.

Figure 6-2 reveals that the propulsion system is sized primarily by the VTO (parallel flow mode with front fan augmentation) thrust-to-weight requirement of 1.17, which meets MIL-STD-83300 Level 1 flying qualities. Minimum wing area is dictated primarily by the sustained load factor guideline

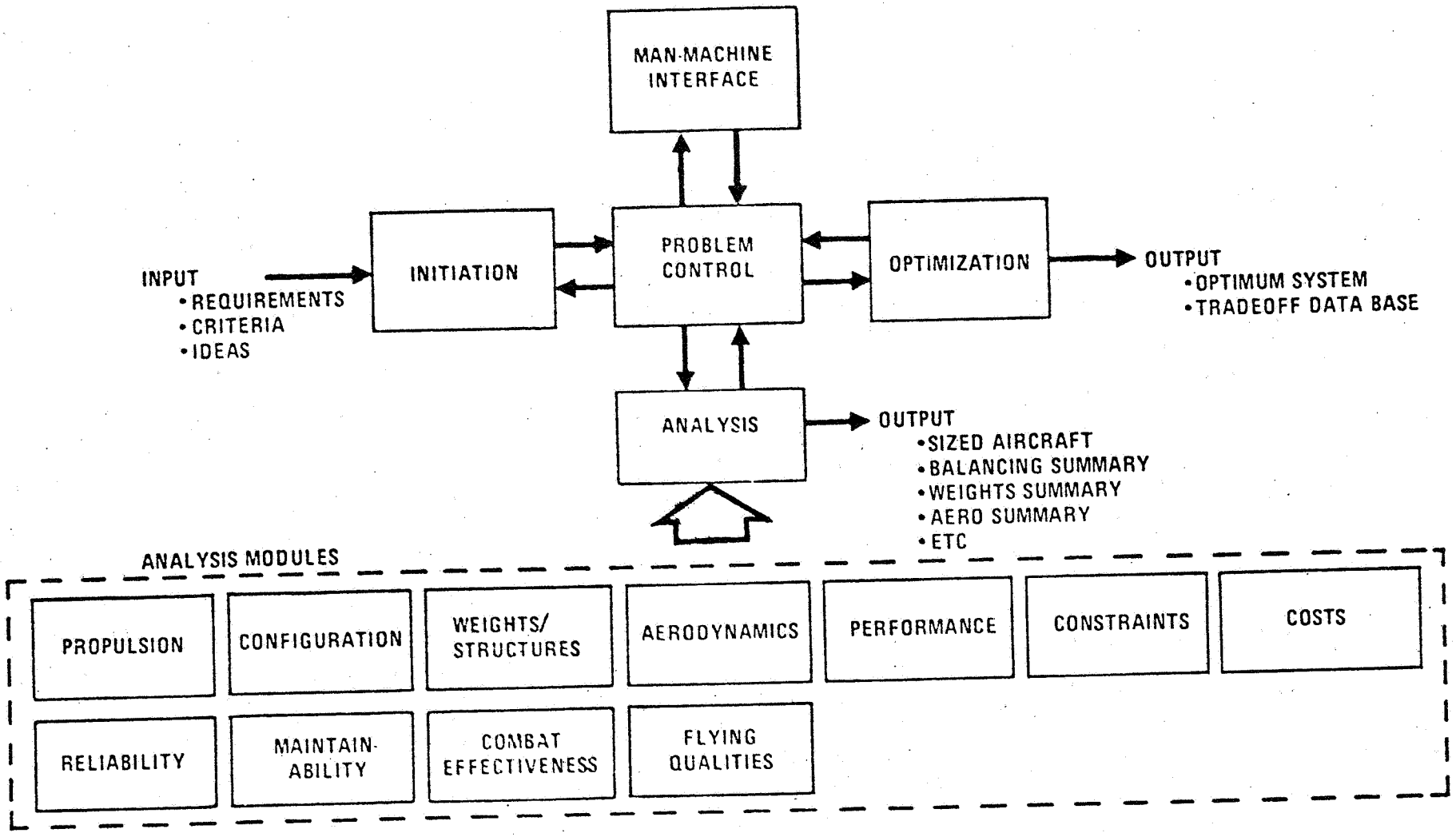

Figure 6-1 - Aircraft Synthesis Analysis Program (ASAP) Architecture

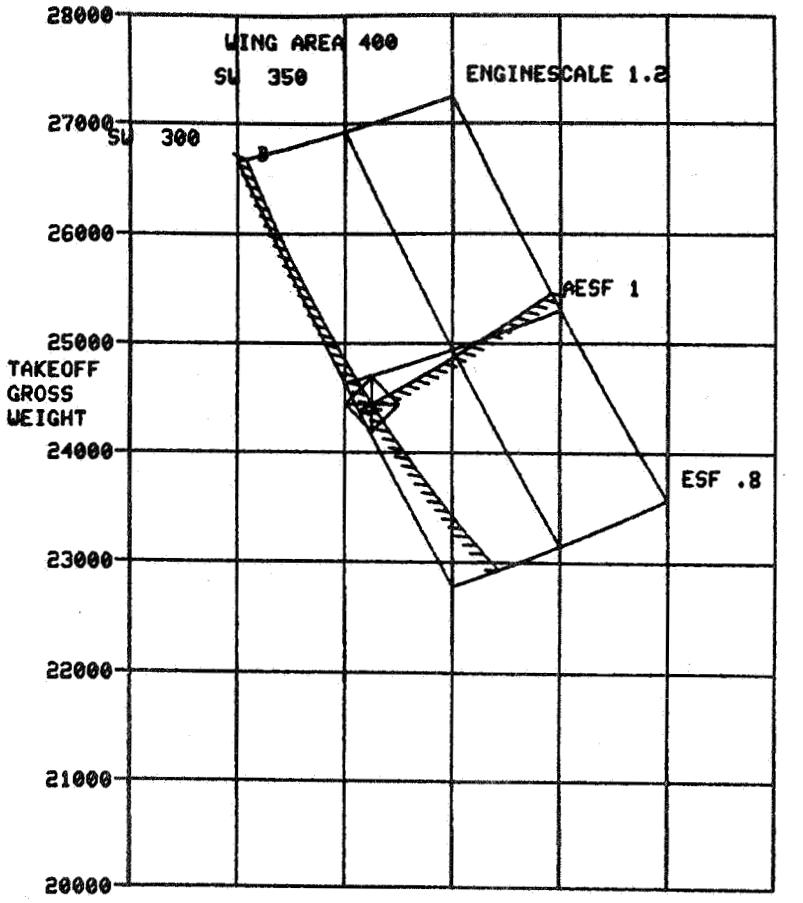

SYMBOL	CONSTRAINT	TYPE	VALUE
A	THRUST TO WEIGHT	GT	1.170
B	EQUIL. NZ - 10KM= .60	GT	6.200

Figure 6-2 - TF120 Parametric Takeoff Weight Sizing

of 6.2 at Mach 0.6, 10,000 ft. The minimum size airplane which satisfies the sizing constraints weights 24,440 lb, has a 307 ft^2 wing area and a 0.98 scale engine (42,960 lbs, installed, series flow mode, max A/B, sea level static).

The baseline aircraft meets the VTO T/W = 1.17 requirement and exceeds the maneuverability guideline with a sustained load factor capability of 6.62 at Mach 0.6, 10,000 ft. This is achieved at a lift coefficient of 1.13. This result is a strong function of high angle of attack trimmed L/D, which is difficult to predict accurately because of the large portion of the theoretical wing enveloped by the wing-body blending. We elected to define the 350 Ft^2 TF120 as the point design and exceed the maneuverability guideline. Detailed mission capability and performance are presented in the following subsections.

6.1.2 Mission Capability

> The TF120 offers good radius of action capability for a variety of fighter and strike mission profiles.

The TF120 design was tested against three basic mission profiles, with variations, depicted in Figure 6-3. The Supersonic Intercept, or Deck Launched Intercept (DLI) was the design mission. A radius of action of 200 NMi with a Mach 1.6 dash at 50,000 ft was specified to establish internal fuel capacity. For all other missions, radius was determined for the same internal fuel load. In all cases air-to-air missiles and aummunition are retained.

Figure 6-4 summarizes the mission capability of the TF120 point design. The 200 NMi radius is feasible at moderate takeoff weight because of excellent acceleration (1.8 minutes from launch to Mach 1.6 at 50,000 ft) and moderate specific fuel consumption in supersonic cruise (1.36 lb/hr/lb). Note that the Supersonic Intercept dash can be performed at Mach 2.0 and the TF120 will still be capable of a 139 NMi radius of action.

Fighter Escort (FE) is an all-subsonic mission, with an internal fuel radius of 541 NMi. With the addition of two 370 gal drop tanks (and two more missiles) the TF120 is capable of an FEX radius of 838 NMi, an increase of 55 percent.

The powerful effect of fuel allowances is illustrated by comparing Fighter Escort radius with combat (2 min Max A/B at Mach 1.0) at an altitude of 30,000 ft vs. 10,000 ft. The lower altitude reduces radius of action from 541 NMi to 322 NMi. A task-oriented combat segment would tend to equalize mission fuel for aircraft with widely differing thrust-to-weight ratios.

The Interdiction (INX) hi-lo-lo-hi missions represented in Figure 6-4 were calculated with a 9,724 lb overload referenced to the VTO takeoff weight. Radius with fixed Mach 0.85 sea level dashes of 50 and 100 NMi were calculated. When the low altitude dash distance is halved, radius increases from 519 NMi to 641 NMi.

SUPERSONIC INTERCEPT (SI)

4 AMRAAM

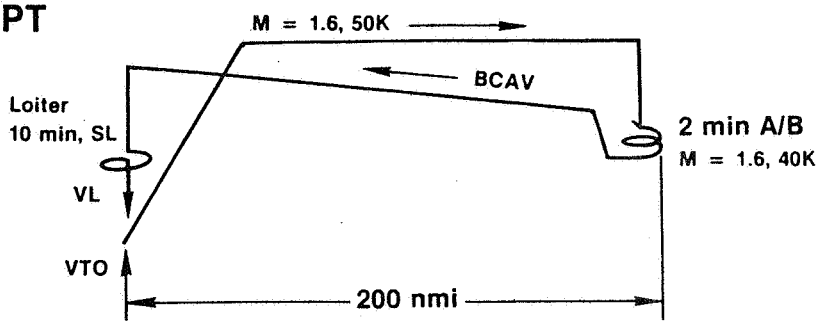

FIGHTER ESCORT (FE)

(FEX)

4 AMRAAM
+2 SRAAM
+2 Tanks

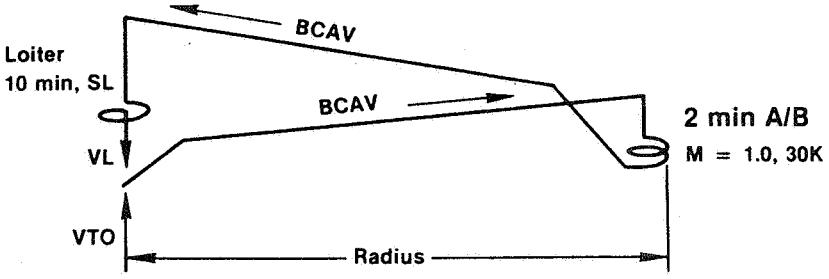

INTERDICTION (INX)

4 LG Bombs
+2 SRAAM
+2 Tanks

400 Rounds 20mm Retained. All Missiles Retained. Tanks Retained until Dash or Combat

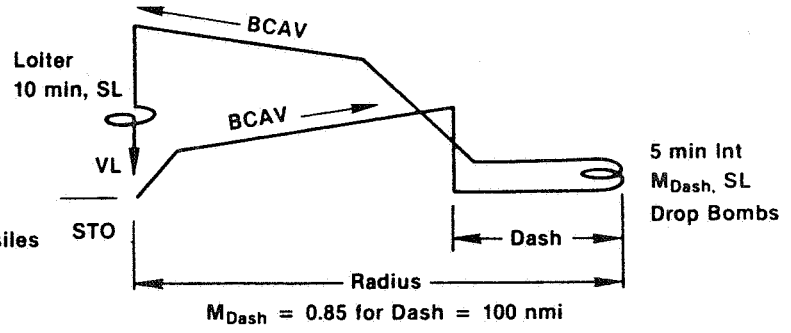

Figure 6-3 - Mission Profiles Used in the Study

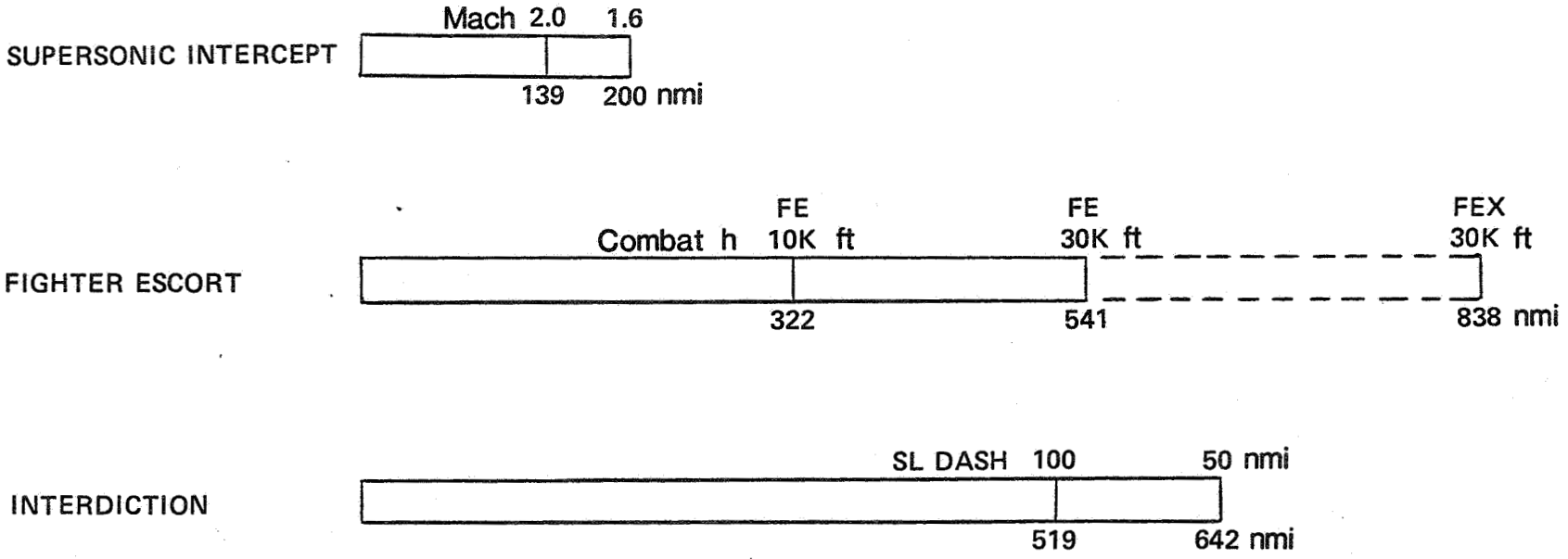

Figure 6-4 - TF120 Mission Capability Summary

6.1.3 Combat Performance

> The TF120 exhibits exceptional energy maneuverability and combat agility.

Point design performance is summarized in Table 6-1. All parameters were calculated at 88 percent of VTO weight, which corresponds to 64.7 percent internal fuel. The TF120 exceeds NASA guidelines by a wide margin. The specific excess power capability is nearly twice the minimum requirement. Acceleration time from Mach 0.8 to 1.6 is a brisk 34 seconds. Maximum speed at altitude is limited to Mach 2.4 by aerodynamic heating. The actual thrust = drag condition occurs at Mach 2.55, despite a rapid decay of inlet pressure recovery above Mach 2. The design dynamic pressure corresponds to Mach 1.2 at sea level.

Note that Mach 1.42 can be sustained without afterburning. This is tactically significant because of the concurrent low infrared signature. Supersonic cruise at Mach 1.6 is possible with near-minimum afterburner assist.

Sustained load factor is 6.62g at the Mach 0.6, 10,000 ft design condition. Of greater significance to the deck launched intercept role is the 4.22g capability at Mach 1.6. This facilitates multiple attacks against supersonic maneuvering targets without decelerating.

Figure 6-5 presents the TF120 operational envelope for both maximum A/B and Intermediate thrust. Contour maps of sustained load factor (NZ) with A/B are given in Figure 6-6, and with Intermediate thrust in Figure 6-7. Note that contours for NZ = 8 and 9 appear on the map; the point design was stressed for 7.5g design load factor. Corresponding maps of specific excess power (SEP) appear in Figures 6-8 and 6-9.

Another presentation of energy maneuverability, max thrust SEP as a function of Mach number and load factor, is provided in Figures 6-10, 6-11 and 6-12, for altitudes of 10,000, 20,000 and 30,000 feet, respectively.

Table 6-1 - TF120 Point Design Performance

PARAMETER	MAX A/B	INTERMEDIATE	NASA GUIDELINES
MAXIMUM MACH NUMBER			
36,089 ft	2.55 (2.4 LIMIT)	1.42	1.6
SEA LEVEL	1.55 (1.2 LIMIT)	0.99	
ABSOLUTE CEILING - FT	66,850	53,580	
COMBAT CEILING (500 FPM)	66,550	52,950	
SPECIFIC EXCESS POWER (1g)			
M=0.9, 10,000 ft - ft/SEC	1,725		900
ACCELERATION TIME			
$0.8 \leq MM \leq 1.6$, 36,089 ft-SEC	34		
SUSTAINED LOAD FACTOR			
M=0.6, 10,000 ft	6.62		6.2
M=0.9, 30,000 ft	4.62		
M=1.6, 40,000 ft	4.22		

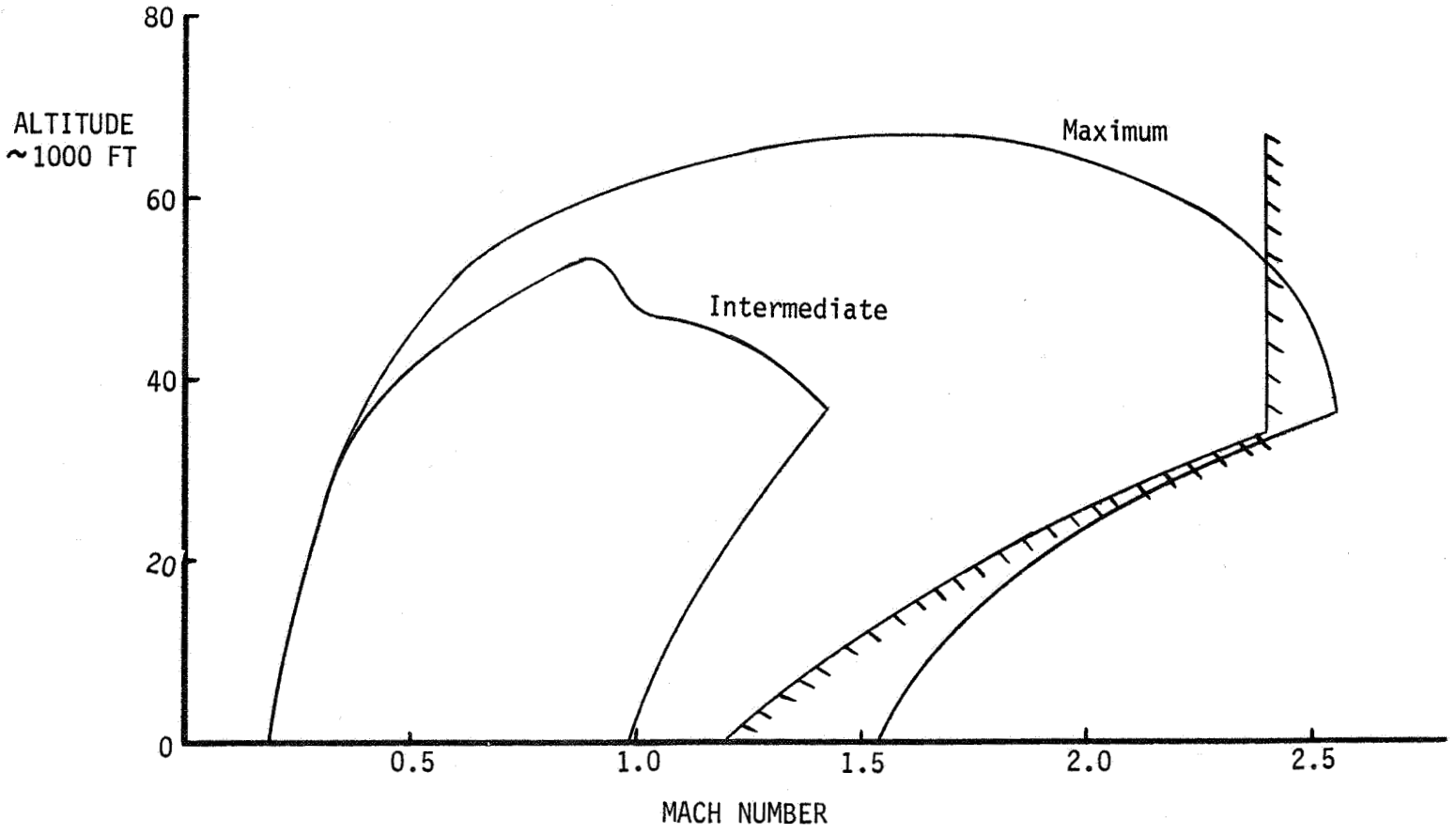

Figure 6-5 - TF120 Operational Envelope

MAXIMUM A/B

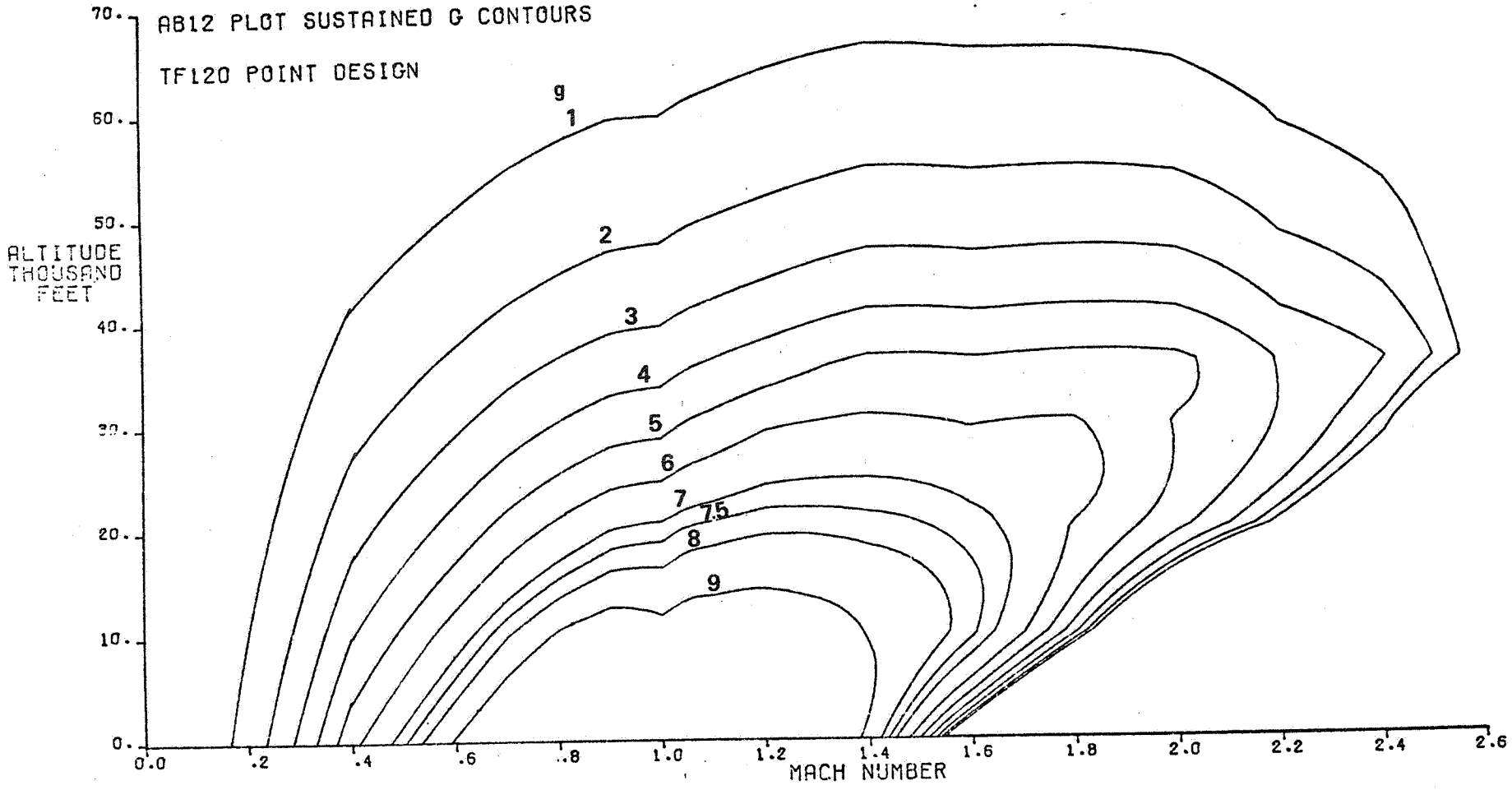

Figure 6-6 - TF120 Sustained Load Factor Capability - Maximum Thrust

INTERMEDIATE

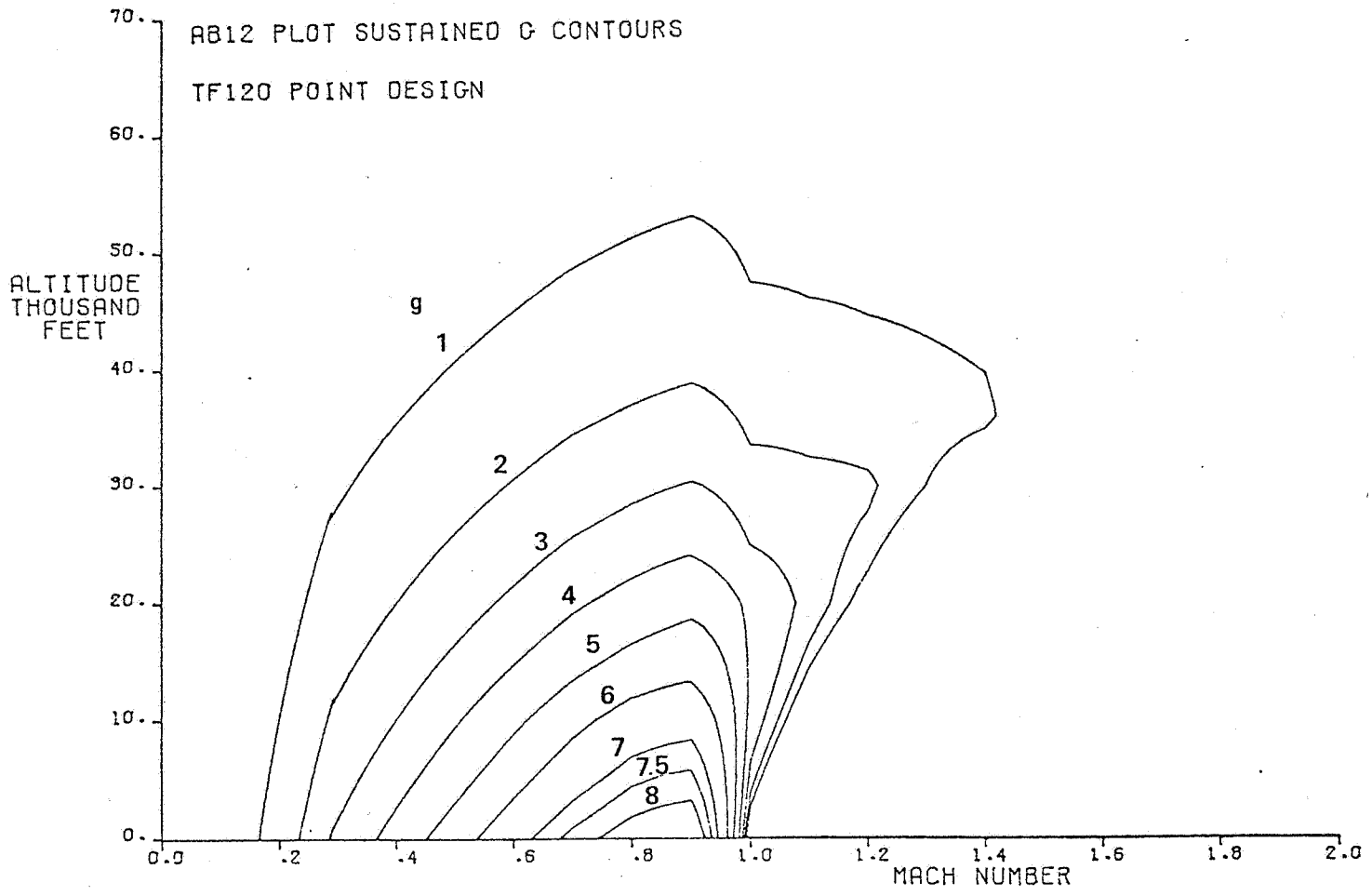

Figure 6-7 - TF120 Sustained Load Factor Capability - Intermediate Thrust

MAXIMUM A/B

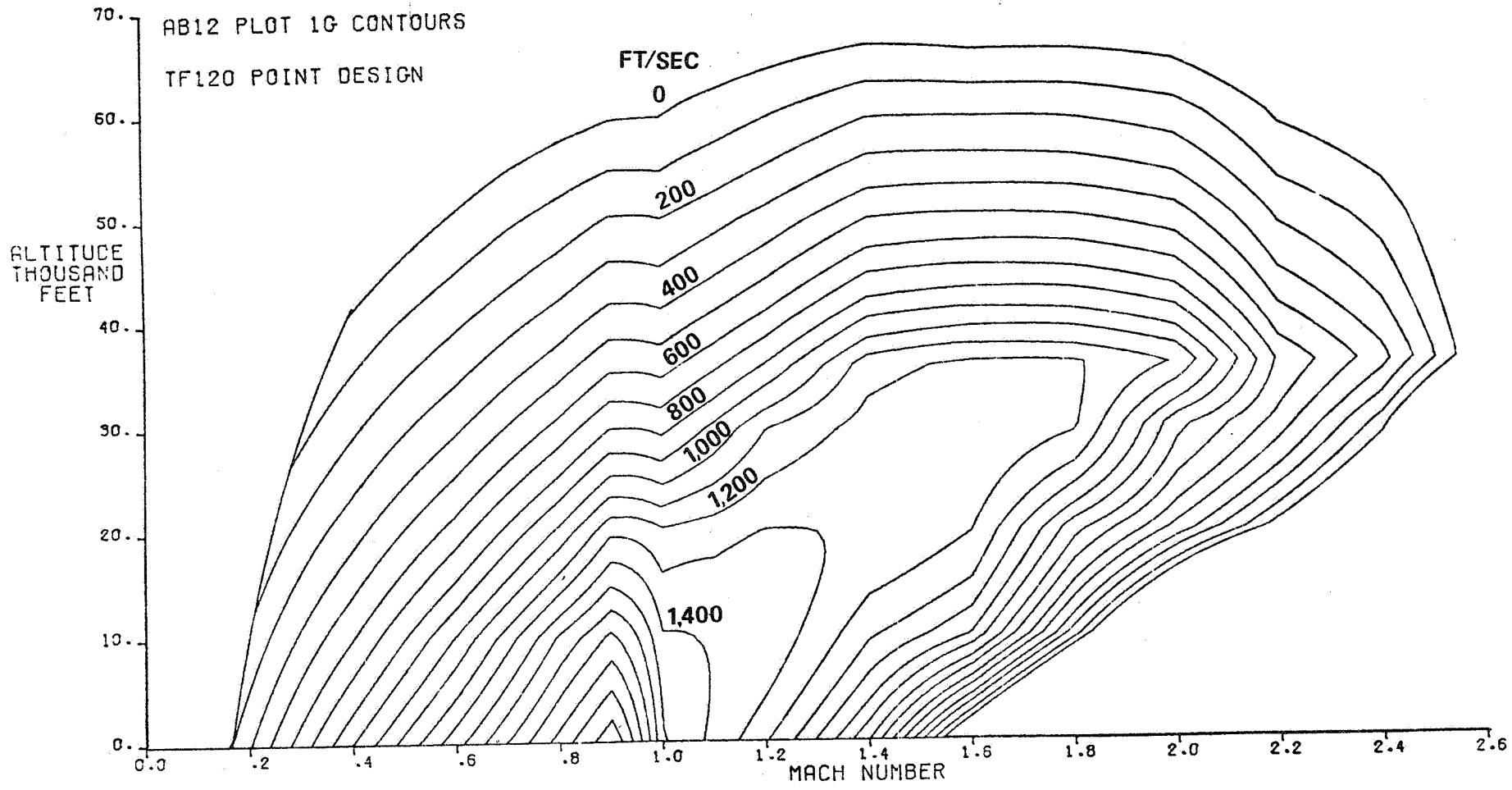

Figure 6-8 – TF120 Specific Excess Power – Maximum Thrust

INTERMEDIATE

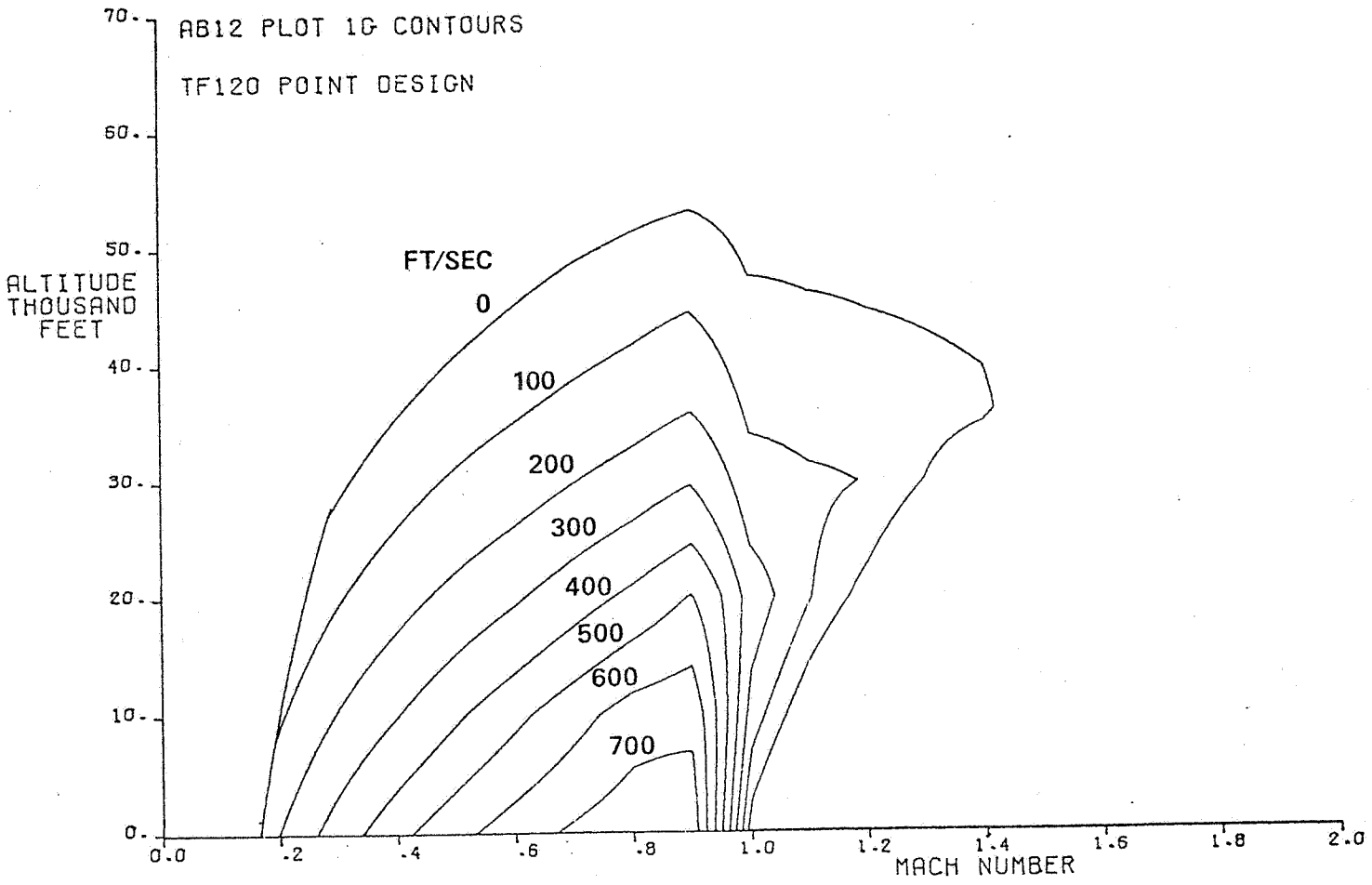

Figure 6-9 - TF120 Specific Excess Power - Intermediate Thrust

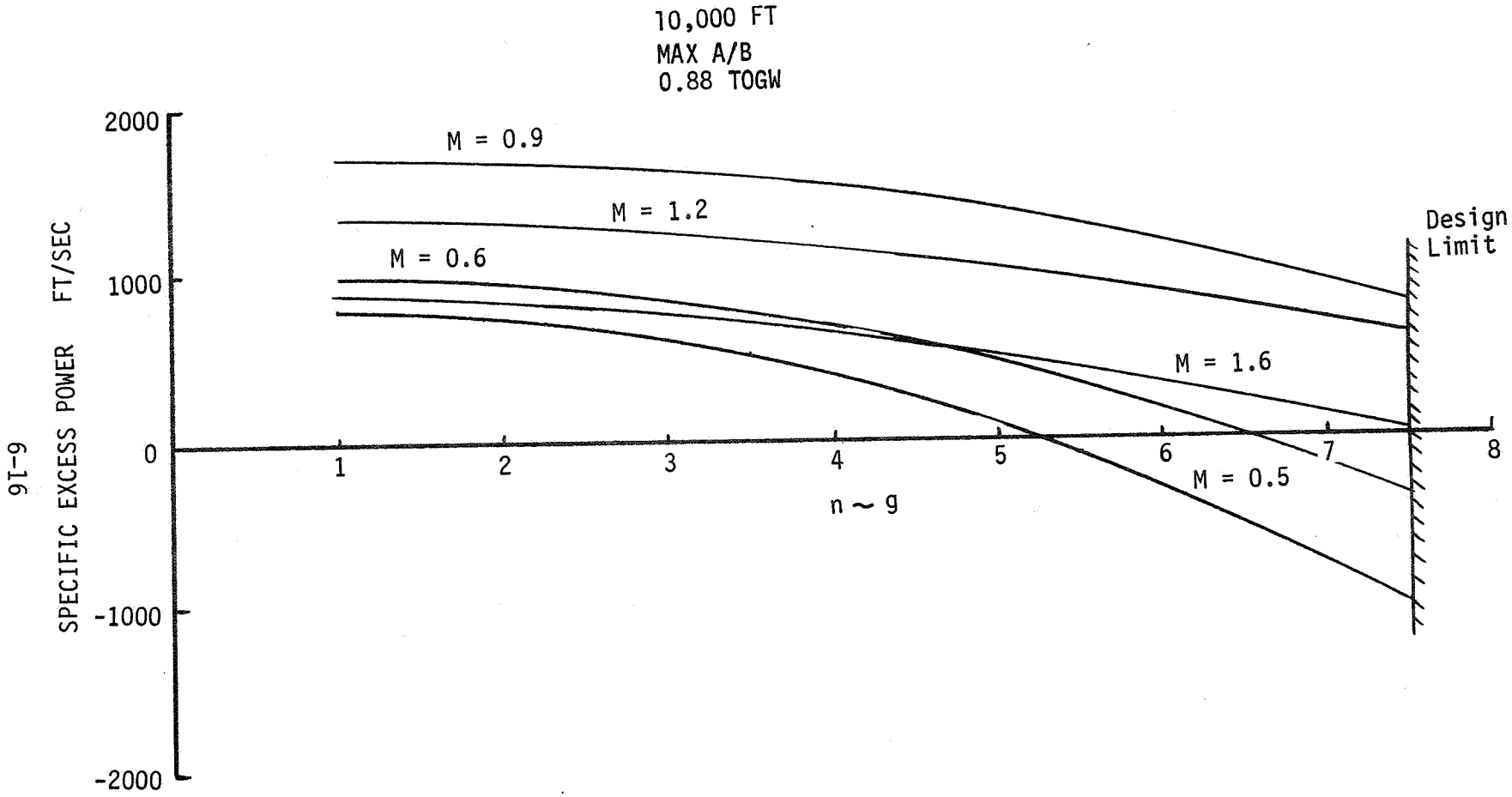

Figure 6-10 - TF120 Energy Maneuverability - 10,000 Ft.

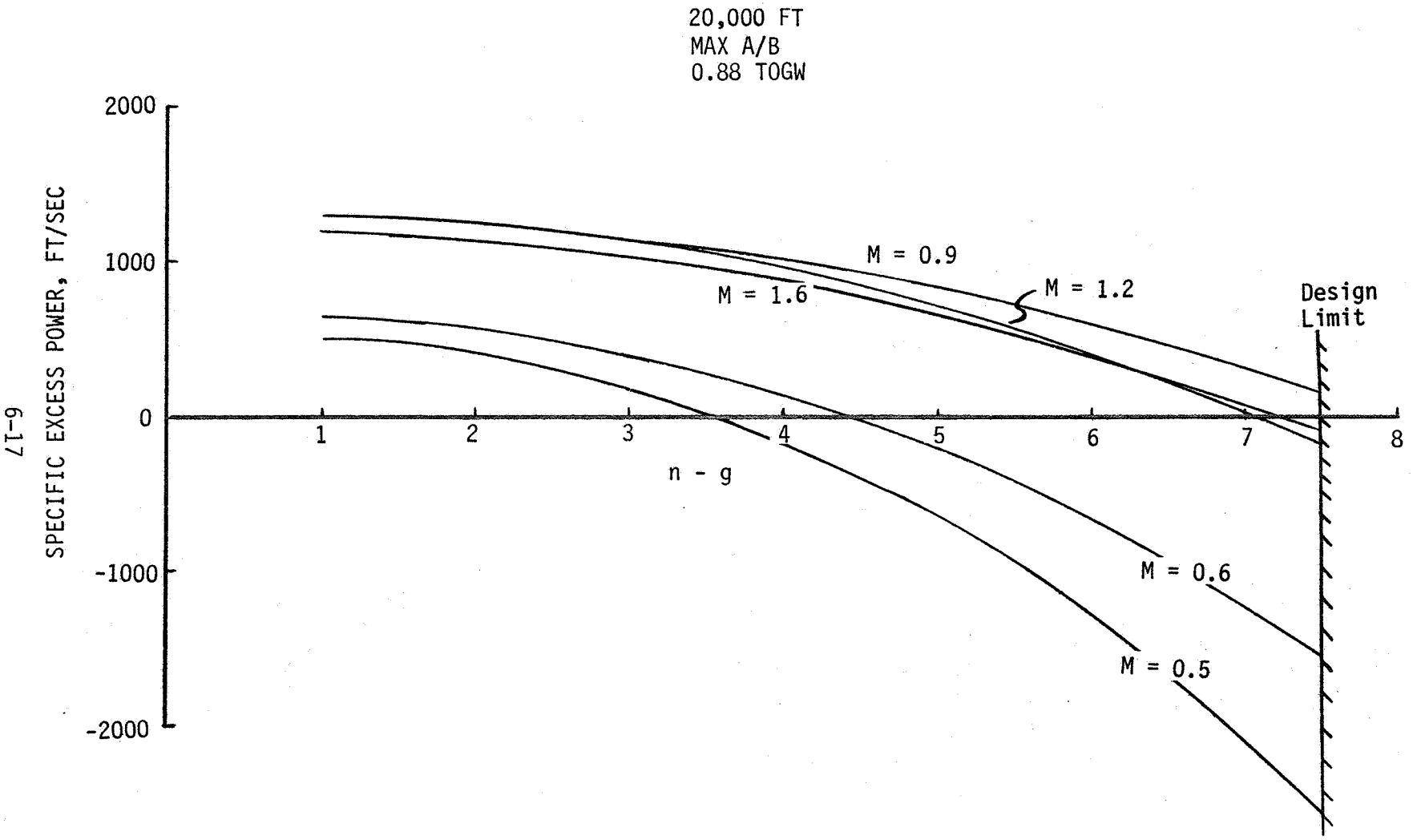

Figure 6-11 - TF120 Energy Maneuverability - 20,000 Ft.

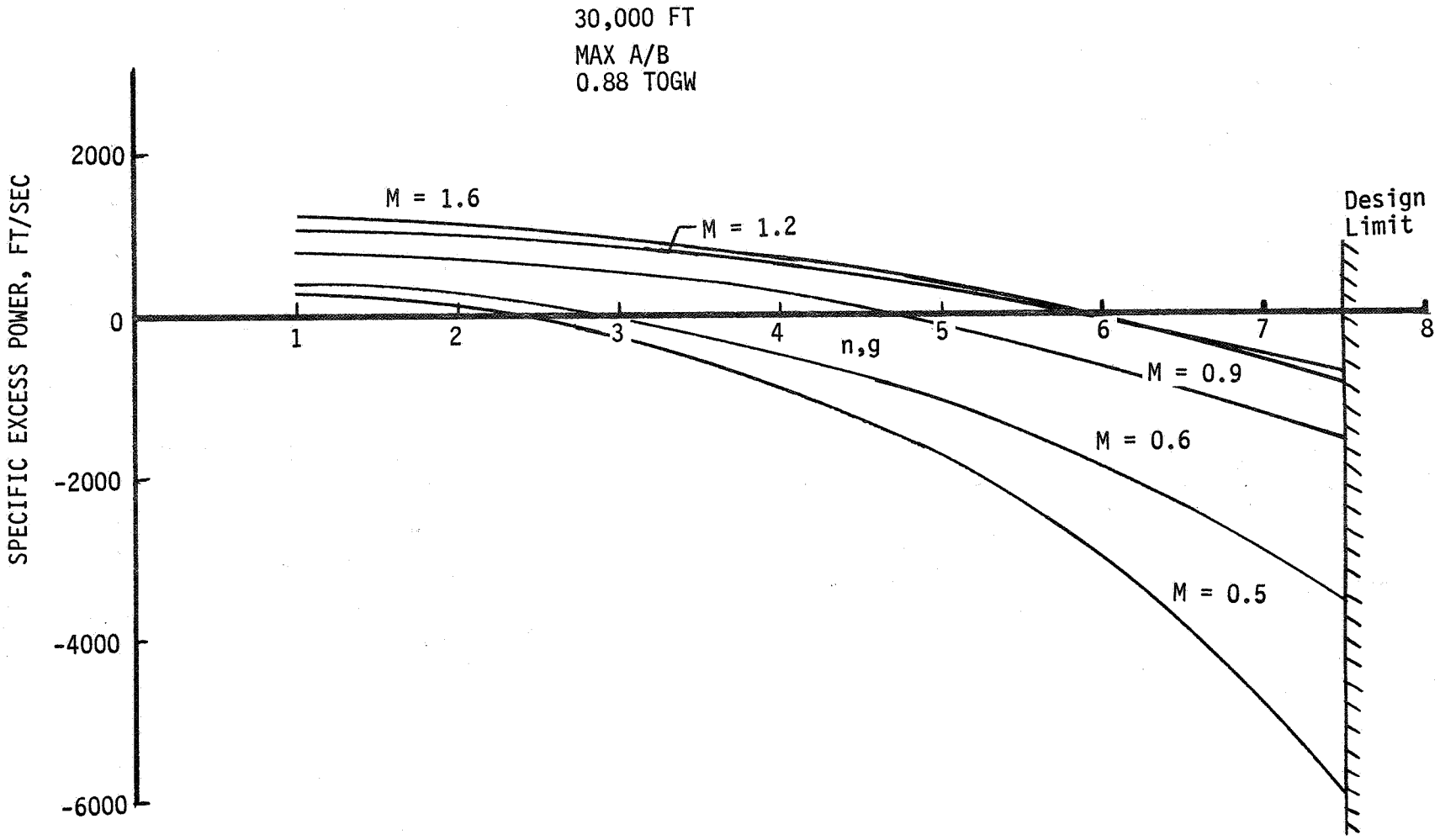

Figure 6-12 - TF120 Energy Maneuverability - 30,000 Ft.

6.2 SENSITIVITIES

6.2.1 Short Takeoff Performance

> TF120 short takeoff performance is exceptional due to aft fan flow augmentation and efficient thrust vectoring of both fan streams.

Usable parallel mode vertical takeoff thrust is constrained by longitudinal balance and by the desire to keep exhaust temperatures impinging on a deck below 1000°F. When deckspace or runway dimensions permit, afterburning can boost the aft fan/core engine thrust for an overall increase of 18 percent. This increment plus the VTO control margin of 18 percent means that the TF120 with a 9,724 lb overload (Interdiction mission stores) has an initial thrust-to-weight ratio of 1.0. However, some of this thrust must be directed aft to accelerate and to maintain longitudinal trim; therefore some aerodynamic lift is required.

We calculated TF120 overload STO performance using conservative ground-rules, requiring that front and rear thrust vector moments be in balance at all times and that deck roll be defined as the actual liftoff point (zero sink). Tropical Day (89.4°F) and zero wind over deck conditions and a flat deck (no ski ramp) were assumed.

The forward fan nozzle can be vectored aft as much as 30 degrees from the vertical without unduly complicating the nozzle mechanism. The TF120 landing gear provides sufficient ground clearance to permit a 20 degree rotational angle of the aircraft. Figure 6-13 shows the effect of forward fan thrust incidence (measured from the horizontal) and angle of attack limit at liftoff on ground (or deck) roll. Even with a nonvectoring forward nozzle (80 degree incidence) less than 450 ft is required. A maximum performance field takeoff can be made in 260 ft, compared to the standard military runway width of 150 ft. On shipboard, rotation of the aircraft can continue to 25 degrees angle of attack once clear of the deck, yielding a 210 ft deck roll. It is apparent that TF120 overload takeoff distance performance is excellent and is not a significant design constraint.

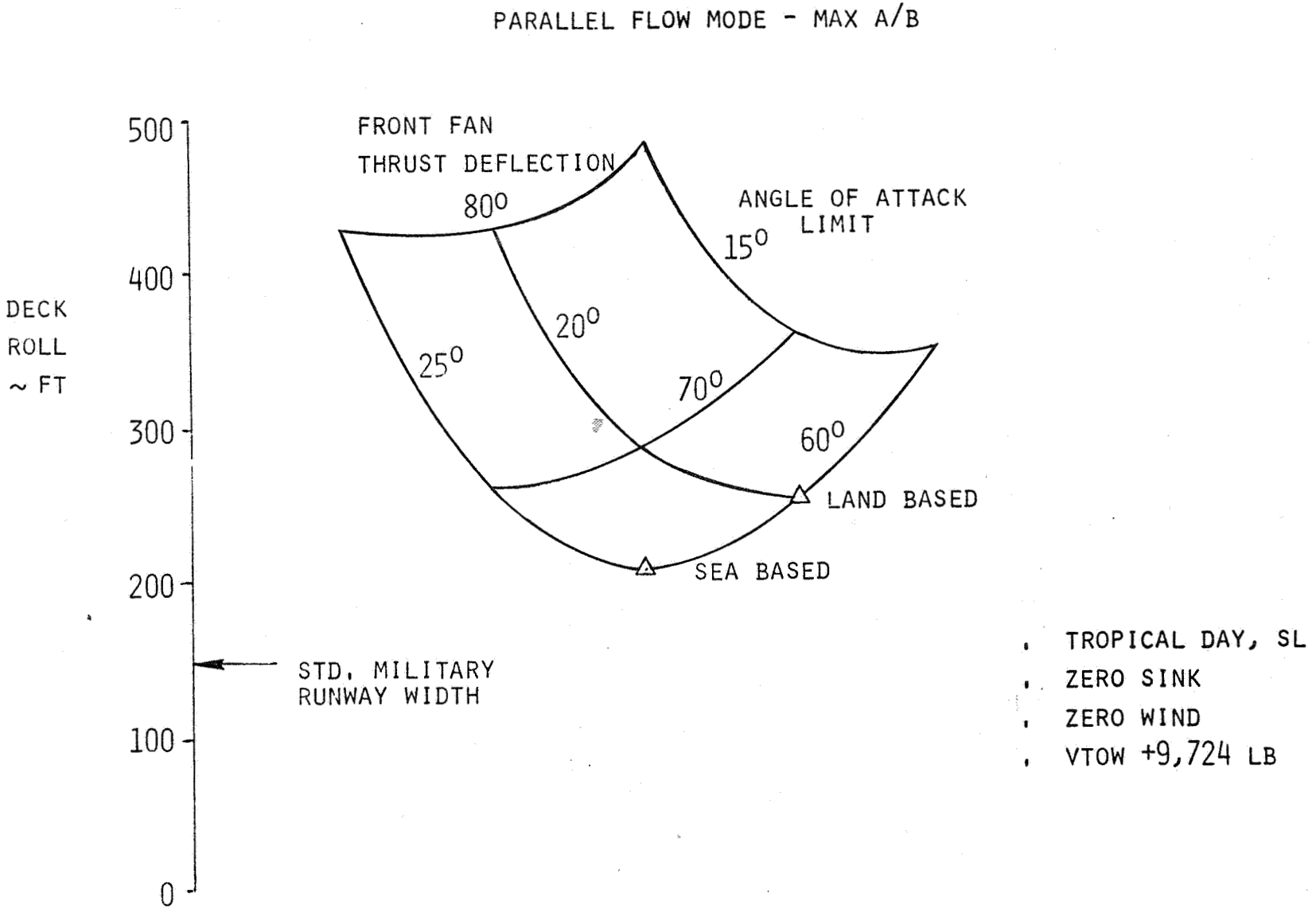

Figure 6-13 - TF120 Short Takeoff Capability

6.2.2 Takeoff and Landing Allowances

> The fuel efficiency of the series flow tandem fan cycle enhances mission performance and minimizes takeoff weight.

Fixed fuel allowances have a dramatic impact on radius of action for high thrust-to-weight fighters. Two takeoff thrust ratings were used to compute TF120 takeoff and mission performance. The vertical takeoff rating is with forward fan augmenation to 950°F and the rear fan unaugmented (which also has a 950°F exhaust temperature). However, for short takeoffs the rear exhaust is augmented to 2800°F. Point design mission performance was calculated with fuel consumption appropriate to the operating mode. However, early sizings simply applied the maximum thrust STO rating across the board to all takeoffs as well as landings, until precise cycle ratings were established. This procedure in effect represented an unfair and unrealistic penalty to VTOL operations.

The consequences of such conservatism are evident in the Supersonic Intercept mission fuel consumption breakdown in Figure 6-14. DLI radius is increased by some 50 NMi by specifying the appropriate VTOL fuel allowances. The other missions exhibit comparable improvements. From this it is clear that mission rules for analyzing V/STOL or other high thrust aircraft should define fuel allowances to be a reasonable simulation of power settings and intervals. Both combat and takeoff and landings should be task oriented to some degree.

SUPERSONIC INTERCEPT MISSION

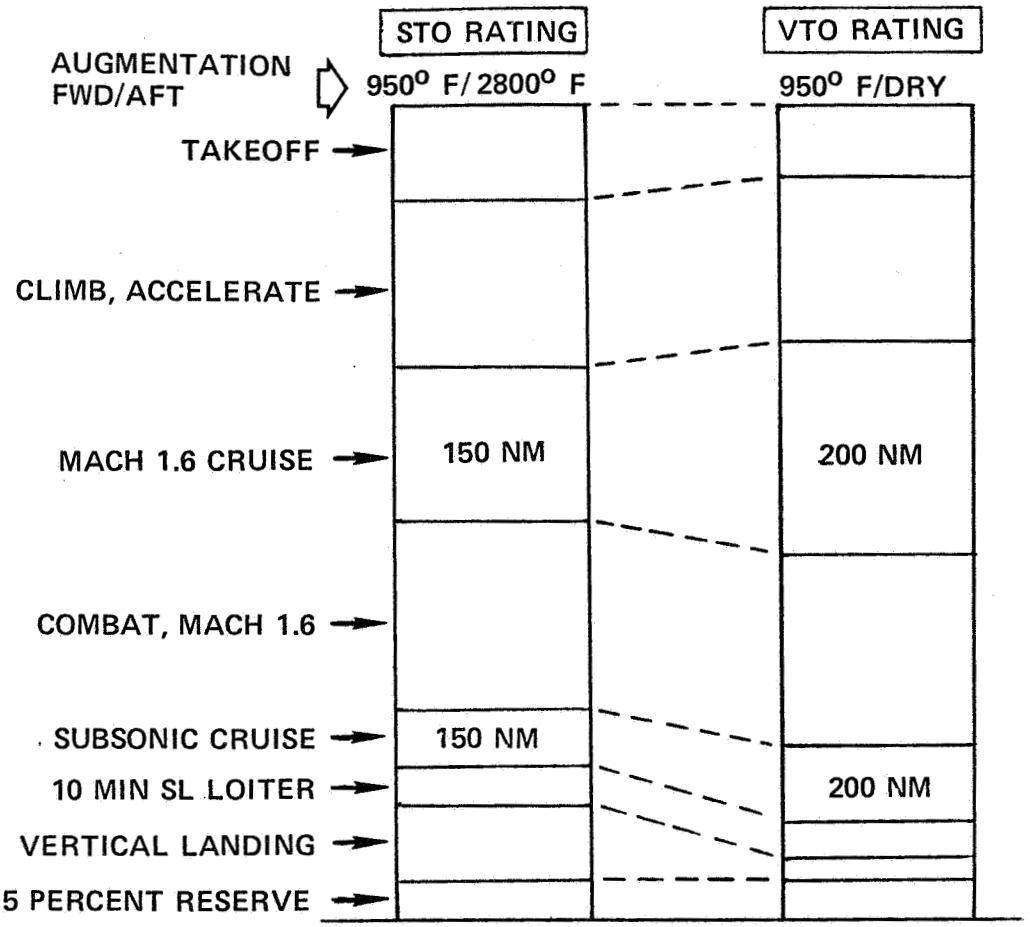

Figure 6-14 - Impact of Fuel Allowances on Radius of Action

6.2.3 Constraint Sensitivities

> The Vought configuration synthesis procedure generates sensitivity data for all performance constraints.

The interactive computer graphics capability integral to ASAP was used to generate design charts of aircraft performance parameters within the design space. These carpet plots allow the analyst to quickly assess the impact of changing any constraint level on takeoff weight, wing area, engine size and all the other performance parameters. Such a trade study can be accomplished without access to the computer.

Appendix III contains ASAP carpets for TF120 performance parameters in the format of Figure 6-2, as functions of wing area (SW) and engine scale factor (SF). The point design constraint lines are overlaid for reference, with numerical value indicated for the minimum weight intersection.

6.3 VTOL TRANSITION

6.3.1 Hover Control Power

> The TF120 meets MIL-F-83300 minimum hover control power requirements, but a greater attitude control power region is recommended.

TF120 hover control power in roll is provided by reaction control jets located near the wingtips and powered by engine bleed air. Pitch and yaw control power is provided by differential inlet guide vane deflections (for pitch) and differential forward and aft fan nozzle deflections (for yaw). Height control is provided by collective changes to the inlet guide vanes.

Minimum control power was established by the same criteria used for the SF-121 VATOL concept (Reference 1). Control power-levels were sized to meet single axis attitude changes in one second as specified in MIL-F-83300 (paragraph 3.2.3.1). This analysis did not consider that portion of the specification which required trimming the aircraft with hover winds from the most critical direction prior to the control inputs. While addressing this portion of the specification was beyond the scope of this study, it warrants analysis when the required aerodynamic data base is available.

The hover control powers provided for the aircraft are:

Axes	Control Power (Single Axis) ~ rad/sec^2	Inertia ~ slug-ft^2
o Roll	0.261	I_{XX} = 12,789
o Pitch	0.176	I_{XY} = 64,469
o Yaw	0.130	I_{ZZ} = 74,622

Considering instantaneous step input of controls, the following airplane attitude displacements were produced.

Axes	MIL-F-83300 Attitude Change in one sec. or less ~ Deg (Level 1)	TF120 Attitude Change (no damping) in one sec or less ~ Deg	TF120 Attitude Change *(with damping) in one sec or less ~ Deg
Roll	$\pm 6^\circ$	7.47°	4.5°
Pitch	$\pm 4^\circ$	5.04°	4.5°
Yaw	$\pm 3^\circ$	3.72°	2.8°

*Damping levels used were based on MIL-H-8501A VFR requirements:

Angular velocity damping ~ ft-lbs/rad/sec	
o Pitch	VFR $\geq 8\ (I_y)^{0.7}$
o Roll	VFR $\geq 18\ (I_x)^{0.7}$
o Yaw	VFR $\geq 27\ (I_z)^{0.7}$

These data indicate that with the control power provided the aircraft will meet the single axis attitude changes required by MIL-F-83300. However, when required to provide adequate artificial damping, the aircraft will probably meet that portion of the hover control power specification.

It is felt, primarily based on comparing the TF120 control power levels with successful VTOL aircraft in the same weight category, that the aircraft will have marginal hover control power levels. Additional control power analyses are required in future program development phases.

6.3.2 Transition Analysis

> Analysis of TF120 transitions to and from hovering flight revealed no major problems.

Vertical takeoff transition characteristics are presented on Figure 6-15 for three acceleration cases (a/g = 0, 0.075 and 0.15) for a flight path angle of zero. Similarily, transitions from cruise flight to vertical landings are shown on Figure 6-16 and Figure 6-17 for descent angles of 0° and 5° and for three deceleration rates (a/g = 0, -0.075 and -0.15).

The transition analyses are based on solutions of the three-degree-of-freedom equations for the forward fan gross thrust, aft fan gross thrust and aft fan effective nozzle deflection angle using the following aircraft data:

- o Aircraft transition weights and relative c.g. locations
- o Pertinent aircraft geometric characteristics; i.e., thrust moment arms, wing area, etc.
- o Ram drag
- o Low speed aerodynamic data
- o Flight path angle and acceleration levels
- o Angle-of-attack/velocity schedule.

The high speed end of the landing and takeoff transitions occurs at an angle of attack of 20.4° (1.225 $V_{STALL_{power\ off}}$, $\delta_{NOZ} = 0°$, and no forward fan thrust). Conventional flight pitch control is provided by operating the canard and elevons simultaneously to produce the necessary pitching moment couple. In this analysis a one-to-one gearing between the elevons and the canard was assumed. A $\delta_{control}$ setting of -7.68° ($\delta_{canard} = -7.68°$ and $\delta_{elevon} = +7.68°$) was required to trim the airplane in conventional flight at 1.224 $V_{STALL_{power\ off}}$. The transitions were analyzed with the longitudinal control surfaces fixed at these settings and forward fan thrust vector was deflected 90° relative to the fuselage reference plane. Transition angle-of-attack/velocity schedules were selected after considering vertical landing

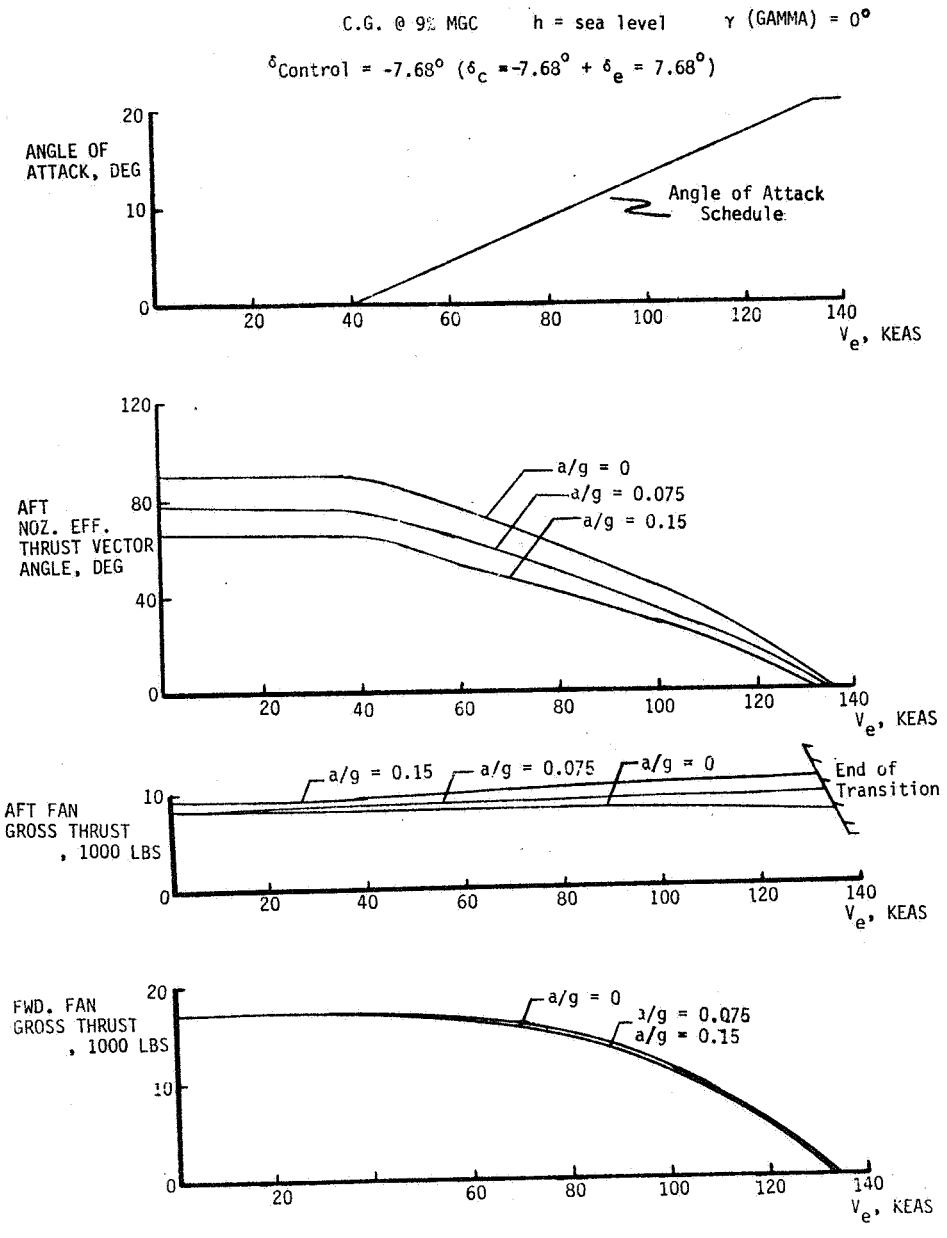

Figure 6-15 - Takeoff Transitions

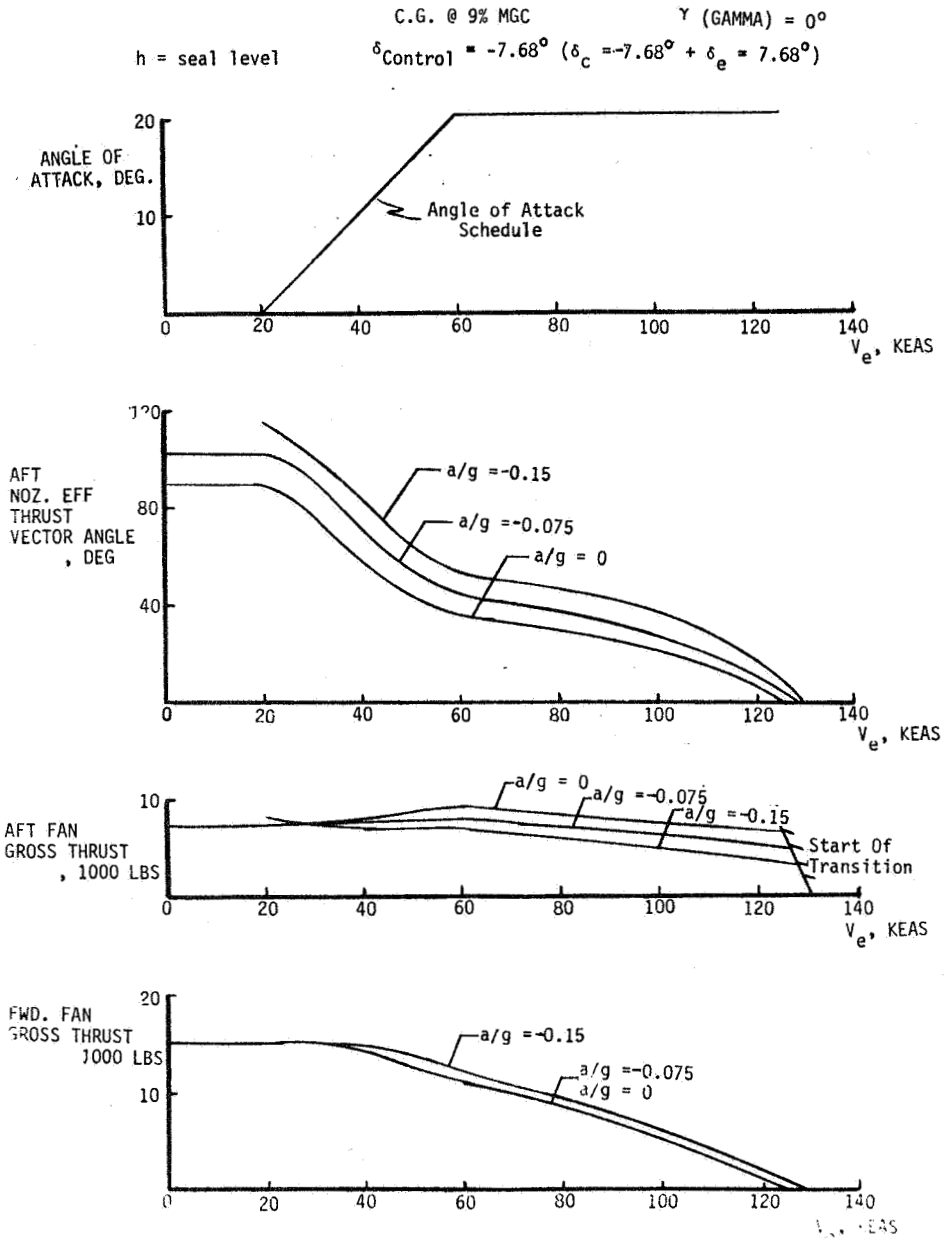

Figure 6-16 – Landing Transitions (γ = 0)

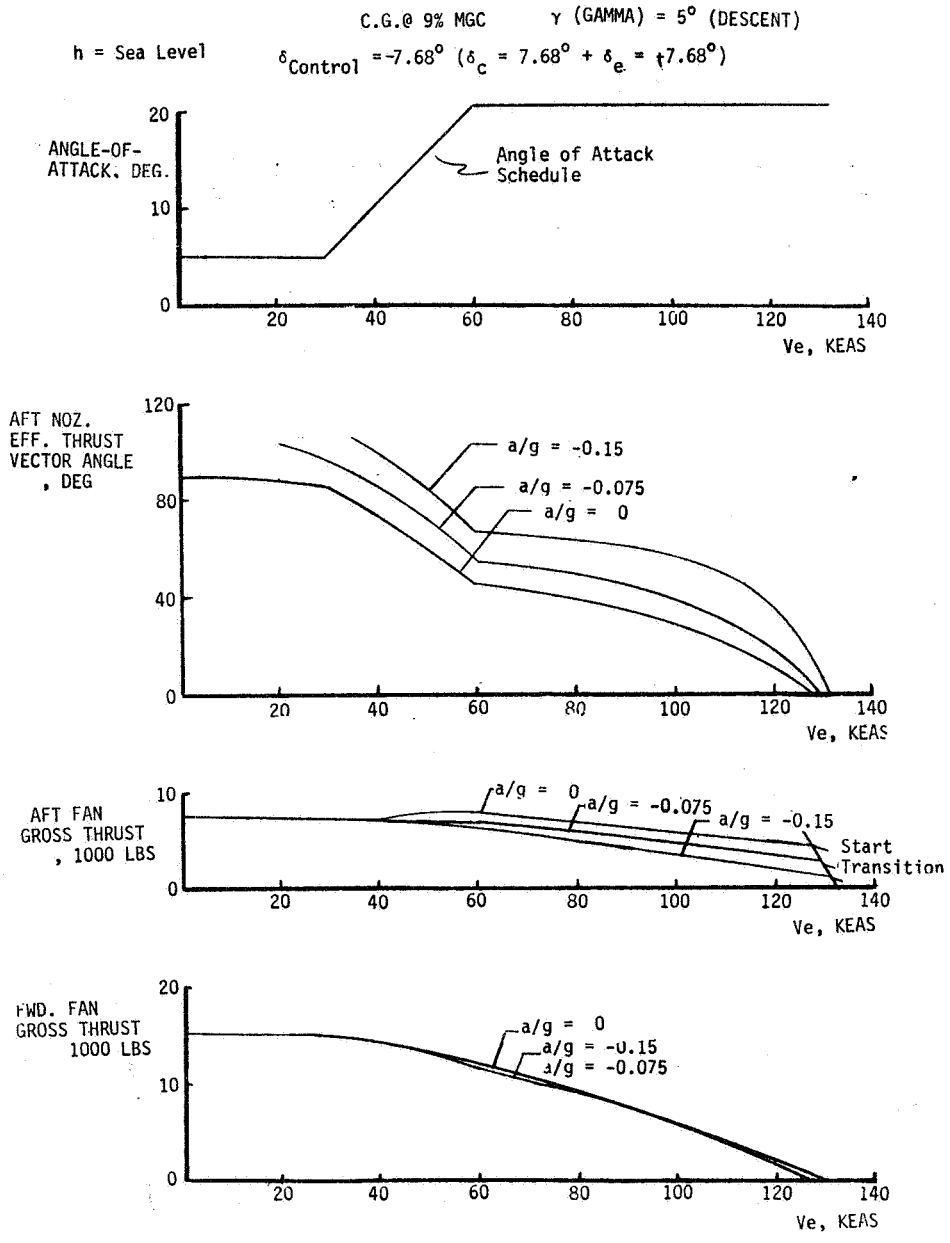

Figure 6-17 - Landing Transitions ($\gamma = -5^{\circ}$)

visibility, touch down attitude and aerodynamic lift variation with angle-of-attack and increasing airspeed. The selected AOA/velocity schedules provide an airplane attitude of 0° during hover, and an AOA = 20.4° at the high speed end of transition. During the landing transitions the angle of attack was held constant at 24.4° down to an airspeed of 60 KEAS, and then reduced as the airspeed approached zero. During the takeoff transition the angle of attack was held to $\alpha = 0°$ until the aircraft reached 40 KEAS. Thereafter the AOA increased linearily to 20.4° at a velocity of 135 KEAS. The takeoff and landing weights were 25,339 and 22,298 lbs., respectively, and center-of-gravity was at 9 percent MGC for both configurations.

Figure 6-18 presents the low speed (M = 0.2) drag and longitudinal stability and control aero coefficient data used in the transition analysis. Pertinent aerodynamic characteristics are listed below:

- $C_{D_o} = 0.0377$ (landing gear down)
- $C_{L_{MAX}}$ (Control neutral) = 1.6
- Aerodynamic center at 4.6 percent MGC

A review of the landing and takeoff transition data shown in Figures 6-15 through 6-17 indicates that the required aft nozzle deflection angles, aft fan thrust levels, and forward fan thrust levels required to meet typical transition performance levels form sets of logical smooth continuous curves which are necessary for a successful V/STOL configuration.

Data from Figure 6-15 for the takeoff transition indicate that:

- Hover flight can be achieved with the aft nozzle deflected 90° with an aft fan thrust level of 8,330 lbs. and a forward fan thrust level of 17,008 lbs.

- Hovering over a spot in a 40 KT head wind or tail wind requires approximately $\pm 1°$ aft nozzle deflection from the nominal 90° position.

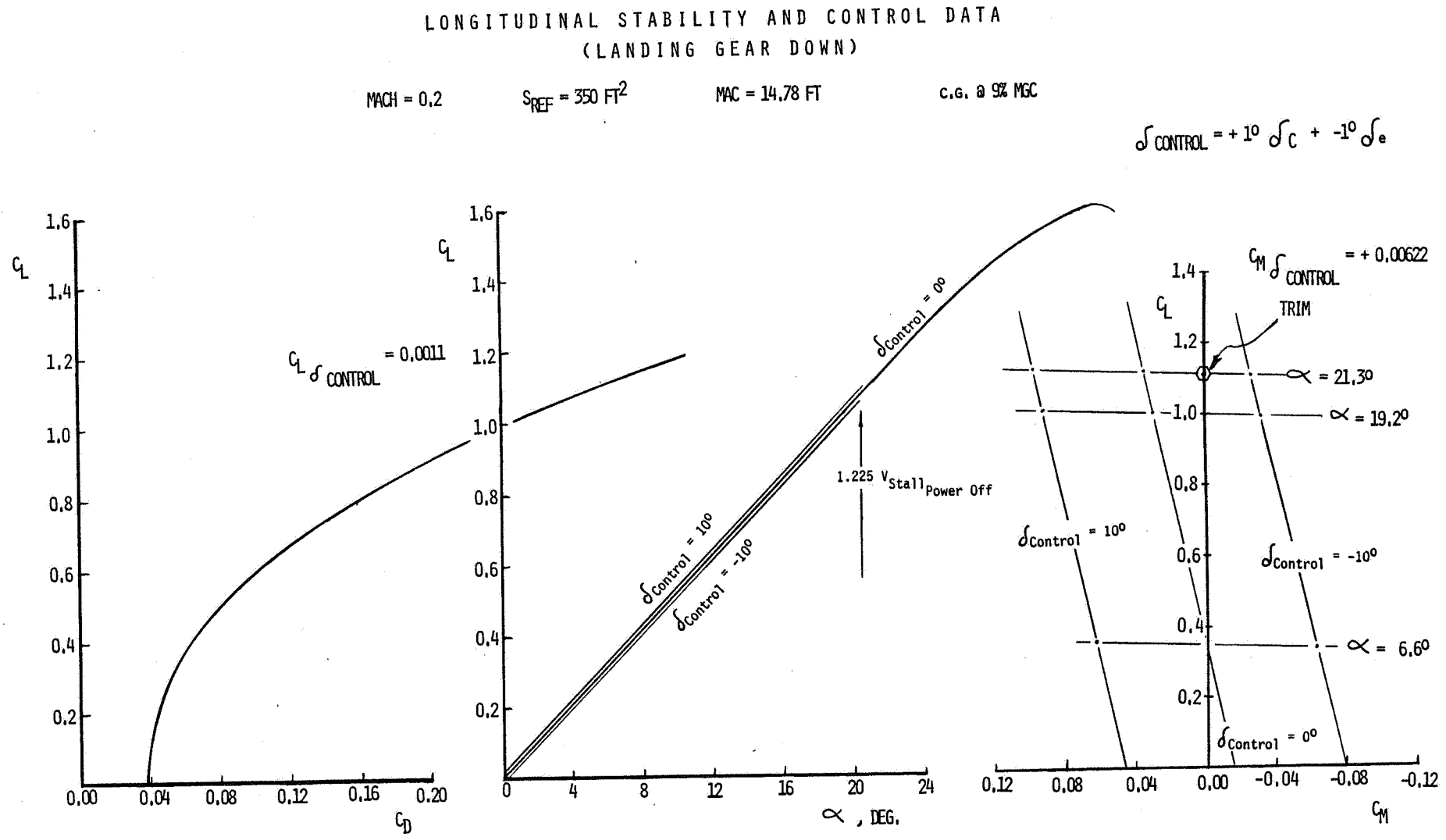

Figure 6-18 – Longitudinal Stability and Control Data (Landing Gear Down)

- If, while hovering in still air, the aft nozzle was deflected to 76° the aircraft will accelerate at a/g = 0.075 at 40 KEAS, and will reach equilibrium flight at 60 KEAS with slight reductions in forward and aft fan thrust levels.

- Forward fan thrust level reduces as airspeed increases and slight variation of thrust levels are required as acceleration levels change. At a given transition speed, higher aircraft accelerations are produced by reduced nozzle deflection angles and increasing aft fan thrust levels.

- Transitions will be complete (forward fan thrust required = 0 lbs and aft nozzle deflection = 0°) when the aircraft reaches approximately 135 KEAS.

- Maximum gross thrust levels available from forward and aft fans exceed the thrust required levels shown in Figure 6-15.

- Aft nozzle deflection rates used in takeoff transition should be limited so that the aft nozzle will not reach the trail position before the aircraft can accelerate to a safe forward velocity.

Data from Figure 6-16 for the landing configuration transitions with flight path angle = 0° indicate that:

- Landing transitions should start in the 125 to 128 KEAS velocity range, depending on the aircraft deceleration characteristics.

- An angle-of-attack of 20.5° should be held down to 60 KEAS. During this portion of the transition, the following changes will occur:

  - Forward fan thrust will increase from 0 lbs to approximately 12,000 lbs.

  - For the a/g = 0 case, the aft nozzle deflection increases from zero to 35°, and the aft fan gross thrust increases from 6,600 to 9,400 lbs.

- For the a/g = -0.075 case, the aft nozzle deflection increases from zero to 43°, and aft fan gross thrust increases from 5,000 to 8,200 lbs.

- For the a/g = -0.15 case, the aft nozzle deflection increases from zero to 52°, and aft fan gross thrust increases from 3,300 to 7,100 lbs.

o Angle-of-attack reduces linearily from α = 20.4° at 60 KEAS to α = 0° at 20 KEAS. The larger aft nozzle deflection required to maintain the AOA profile increases as the deceleration rate required becomes more negative.

  At the 20 KEAS point in the transition, the forward fan gross thrust level requirement are about 15,000 lbs for the three deceleration cases. To produce an a/g of -.15, the aft nozzle deflection required is 114° with an aft fan gross thrust level of 7,600 lbs.

o Hover flight can be achieved in still air with the aft nozzle deflected 90° with an aft fan thrust level of 7,300 lbs and forward fan thrust level of 15,000 lbs.

From Figure 6-17 for the landing with 5° descent angle transition, data trends similar to those discussed above are seen. However, the 5° descent angle at a given transition speed requires an increased aft nozzle deflection and a reduction in aft gross thrust requirements.

7.0 AERODYNAMIC UNCERTAINTIES

This section summarizes and discusses the principal uncertainties in aeropropulsion estimates and analysis uncovered in the Phase I study.

This section contains:

7.1 CONFIGURATION DEPENDENT UNCERTAINTIES

Aerodynamic and aeropropulsive uncertainties have been identified for the study configuration. Some uncertainties in the prediction of detailed aerodynamic characteristics can be attributed to unique features of the TF120; others are inherent limitations in available analytical tools. We will first concentrate on the configuration-dependent issues and their significance. Section 7.2 addresses the broader subject of inadequacies in preliminary design prediction methods.

Aerodynamic Center: Accurate determination of aerodynamic center is essential to confirming the viability of V/STOL configurations. The vertical mode thrust vector, center of mass and subsonic aerodynamic center must be precisely aligned. Failure to achieve correct placement may use up control margins and complicate V/STOL transition. The highly integrated TF120 configuration will not accommodate arbitrary relocation of wing or propulsion system to achieve vector alignment. The TF120 planform is complex and curvilinear; strong interactions are expected between the canard and wing. At high angles of attack, strong vortex flow and separated wakes will appear, causing possible migration of the aerodynamic center. The combination of highly swept strakes and moderately swept leading edges is intended to minimize a.c. shift over the Mach number spectrum; the degree to which this is achieved will have a direct bearing on supercruise mission capability. APAS a.c. estimates were found to be highly sensitive to blended body cross section, raising doubts about the validity of aerodynamic center predictions.

Trimmed Lift and Drag: High sustained load factor capability at Mach 0.6 was a constraining design guideline. Drag due to lift at lift coefficients in excess of 1.0 sizes wing area. The TF120 planform will generate significant vortex lift (and vortex drag). The close-coupled canard will produce favorable interference, but the coplanar relationship of canard and wing, canard dihedral and canard incidence make accurate prediction of the overall effects difficult. Even for subsonic cruise ($C_L \sim 0.32$) mission fuel requirements are sensitive to trimmed lift/drag. This is the very region in which leading edge suction usually begins to break down.

Minimum Drag: We believe subsonic minimum drag estimates for the TF120 to be reasonably accurate. The basically clean intersections of wing-body and canard-strake should yield moderate interference factors. However, the inlet boundary layer diverter, nozzle-afterbody and wing-mounted vertical fin interference estimates may not adequately account for accelerated flows and possible corner separation. The dominant aerodynamic uncertainity is transonic and supersonic wave drag. APAS solutions were highly sensitive to wing-afterbody definition and failed entirely at Mach 2.0 and 2.4. Wind tunnel tests of a sting-mounted model will not completely resolve the afterbody effects, but will provide the data base on all other configuration elements necessary to validate APAS and other supersonic drag methods. The Phase II wind tunnel model will include provisions for a blade support to permit accurate nozzle-afterbody simulation in future tests.

Longitudinal Control Power. The TF120 elevons and all-moving canards are powerful moment generators at moderate angle of attack. However the estimated control power is implicitly restricted to the linear angle of attack region and small deflections. The elevons will lose effectiveness at high deflections and when the wing stalls. The all-moving canard controls can be driven to whatever incidence is required to prevent canard stall. However, unporting will spill air at the canard root and the degree to which canard effectiveness is reduced is not known. We were unable to quantitatively address the characteristics of the tail flap within the scope of the Phase I analysis. This control is exposed to the exhaust stream on the underside, thus yielding pitching moments dependent on both dynamic pressure and power setting. Its principal function is static longitudinal trim, thus leaving canards and elevons undeflected in equilibrium flight. At this point we do not know if it will show a payoff for either high speed thrust vectoring, or as an aid to recovery from a deep stall.

Stall Departure Characteristics: An air combat fighter must have good flying qualities near the stall in order to fully utilize maneuver capability. Indeed, intentional excursions into the post-stall regime may yield tactical advantages. The TF120 is designed to be controllable at extreme angles of attack by maintaining the four ventral fins and the canard in the windward flow field. However, none of the analysis methods used in this study can be relied upon to predict either high angle of attack (nonlinear) lateral/

directional stability deviations or large amplitude control effectiveness. Such information is prerequisite to assessing flying qualities near and beyond the stall. Data should be acquired for variations in control fin size and location. Interactions of the canard wake on the vertical fins may require changes in spanwise and chordwise location of the fins.

Unconventional Controls: The remarkable aerodynamic interactions arising from control surface deflections as predicted by the APAS code must be independently verified before serious exploitation of the phenomenon can begin. Both the magnitude of the small amplitude effects and the nonlinear high-deflection/high-C_L region must be known to permit design and simulation of an adaptive, multiple-deflection control system. The potential for such a control-configured vehicle is high, but so is the technical risk if based solely on our present understanding of the cross-coupling effect.

V/STOL Induced Effects: The emphasis in the Phase I effort and in the proposed Phase II wind tunnel program has been on up-and-away flight. This is appropriate in order to first validate the configuration for its intended role as a high performance fighter/attack weapon system. We performed a first order suckdown estimate, hover control power analysis and transition analysis, all of which indicated no serious deficiencies in the V/STOL flight mode. It should not be concluded that no problems exist. In-depth analysis, backed by powered model tests of propulsion-induced effects (suckdown, fountains, damping, adverse wind effects, reingestion and reaction control system characteristics) must ultimately be performed before even a flight demonstrator can be developed. This will necessitate a research program paralleling the Phase II effort directed at the high speed regime.

Inlet Performance: The one substantial compromise to V/STOL capability for the TF120 configuration is in the air induction system. The short duct may introduce substantial flow distortion at the front fan face. The inlet guide vanes should help the fans tolerate flow distortion but a consequence could be reduced control margin for hover mode height and longitudinal control. The blow-in doors needed for V/STOL operation and the bypass system for supercritical inlet conditions require more analysis. Development of the top auxiliary inlet for the aft fan is expected to be less challenging than the front

inlet, since it is designed only for the V/STOL region and is closed for high speed flight. A possibility not yet explored, however, is to configure the top inlet to permit subsonic cruise or loiter in the parallel flow mode. Combat air patrol time on station might benefit substantially from a increasing bypass ratio from 1.0 to 3.43. Some of these SFTF propulsion system issues can be addressed by additions to the powered model test hardware tested at the Lewis Research Center.

7.2 PREDICTION METHODS UNCERTAINTIES

The principal tools used to analyze the TF120 configuration were APAS, and to some extent Vortex-Lattice. Both methods are limited to linear aerodynamic predictions. Digital Datcom offers nonlinear prediction methods, but the quality of the results obtained in this study for the TF120 configuration were unsatisfactory and thus were not used. The following discussion outlines those areas for which no satisfactory prediction methods exist.

Nonlinear aerodynamics: In a configuration like the TF120 the limit of the linear angle of attack range is lower than for more conventional configurations. Due to the close-coupled canard, the wing root strakes, the blended body, and the low aspect ratio highly tapered wings, the TF120 configuration will generate a very complex and nonlinear flow field. Neither APAS nor Vortex-Lattice methods can successfully treat this type of flow field. Datcom and Digital Datcom offer nonlinear predictions, but the quality of the results obtained for the TF120 configuration were unsatisfactory. In order to adequately define the flying qualities of the TF120 improved methods of determining the onset of nonlinear aerodynamics and of determining the configuration aerodynamics at larger angles of attack are needed. At subsonic and transonic speeds corresponding to maneuvering flight, better methods of predicting buffet onset $C_{m_{bo}}$, control effectiveness and maximum lift coefficients are needed to more clearly define the maneuvering envelope of the aircraft.

Closely associated with the need for methods treating the prediction of aerodynamic quantities in the nonlinear aerodynamics region is the need for methods to predict higher order derivatives. For example, the variation of C_{n_β} with angle of attack is needed to define the aircraft stall departure and characteristics. At the present time no general methods for treating these predictions exist. The designer is forced to rely on rough approximations, data for similar configurations.

Control effectiveness at large angles of attack and large deflection angles: The analyses of the control systems presented in this report are based on the assumption of linear control effectiveness. Again, due to the highly integrated nature of the TF120 configuration, there will be significant interactions between the various control surfaces and the vehicle lifting surfaces. APAS and Vortex-Lattice analyses account for some of the aerodynamic interactions. However, the reduced effectiveness at large angles of attack and/or deflections is not accounted for. Datcom does offer a correlation for this reduction in effectiveness but these correlations are based on conventional configurations. An improved method of predicting control effectiveness on a highly integrated configuration is needed.

Supersonic Zero Lift Drag: Supersonic aircraft have been flying for a number of years. At this late date, the principal wave drag analysis tool is still the Hays-Emmington type analysis. This method is only suitable for use with slender, well streamlined configuration. For compact fighter configurations such as the TF120 the initial and final slopes of the area distribution curve may locally violate the slenderness criterion required by the theory. In addition, the area distribution tends to be "two-humped" due to the canard and wing. The accuracy obtained when using Hays-Emmington methods on these types of configurations is questionable. Accurate results can be obtained through the use of the Boeing-developed PANAIR program, but long run times and complexity of inputs limit its usefulness during the early stages of aircraft development. Better methods of predicting wave drag in the conceptual and preliminary design phases of an aircraft design are urgently needed.

Design of Optimum Camber and Twist: Methods exist for the design of optimum camber and twist for relatively conventional configurations. For complex planform configurations such as the TF120 the adequacy of the existing methods is questionable. Better methods for rapid design of camber and twist distributions are needed.

8.0 RESEARCH PROGRAM

This section presents Vought's recommended approach to the resolution of principal aerodynamic uncertainties discovered in Phase I. The Phase II program will develop a wind tunnel data base.

This section includes:

8.1 WIND TUNNEL MODEL

8.1.1 Model Design Concept

> A versatile high speed wind tunnel model is described which is sized for compatibility with NASA facilities and with the XM2R propulsion simulator.

Vought will design and fabricate a high speed wind tunnel model of the Phase I configuration as a portion of the Phase II effort. This model will have flow-through inlets with a rear sting support. Provisions in the design will permit installation of one XM2R compact propulsion simulator and a blade mount for future powered tests. Design, size and structure of the model and sting system will be compatible with use in the NASA Ames 11-foot and 14 foot Transonic and 9 x 7-foot Supersonic Wind Tunnels. Several configuration variables will be available to provide experimental data for the aerodynamic and aerodynamic/propulsion interaction uncertainties identified in Phase I.

A model scale of 0.087 (2.65 ft^2 wing area) is recommended for the proposed configuration. The scale was chosen for optimum data quality for the flow-through configuration in the applicable tunnel facilities and for acceptable scaling when the XM2R propulsion simulator is used. The model wing area is less than the published maximum wing area for Ames 11-foot tunnel (3.63 ft^2), yet is sufficiently large for good dimensional scaling accuracy. By using a model of this size, problems associated with configuration changes, balance installation, and future installation of the XM2R engine simulator will be minimized. Table 8.1 (Page 8-4) shows how this model size relates to the NASA tunnel facilities that Vought feels are applicable to this program. The final selection of tunnel facilities, model balances and types of stings to be used will be made in conjunction with NASA Ames personnel.

The preliminary design for the model is shown in Figure 8-1. This design emphasizes ease of parametric changes in configuration.

Aerodynamic forces and moments will be measured with an internally mounted six-component balance from either Vought or NASA inventory. Internal flow drag and base pressure will be determined from internal static and total pressures measured with Government-furnished Scanivalves mounted within the model.

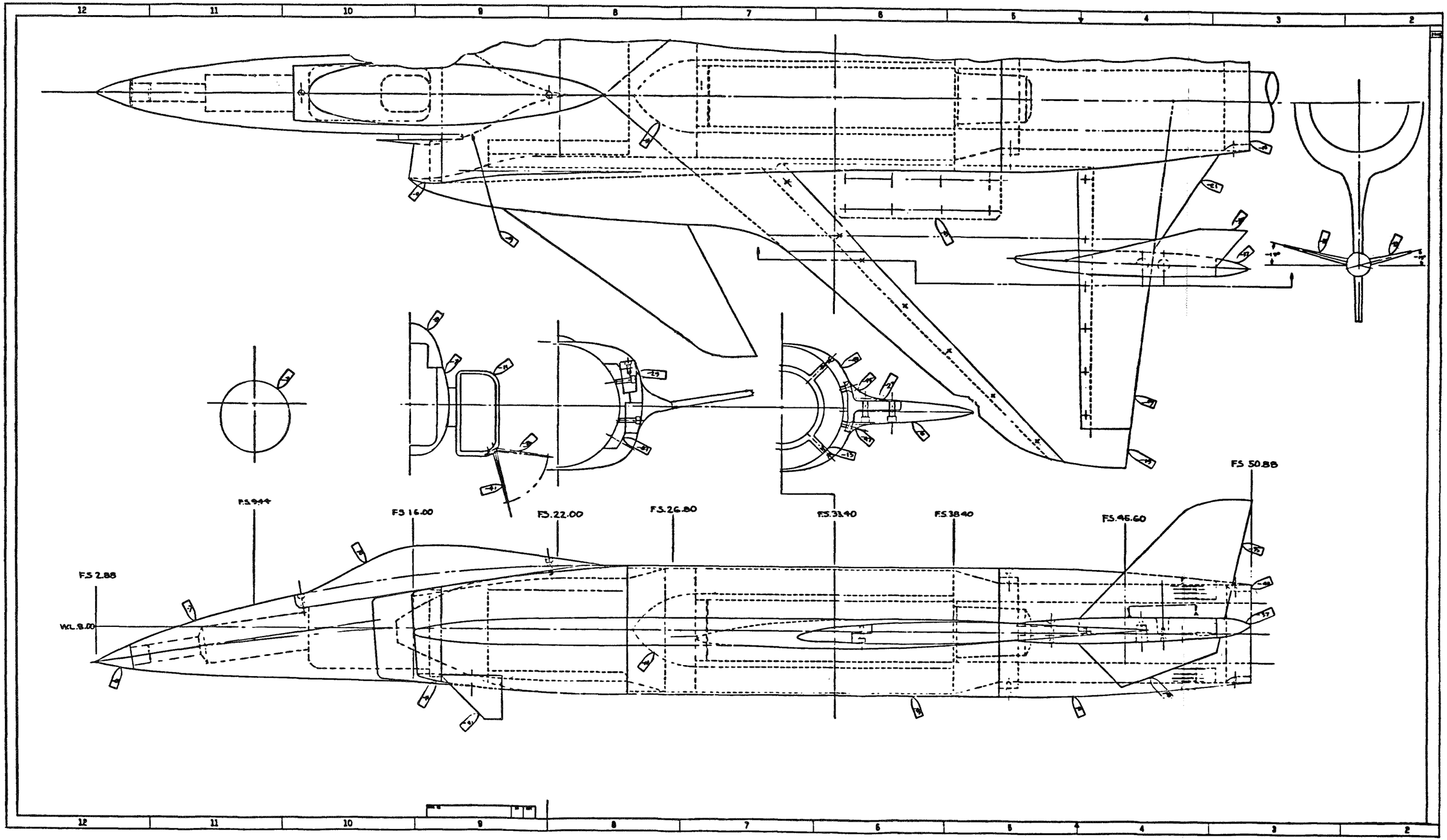

Figure 8-1 - 0.087 Scale TF120 Wind Tunnel Model Assembly

FOLD-OUT #1

FOLD-OUT #2

Table 8.1 - Comparison of Model and Wind Tunnel Sizes
(8.7 Percent Model)

PARAMETERS	AMES 11' TUNNEL	AMES 14' TUNNEL	AMES 9x7' TUNNEL
WING REFERENCE AREA			
FULL SCALE = 350 FT^2			
MODEL SCALE = 2.65 FT^2			
PERCENT TUNNEL CROSS-SECTION AREA:	2.2	1.42	4.2
MAXIMUM FRONTAL AREA			
FULL SCALE = 36.54 FT^2			
MODEL SCALE = 0.277 FT^2			
PERCENT TUNNEL CROSS-SECTION AREA:	0.23	0.15	0.44
WING SPAN			
FULL SCALE = 29.24 FT			
MODEL SCALE = 2.54 FT			
PERCENT TUNNEL WIDTH:	23.1	18.4	28.2
PLANFORM AREA			
FULL SCALE = 5.66 FT^2			
MODEL SCALE = 4.28 FT^2			
PERCENT TUNNEL CROSS-SECTION AREA:	3.5	2.3	6.8

A duct calibration performed at Vought will relate the pressure measurements to internal drag and mass flow in the duct.

The final choice of a balance will be made during the Phase II design effort. A rear sting (nominally 2 1/2-inch diameter) will be provided to support the model and will mount to the existing model support systems in the NASA tunnels.

Total and static pressure instrumentation will be provided near the exit nozzle and inlet throat. Balance cavity and base pressure orifices will also be provided. The pressure instrumentation will be designed and located such that the internal flow drag, mass flow and base pressure may be measured. Final design of the duct instrumentation will be subject to NASA approval to ensure that it is consistent with NASA equipment and standard practice. A cavity and mounting bracket is provided in the model nose for securing a government-furnished Scanivalve and, if desired, a government-furnished bubble pack to precisely measure the model angle of attack.

A preliminary stress analysis was conducted during the proposal design effort to support the conceptual approach to the model design and to define the nominal balance and sting requirements. A detailed stress analysis of the model and sting will be performed during detail design based on predicted maximum loads existing on the model for proposed critical test conditions in the Ames 11-foot, 14-foot and 9 x 7-foot wind tunnels. A stress report will be provided that outlines the calculations and confirms the design has a factor of safety of five based on the ultimate strength of the material, or three based on the yield strength, whichever is more conservative. In addition, the design shall satisfy the 9 x 7-foot wind tunnel starting load requirement.

Vought will furnish preliminary detailed manufacturing drawings and stress analysis of the model and support structure design to the NASA Ames Contracting Officer within seven weeks following the start of Phase II. Fabrication shall commence when written approval is given by the Contracting Officer. Any proposed changes to the approved design will be implemented only when approved by the Contracting Officer.

8.1.2 Parametric Design Variations

> Control deflections and variations on the baseline wind tunnel model configuration are recommended.

The design of the primary structure and the use of joints in the fuselage and wing and detachable canopy, canard, wing and tail make possible low cost variations in the aircraft configruation.

The basic model (with neutral settings on all deflectable surfaces) has the following components removable and appropriate off-blocks provided for aerodynamic buildup testing:

- Vertical tails
- Canard
- Inlet fins
- Wing-to-inlet strakes
- Wing-to-body fillets (upper and lower)

Configuration variables required for the Phase II model are noted below:

- Elevon, right and left hand; each has five deflections (0, $\pm$5, $\pm$10 degrees)
- Vertical fin, right and left; upper and lower, each has four deflections (one way only) (0, 5, 10, 15 degrees)
- Inlet fin, right and left; each has three deflections (one way only) (0, 10, 20 degrees)

- Canard, right and left hand, each has three incidence settings (0, $\pm$5, $\pm$10 degrees)

Alternate locations will be provided for the control surfaces alternate locations, while retaining the range of movements cited above:

- Vertical fins, 3 longitudinal and and 2 spanwise movements
- Inlet fins, 2 longitudinal movements
- Canard, two longitudinal movements and one lower position (coplanar with wing)

Added surfaces of other size or geometry located in basic location:

- One canard set
- One vertical fin set
- One inlet fin set (vertical position) and one inlet fin set (horizontal position)
- Wing leading edges

8.2 WIND TUNNEL TEST PLAN

> The wind tunnel test plan has been designed to supply data necessary to resolve major aerodynamic uncertainties.

The wind tunnel test plan has been designed to supply data necessary to reduce the uncertainties discussed in Section 7.0 to acceptable levels since it is recognized that it may be uneconomical to completely resolve all the uncertainties.

Three Ames Research Center tunnels were considered for this test program. Each offers important capabilities ultimately useful to the aircraft design under study. Primary emphasis has been placed on maneuvering capability for an airframe compatible with V/STOL operation. Very low speed and landing/takeoff modes, and which with representation of the landing configuration (landing gear and deflected nozzles require utilization of the Ames 12-foot pressure tunnel) are reserved for future investigations.

The 11-Foot Transonic Tunnel and/or the 14-Foot Transonic Tunnel will be used for Mach numbers ranging from 0.6 to 1.4 and will cover an angle of attack range from -5 to approximately +50 degrees in two stages. Offset stings will be used to obtain the high angles desired. One sting will cover the -5 to 25 degrees test range, and the second the 20 to 50 degrees range. The 5 degree angle of attack overlap will provide continuity between data taken using the two stings. Supersonic testing will be done in the 9 x 7-Foot Tunnel at Mach numbers of 1.6, 1.8 and 2.0. Angles of attack will range from -5 to 15 degrees. The selection of the tunnel facilities for the transonic speeds will be done in conjunction with NASA personnel. The 11-Foot Transonic Tunnel will not allow the fairly high angles of attack desired but it does provide reasonable levels of Reynolds Number. The 14-Foot Transonic Tunnel will permit the angle of attack range, with appropriate sting arrangements, but does not produce the Reynolds Number levels of the 11-Foot Tunnel. Therefore, the final decision on which tunnels will be used will be based on availability and applicability as ascertained by both Vought and NASA.

Testing in the 12-Foot Pressure Tunnel would be of great value in the evaluation of aerodynamics at high angles of attack for subsonic flight. Since this study has concentrated on high subsonic, transonic and supersonic capabilities, testing in this tunnel is recommended for future effort after the configuration has been further defined and powered testing has been implemented.

In order to understand the aerodynamics of the configuration a complete drag buildup is needed, extending from the low subsonic to high supersonic speeds as shown in Table 8-2. Control effectiveness must be investigated over the same range, but in lesser detail as shown in Table 8-3. This series of tests is intended to evaluate the changes in effectiveness of the various controls with angle of attack and the cross coupling of the controls.

A series of investigative runs is needed to determine the effects of configuration changes. The vertical control surfaces must be moved fore and aft, as well as inboard and outboard, to evaluate the mutual interaction effects. The canards must be raised to the shoulder of the inlet, and the forward ventrals must be moved fore and aft for the same reason. These exploratory runs are not required at each and every Mach number as shown in Table 8-4.

Table 8-2 - Basic Configuration Test Plan

α Range A = -4° to 24° (2 deg increments)
α Range B = -4° ~ 50° (increments to be selected)
β Range A = -4° to 10° (2 deg increments)
β Range B = -4° to tunnel limit (increments to be selected)
(Maximum of 4 β sweeps per α sweep)

I - BASIC CONFIGURATION INCLUDING BUILD UP											
			MACH NUMBER								
CONFIGURATION	α	β	.6	.8	.9	1.1	1.2	1.4	1.6	1.8	2.0
B	B	B	X	X							
"	A	A			X	X	X	X	X	X	X
BW_1	B	B	X	X							
"	A	A			X	X	X	X	X	X	X
BW_1S_1	B	B	X	X							
"	A	A			X	X	X	X	X	X	X
$BW_1S_1C_1$	B	B	X	X							
	A	A			X	X	X	X	X	X	X
$BW_1S_1C_1Vu_1$	B	B	X	X							
	A	A			X	X	X	X	X	X	X
$BW_1S1C_1Vu_1VA_1$	B	B	X	X							
	A	A			X	X	X	X	X	X	X
$BW_1S_1C_1Vu_1VA_1VI_1$	B	B	X	X							
	A	A			X	X	X	X	X	X	X
$BW_1S_1C_1Vv_1VA_1VL_1+F_{1v}$	B	B	X	X							
	A	A			X	X	X	X	X	X	X
$BW_1S_1C_1Vu_1VA_1VI_1+F_{1v}+F_{1L}$	B	B	X	X							
	A	A			X	X	X	X	X	X	X

Table 8-3 - Control Effectiveness Test Plan

II - SURFACE DEFLECTION AND POSITION STUDY								
$G = BW_1S_1C_1$ $Vu_1VA_1VI_1F_1uF_1L$ α and β ranges same as in 1 M range: A = .6, .9 B = 1.1, 1.4, 1.6, 1.8, 2.0								
CONFIGURATION	δ_e	δ_{v_1}	δ_{v_2}	δ_i	δ_c	α	β	M
G	$\pm5,\pm10$	0	0	0	0	B	B	A
	$\pm5,\pm10$					A	A	B
G	0	5,10,15	0	0	0	B	B	A
		5,10,15	0	0	0	A	A	B
G	0	0	5,10,5	0	0	B	B	A
	0	0	5,10,15	0	0	A	A	B
G	0	0	0	10,20	0	B	B	A
	0	0	0	10,20	0	A	A	B
G	0	0	0	0	$\pm5,\pm10$	B	B	A
	0	0	0	0	$\pm5,\pm10$	A	A	B

The above test program will also include combinations of deflections and variation of position. The vertical fins will be moved fore and aft through a range of 1 MAC of the vertical. They will also be tested in 2 spanwise positions. The inlet fins will be moved aft approximately one fin root chord. The canard will be moved fore and aft and will be tested coplanar with the wing. Therefore the above matrix shows only an outline of the testing to be done.

Table 8-4 - Configuration Effects Test Plan

III - CONFIGURATION GEOMETRY STUDY			
M Range: A = .6,.9 B = 1.2, 1.6, 1.8, 2.0 α, β Ranges same as in I and II			
CONFIGURATION	M	α	β
(Canard Study) G - C_1 + Cw	A B	B A	B A
(Vertical Study) G - Vu_1 + Vu_L	A B	B A	B A
(Aft Ventral Study) G - VA_1 + VA_2	A B	B A	B A
(Forward Ventral Study) G - VI_1 + VI_2	A B	B A	B A
(Wing Leading Edge Study) G - W_1 + W_2	A B	B A	B A

9.0 CONCLUSIONS

The principal Phase I study findings are summarized.

9.0 CONCLUSIONS

Conclusions resulting from the Phase I design and analysis effort can be grouped in three categories: configuration, aerodynamic and propulsion uncertainties. The principal conclusions are:

CONFIGURATION

- The TF120 aerodynamic configuration is essentially uncompromised by installation of the SFTF propulsion system.

- The aerodynamic configuration can be applied to STOL or CTOL roles with minimal change.

- The SFTF-powered TF120 exhibits excellent fighter performance, well in excess of study guidelines

- The aerodynamic analysis suggests potential payoffs for the unconventional usage of the multiple all-moving aerodynamic control surfaces.

- The short air induction system requires development.

AERODYNAMICS

- The angle of attack at which TF120 aerodynamics become seriously nonlinear is uncertain because of the vortex patterns associated with the forebody/strake/canard/wing complex. Principal concerns are elevon effectiveness, pitchup tendencies and yaw departure tendencies.

- The design goal of post-stall maneuverability was not confirmed due to a lack of suitable analysis methods. We see no alternative to subsonic wind tunnel tests to the highest feasible angle of attack, and including large amplitude control deflections.

- Theoretical methods predict strong induced responses to aerodynamic control deflections. The existence of such effects has been confirmed, but the absolute magnitudes and behavior at large control deflections must be confirmed by test.

- The ability to generate pure single-axis response by simultaneous deflection of multiple aerodynamic controls was demonstrated for a linear system. The feasibility and performance payoffs for this approach with nonlinear aerodynamics must await a more comprehensive data base.

- APAS far-field wave drag solutions were sensitive to minor math model changes. Estimates at Mach 2.0 and above were not consistent with Mach 1.2 - 1.8 values. The anomalies encountered warrant further study of APAS and comparison with alternative methods. The proposed Phase II sting-mounted wind tunnel model will provide a data base on all interactions except afterbody drag.

- Drag due to lift estimation methods varied widely, at a given Mach number and the relative trends with Mach number. Loss of leading edge suction as lift coefficient increased was not properly accounted for by most methods.

PROPULSION

- The Series Flow Tandem Fan (SFTF) cycle in the series flow (high speed) mode is an afterburning turbofan, which permits speeds in excess of Mach 2.4.

- Parallel flow operation for VTOL exhibits low specific fuel consumption (0.94 lb/hr/lb with fan augmentation, 0.54 dry), with a favorable effect on mission radius.

- Low jet velocities and moderate exhaust temperatures ($950^{o}F$ during VTO) make the SFTF attractive for shipboard operation.

- Augmentation of the aft fan flow stream during free deck takeoffs yields a deck roll of 210 feet with a 9,724 lb overload.

- The SFTF cycle can be implemented using conventional core engine and fan technology.

- Major elements of technical risk are the series/parallel flow transition section and the front fan burner.

10.0 REFERENCES

REFERENCES

1. Driggers, H. H.: Study of Aerodynamic Technology for VSTOL Fighter/Attack Aircraft. NASA CR-152132, May 1978.

2. Boruff, W. R. and Roch, A. J., Jr.: Impact of Mission Requirements on V/STOL Propulsion Concept Selection. Paper 79-1283, presented at AIAA/SAE/ASME 15th Joint Propulsion Conference, Las Vegas, Nevada, June 18-20, 1979.

3. Anderson, C. J.: Study of Aerodynamic Technology for Single-Cruise-Engine VSTOL Fighter/Attack Aircraft. NASA Request for Proposal NAS2-28182, September 1980.

4. Driggers, H. H.: SF-122 VSTOL Strike Fighter Concept and Performance. Vought Corporation Report 2-38100/8R-51534, March 1978.

5. Aircraft Synthesis Analysis Program. 2-53600/1R-507R, Vought Aeronautics, June 1971.

6. USAF Stability and Control DATCOM, McDonnell Douglas Corporation, February 1972.

7. Bonner, E., Clever, W. and Dunn, K.: Aerodynamic Preliminary Analysis System. Part I NASA CR 145284, Part II NASA CR 145300.

8. Benepe, D. B., Kouri, B. G., and Webb, J. B.: Aerodynamic Characteristics of Non-Straight-Taper Wings. AFFDL-TR-66-73, October 1966.

9. Margason, Richard J., and Lamar, John E.: Vortex-Lattice FORTRAN Program for Estimating Subsonic Aerodynamic Characteristics of Complex Planforms. NASA TND-6142, 1971.

10. The USAF Stability and Control Digital Datcom. Technical Report AFFDL-TR-6-45, Volume 1, 1976.

11. Marti, V. M. and Vetsch, G. J.: Preliminary Development of Digital Flight Control System. AFFDL-TR-79-3017, April 1978.

12. Hendersen, C., Clark, J., Walters, M.: V/STOL Aerodynamics and Stability Control Manual. NADC-80017-60, January 1980.

13. Gentry, Carl L. and Margason, Richard: Jet-Induced Lift Losses on VTOL Configuration Hovering In and Out-of-Ground Effect. NASA TND-3166, 1966.

14. Shumpert, P. K., and Tibbets, J. G.: Model Tests of Jet-Induced Lift Effects on a VTOL Aircraft in Hover. NASA CR-1297, 1969.

15. Margason, Richard, J., and Gentry, Carl L., Jr.: Aerodynamic Characteristics of a Five-Jet VTOL Configuration in the Transition Speed Range. NASA TND-4812, 1968.

APPENDICES

Supplementary data developed in the course of the Phase I study effort are grouped here:

This section includes:

APPENDIX I - U.S. CUSTOMARY UNITS TO METRIC (SI) CONVERSION

APPENDIX II - AERODYNAMIC DATA

APPENDIX III - PERFORMANCE SENSITIVITIES

APPENDIX I

U.S. CUSTOMARY UNITS TO METRIC (SI) CONVERSION

MULTIPLY U.S.	BY	TO OBTAIN SI
Degrees	1/0.9	Grads
Feet (ft)	0.3048	Meters (M)
Inches (in)	2.54	Centimeters (cm)
ft^2	0.0929	M^2
in^2	6.4516	cm^2
ft/sec	0.3048	M/sec
Knots (kts)	1.852	KM/hr
Pounds (Mass) (lb)	0.4536	Kilograms (Kg)
Pounds (Force) (lb)	4.448	Newtons (N)
lb/ft^2	47.88	N/M^2
lb/in^2	0.6895	N/cm^2
$Slug-ft^2$	0.7375	$Kg-M^2$
Horsepower (hp)	0.7457	KW

Temperature Conversion:

$$^{\circ}C = (^{\circ}F-32)/1.8$$

APPENDIX II

AERODYNAMIC DATA

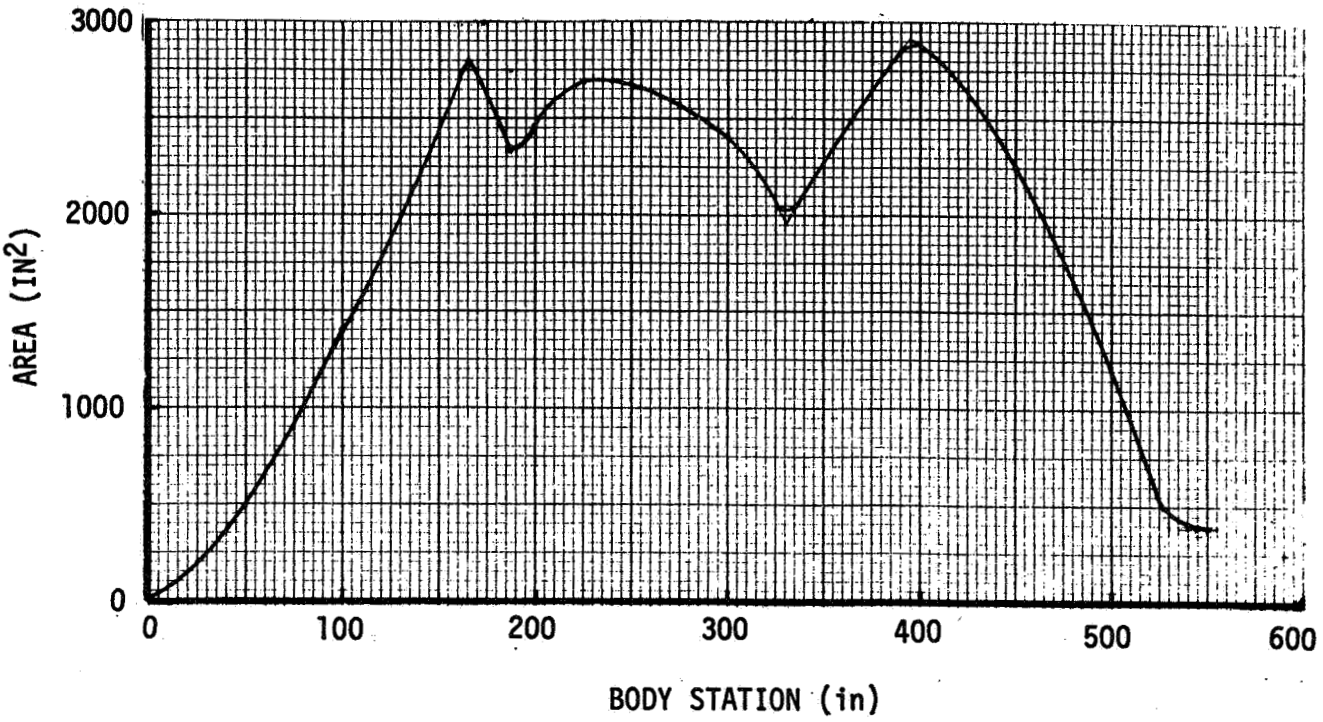

MACH 1 AREA DISTRIBUTION FOR TF120 CONFIGURATION

ZERO LIFT DRAG BUILDUP

	MACH NUMBER											
	0.2	0.4	0.6	0.8	0.9	1.2	1.4	1.6	1.8	2.0	2.2	2.4
Miscellaneous	.0019	.0019	.0020	.0022	.0024	.0038	.0039	.0037	.0036	.0034	.0033	.0033
Friction	.0123	.0111	.0102	.0091	.0090	.0081	.0077	.0075	.0070	.0066	.0063	.0061
Form and Interference	.0013	.0018	.0018	.0021	.0022	0	0	0	0	0	0	0
Wave Drag	0	0	0	0	0	.0330	.0320	.0310	.0300	.0290	.0281	.0270
TOTAL $C_{D_{MIN}}$	.0155	.0148	.0140	.0134	.0316	.0440	.0436	.0422	.0406	.0390	.0377	.0364

MISCELLANEOUS DRAG

	MACH NUMBER											
MISCELLANEOUS D/q	0.2	0.4	0.6	0.8	0.9	1.2	1.4	1.6	1.8	2.0	2.2	2.4
Protuberance, Cooling, Ventilation	0.382	.380	.377	.401	.435	.659	.603	.557	.527	.498	.485	.473
Roughness, Waviness, Leakage	.266	.268	.269	.282	.298	.469	.404	.355	.332	.308	.301	.294
Boundary Layer Diverter	.009	.030	.052	.082	.100	.192	.369	.413	.400	.388	.382	.377
TOTAL	0.657	0.678	0.698	0.765	0.833	1.320	1.376	1.325	1.259	1.194	1.168	1.144

TF120 SPAN EFFICIENCY FACTORS

M = 0		M = 0.6		M = 0.7		M = 0.8		M = 0.85		M = 0.9	
C_L	e	C_L	e	C_L	e	C_L	e	C_L	e	C_L	e
0	0.860	0	0.860	0	0.860	0	0.860	0	0.860	0	0.840
0.5	0.860	0.5	0.860	0.45	0.860	0.375	0.860	0.35	0.860	0.33	0.840
0.7	0.782	0.7	0.782	0.7	0.768	0.7	0.697	0.7	0.626	0.62	0.596
0.9	0.718	0.9	0.718	0.9	0.704	0.9	0.643	1.3	0.555	1.20	0.538
1.1	0.672	1.1	0.672	1.1	0.658	1.1	0.608	2.0	0.499	1.50	0.512
1.3	0.636	1.3	0.636	1.3	0.621	1.3	0.577			1.80	0.495
1.6	0.595	1.6	0.595	1.6	0.582	1.6	0.542				
2.0	0.560	2.0	0.560	2.0	0.544	2.0	0.512				

M = 0.95		M = 1.00		M = 1.05		M = 1.2		M = 1.6		M = 2.0	
C_L	e	C_L	e	C_L	e	C_L	e	C_L	e	C_L	e
0	0.805	0	0.765	0	0.73	0	0.624	0	0.375	0	0.315
0.29	0.805	0.22	0.765	0.2	0.73	0.2	0.624	0.2	0.375	0.2	0.315
0.56	0.586	0.5	0.600	0.4	0.627	0.4	0.556	0.4	0.332	0.4	0.277
1.2	0.538	1.2	0.538	1.0	0.535	0.6	0.523	0.6	0.304	0.9	0.206
1.5	0.512	1.5	0.512	1.6	0.480	1.6	0.440	1.4	0.229		
1.8	0.495	1.8	0.495	1.7	0.473						

M = 2.4	
C_L	e
0	0.260
0.2	0.260
0.5	0.194

TF120 Aerodynamic Force and Moment Coefficients

	Mach .2	Mach .6	Mach .9	Mach 1.2	Mach 1.6	Mach 2.0	Mach 2.4
C_{L_o}	.00815	.00824	.00838	.00536	.0008	.00456	.00470
C_{m_o}	- .01493	- .01540	- .01662	- .01452	- .00775	- .00731	- .00780
C_{L_α}	.05175	.05579	.06532	.05870	.04949	.03835	.03036
C_{m_α}	.00227	.00074	- .00376	- .00413	- .00419	- .0216	- .00037
C_{L_q}	4.24339	4.564	5.39274	4.1846	2.80243	2.31781	1.03845
C_{m_q}	-1.56824	-1.8106	-2.47634	-2.4676	-1.71472	-1.27889	-1.93845
C_{Y_β}	- .01033	- .01084	- .01182	- .01352	- .01214	- .00912	- .0075
C_{l_β}	- .00150	- .00167	- .00202	- .0019	- .00119	- .00086	- .0064
C_{n_β}	.00119	.00138	.00174	.00254	.00208	.00094	.00041
C_{L_p}	.00531	.00531	.00531	.00531	.00531	.00531	.00531
C_{Y_p}	- .03432	- .03216	- .02962	.01344	.03745	- .00907	- .03921
C_{l_p}	- .21226	- .21776	- .22791	- .24396	- .24667	- .23056	- .20447
C_{m_p}	.00163	.00163	.00163	.00163	.00163	.00163	.00163
C_{n_p}	- .01485	- .01596	- .01738	- .03738	- .04988	- .02584	- .01088
C_{l_r}	.00692	.00692	.00692	.00692	.00692	.00692	.00692
C_{Y_r}	.50766	.53683	.59438	.66918	.48190	.39563	.33476
C_{l_r}	.06528	.07241	.08756	.07635	.04266	.02088	.01676
C_{m_r}	.01121	.01121	.01121	.01121	.01121	.01121	.01121
C_{n_r}	- .36393	- .38054	- .41398	- .47029	- .3853	- .32626	- .28094

	Mach .2	Mach .6	Mach .9	Mach 1.2	Mach 1.6	Mach 2.0	Mach 2.4
SYMMETRIC DEFLECTION							
$C_{l_{\delta_a}}$	.00324	.00306	.00234	.00216	.00197	.0016	.00135
$C_{m_{\delta_a}}$	- .00211	- .00214	- .00202	- .00183	- .00167	- .00135	- .00113
$C_{l_{\delta_c}}$	.00435	.00455	.00476	.00464	.0064	.00485	.00368
$C_{m_{\delta_c}}$	.00411	.00439	.00510	.00595	.00324	.00279	.00222
ASYMMETRIC DEFLECTIONS							
$C_{Y_{\delta_a}}$	- .00107	- .00124	- .00165	- .00211	- .00076	- .0003	- .00015
$C_{l_{\delta_a}}$	.00099	.00098	.00097	.00069	.00062	.00052	.00044
$C_{n_{\delta_w}}$	.00051	.00059	.00078	.00106	.00041	.00016	.00009
$C_{Y_{\delta_V}}$	.00818	..00864	.00945	.01085	.00937	.00675	.00547
$C_{l_{\delta_v}}$	.00285	.00318	.00384	.00347	.00211	.00116	.00081
$C_{n_{\delta_v}}$	- .00383	- .00405	- .00443	- .00524	- .0047	- .00344	- .0028
$C_{Y_{\delta_{av}}}$	.00109	.00114	.0013	.0018	.00116	.00133	.00113
$C_{l_{\delta_{av}}}$	- .00156	- .00174	- .00208	- .00173	- .00108	- .00057	- .00038

TF120 Control Effectiveness (Continued)

	Mach .2	Mach .6	Mach .9	Mach 1.2	Mach 1.6	Mach 2.0	Mach 2.4
$C_{n_{\delta_{av}}}$	- .00047	- .00049	- .00056	- .0008	- .00051	- .00061	- .00052
$C_{Y_{\delta_{fv}}}$	.00083	.00086	.00094	.00099	.00156	.00087	.00054
$C_{l_{\delta_{fv}}}$	.00018	.00021	.00026	.00026	.00018	.00015	.00007
$C_{n_{\delta_{fv}}}$	.00042	.00044	.00049	.00059	.00028	.00037	.00030
$C_{Y_{\delta_c}}$	.00076	.00079	.00084	.00072	.00041	.00025	.00063
$C_{l_{\delta_c}}$	.00040	.00040	.00038	- .00008	.00007	.00058	.00079
$C_{n_{\delta_c}}$	.00023	.00025	.00028	.00041	.00044	.00044	.00015

APPENDIX III

PERFORMANCE SENSITIVITIES

The following parametric carpet plots for the TF120 were generated by the Vought Aircraft Synthesis Analysis Program (ASAP). They may be used to determine the sensitivity of takeoff weight or other performance parameters to changes in performance requirementes (constraints). All points in the design space represent airplanes fuel-balanced for the 200 NM radius, Mach 1.6 Supersonic Intercept mission defined in Figure 6-3.

The baseline design for the Phase I design analysis, the center of the design space, was selected as the point design. The minimum weight airplane which satisfies the design constraints (VTO T/W = 1.17 and sustained nz = 6.2, M = 0.6, 10,000 ft) is indicated on each chart.

TF120 PERFORMANCE SENSITIVITIES
SSTF011 *

1= CHANGE INDEPENDENT VAR.
2= CHANGE DEPENDENT VAR.
3= NEXT DEPENDENT VAR.
4= ADD A CONSTRAINT
5= DELETE A CONSTRAINT
6= CONSTRAINT INTERSECTIONS
7= COORDINATE PICK
8= INSERT/DELETE GRID
9= REPAINT
10= DELETE MARKER COORDINATES
11= BATCH PLOT
12= EXIT 8

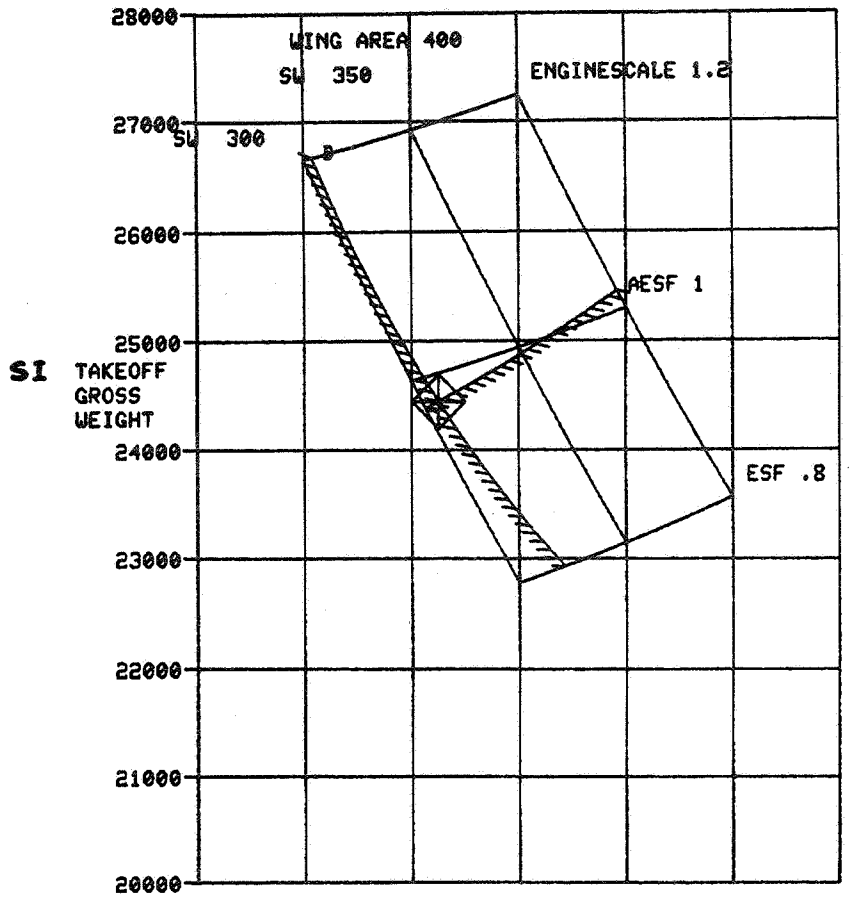

SYMBOL	CONSTRAINT	TYPE	VALUE
A	THRUST TO WEIGHT	GT	1.170
B	EQUIL. NZ - 10KM= .60	GT	6.200

MARKER COORDINATES

	ENGINESCALE	WING AREA	TAKEOFF GROSS WEIGHT
*1.	.97649998	306.58827622	24440.29511514

SUPERSONIC INTERCEPT
M = 1.6 h = 50K FT

TF120 PERFORMANCE SENSITIVITIES
SSTF011 *

1- CHANGE INDEPENDENT VAR.
2- CHANGE DEPENDENT VAR.
3- NEXT DEPENDENT VAR.
4- ADD A CONSTRAINT
5- DELETE A CONSTRAINT
6- CONSTRAINT INTERSECTIONS
7- COORDINATE PICK
8- INSERT/DELETE GRID
9- REPAINT
10- DELETE MARKER COORDINATES
11- BATCH PLOT
12- EXIT 8

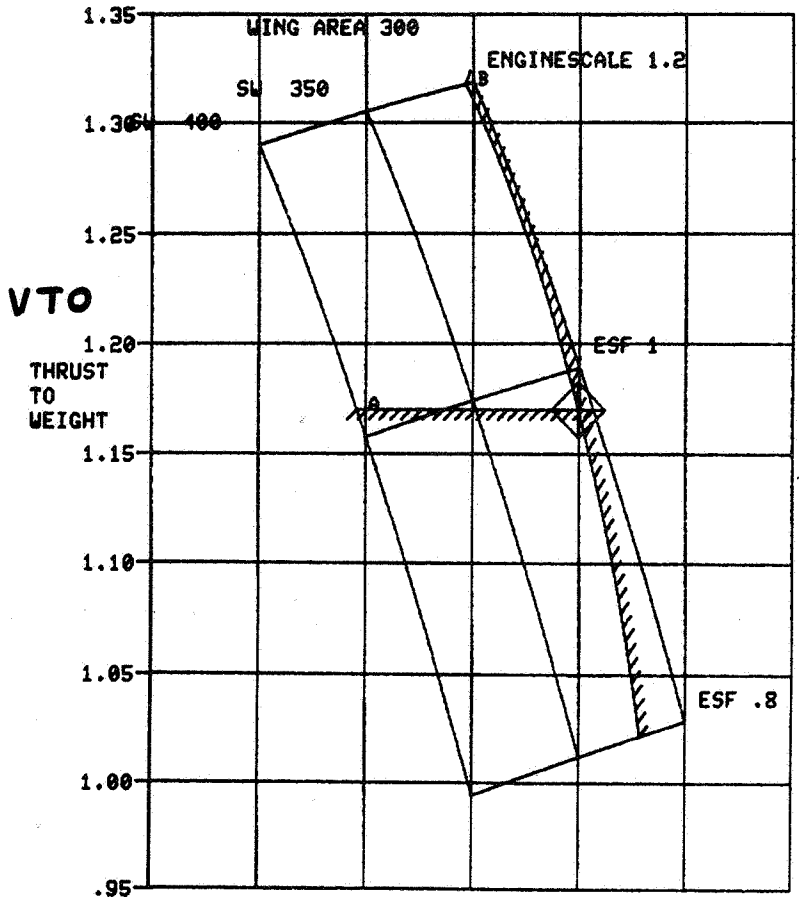

SYMBOL	CONSTRAINT	TYPE	VALUE
A	THRUST TO WEIGHT	GT	1.170
B	EQUIL. NZ - 10KM= .60	GT	6.200

MARKER COORDINATES

	ENGINESCALE	WING AREA	THRUST TO WEIGHT
*1.	.97649998	306.58827622	1.16998288

VTO NORMAL THRUST
950°F FRONT AUGMENTATION ONLY

TF120 PERFORMANCE SENSITIVITIES
SSTF011 *

1= CHANGE INDEPENDENT VAR.
2= CHANGE DEPENDENT VAR.
3= NEXT DEPENDENT VAR.
4= ADD A CONSTRAINT
5= DELETE A CONSTRAINT
6= CONSTRAINT INTERSECTIONS
7= COORDINATE PICK
8= INSERT/DELETE GRID
9= REPAINT
10= DELETE MARKER COORDINATES
11= BATCH PLOT
12= EXIT

8

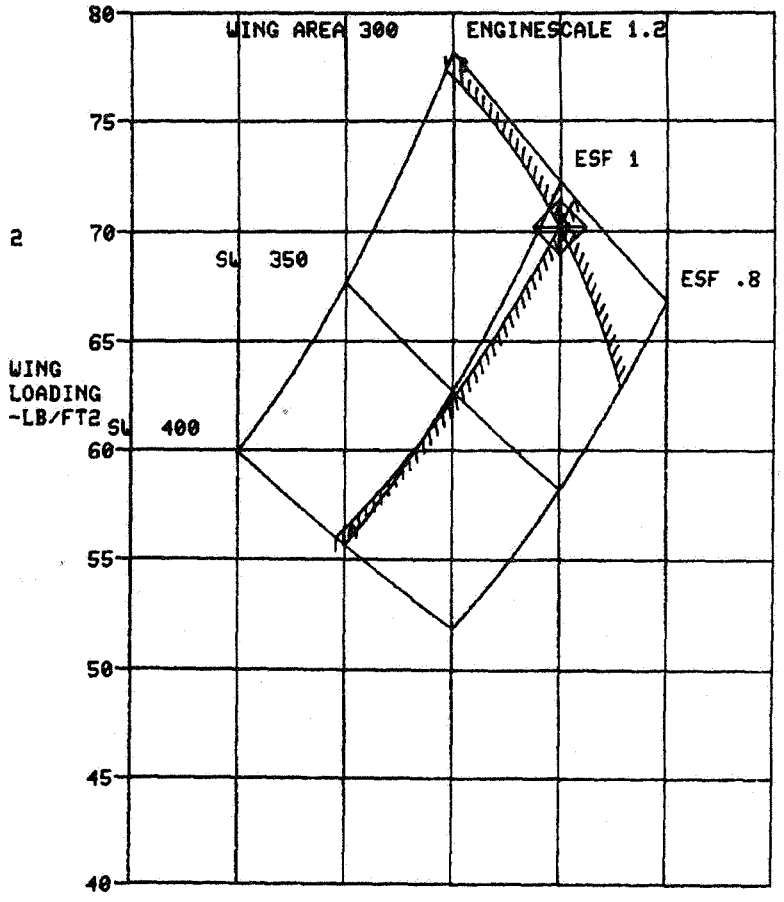

SYMBOL	CONSTRAINT	TYPE	VALUE
A	THRUST TO WEIGHT	GT	1.170
B	EQUIL. NZ - 10KM= .60	GT	6.200

MARKER COORDINATES

	ENGINESCALE	WING AREA	WING LOADING -LB/FT
*1.	.97649998	306.58827622	70.19551707

AT 0.88 VTO WEIGHT

TF120 PERFORMANCE SENSITIVITIES
SSTF011 *

1= CHANGE INDEPENDENT VAR.
2= CHANGE DEPENDENT VAR.
3= NEXT DEPENDENT VAR.
4= ADD A CONSTRAINT
5= DELETE A CONSTRAINT
6= CONSTRAINT INTERSECTIONS
7= COORDINATE PICK
8= INSERT/DELETE GRID
9= REPAINT
10= DELETE MARKER COORDINATES
11= BATCH PLOT
12= EXIT 8

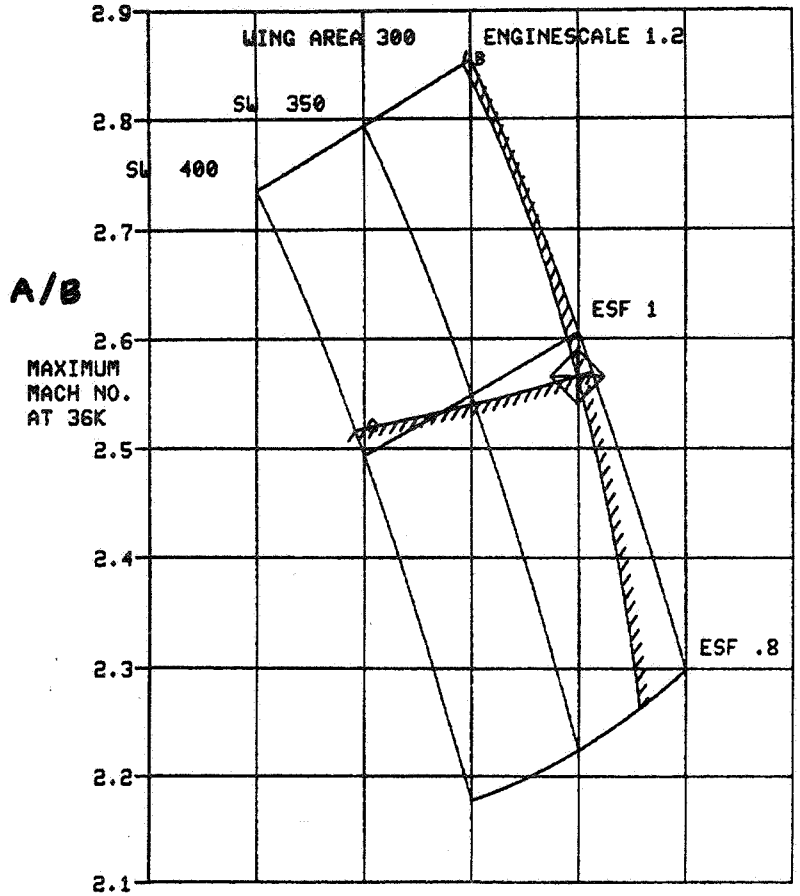

SYMBOL	CONSTRAINT	TYPE	VALUE
A	THRUST TO WEIGHT	GT	1.170
B	EQUIL. NZ - 10KM= .60	GT	6.200

MARKER COORDINATES

	ENGINESCALE	WING AREA	MAXIMUM MACH NO.AT 36K
*1.	.97649998	306.58827622	2.56571119

NOTE: THRUST = DRAG CONDITION

MACH 2.4 AIRFRAME LIMIT

TF120 PERFORMANCE SENSITIVITIES
SSTF011 *

1= CHANGE INDEPENDENT VAR.
2= CHANGE DEPENDENT VAR.
3= NEXT DEPENDENT VAR.
4= ADD A CONSTRAINT
5= DELETE A CONSTRAINT
6= CONSTRAINT INTERSECTIONS
7= COORDINATE PICK
8= INSERT/DELETE GRID
9= REPAINT
10= DELETE MARKER COORDINATES
11= BATCH PLOT
12= EXIT 8

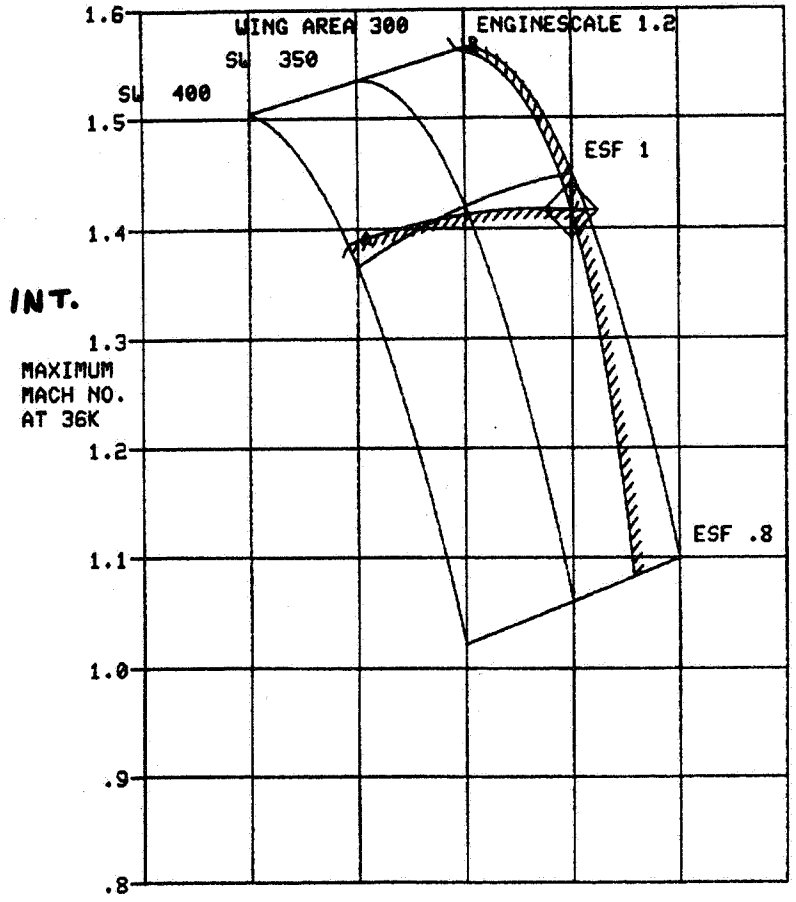

SYMBOL	CONSTRAINT	TYPE	VALUE
A	THRUST TO WEIGHT	GT	1.170
B	EQUIL. NZ - 10KM= .60	GT	6.200

MARKER COORDINATES

	ENGINESCALE	WING AREA	MAXIMUM MACH NO.AT 36K
*1.	.97649998	306.58827622	1.41654718

INTERMEDIATE THRUST

TF120 PERFORMANCE SENSITIVITIES
SSTF011 *

1= CHANGE INDEPENDENT VAR.
2= CHANGE DEPENDENT VAR.
3= NEXT DEPENDENT VAR.
4= ADD A CONSTRAINT
5= DELETE A CONSTRAINT
6= CONSTRAINT INTERSECTIONS
7= COORDINATE PICK
8= INSERT/DELETE GRID
9= REPAINT
10= DELETE MARKER COORDINATES
11= BATCH PLOT
12= EXIT 8

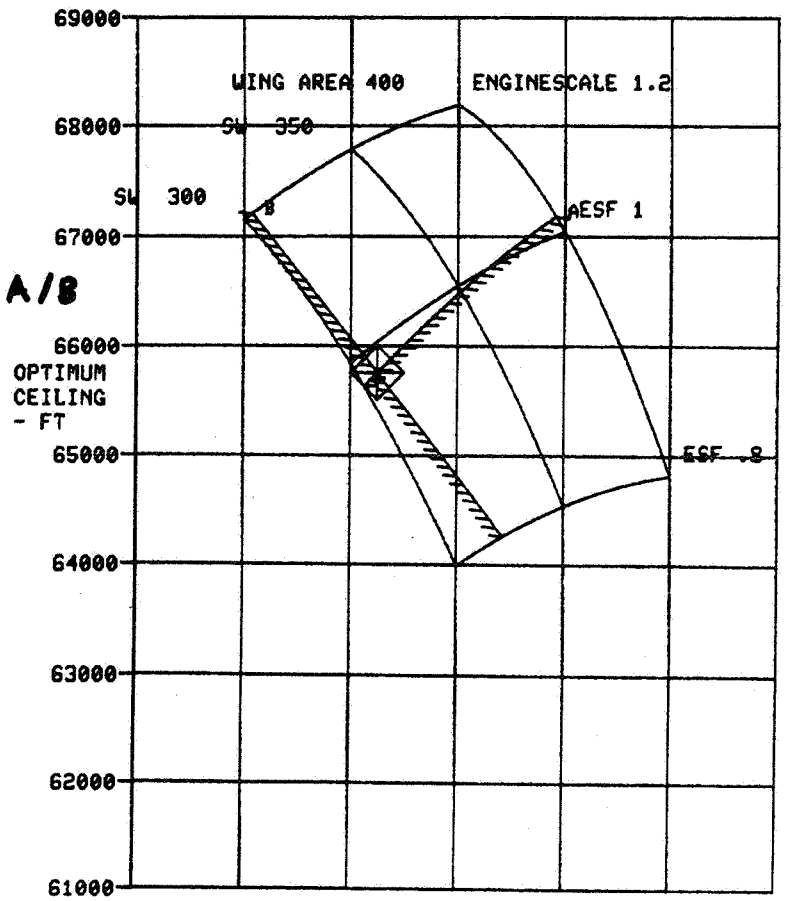

SYMBOL	CONSTRAINT	TYPE	VALUE
A	THRUST TO WEIGHT	GT	1.170
B	EQUIL. NZ - 10KM= .60	GT	6.200

MARKER COORDINATES

	ENGINESCALE	WING AREA	OPTIMUM CEILING - FT
*1.	.97649998	306.58827622	65754.53112478

MAXIMUM A/B

R/C = 500 FPM

TF120 PERFORMANCE SENSITIVITIES
SSTF011 *

1= CHANGE INDEPENDENT VAR.
2= CHANGE DEPENDENT VAR.
3= NEXT DEPENDENT VAR.
4= ADD A CONSTRAINT
5= DELETE A CONSTRAINT
6= CONSTRAINT INTERSECTIONS
7= COORDINATE PICK
8= INSERT/DELETE GRID
9= REPAINT
10= DELETE MARKER COORDINATES
11= BATCH PLOT
12= EXIT

8

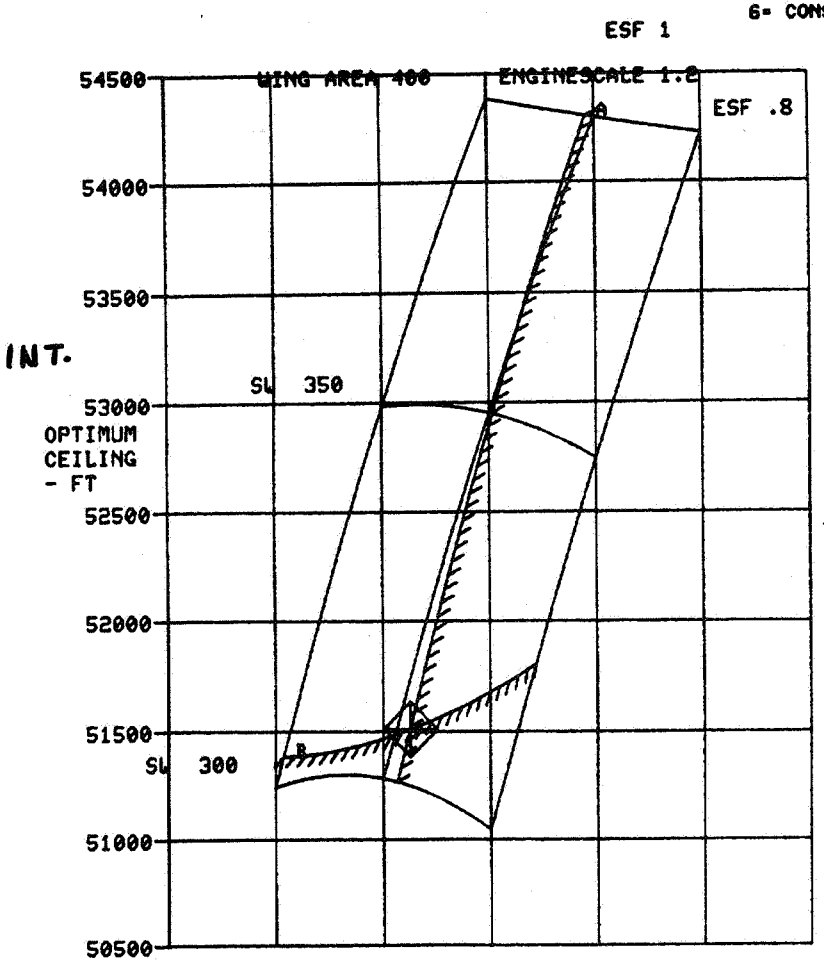

SYMBOL	CONSTRAINT	TYPE	VALUE
A	THRUST TO WEIGHT	GT	1.170
B	EQUIL. NZ - 10KM= .60	GT	6.200

MARKER COORDINATES

	ENGINESCALE	WING AREA	OPTIMUM CEILING - FT
*1.	.97649998	306.58827622	51509.27759566

INTERMEDIATE THRUST
R/C = 500 FPM

TF120 PERFORMANCE SENSITIVITIES
SSTF011 %

1= CHANGE INDEPENDENT VAR.
2= CHANGE DEPENDENT VAR.
3= NEXT DEPENDENT VAR.
4= ADD A CONSTRAINT
5= DELETE A CONSTRAINT
6= CONSTRAINT INTERSECTIONS
7= COORDINATE PICK
8= INSERT/DELETE GRID
9= REPAINT
10= DELETE MARKER COORDINATES
11= BATCH PLOT
12= EXIT 8

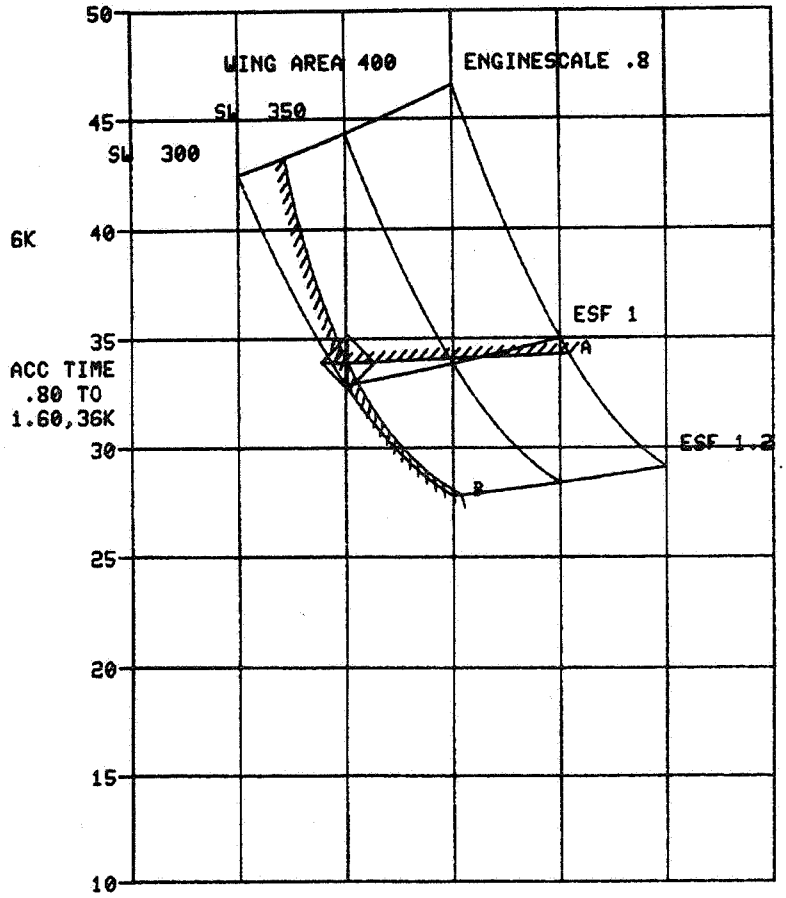

SYMBOL	CONSTRAINT	TYPE	VALUE
A	THRUST TO WEIGHT	GT	1.170
B	EQUIL. NZ - 10KM= .60	GT	6.200

MARKER COORDINATES

	ENGINESCALE	WING AREA	ACC TIME .80 TO 1.60,3
%1.	.97649998	306.58827622	33.89700662

MAXIMUM A/B

TF120 PERFORMANCE SENSITIVITIES
SSTF011 *

1- CHANGE INDEPENDENT VAR.
2- CHANGE DEPENDENT VAR.
3- NEXT DEPENDENT VAR.
4- ADD A CONSTRAINT
5- DELETE A CONSTRAINT
6- CONSTRAINT INTERSECTIONS
7- COORDINATE PICK
8- INSERT/DELETE GRID
9- REPAINT
10- DELETE MARKER COORDINATES
11- BATCH PLOT
12- EXIT

8

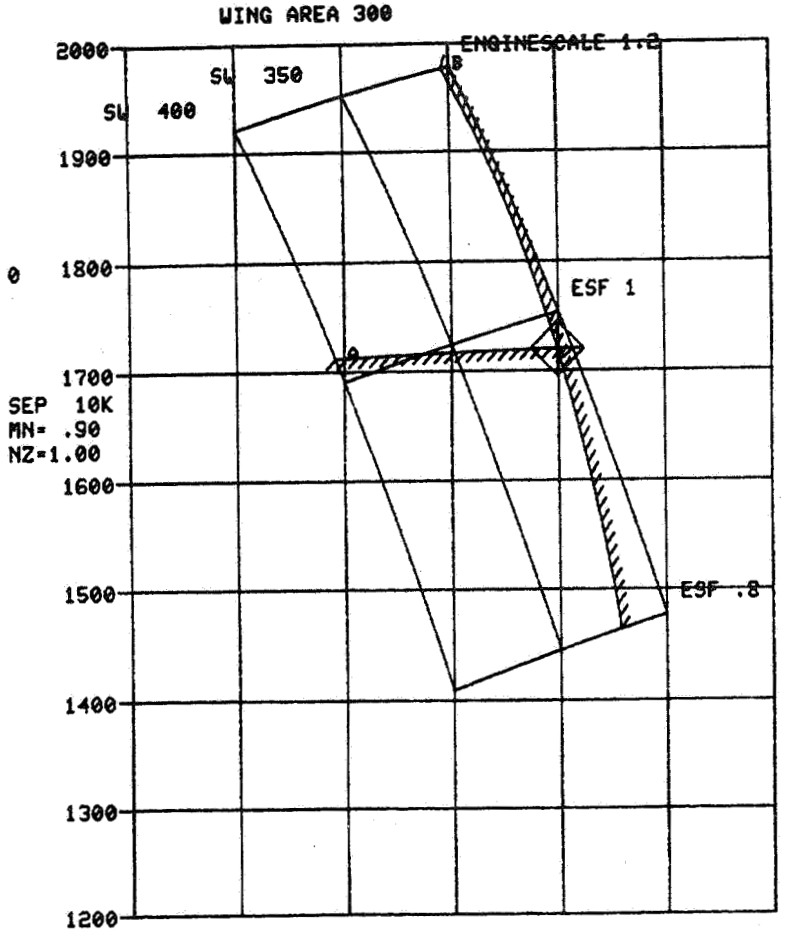

SYMBOL	CONSTRAINT	TYPE	VALUE
A	THRUST TO WEIGHT	GT	1.170
B	EQUIL. NZ - 10KM= .60	GT	6.200

MARKER COORDINATES

	ENGINESCALE	WING AREA	SEP 10KMN= .90 NZ=1.0
*1.	.97649998	306.58827622	1720.23574999

TF120 PERFORMANCE SENSITIVITIES
SSTF011 *

1= CHANGE INDEPENDENT VAR.
2= CHANGE DEPENDENT VAR.
3= NEXT DEPENDENT VAR.
4= ADD A CONSTRAINT
5= DELETE A CONSTRAINT
6= CONSTRAINT INTERSECTIONS
7= COORDINATE PICK
8= INSERT/DELETE GRID
9= REPAINT
10= DELETE MARKER COORDINATES
11= BATCH PLOT
12= EXIT

8

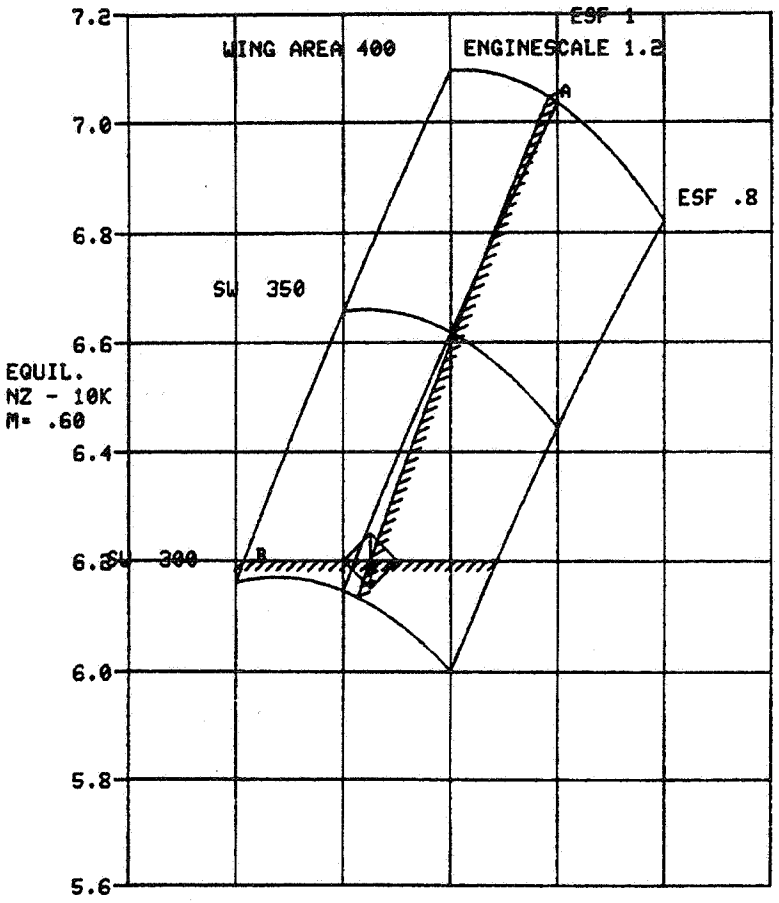

SYMBOL	CONSTRAINT	TYPE	VALUE
A	THRUST TO WEIGHT	GT	1.170
B	EQUIL. NZ - 10KM= .60	GT	6.200

MARKER COORDINATES

	ENGINESCALE	WING AREA	EQUIL. NZ - 10KM= .60
*1.	.97649998	306.58827622	6.20010403

TF120 PERFORMANCE SENSITIVITIES
SSTF011 *

1= CHANGE INDEPENDENT VAR.
2= CHANGE DEPENDENT VAR.
3= NEXT DEPENDENT VAR.
4= ADD A CONSTRAINT
5= DELETE A CONSTRAINT
6= CONSTRAINT INTERSECTIONS
7= COORDINATE PICK
8= INSERT/DELETE GRID
9= REPAINT
10= DELETE MARKER COORDINATES
11= BATCH PLOT
12= EXIT

8

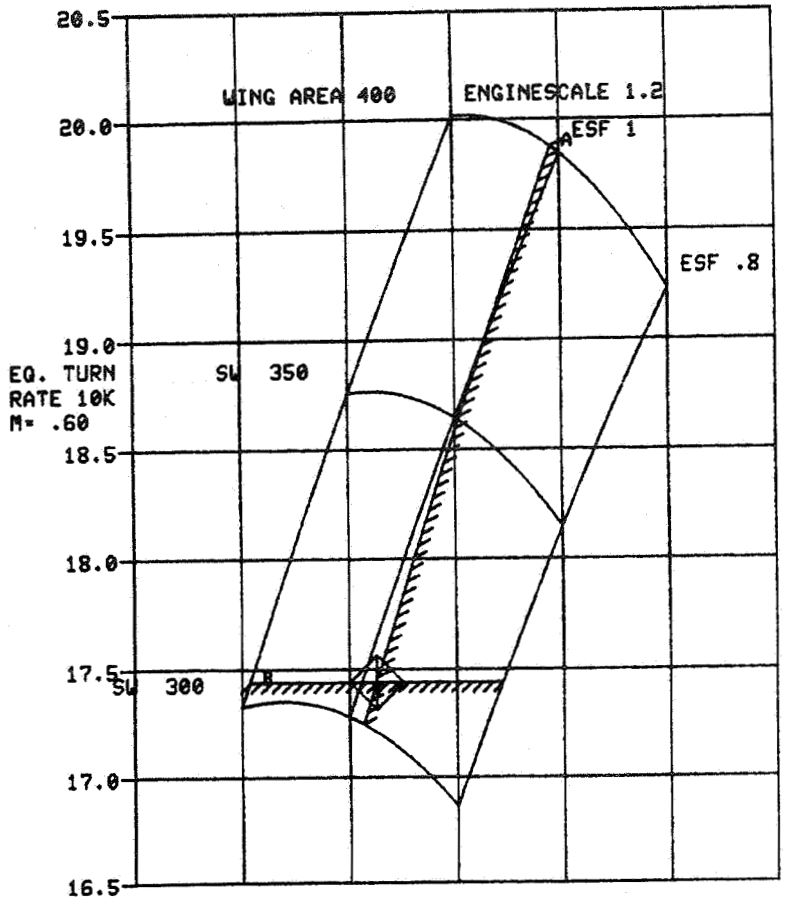

SYMBOL	CONSTRAINT	TYPE	VALUE
A	THRUST TO WEIGHT	GT	1.170
B	EQUIL. NZ - 10KM= .60	GT	6.200

MARKER COORDINATES

	ENGINESCALE	WING AREA	EQ. TURNRATE 10KM= .60
*1.	.97649998	306.58827622	17.43863227

TF120 PERFORMANCE SENSITIVITIES
SSTF011 *

1- CHANGE INDEPENDENT VAR.
2- CHANGE DEPENDENT VAR.
3- NEXT DEPENDENT VAR.
4- ADD A CONSTRAINT
5- DELETE A CONSTRAINT
6- CONSTRAINT INTERSECTIONS
7- COORDINATE PICK
8- INSERT/DELETE GRID
9- REPAINT
10- DELETE MARKER COORDINATES
11- BATCH PLOT
12- EXIT

8

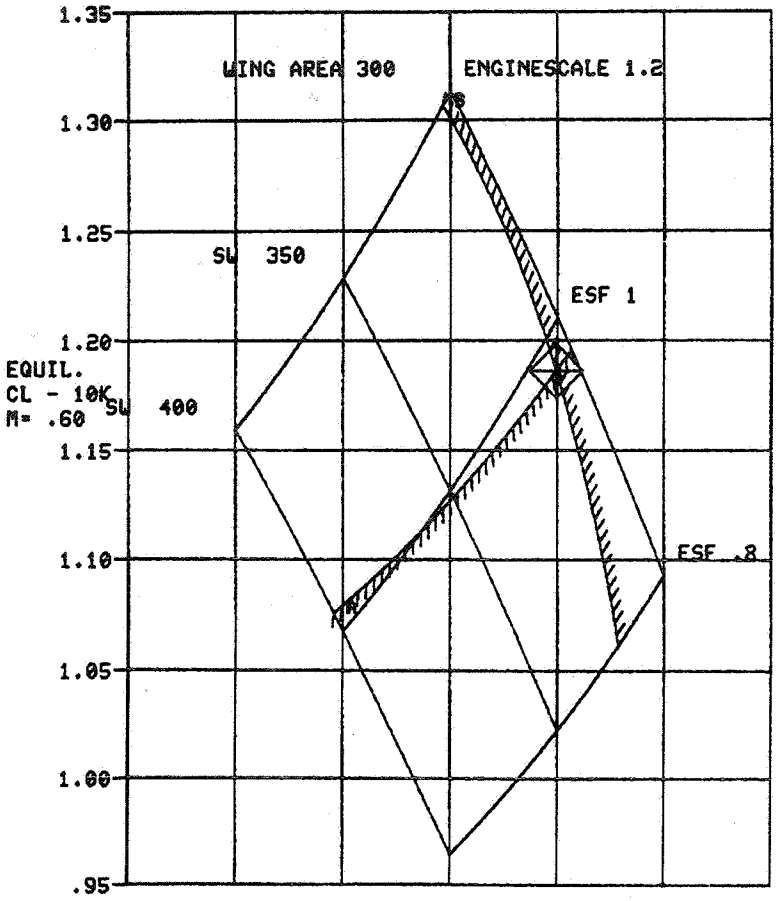

SYMBOL	CONSTRAINT	TYPE	VALUE
A	THRUST TO WEIGHT	GT	1.170
B	EQUIL. NZ - 10KM= .60	GT	6.200

MARKER COORDINATES

	ENGINESCALE	WING AREA	EQUIL. CL - 10KM= .60
*1.	.97649998	306.58827622	1.18604906

TF120 PERFORMANCE SENSITIVITIES
SSTF011 *

1= CHANGE INDEPENDENT VAR.
2= CHANGE DEPENDENT VAR.
3= NEXT DEPENDENT VAR.
4= ADD A CONSTRAINT
5= DELETE A CONSTRAINT
6= CONSTRAINT INTERSECTIONS
7= COORDINATE PICK
8= INSERT/DELETE GRID
9= REPAINT
10= DELETE MARKER COORDINATES
11= BATCH PLOT
12= EXIT

8

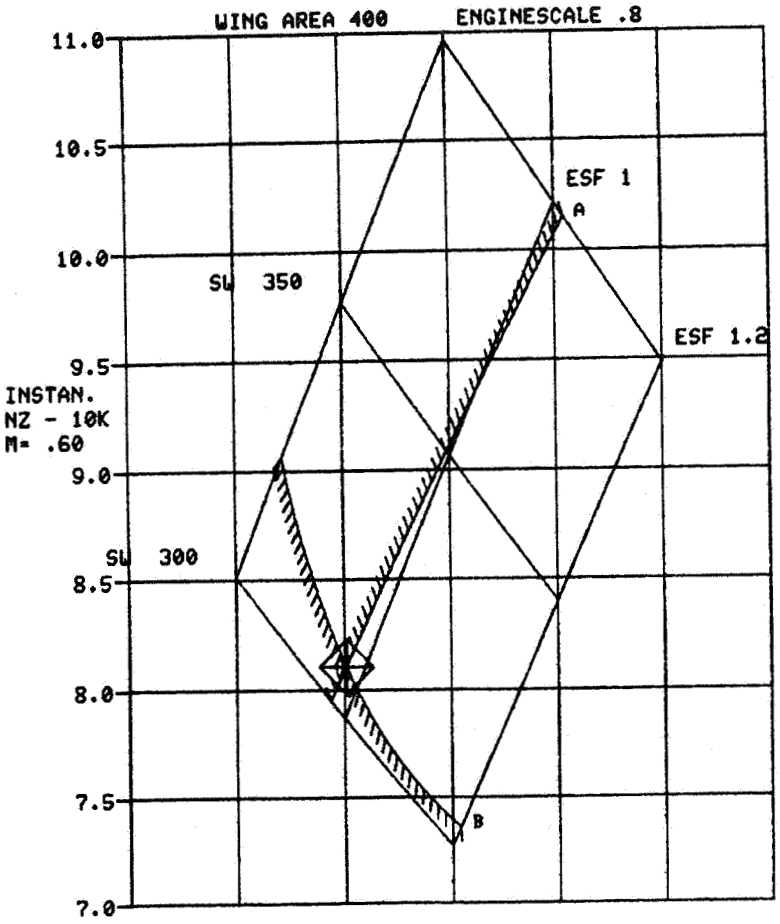

SYMBOL	CONSTRAINT	TYPE	VALUE
A	THRUST TO WEIGHT	GT	1.170
B	EQUIL. NZ - 10KM= .60	GT	6.200

MARKER COORDINATES

	ENGINESCALE	WING AREA	INSTAN. NZ - 10KM= .60
*1.	.97649998	306.58827622	8.10429276

TF120 PERFORMANCE SENSITIVITIES
SSTF011 *

1= CHANGE INDEPENDENT VAR.
2= CHANGE DEPENDENT VAR.
3= NEXT DEPENDENT VAR.
4= ADD A CONSTRAINT
5= DELETE A CONSTRAINT
6= CONSTRAINT INTERSECTIONS
7= COORDINATE PICK
8= INSERT/DELETE GRID
9= REPAINT
10= DELETE MARKER COORDINATES
11= BATCH PLOT
12= EXIT

8

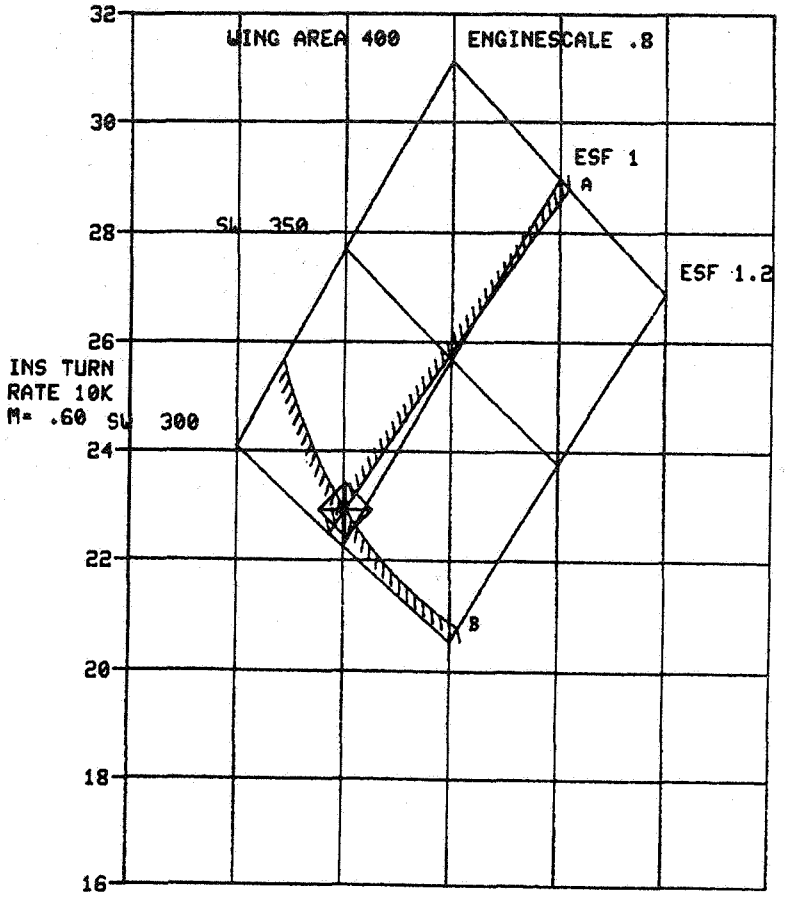

SYMBOL	CONSTRAINT			TYPE	VALUE
A	THRUST TO	WEIGHT		GT	1.170
B	EQUIL. NZ -	10KM= .60		GT	6.200

MARKER COORDINATES

	ENGINESCALE	WING AREA	INS TURNRATE 10KM= .60
*1.	.97649998	306.58827622	22.92027327

TF120 PERFORMANCE SENSITIVITIES
SSTF011 *

1= CHANGE INDEPENDENT VAR.
2= CHANGE DEPENDENT VAR.
3= NEXT DEPENDENT VAR.
4= ADD A CONSTRAINT
5= DELETE A CONSTRAINT
6= CONSTRAINT INTERSECTIONS
7= COORDINATE PICK
8= INSERT/DELETE GRID
9= REPAINT
10= DELETE MARKER COORDINATES
11= BATCH PLOT
12= EXIT 8

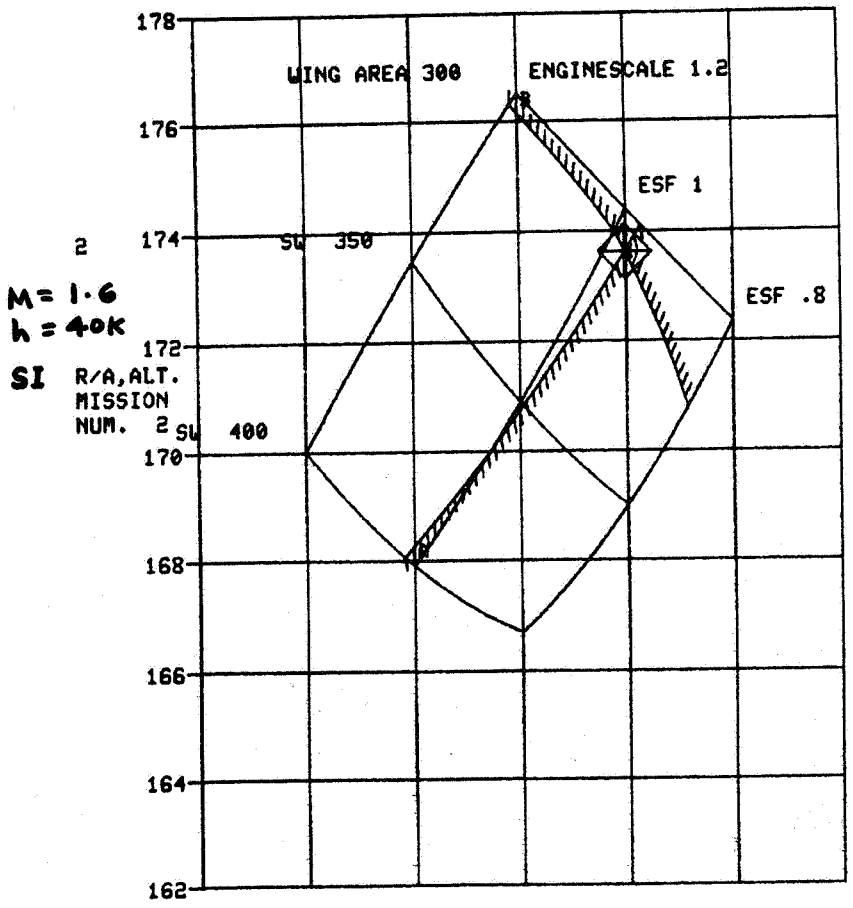

SYMBOL	CONSTRAINT	TYPE	VALUE
A	THRUST TO WEIGHT	GT	1.170
B	EQUIL. NZ - 10KM= .60	GT	6.200

MARKER COORDINATES

	ENGINESCALE	WING AREA	R/A,ALT.MISSION NUM.
*1.	.97649998	306.58827622	173.62256202

TF120 PERFORMANCE SENSITIVITIES
SSTF011 *

1= CHANGE INDEPENDENT VAR.
2= CHANGE DEPENDENT VAR.
3= NEXT DEPENDENT VAR.
4= ADD A CONSTRAINT
5= DELETE A CONSTRAINT
6= CONSTRAINT INTERSECTIONS
7= COORDINATE PICK
8= INSERT/DELETE GRID
9= REPAINT
10= DELETE MARKER COORDINATES
11= BATCH PLOT
12= EXIT 8

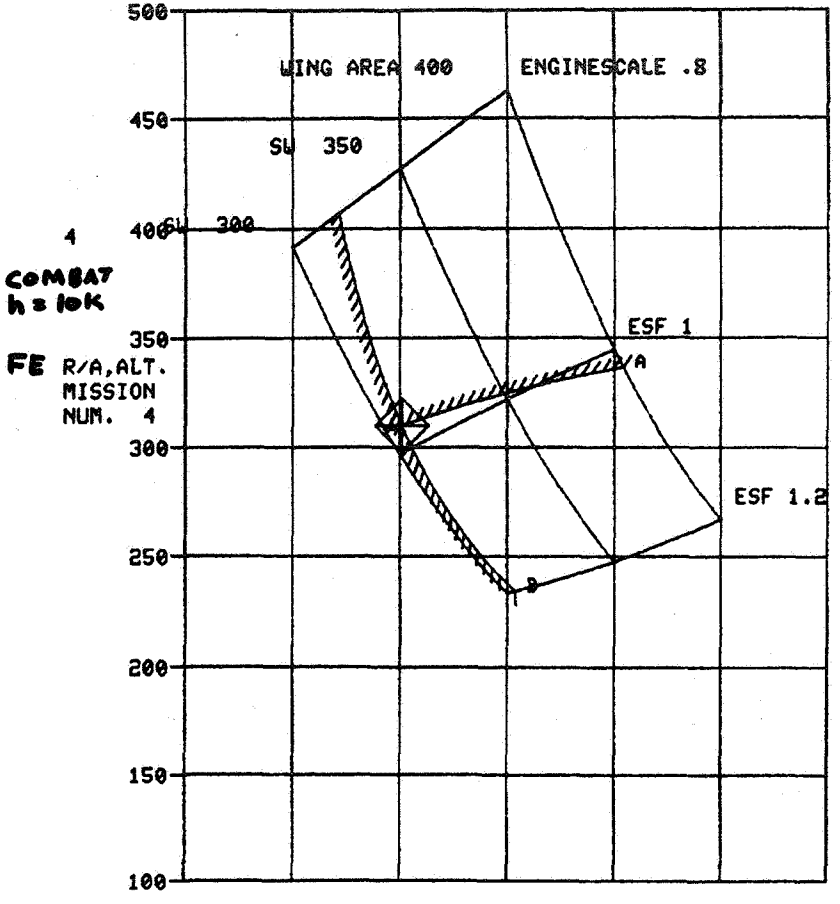

SYMBOL	C O N S T R A I N T	TYPE	VALUE
A	THRUST TO WEIGHT	GT	1.170
B	EQUIL. NZ - 10KM= .60	GT	6.200

M A R K E R C O O R D I N A T E S

	ENGINESCALE	WING AREA	R/A,ALT.MISSION NUM.
*1.	.97649998	306.58827622	309.89040396

TF120 PERFORMANCE SENSITIVITIES
SSTF011 *

1- CHANGE INDEPENDENT VAR.
2- CHANGE DEPENDENT VAR.
3- NEXT DEPENDENT VAR.
4- ADD A CONSTRAINT
5- DELETE A CONSTRAINT
6- CONSTRAINT INTERSECTIONS
7- COORDINATE PICK
8- INSERT/DELETE GRID
9- REPAINT
10- DELETE MARKER COORDINATES
11- BATCH PLOT
12- EXIT

8

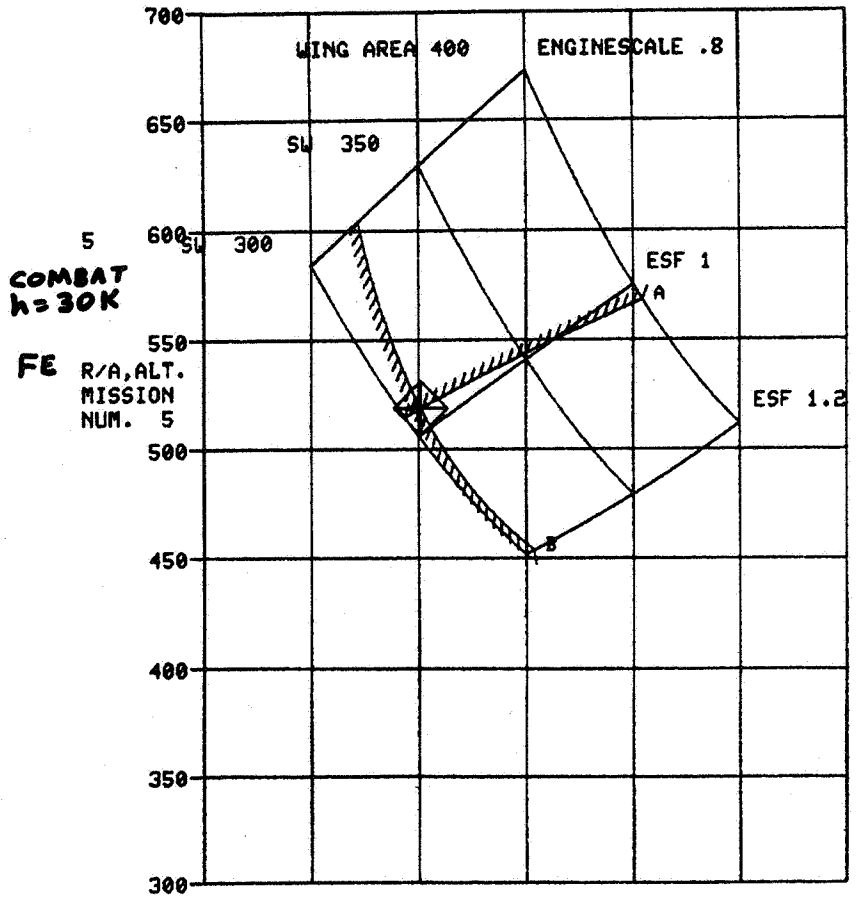

SYMBOL	CONSTRAINT	TYPE	VALUE
A	THRUST TO WEIGHT	GT	1.170
B	EQUIL. NZ - 10KM- .60	GT	6.200

MARKER COORDINATES

	ENGINESCALE	WING AREA	R/A,ALT.MISSION NUM.
*1.	.97649998	306.58827622	518.62850420

TF120 PERFORMANCE SENSITIVITIES
SSTF011 *

1= CHANGE INDEPENDENT VAR.
2= CHANGE DEPENDENT VAR.
3= NEXT DEPENDENT VAR.
4= ADD A CONSTRAINT
5= DELETE A CONSTRAINT
6= CONSTRAINT INTERSECTIONS
7= COORDINATE PICK
8= INSERT/DELETE GRID
9= REPAINT
10= DELETE MARKER COORDINATES
11= BATCH PLOT
12= EXIT 8

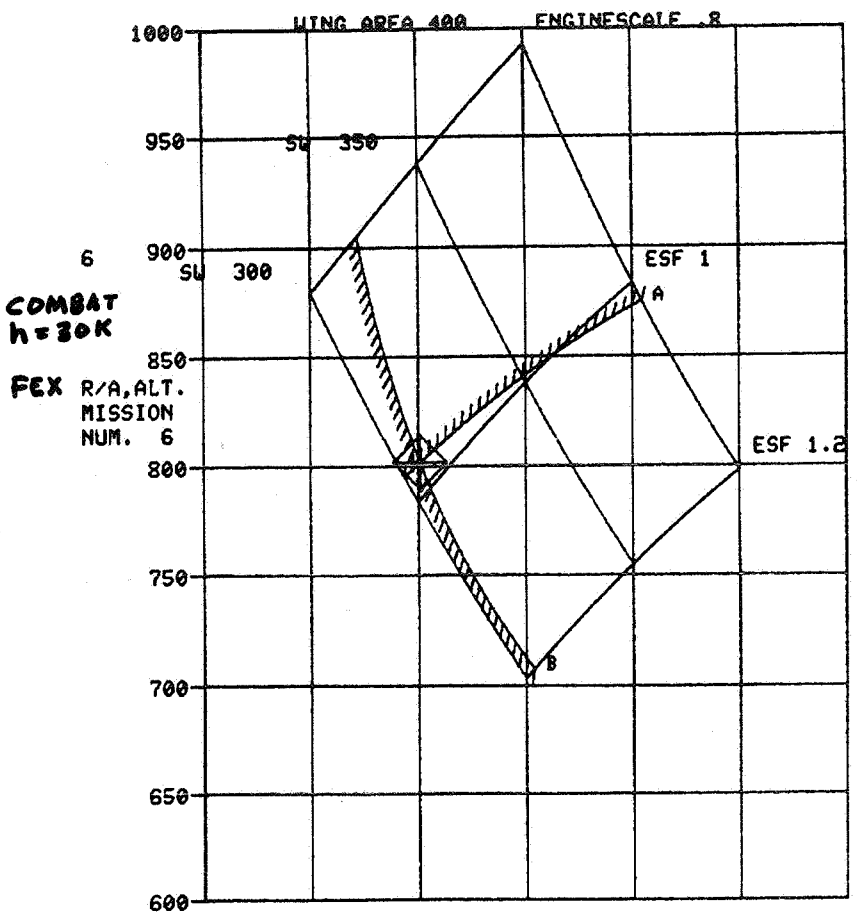

SYMBOL	CONSTRAINT	TYPE	VALUE
A	THRUST TO WEIGHT	GT	1.170
B	EQUIL. NZ - 10KM= .60	GT	6.200

MARKER COORDINATES

	ENGINESCALE	WING AREA	R/A,ALT.MISSION NUM.
*1.	.97649998	306.58827622	801.58853576

TF120 PERFORMANCE SENSITIVITIES
SSTF011 X

1= CHANGE INDEPENDENT VAR.
2= CHANGE DEPENDENT VAR.
3= NEXT DEPENDENT VAR.
4= ADD A CONSTRAINT
5= DELETE A CONSTRAINT
6= CONSTRAINT INTERSECTIONS
7= COORDINATE PICK
8= INSERT/DELETE GRID
9= REPAINT
10= DELETE MARKER COORDINATES
11= BATCH PLOT
12= EXIT 8

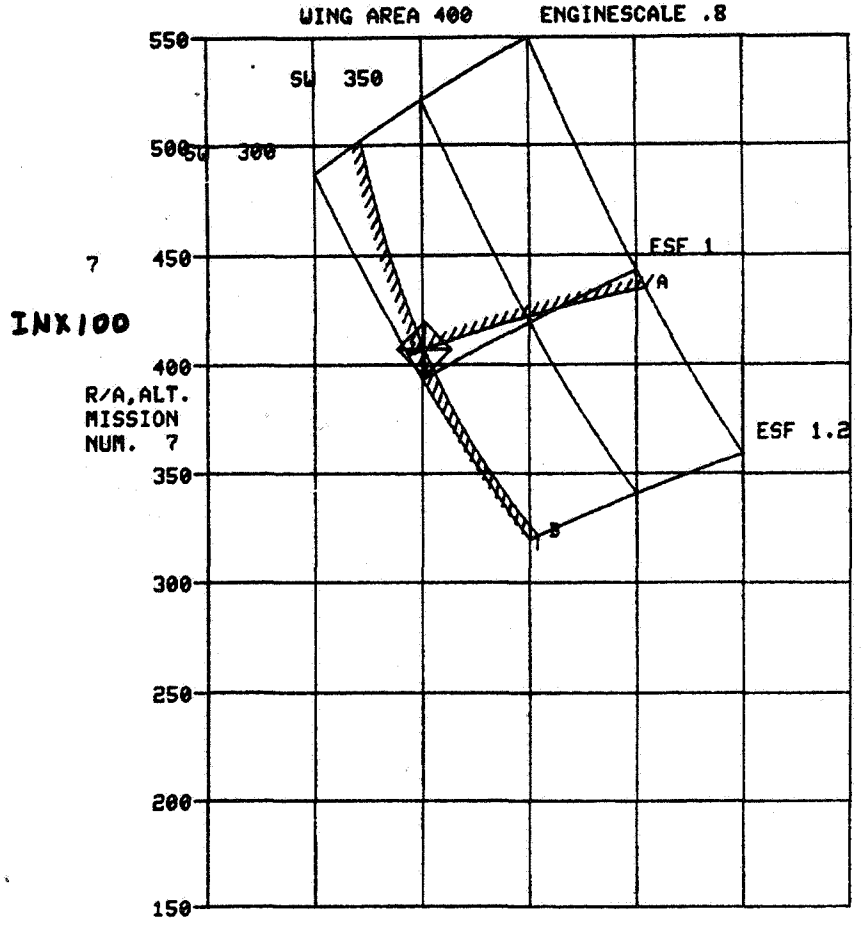

SYMBOL	CONSTRAINT	TYPE	VALUE
A	THRUST TO WEIGHT	GT	1.170
B	EQUIL. NZ - 10KM= .60	GT	6.200

MARKER COORDINATES

	ENGINESCALE	WING AREA	R/A,ALT.MISSION NUM.
X1.	.97649998	306.58827622	406.96590068

NOTE: ADD 100 NMI RADIUS TO CARPET VALUES

TF120 PERFORMANCE SENSITIVITIES
SSTF011 *

1= CHANGE INDEPENDENT VAR.
2= CHANGE DEPENDENT VAR.
3= NEXT DEPENDENT VAR.
4= ADD A CONSTRAINT
5= DELETE A CONSTRAINT
6= CONSTRAINT INTERSECTIONS
7= COORDINATE PICK
8= INSERT/DELETE GRID
9= REPAINT
10= DELETE MARKER COORDINATES
11= BATCH PLOT
12= EXIT 8

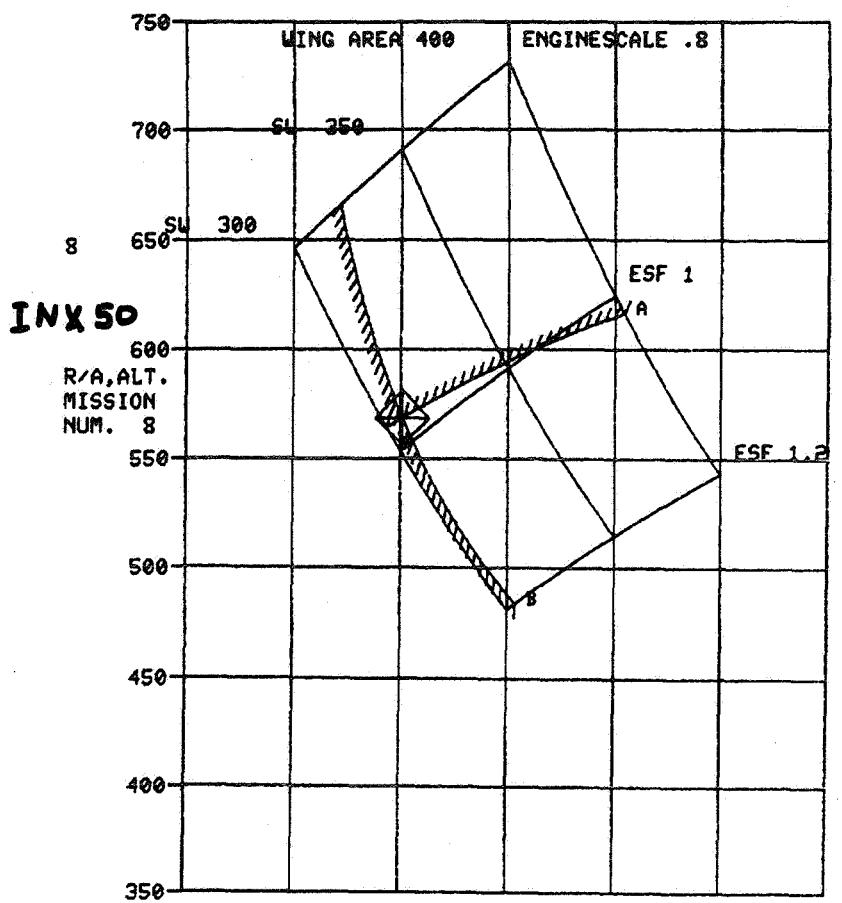

SYMBOL	CONSTRAINT			TYPE	VALUE
A	THRUST TO		WEIGHT	GT	1.170
B	EQUIL.	NZ -	10KM= .60	GT	6.200

MARKER COORDINATES

	ENGINESCALE	WING AREA	R/A,ALT.MISSION NUM.
*1.	.97649998	306.58827622	568.56176250

NOTE: ADD 50 NM: RADIUS TO CARPET VALUES

TF120 PERFORMANCE SENSITIVITIES
SSTF011 *

1= CHANGE INDEPENDENT VAR.
2= CHANGE DEPENDENT VAR.
3= NEXT DEPENDENT VAR.
4= ADD A CONSTRAINT
5= DELETE A CONSTRAINT
6= CONSTRAINT INTERSECTIONS
7= COORDINATE PICK
8= INSERT/DELETE GRID
9= REPAINT
10= DELETE MARKER COORDINATES
11= BATCH PLOT
12= EXIT 8

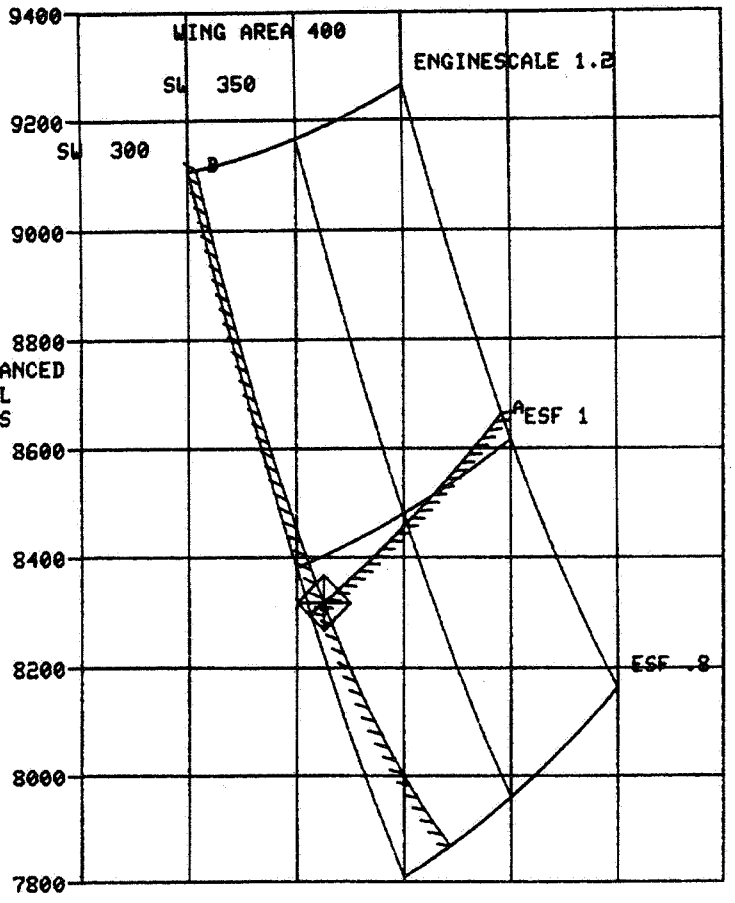

SYMBOL	CONSTRAINT			TYPE	VALUE
A	THRUST	TO	WEIGHT	GT	1.170
B	EQUIL.	NZ - 10KM=	.60	GT	6.200

MARKER COORDINATES

	ENGINESCALE	WING AREA	BALANCEDFUEL -LBS
*1.	.97649998	306.58827622	8317.40279324

1. Report No.	2. Government Accession No.	3. Recipient's Catalog No.
NASA CR-166271		

4. Title and Subtitle	5. Report Date
Study of Aerodynamic Technology for Single-Cruise Engine V/STOL Fighter/Attack Aircraft	6. Performing Organization Code

7. Author(s)	8. Performing Organization Report No.
H. H. Driggers, S. A. Powers, R. T. Roush	2-52300/2R-53020
	10. Work Unit No.

9. Performing Organization Name and Address	11. Contract or Grant No.
Vought Corporation P.O. Box 225907 Dallas, TX 75265	Contract NAS2-11003
	13. Type of Report and Period Covered Contractor Final Report June 1981 to February 1982
12. Sponsoring Agency Name and Address National Aeronautics and Space Administration, Washington, DC 20546 David Taylor Naval Ship R&D Center, Carderock, MD 20034 Naval Air Systems Command, Washington, DC 23061	14. Sponsoring Agency Code RTOP 505-43-01

15. Supplementary Notes

Technical Monitors: D. A. Durston/W. P. Nelms, NASA-Ames Research Center, MS 227-2, Moffett Field, CA, (415) 964-5855/5879, FTS 448-5855/5879

Point of Contact: J. H. Nichols, Jr., DTNSRDC; M. W. Brown, NAVAIR

16. Abstract

A conceptual design analysis was performed on a single engine V/STOL supersonic fighter/attack concept powered by a series flow tandem fan propulsion system. Forward and aft mounted fans have independent flow paths for V/STOL operation and series flow in high speed flight. Mission, combat and V/STOL performance was calculated.

Detailed aerodynamic estimates were made and aerodynamic uncertainties associated with the configuration and estimation methods identified. A wind tunnel research program was developed to resolve principal uncertainties and establish a data base for the baseline configuration and parametric variations.

17. Key Words (Suggested by Author(s))	18. Distribution Statement
V/STOL Fighter/Attack Aircraft Aerodynamic Estimates Tandem Fan Propulsion Cycle	FEDD Distribution Subject Category 02

19. Security Classif. (of this report)	20. Security Classif. (of this page)	21. No. of Pages	22. Price*
Unclassified	Unclassified	209	

Available: NASA's Industrial Applications Centers